

Signal transduction pathways
in the fungal wheat pathogen *Fusarium graminearum*

Dissertation

A thesis submitted for the degree of Dr. rer.nat. (*rerum naturalium*)
to the Biology Department,
the Faculty of Mathematics, Informatics and Natural Sciences,
University of Hamburg

by

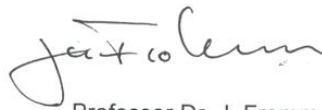
Thuat Van Nguyen

Thanh Hoa, Vietnam

Hamburg, 2013

Genehmigt vom Fachbereich Biologie
der Fakultät für Mathematik, Informatik und Naturwissenschaften
an der Universität Hamburg
auf Antrag von Professor Dr. W. SCHÄFER
Weiterer Gutachter der Dissertation:
Professor Dr. C. VOIGT
Tag der Disputation: 15. Februar 2013

Hamburg, den 31. Januar 2013

A handwritten signature in black ink, appearing to read 'J. Fromm', with a stylized flourish at the end.

Professor Dr. J. Fromm
Vorsitzender des Promotionsausschusses
Biologie

Prof. PhD. Myron A. Peck
Institute of Hydrobiology and
Fisheries Science

Olbersweg 24 • D-22767 •
Hamburg

Tel +49 4042 838 6602

Fax +49 4042 838 6618

myron.peck@uni-hamburg.de

Promotionsausschuss der Universität Hamburg
Department Biologie

Hiermit wird bestätigt, dass die sprachliche Ausarbeitung der kumulativen Dissertation in Englisch mit dem Titel „Signal transduction pathways in the fungal wheat pathogen *Fusarium graminearum*“ vorgelegt von Thuat Van Ngueyen wissenschaftlichen Standards genügt.

Mit freundlichen Grüßen



Prof. PhD. Myron A. Peck

Hamburg 5.11.2012

Contents

1. Introduction	1
1.1. The phytopathogenic fungus <i>Fusarium graminearum</i>	1
1.2. Transmembrane receptors	3
1.3. The MAPK (mitogen-activated protein kinase) cascade.....	7
1.4. The stress-activated MAP kinase pathway	10
1.4.1. Yeast stress-activated MAP kinase pathway (The HOG1 pathway).....	10
1.4.2. The stress-activated MAP kinase pathway in filamentous fungi	11
1.5. The Activating Transcription Factor Atf1 in fungi.....	13
1.6. Aims of this study	14
2. Materials and Methods	15
2.1. Fungal strains and culture conditions	15
2.2. Oligonucleotide primers.....	17
2.3. Vector construction	23
2.3.1. Vector construction for deletion of <i>FgOS-2</i> , <i>Fgatf1</i> and the TMRs.....	23
2.3.2. Vector construction for <i>Fgatf1</i> overexpression	24
2.3.3. Bimolecular fluorescence complementation experiments	24
2.4. Transformation of <i>F. graminearum</i>	25
2.5. Southern blot analysis.....	26
2.6. Virulence assays on wheat, maize, and <i>Brachypodium distachyon</i>	26
2.7. Deoxynivalenol (DON) and zearalenone (ZEA) production analysis	27
2.8. Reactive oxygen species (ROS) and catalase activity measurements	28
2.9. Detection of extracellular lipolytic activity	29
2.10. cAMP level measurement	30
2.11. DAPI-nuclei staining, BiFC assays and microscopy.....	30
2.12. Expression analysis by semi-quantitative and quantitative real-time PCR.....	31
3. Results	32
3.1. The role of transmembrane receptors in <i>Fusarium graminearum</i>	32
3.1.1. Identification of transmembrane receptors from <i>F. graminearum</i>	32
3.1.2. Generation of TMR deletion mutants.....	33
3.1.3. Putative carbon sensor FGSG_05006 is necessary for utilization of poor carbon sources but not for virulence toward wheat and maize	38

3.1.4. The pheromone receptor FGSG_02655 is involved in sexual reproduction and virulence	42
3.1.5. Deletion of <i>FGSG_01861</i> enhances stress tolerance towards oxidative, osmotic, fungicide, temperature and cell wall stress	46
3.1.6. Deletion of <i>FGSG_03023</i> attenuates virulence towards wheat and maize.....	50
3.2. The role of FgOS-2 in <i>Fusarium graminearum</i>	53
3.2.1. Identification of FgOS-2 from <i>F. graminearum</i>	53
3.2.2. Generation of <i>FgOS-2</i> deletion mutants	55
3.2.3. <i>FgOS-2</i> deletion mutants are sensitive to osmotic stress but not to oxidative stress or fungicides	57
3.2.4. FgOS-2 is involved in sexual but not asexual reproduction	62
3.2.5. The deletion of <i>FgOS-2</i> leads to reduced virulence towards wheat and maize	63
3.2.6. Secondary metabolism is controlled by FgOS-2.....	66
3.2.7. Osmotic stress leads to a strongly increased oxidative burst in FgOS-2-mutants...71	
3.3. The role of the Activating Transcription Factor Atf1 in <i>Fusarium graminearum</i>	76
3.3.1. Computer-based identification of transcription factor Atf1 from <i>F. graminearum</i> ...76	
3.3.2. Generation of <i>Fgatf1</i> deletion mutants.....	76
3.3.3. Generation of <i>Fgatf1</i> overexpressing mutants (<i>Fgatf1^{oe}</i>)	78
3.3.4. Generation of <i>FgOS-2</i> deletion mutants in a <i>Fgatf1</i> overexpression mutant (<i>Fgatf1^{oe}::ΔFgOS-2</i>)	79
3.3.5. Functional <i>Fgatf1</i> is necessary for proper vegetative growth and interacts with FgOS-2 under osmotic stress conditions	81
3.3.6. Overexpression of <i>Fgatf1</i> restores sexual reproduction in <i>FgOS-2</i> deletion strains.85	
3.3.7. Deletion of <i>Fgatf1</i> attenuates virulence towards wheat and maize.....	87
3.3.8. <i>Fusarium graminearum</i> Atf1 orchestrates secondary metabolite production	91
3.3.9. <i>Fusarium graminearum</i> Atf1 is involved in regulation of ROS metabolism and catalase gene expression	97
3.3.10. <i>Fusarium graminearum</i> Atf1 is involved in the regulation of light-dependent processes	102
4. Discussion.....	105
4.1. Osmotic stress and altered ROS metabolism influences spore development, germination and mycelial growth in different mutants	105
4.2. Deletion of <i>FgOS-2</i> , <i>Fgatf1</i> and TMR <i>FGSG_01861</i> alters the fungal sensitivity towards the phenylpyrrolic fungicide	110

4.3. Cell wall integrity and ergosterol biosynthesis relies on the activation of MAP-kinase cascades by FGSG_01861.....	112
4.4. The putative transmembrane receptor FGSG_05006 regulates vegetative growth and intracellular cAMP levels on poor carbon sources via the cAMP-PKA or MAP kinase signaling pathways.....	114
4.5. The activating transcription factor Fgatf1 and the TMR FGSG_02655 are prerequisite for sexual reproduction.....	115
4.6. Virulence of <i>F. graminearum</i> relies on FgOS-2 and Fgatf1 in concert with the function of the TMRs FGSG_03023 and FGSG_02655.....	118
4.7. Normal secondary metabolite production depends on functional FgOS-2 and Fgatf1.....	121
4.8. FgOS-2 and Fgatf1 influence the expression of genes involved light reception and circadian rhythmicity.....	124
5. Summary	128
6. Zusammenfassung	130
7. References	132

List of Figures and Tables

Figures

Figure 1. The life cycle of <i>F. graminearum</i>	1
Figure 2. Schematic representation of a signal transduction cascade.....	2
Figure 3. The G protein cycle	4
Figure 4. Nutrient-sensing pathway in <i>N. crassa</i> and <i>C. neoformans</i>	5
Figure 5. General scheme of a MAPK pathway.....	8
Figure 6. MAP kinase pathways in fungi.....	9
Figure 7. Model for the pheromone response, HOG, and pseudohyphal growth pathways in <i>S. cerevisiae</i>	10
Figure 8. The HOG pathway of <i>S. cerevisiae</i>	11
Figure 9. Gene replacement strategy using double homologous recombination method	24
Figure 10. Gene replacement strategies and Southern analysis of TMR deletion.....	36
Figure 11. Gene replacement strategy and PCR analysis of <i>FGSG_09693</i> deletion.....	37
Figure 12. Vegetative growth of the wild type and $\Delta FGSG_05006$ mutant strains on different poor carbon sources	39
Figure 13. Steady-state intracellular cAMP level measurements of the wild type (WT:PH1) and $\Delta FGSG_05006$ mutant strains on minimal-glycerol medium	40
Figure 14. Pathogenicity assay on wheat and maize and DON concentrations measurement in wheat heads. Pathogenicity on wheat heads (A, upper) and maize (B, lower) infected with conidia of the wild type (WT:PH1) and <i>FGSG_05006</i> deletion strains	41
Figure 15. Assay for perithecia formation. Conidia of the wild type (WT:PH1) and <i>FGSG_02655</i> deletion strains were placed on wheat nodes (A) and carrot agar (B).....	42
Figure 16. Pathogenicity assay on wheat and maize. Wheat heads (A, upper) and maize (B, lower) were infected with conidia of the wild type (WT:PH1) and <i>FGSG_02655</i> deletion strains.....	43
Figure 17. DON concentrations of the wild type (WT:PH1) and <i>FGSG_02655</i> deletion strains in wheat heads (A) and submerged culture (B).....	44
Figure 18. Extracellular lipolytic activity of the wild type and <i>FGSG_02655</i> deletion mutant strains after induction by 2% (v/v) wheat germ oil.....	45
Figure 19. Colony morphology of the wild type (WT:PH1) and <i>FGSG_01861</i> deletion strains after 3 days of growth under different stress conditions	46
Figure 20. Colony morphology of the wild type (WT:PH1) and <i>FGSG_01861</i> deletion strains after 3 days and 5 days of growth under osmotic conditions.....	47

Figure 21. Fungicide sensitivity assay.....	47
Figure 22. Conidia germination assay	48
Figure 23. Pathogenicity assay on wheat and maize. Wheat heads (A, upper) and maize (B, lower) were infected with conidia of the wild type (WT:PH1) and <i>FGSG_01861</i> deletion strains.....	49
Figure 24. Pathogenicity assay on wheat and maize. Wheat heads (A, upper) and maize (B, lower) were infected with conidia of the wild type (WT:PH1) and <i>FGSG_03023</i> deletion strains	50
Figure 25. DON concentrations of the wild type (WT:PH1) and <i>FGSG_03023</i> deletion strains in wheat heads (A) and submerged culture (B).....	51
Figure 26. Extracellular lipolytic activity of the wild type and Δ <i>FGSG_03023</i> mutant strains after induction by 2% (v/v) wheat germ oil	52
Figure 27. Alignment of the predicted amino acid sequence of the putative osmolarity MAP kinase from <i>F. graminearum</i> and several fungal MAP kinases.....	54
Figure 28. Replacement and Southern hybridization strategy for <i>FgOS-2</i>	56
Figure 29. Colony morphology of the wild type (WT:PH1), ectopic (ECT) and <i>FgOS-2</i> deletion strains after 3 days of growth on the osmotic stress medium.....	57
Figure 30. Conidia germination assay.	58
Figure 31. Agar plate assay for oxidative stress	59
Figure 32. Agar plate assay for different nitrogen sources	59
Figure 33. Agar plate assay for different pH values.....	60
Figure 34. Agar plate assay for different temperatures.....	60
Figure 35. Fungicide sensitivity assay.....	61
Figure 36. Assay for perithecia formation. Conidia of the wild type (WT:PH1) and <i>FgOS-2</i> deletion strains were placed on detached wheat nodes (on water agar) and on carrot agar	62
Figure 37. Pathogenicity assay on wheat and maize. Maize cobs (A, left) and wheat heads (A, right) were infected with conidia of the wild type and <i>FgOS-2</i> deletion strains	64
Figure 38. Infection assay. Cross-sections of inoculated wheat spikelets.....	65
Figure 39. Infection assay. Cross-sections of wheat rachis nodes inoculated with dsRed-expressing wild type (WT:PH1) and Δ <i>FgOS-2</i> mutant strains.....	66
Figure 40. Pigmentation assay and corresponding gene expression analysis	66
Figure 41. DON concentration and gene expression analysis of the wild type and <i>FgOS-2</i> deletion strains in wheat heads (A), submerged culture (B) and wheat kernels (C).....	68
Figure 42. ZEA concentration and gene expression analysis of the wild type and <i>FgOS-2</i> deletion strains in wheat heads (A), submerged culture (B)	70

Figure 43. ROS production assay in the wild type (WT:PH1) and *FgOS-2* deletion strains72

Figure 44. NADPH-oxidase (Nox) expression assay in the wild type (WT:PH1) and *FgOS-2* deletion strains.....73

Figure 45. Gene expression analysis of the putative transcriptional regulator of ROS metabolic genes, *atf1* (A) and the putative calcium-responsive NADPH-oxidase *noxC* (B)74

Figure 46. Catalase expression and activity assay74

Figure 47. Growth performance of the *FgOS-2* deletion and wild type (WT:PH1) strains on CM agar plates containing 0.2 M NaCl and increasing concentrations of purified catalase.75

Figure 48. Protein alignment (CLUSTALW) of the basic-leucine zipper (bZIP) domain for DNA binding of *F. graminearum* Atf1 (Genebank accession number XP_390318.1) and other (putative) Atf1 orthologues76

Figure 49. Gene replacement and Southern hybridization strategy for *Fgatf1*.....77

Figure 50. Scheme representation for the generation of the *Fgatf1* overexpression construct..79

Figure 51. Replacement and Southern hybridization strategy for *FgOS-2*.....80

Figure 52. Colony morphology of the wild type (WT:PH1) and the mutants $\Delta Fgatf1$, *Fgatf1^{oe}*, $\Delta FgOS-2$ and *Fgatf1::\Delta FgOS-2* after 3 days of growth on the osmotic stress media.81

Figure 53. Colony morphology of the wild type (WT:PH1), $\Delta FgOS-2$ and *Fgatf1^{oe}::\Delta FgOS-2* strains after 3 days of growth on the mild osmotic stress medium82

Figure 54. Bright-field microscopy of germinating conidia of the wild type and $\Delta Fgatf1$ mutant strains in liquid CM and liquid CM supplemented with 0.8 M NaCl.....83

Figure 55. Colony morphology of the wild type (WT:PH1) and the mutants $\Delta FgOS-2$, $\Delta Fgatf1$, *Fgatf1^{oe}* and *Fgatf1^{oe}::\Delta FgOS-2* after 4 days of growth on oxidative stress and fungicide agar plates84

Figure 56. Bimolecular fluorescence complementation assay85

Figure 57. Assay for perithecia formation. Conidia of the wild type, the mutants $\Delta Fgatf1$, *Fgatf1^{oe}*, $\Delta FgOS-2$ and *Fgatf1^{oe}::\Delta FgOS-2* were placed on carrot agar plates.....86

Figure 58. Perithecia and ascospore development on detached wheat nodes86

Figure 59. Pathogenicity assay on wheat and maize. Wheat heads (cv. Nandu; upper panel) and maize cobs (lower panel) were infected with conidia of the wild type (WT:PH1) and the mutants $\Delta Fgatf1$, *Fgatf1^{oe}* and *Fgatf1^{oe}::\Delta FgOS-2*.....87

Figure 60. Pathogenicity assay on wheat cultivar Amaretto88

Figure 61. Infection assay. Cross-sections of inoculated wheat spikelets. The spikelets were infected with strains that constitutively express dsRed in the cytosol and that were derived from the wild type (WT:PH1) and a $\Delta Fgatf1$ strain89

Figure 62. Infection assay. Longitudinal sections of the inoculated and adjacent spikelets90

Figure 63. Pathogenicity assay on *Brachypodium distachyon*.....90

Figure 64. DON concentrations and gene expression analysis of the wild type and *Fgatz1* deletion strains in wheat heads (A) and submerged culture (B).....92

Figure 65. DON concentrations of the wild type (WT:PH1) and the mutants $\Delta Fgatz1$, *Fgatz1^{oe}* and *Fgatz1^{oe}:: $\Delta FgOS-2$* and $\Delta FgOS-2$ in wheat heads.....94

Figure 66. ZEA concentrations and gene expression analysis of the wild type and *Fgatz1* deletion strains in wheat heads (A), submerged culture (B).95

Figure 67. Pigmentation assay and corresponding gene expression analysis97

Figure 68. Nitroblue tetrazolium (NBT) staining for reactive oxygen species (ROS) production of the wild type (WT:PH1), $\Delta FgOS-2$ mutant and the *Fgatz1* mutants.....98

Figure 69. Catalase expression and activity assay99

Figure 70. Catalase gene expression analysis. Quantitative RT-PCR using cDNA obtained from induction medium containing 0.8 M NaCl.....101

Figure 71. Catalase gene expression analysis. Quantitative RT-PCR using cDNA obtained from inoculated wheat spikelets.....102

Figure 72. Growth assay in different light conditions103

Figure 73. Expression analysis of genes encoding for putative light receptors and putative circadian clock receptor proteins.....104

Figure 74. Hypothetical regulation network of ROS metabolic genes.....106

Figure 75. Model for the *S. pombe* Sty1 signaling pathway and hypothesized model for ROS metabolism-mediated signaling pathway in *F. graminearum*110

Figure 76. Proposed model for the FgOS2/*Fgatz1* signaling pathway in response to fludioxonil in *F. graminearum*.....111

Figure 77. Proposed signaling pathway mediating cell wall integrity and heat stress response in *F. graminearum*.....113

Figure 78. Hypothesized model for the putative carbon sensor TMR FGSG_05006 -mediated signaling cascade in *F. graminearum*115

Figure 79. Hypothesized model for the pheromone receptor FGSG_02655 -mediated signaling cascades in *F. graminearum*.....117

Figure 80. Hypothesized model for TMRs FGSG_03023 and FGSG_02655-mediated signaling pathways involved in pathogenesis of *F. graminearum*.121

Figure 81. Proposed regulation model for secondary metabolite production by the FgOS-2/*Fgatz1* signaling pathway in *F. graminearum*123

Figure 82. Proposed model: FgOS-2 orchestrates numerous physiological functions like sexual reproduction, secondary metabolism, virulence and stress response in *F. graminearum*.....127

Tables

Table 1. Primers for generation of TMR gene replacement constructs.....	17
Table 2. Primers for generation of gene replacement construct of <i>FgOS-2</i>	20
Table 3. Primers for generation of gene replacement construct of <i>Fgatf1</i> , <i>Fgatf1</i> overexpression, and bifluorescence complementation experiments.	20
Table 4. Primers for semi-quantitative RT-PCR.....	21
Table 5. Primers for quantitative RT-PCR.....	22
Table 6. Dry mass of and the wild type (WT:PH1) and <i>FGSG_05006</i> deletion strains.....	40
Table 7. ELISA analysis of DON production under different growth conditions in the wild type (WT:PH1) and <i>FGSG_02655</i> deletion strains.	44
Table 8. Extracellular lipolytic activity of the wild type and <i>FGSG_02655</i> deletion strains after induction by 2% wheat germ oil.....	45
Table 9. ELISA analysis of DON production under different growth conditions in the wild type (WT:PH1) and <i>FGSG_03023</i> deletion strains.	51
Table 10. Extracellular lipolytic activity of the wild type and <i>FGSG_03023</i> deletion strains after induction by 2% wheat germ oil.....	52
Table 11. Gene expression analysis of genes involved in aurofurasin biosynthesis.....	67
Table 12. ELISA analysis of DON production under different growth conditions in the wild type and $\Delta FgOS-2$ mutant strains	69
Table 13. Gene expression analysis of genes involved in DON biosynthesis.	69
Table 14. ELISA analysis of ZEA production under different growth conditions in the wild type and $\Delta FgOS-2$ mutant strains	71
Table 15. Gene expression analysis of genes involved in ZEA biosynthesis.....	71
Table 16. Gene expression analysis of genes involved in ROS metabolism.....	75
Table 17. ELISA analysis of DON production under different growth conditions in the wild type (WT:PH1) and <i>Fgatf1</i> deletion strains.....	93
Table 18. Gene expression analysis of genes involved in DON biosynthesis	93
Table 19. ELISA analysis of mycotoxin production <i>in planta</i> of the wild type (WT:PH1) and the mutants $\Delta Fgatf1$, $\Delta FgOS-2$, <i>Fgatf1^{oe}</i> and <i>Fgatf1^{oe}::$\Delta FgOS-2$</i>	94
Table 20. ELISA analysis of ZEA production under different growth conditions in the wild type (WT:PH1) and <i>Fgatf1</i> deletion strains.....	96
Table 21. Gene expression analysis of genes involved in ZEA biosynthesis.....	96
Table 22. Gene expression analysis of putative catalase genes.	100
Table 23. Gene expression analysis of putative catalase genes in osmotic stress medium	101

Table 24. Gene expression analysis of putative catalase genes of *F. graminearum* during wheat infection.....102

Abbreviations	Full name
%	Percentage
Δ	Delta/deletion mutant
°C	Degree Celsius
μl	microliter
μm	micrometer
aa	amino acid
Amp	Ampicillin
ATF1	Activating Transcription Factor 1
ATP	Adenosintriphosphate
BiFC	Bimolecular fluorescence complementation
BLAST	Basic Local Alignment Search Tool
bp	base pairs
cAMP	Adenosine 3',5'-cyclic monophosphate
cat	catalase
cDNA	complementary Deoxyribonucleic Acid
CM	Complete medium
cv	Cultivated variety; cultivar
DAB	Diaminobenzidine
DAPI	4',6-diamidino-2-phenylindole
DIG	Digoxigenin
DNA	Deoxyribonucleic Acid
dNTPs	Deoxyribonucleotide triphosphates
DON	Deoxynivalenol
dpi	days post inoculation
DsRed	Discosoma sp. red fluorescent protein
dsRNA	double stranded RNA
dUTP	Deoxyuridine triphosphate
E. coli	Escherichia coli
EDTA	Ethylenediaminetetraacetic acid
EIA	Enzyme immunoassay
et al.	et alii = and others
F _{do}	downstream fragment
FHB	Fusarium Head Blight

Frq	Putative circadian regulatory protein Frequency
F _{up}	upstream fragment
g	gram; the metric unit of mass
gDNA	genomic DNA
GDP	Guanosine diphosphate
GFP	Green fluorescent protein
gip	Gibberella zeae pigment
GPCR(s)	G protein-coupled receptor(s)
GTP	Guanosine triphosphate
h	hour
HOG	High Osmolarity Glycerol
hph (hyg)	hygromycin B phosphotransferase
IEF	Isoelectric focusing
kb	kilo bases (= 1000 bp)
kDa	kilo Dalton (= 1000 Da)
KP	Potassium phosphate
L	Liter
LB	Luria-Bertani medium
M	Molar (mol/L)
MAP	Mitogen-activated protein
MAPK	Mitogen-activated protein kinase
MAPKK	Mitogen-activated protein kinase kinase
min	minute
MIPS	Munich Information Center for Protein Sequences
ml	milliliter
mM	millimolar
MM	Minimal medium
mRNA	messenger RNA
NBT	Nitro blue tetrazolium
NCBI	National Center for Biotechnology Information
NIV	Nivalenol
nptII	neomycin phosphotransferase
OD	Optical Density
Ops	Opsins
ORF	Open Reading Frame

PCR	Polymerase Chain Reaction
PDA	Potato Dextrose Agar
PDB	Potato Dextrose Broth
PEG	Polyethylene glycol
pH	Potential Hydrogen
PKA	Protein kinase A
PKC	Protein kinase C
PKS12	Polyketide synthase 12
pNP	para-Nitrophenol
pNPP	para-Nitrophenyl Palmitate
qRT-PCR	quantitative Reverse Transcription-Polymerase Chain Reaction
RGS	Regulator of G-protein signaling
RNA	Ribonucleic Acid
ROS	Reactive oxygen species
rpm	round per minute
RT	room temperature
RT-PCR	Reverse transcription- Polymerase Chain Reaction
SDS	Sodium dodecyl sulphate
SNA	Synthetic Nutrient Agar
TBE	Tris-Borate-EDTA
TEMED	Tetramethylethylenediamine
T _m	Annealing Temperature
TMR(s)	Transmembrane receptor(s)
Tri	Trichothecene synthase gene
Tris	Tris-(hydroxymethyl) aminomethane
UV	Ultra violet
v	Volume
v/v	Volume per volume
Vvd	Putative blue-light receptor Vivid
w/v	Weight per volume
WT	Wild-type
YES	Yeast extract/Sucrose/ MgSO ₄ x 7H ₂ O medium
YFP	Yellow Fluorescent Protein
YPD	Yeast-extract PeptonDextrose

YPG	Yeast-extract Peptone Glucose
ZEA	Zearalenone

1. Introduction

1.1. The phytopathogenic fungus *Fusarium graminearum*

Fusarium graminearum [teleomorph *Gibberella zeae* (Schwein.)] is one of the most destructive pathogens of cereals and a threat to food and feed production worldwide. It is an ascomycetous plant pathogen and the causal agent of Fusarium head blight disease in small grain cereals and of cob rot disease in maize. Infection with *F. graminearum* leads to the reduction of yield and quality of the harvested grain. Importantly, *F. graminearum* produces several mycotoxins that contaminate food and have harmful impact on animal and human health. The most prominent mycotoxins are the trichothecenes deoxynivalenol (DON) and the estrogenic polyketide zearalenone (ZEA). ZEA and DON are hazardous to animals and humans; the latter DON is necessary for virulence towards wheat (Sutton, 1982; Goswami and Kistler, 2004).

F. graminearum is a haploid homothallic ascomycete. Ascospores produced by sexual reproduction play crucial roles in the completion of the disease cycle of Fusarium head blight. Fruiting bodies called perithecia develop on plant debris and give rise to ascospores which are forcibly discharged from perithecia and initiate primary infection on susceptible parts of wheat, barley, and other grass species as well as ear rot on corn during the next spring. In asexual stage, *F. graminearum* produces conidia on crop residues to overwinter. When environmental conditions are warm, humid and wet, the sexual stage starts develop on the plant debris (Beyer et al., 2004; Trail, 2009). The *F. graminearum* life cycle can be summarized as follows (Fig. 1).

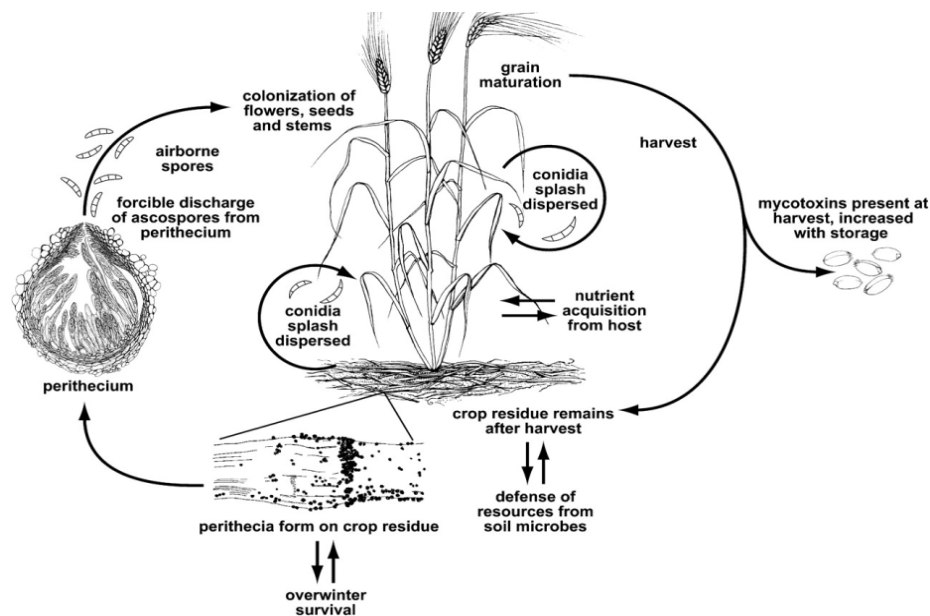


Figure 1. The life cycle of *F. graminearum* (sexual phase, *Gibberella zeae*), causal agent of Fusarium head blight on wheat (Trail, 2009).

In order to survive in changing environments, *F. graminearum* responds to diverse stimuli such as light, pheromones, temperature, hormones, and nutrients by signal transduction cascades. Signal transduction cascades usually start with transmembrane receptors and end with the alteration of transcription in the nucleus. Transmembrane receptors (TMRs) are specialized integral membrane proteins that perceive external signals and communicate them to intracellular signaling cascades. These signaling cascades convert diverse physical or chemical signals detected at the cell surface into changes in gene expression through a series of reversible protein phosphorylation events. The signal is finally shifted to downstream effectors facilitating changes in corresponding target gene expression. The change in expression of these target genes is essential for the response of *F. graminearum* to an activating signal. Errors in these signaling pathways caused by mutations will activate or inhibit the expression of target genes. Consequently, cellular functions such as stress adaptation, filamentous growth, secondary metabolite production and virulence might be changed (Fig. 2).

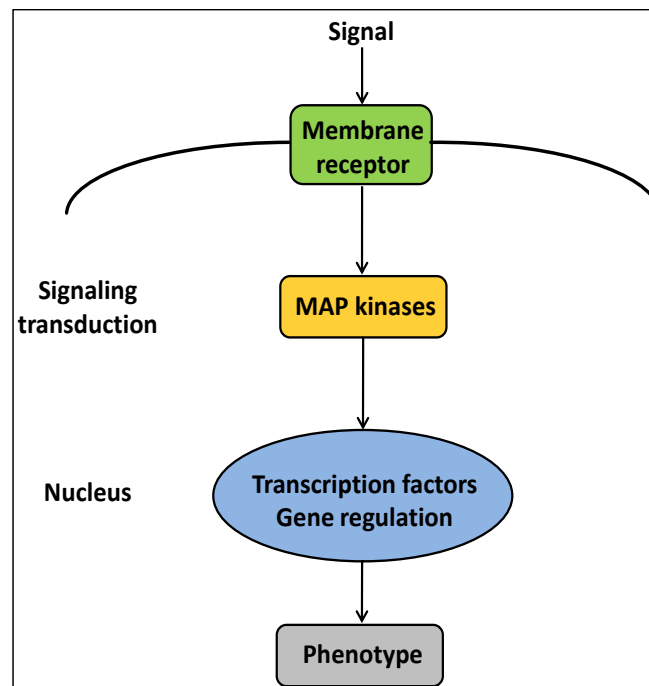


Figure 2. Schematic representation of a signal transduction cascade. A specific receptor protein at the plasma membrane perceives an external stimulus and communicates to a MAP kinase signaling cascade. The diverse physical or chemical signals detected at the cell surface are converted into changes in gene expression through this signaling cascade. The change in expression of these target genes is essential for the response of *F. graminearum* to an activating stimulus.

In the following I will present results on the functional characterization of transmembrane receptors, the stress-activated MAP kinase FgOS-2 and a putative downstream target of FgOS-2, the ATF/CREB activating transcription factor Fgatf1 in *F. graminearum*, in order to elucidate their functions in the signaling transduction cascades.

1.2. Transmembrane receptors

Transmembrane receptors are specialized integral membrane proteins that perceive external signals and communicate to intracellular signaling cascades. TMRs play an important role in cellular communications and signal transduction.

Based on structural and functional similarities, transmembrane receptors are mainly divided into 3 classes: the ion channel-linked receptor, the enzyme-linked receptor and G protein-coupled receptors (Alberts et al., 2002).

Ion channel-linked receptors are cell membrane bound receptors, also called ligand-gated channels. These receptors are involved in controlling the flow of ions into cells and open in response to signals from nerve cells. When a ligand binds to these receptors, they undergo a conformational change. Subsequently, ion channels for extracellular ions such as sodium (Na^+) or potassium (K^+) open. Consequently, the extracellular chemical signal is converted into intracellular electric signal, which alter the excitability of the cell. The ion channels are opened only for a short time. When the ligand dissociates from the receptor, the receptor is available once again for a new ligand to bind. Ion channel-linked receptors usually consist of five subunits which form a pore through the membrane. Each individual subunit spans the membrane four times (Lodish et al., 2003).

Enzyme-linked receptors are catalytic receptors, where an extracellular ligand binds to and causes a conformational change on the catalytic function located on the receptor inside of the cell. They have two important domains: an extracellular ligand binding domain and an intracellular domain, which has a catalytic function and a transmembrane helix without an association with heterotrimeric G proteins. Enzyme-linked receptors are divided into 6 classes: tyrosine kinase receptors, tyrosin kinase associated receptors, receptor-like tyrosine phosphatases, receptor serine/threonine kinases, receptor guanylyl cyclases and histidine kinase associated receptors (Cuatrecasas, 1974; Alberts et al., 2002).

The third group, the G protein-coupled receptors (GPCRs), comprises seven membrane-spanning domains, three extracellular loops and three intracellular loops with an extracellular amino terminus and an intracellular carboxyl tail extending into cytoplasm. GPCRs are pivotal for the rapid response to extracellular stimuli including light, odors, Ca^{2+} , pheromones, hormones, neurotransmitters and other signals. When an extracellular ligand binds, the receptor undergoes a conformational change and thereby gets active. The signal transduction begins. The signal activates the heterotrimeric G-protein (heterotrimeric G-proteins are intracellular membrane-associated proteins activated by several receptors) by inducing the exchange of GDP for GTP at the G_α . Subsequently, the dissociation of G_α -GTP from the $G_{\beta\gamma}$

dimer allows G_α and/or $G_{\beta\gamma}$ to interact with downstream effector proteins (Fig. 3) (Li et al., 2007).

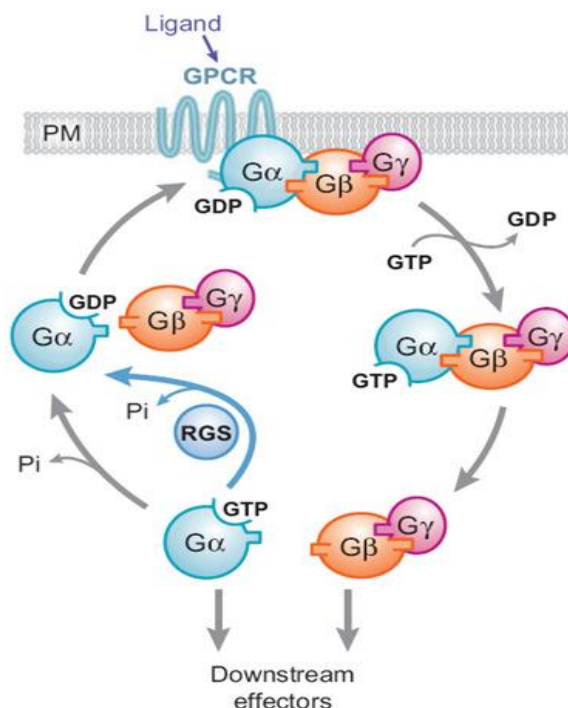


Figure 3. The G protein cycle. When a ligand binds to the G protein-coupled receptor (GPCR), the GPCR undergoes a conformational change and activates a heterotrimeric G-protein by stimulating the exchange of GDP to GTP associated with the G_α subunit. Subsequently, the G_α -GTP dissociates from $G_{\beta\gamma}$ dimer and both may act on their downstream effectors. Consequently completing the cycle a reassociation of G_α -GDP with the $G_{\beta\gamma}$ dimer and the GPCR takes place, as the GTP is hydrolyzed to GDP. The rate of GTP hydrolysis is accelerated by RGS (regulator of G-protein signaling) proteins (blue arrow). Reproduced from Li et al. (2007).

In filamentous fungi (including *F. graminearum*), G protein-coupled receptors are divided into five distinct groups: pheromone receptors, cAMP receptor-like proteins, carbon sensors, putative nitrogen sensors, and microbial opsins. Some proteins have sequences which are similar to GPCRs but do not contain seven transmembrane helices; these results seem to appear from annotation or sequence errors (Li et al., 2007).

Several TMR carbon sensors have been characterized in fungi to elucidate their functions. In *Saccharomyces cerevisiae*, GPCR Gpr1 senses glucose and sucrose and activates cAMP signaling through Gpa2 (Lemaire et al., 2004b). *Candida albicans* heterotrimeric G_α subunit Gpa2 acts downstream of GPCR Gpr1 to regulate filamentous growth in cAMP/PKA signaling pathway. Deletion of *Gpr1* leads to a severe defect in hyphal formation during growth on solid media containing low concentrations of glucose and amino acids such as methionine. The supplementation of exogenous cAMP partially restores wild-type hyphal formation. Moreover, constitutive overexpression of *Gpa2* or catalytic protein kinase A subunit *TPK1* restores the

wild-type phenotype of *Gpr1* deletion strains. However, *Gpr1* plays a minor role in virulence and invasion in human tissue (Maidan et al., 2005). Carbon sensor *Gpr-4* of *Neurospora crassa* is homologous to carbon sensing GPCR *Gpr1* from *S. cerevisiae* and *C. albicans*. It is also required for carbon source utilization. $\Delta Gpr-4$ mutants accumulate less biomass compared to the wild type on poor carbon sources. The supplementation of exogenous cAMP can partially restore the biomass defects of $\Delta Gpr-4$ mutants on solid glycerol medium. However, *Gpr-4* is unnecessary for the regulation of steady-state intracellular cAMP levels but necessary for transient increase in cAMP levels when shifted from glycerol to glucose medium. Deletion of G_α subunit *GNA-1* causes a severe reduction biomass on glycerol medium. Double deletion mutants ($\Delta\Delta Gpr-4GNA-1$) showed the same biomass accumulation on glycerol medium like of the $\Delta GNA-1$ mutants. Constitutive expression of *GNA-1* suppressed the growth defect of *Gpr-4* deletion mutant on glycerol medium. These results indicate that *Gpr-4* functions upstream of the G_α subunit *GNA-1* in cAMP/PKA signaling pathway (Fig. 4) (Li and Borkovich, 2006). In *Cryptococcus neoformans*, GPCR *Gpr4* is described as a methionine sensor. *Gpr4* interacts with downstream G_α subunit *Gpa1* to regulate cAMP levels and mating in a cAMP/PKA signaling cascade on medium containing methionine. However, *Gpr4* is not essential for virulence on mice (Fig. 4) (Xue et al., 2006).

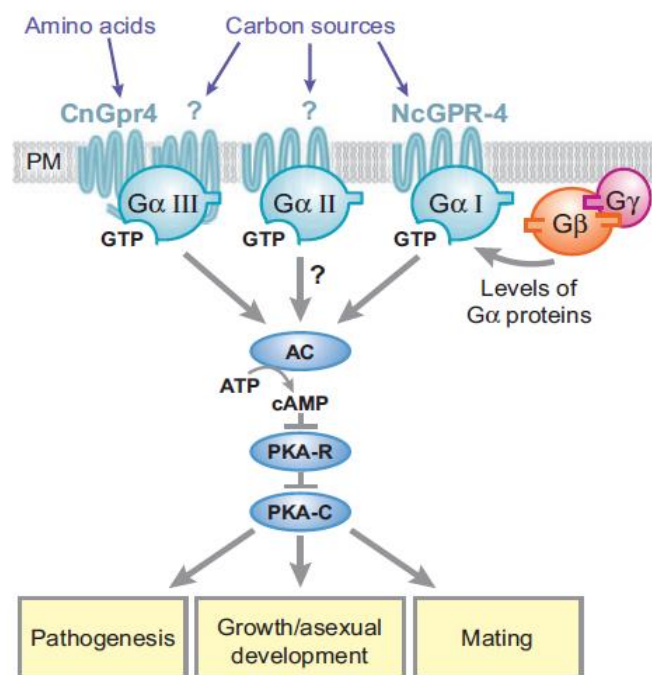


Figure 4. Nutrient-sensing pathway in *N. crassa* and *C. neoformans*. GPR-4 in *N. crassa* is sensor for carbon sources. As a carbon-source ligand binds to and activates GPR-4. This leads to an activation of the associated G_α I (*GNA-1*) and downstream effectors in the cAMP signaling pathway. Activation of this cascade regulates vegetative growth and pathogenicity. *Gpr4* (*CnGPR4*) in *C. neoformans* is an amino acid sensor. It functions upstream of the group G_α III (*Gpa1*) and the cAMP signal transduction pathway to regulate growth, sexual development, and pathogenicity. Reproduced from Li et al. (2007).

TMRs and G proteins-related regulation of sexual development also have been characterized in so many fungi. In *S. cerevisiae* the pheromone response pathway consists of the peptide pheromones α -factor and a-factor, the pheromone receptors Ste2p and Ste3p, a heterotrimeric G protein (including Gpa1p (G_{α}) and Ste4p/Ste18p ($G_{\beta\gamma}$ dimer)), and the MAP kinase cascade (Ste11, Ste7, and Fus3/Kss1) (Fig. 7). When the cell responds to mating pheromones, Gpa1p is activated by Ste2p and the signal is transmitted to the MAP kinase cascade via the Ste20 kinase (Leberer et al., 1997; O'Rourke and Herskowitz, 1998). Disruption of GPCR *gpr1* (a cAMP receptor-like GPCR) in *N. crassa* causes deficiency in perithecial development and ascospore discharge. Perithecia produced by Δ *gpr-1* mutants are hairy, had deformed beaks and lack pores at the tips. Furthermore, perithecia are frequently ruptured and generally do not reach maturity (Krystofova and Borkovich, 2006). The *Aspergillus nidulans* genome has two pheromone receptors, *gprA* and *gprB*. The absence of *gprA* and *gprB* in *A. nidulans* leads to pleiotropic phenotypic defects during sexual development. The single mutants Δ *gprA* or Δ *gprB* are able to produce cleistothecia. However, cleistothecia are smaller and contain less ascospores compared to the wild type. Double-receptor mutants completely fail to produce cleistothecia (Seo et al., 2004). The *C. neoformans* genome has two pheromone receptors CPR α and CPR β . Deletion of *CPR α* decreases mating efficiency and the ability to sense to the MAT α pheromone (Chung et al., 2002). Loss of *CPR α* increases mating and virulence (Chang et al., 2003). The *Magnaporthe grisea* G_{α} subunits *magA*, *magB*, and *magC* are involved in sexual development. Δ *magA* and Δ *magC* mutants can produce perithecia. Nevertheless, ascospores have never reached maturity. Deletion mutants of *magB* fail to form perithecia (Liu and Dean, 1997b). *F. graminearum* has two putative pheromone precursor genes (*ppg1* and *ppg2*) and their corresponding pheromone receptor genes (*pre1* and *pre2*). Disruption of *ppg1* and *pre2* leads to significantly reduced perithecia maturation rate and ascospore formation. However, *ppg2* and *pre1* have no effects on sexual development (Lee et al., 2008).

TMRs and heterotrimeric G proteins are also involved in pathogenicity. In filamentous fungi G_{α} I or G_{α} III is associated with the cAMP signaling cascade and is necessary for pathogenicity. $G_{\beta\gamma}$ proteins may also be required for pathogenicity since they may function upstream of other MAP kinase signaling cascades. For example, in *M. grisea* *magB* (G_{α} I) is associated with the cAMP/PKA pathway and regulates vegetative growth, appressorium formation, asexual and sexual development, and pathogenicity (Liu and Dean, 1997). Also, in *M. grisea*, Deletion of *mgb1* (G_{β}) or *mgg1* (G_{γ}) causes a defect in appressorium penetration and infectious growth. The supplementation of exogenous cAMP does not restore normal appressorium formation and infectious growth of these mutants suggesting that *mgb1* and *mgg1* may function upstream of

other MAPK pathways but not the cAMP/PKA pathway (Liu and Dean, 1997; Nishimura M. et al., 2003; Liang et al., 2006). The putative TMR Pth11 in *M. grisea* also regulates appressorium differentiation. The absence of *Pth11* causes avirulence towards barley. These results suggest that TMR Pth11 associates with heterotrimeric G proteins and intracellular signaling cascades to regulate appressorium differentiation and pathogenicity (DeZwaan et al., 1999). Tmpl, a transmembrane protein in both *Alternaria brassicicola* and *A. nidulans* containing six putative transmembrane domains, is necessary for intracellular redox homeostasis and pathogenicity (Kim et al., 2009). Fungal tetraspanins (small integral membrane proteins consisting of four putative transmembrane domains) are also required for the formation of the penetration peg and thus pathogenicity in *M. grisea*, *Botrytis cinerea* and *Colletotrichum lindemuthianum* (Clergeot et al., 2001; Gourgues et al., 2004; Veneault-Fourrey et al., 2005).

1.3. The MAPK (mitogen-activated protein kinase) cascade

MAPK cascades are perhaps one of the most conserved and crucial signaling pathways possessed by eukaryotes. They can be found in all eukaryotic kingdoms from animal to fungi. These pathways convert diverse physical or chemical signals detected at the cell surface into changes in gene expression through a phosphorylation MAP kinase cascade consisting of three highly conserved protein kinases (the core of each MAP kinase cascade): the MAP kinase kinase kinase (MAPKK kinase), MAP kinase kinase (MAPK kinase) and MAP kinase (MAPK) (Fig. 5). The activating stimulus is detected at the cell surface by membrane receptors. The signal is then transmitted either directly to the MAPKK kinase or via an adaptor module composed of an additional protein kinase. The activated MAPKK kinase then phosphorylates the MAPK kinase at specific serine/threonine residues, which in turn phosphorylates the MAP kinase. The signal is finally shifted to downstream effectors facilitating changes in corresponding target gene expression. The change in expression of these target genes is essential for the response of a cell to an activating stimulus (Román et al., 2007).

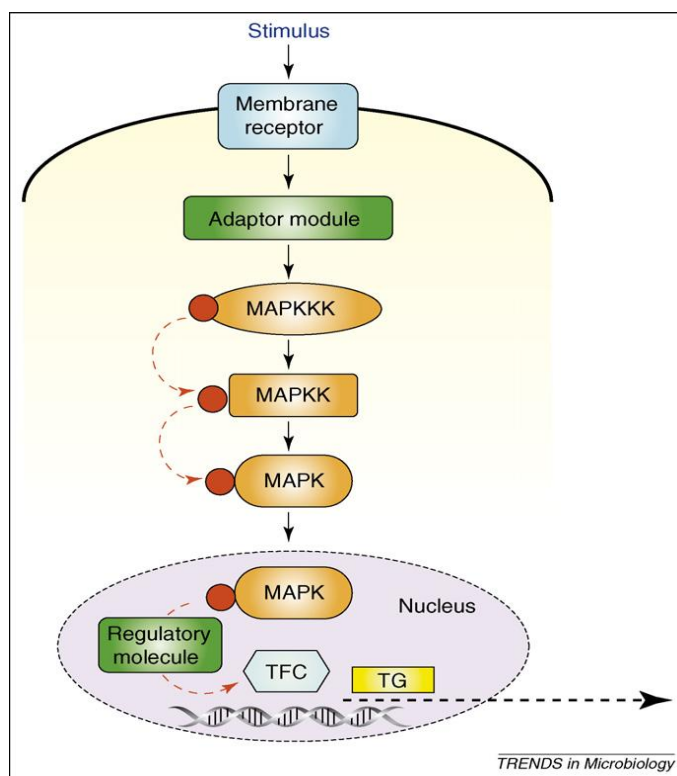


Figure 5. General scheme of a MAPK pathway. A specific receptor protein at the plasma membrane perceives an external stimulus. This receptor then transmits the signal through adaptor molecules to the core MAP kinase phosphorylation cascade. This cascade consists of three highly conserved protein kinases, the MAP kinase kinase kinase (MAPKKK), the MAP kinase kinase (MAPKK) and MAP kinase (MAPK). These kinases are sequentially phosphorylated and activated. Upon phosphorylation, the MAPK generally translocates to the nucleus where it activates target transcription factor complexes (TFC), leading to changes in target gene (TG) expression. The MAPK may also phosphorylate other regulatory molecules such as repressor complexes, relieving the repression of gene expression. Reproduced from Román et al. (2007).

MAPK cascades are found both in higher and lower eukaryotic organism, including yeasts, plants, and mammals (Waskiewicz and Cooper, 1995). Each organism has multiple distinct MAPK cascades that transduce different signals. In the model organism, *S. cerevisiae*, four MAP kinase pathways are involved in cell-wall integrity (protein kinase C, PKC), mating-pheromone response (Fus3), filamentous/invasive growth (Kss1), and high osmolarity growth (HOG1) (Fig. 6). A fifth MAP kinase pathway (Smk1) involved in spore wall assembly is active only during sporulation (Michael et al., 1998). Most filamentous fungi possess only three MAP kinase pathways. Nonetheless, in the *Aspergilli*, the number of MAP kinases has been expanded with *Aspergillus fumigatus* and *A. nidulans* having four, and *Aspergillus oryzae* possessing five due to redundancy of the HOG1-like MAP kinase (Kobayashi et al., 2007). In pathogenic fungi MAP kinase pathways have been found to play important roles in virulence (Román et al., 2007). For example, in *M. grisea*, two of three MAP kinase pathways have been addressed to function in virulence with the MPS1 pathway (homologous to *S. cerevisiae* Slt2 pathway)

involved in penetration peg formation, and the PMK1 pathway (homologous to *S.cerevisiae* Fus3 and Kss1 pathways) involved in appressorium formation. The third pathway (OSM1 pathway homologous to *S. cerevisiae* Hog1 pathway) is involved in the hyperosmotic response (Dean et al., 2005).

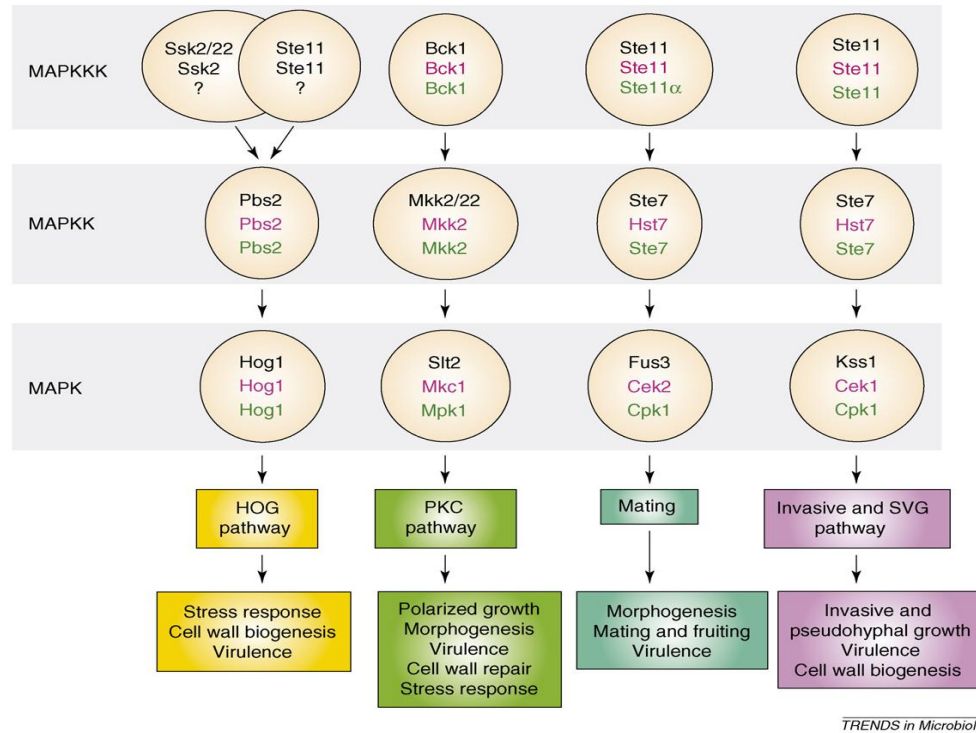


Figure 6. MAP kinase pathways in fungi. The central core proteins of MAPK pathways in three selected fungal models are shown: *Saccharomyces cerevisiae* (black), *Candida albicans* (pink) and *Cryptococcus neoformans* (green). The functions associated to each of them are indicated beneath the core proteins. Reproduced from Román et al. (2007).

However, cross-talk between pathways is prevented, probably because of the formation of multi-component signaling complexes. Recent experimental evidence indicates that Hog1 and Pbs2 have a negative feedback regulation on the pheromone response pathway in *S. cerevisiae*. Under osmotic conditions, Hog1 and Pbs2 mutants activate the pheromone response pathway. This pathway includes a functional Sho1 osmosensor, as well as Ste20, Ste50, the pheromone response MAPK cascade (Ste11, Ste7, and Fus3/Kss1), and Ste12. Ste20 and Ste50 both function in the Sho1 branch of the HOG pathway and another unknown osmosensor distinct from Sho1. Ste11 may be triggered by Sln1 through Ste12. Additionally, pseudohyphal growth depends on Sho1, suggesting that Sho1 is not only an osmosensor for the HOG signaling but also a receptor for pseudohyphal growth cascade (Fig. 7) (O'Rourke and Herskowitz, 1998).

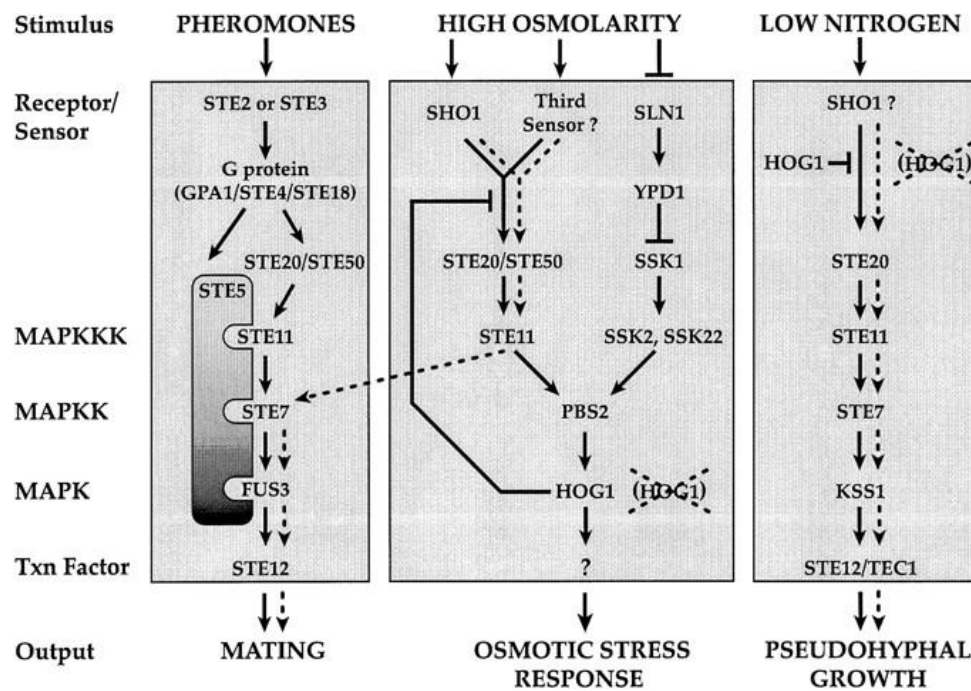


Figure 7. Model for the pheromone response, HOG, and pseudohyphal growth pathways in *S. cerevisiae*. Hog1p has feedback regulation on the Sho1p osmosensor in the HOG pathway. Ste50p and Ste20p participate in both the pheromone response and HOG pathways. Sho1p is not only a sensor for the pseudohyphal growth but also for HOG pathways. Dashed lines indicate that Hog1 mutants activate pheromone response and hyperpseudohyphal growth pathways under osmotic conditions. Reproduced from O'Rourke and Herskowitz (1998).

1.4. The stress-activated MAP kinase pathway

1.4.1. Yeast stress-activated MAP kinase pathway (The HOG1 pathway)

The name HOG1 (high osmolarity glycerol) derives from the fact that deletion mutants not only exhibit retarded growth under high osmolarity but also have a greatly reduced glycerol response. These mutants also displayed altered cell morphology under high osmotic media, forming large multinucleated cells with multiple elongated buds (Brewster et al., 1993). The HOG pathway in *S. cerevisiae* is essential for cells to grow under hyperosmotic conditions to maintain the osmotic gradient across the plasma membrane by accumulating glycerol. The HOG signaling cascade in *S. cerevisiae* consists of three major components: one MAP kinase (HOG1), one MAP kinase kinase (Pbs2), and three MAP kinase kinase kinases (Ste11, Ssk2, and Ssk22). The HOG1 MAP kinase can be activated by two branches of upstream osmosensing pathways that converge at Pbs2. One branch comprises a two-component histidine kinase phosphor-relay system consisting of three components, Sln1, Ypd1, and Ssk1. A putative membrane protein, Sho1 is another upstream osmosensing branch that can activate the Pbs2 via Ste11 (Fig. 8). *S. cerevisiae* mutants defective in the HOG pathway, such as single mutants *hog1* or *Pbs2*, show an osmosensitive phenotype (Michael et al., 1998).

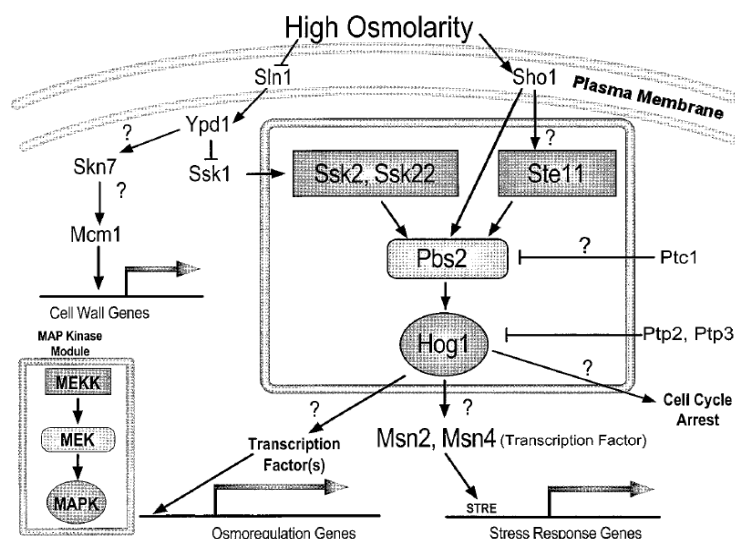


Figure 8. The HOG pathway of *S. cerevisiae*. The HOG1 MAP kinase in *S. cerevisiae* can be activated by external signals which are perceived by two transmembrane sensors Sln1 and Sho1 and transmitted via other components. Uncertainty that require further experimental evidence are indicated by question marks. Reproduced from Michael et al. (1998).

The HOG-pathway has classically been considered to be specific to osmotic stress in fungi (Brewster et al., 1993). However, following studies announced additional function for the HOG-pathway. The HOG-pathway is crucial for adaptation to both citric acid (Lawrence et al., 2004) and heat stress (Winkler et al., 2002) in *S. cerevisiae*. Moreover, the HOG-pathway is involved in the regulation of cell-wall composition (Alonso-Monge et al., 2001). Furthermore, in *Schizosaccharomyces pombe*, the *S. pombe* HOG1 homologue Sty1 (also known as Spc1 and Phh1) is associated in response to a number of stresses including heat shock, ultraviolet (UV) radiation, osmotic, cold and oxidative stresses (Gacto et al., 2003). It is also implicated in cell cycle control, since gene-deletion mutants display a delay in the G2 phase of mitosis, resulting in increased cell length (Shiozaki and Russell, 1995; Millar et al., 1995).

1.4.2. The stress-activated MAP kinase pathway in filamentous fungi

Up to date, several stress-activated MAP kinase HOG1 homologues have been characterized in a number of filamentous fungi ranging from saprobes to animal and plant pathogens. They have diverse and distinct functions in filamentous fungi. In *N. crassa*, the OS-2 MAPK cascade is required not only for growth under osmotic conditions, but also for sensitivity to phenylpyrrole fungicides. Moreover, OS-2 positively regulates catalase gene expression, a component of the antioxidant system (Zhang et al., 2002; Noguchi et al., 2007). The *Fusarium proliferatum* HOG1 seems to maintain apoptotic phenotypes under stress conditions, since $\Delta FpHOG1$ mutants show retarded growth, inhibition of conidial germination, morphological abnormalities and an up regulation of genes involved in programmed cell death under

hyperosmotic conditions (Ádám et al., 2008). In *A. nidulans*, the HOG1 homologue SakA is involved in stress signaling after exposure to oxidative and heat stresses but not osmotic stress. *SakA* deletion mutants show defective sexual development and the spores are sensitive to stress and unable to survive long storage periods. Moreover, chitin deposition alteration in the mutants also suggests a possible role of SakA in cell wall biogenesis. Furthermore, disruption of the *SakA* gene in *A. nidulans* result in a de-repression of *noxA*, encoding a NADPH oxidase known to produce ROS (Han and Prade., 2002; Kawasaki et al., 2002; Lara-Ortíz et al., 2003). Deletion of *SakA* in *Epichlöe festucae* leads to an increased sensitivity to both temperature and osmotic stress but not to oxidative stress and phenylpyrrole fungicide fludioxonil (Carla et al., 2008). The importance of HOG1 homologues regarding pathogenic development varies between different fungal organisms. In many fungi the stress-activated MAP kinase is dispensable for virulence. The *M. grisea* HOG1 homologue, Osm1, is dispensable for appressorium formation and virulence towards rice but essential for proper growth in hyperosmotic media and conidia production (Dixon et al., 1999). Similarly, in *Bipolaris oryzae*, the causal agent of brown leaf spot disease of rice, *srm1* deletion mutants are sensitive to osmotic stress, hydrogen peroxide and UV but remain fully pathogenic (Kojima et al., 2004; Moriwaki et al., 2006). Additionally, loss of *Colletotrichum lagenarium osc1* also has no effect on pathogenicity, although the mutants are sensitive to osmotic stress (Kojima et al., 2004; Moriwaki et al., 2006). In contrast, the stress-activated MAP kinase is essential for normal virulence in a number of other fungi. The HOG1 homologue *Bcsak1* of *B. cinerea* was found to be involved in pathogenicity. $\Delta Bcsak1$ mutants are drastically reduced in virulence. They are unable to produce pseudo-appressoria formation and to penetrate unwounded plant tissue. In addition, *Bcsak1* deletion strains are sensitive to H₂O₂ but resistant to the dicarboximide antibiotic iprodione (Segmüller et al., 2007). In *Cochliobolus heterotrophus*, the causal agent of southern corn leaf blight, *hog1* mutants produce smaller appressoria than the wild type. This leads to a reduction in disease symptoms development on maize. Moreover, *hog1* deletion mutants show an increased susceptibility towards osmotic and oxidative stress (Igbaria et al., 2008). Cpmk1, the stress-activated MAP kinase of the chestnut blight fungus *Cryphonectria parasitica* is also required for virulence, although this is complicated by a involvement of the mycovirus that specially targets Cpmk1 (Park et al., 2004). In the cereal pathogen *F. graminearum*, the two response-regulator proteins within the HOG1-pathway, termed FgRrg1 and FgRrg2 were disrupted by Jiang and co-workers (2011). While deletion of *FgRrg2* evokes no obvious phenotype, disruption of *FgRrg1* leads to an increased sensitivity towards osmotic stress. Furthermore, $\Delta FgRrg1$ mutants exhibit a significant reduction in virulence, DON production and conidiation (Jiang et al., 2011). FgOS-2, the HOG1

orthologue of *F. graminearum* was first described by Ochiai and associates (2007a). FgOS-2 plays a significant role in regulation of secondary metabolism. Deletion of *FgOS-2* leads to an up-regulation of the red pigment aurofusarin and a complete lack of DON-production under *in-vitro* conditions. Moreover, $\Delta FgOS-2$ mutants are sensitive to oxidative stress (Ochiai et al., 2007a).

In general, mitogen-activated protein kinase (MAPK) signaling is a ubiquitous and well preserved regulation system for nearly all developmental processes throughout all eukaryotic organisms in response to several external stimuli like biotic or abiotic stresses or hormones. In filamentous fungi and yeasts, the stress-activated MAP kinase signaling cascade regulates stress response, sexual and vegetative reproduction, cell cycle, virulence, apoptosis, cell wall integrity, and secondary metabolism.

1.5. The Activating Transcription Factor Atf1 in fungi

The activating transcription factor 1 (Atf1) belongs to the ATF subfamily of bZIP (basic-region leucine zipper) transcription factors. Atf1 influences diverse physiological processes through interacting or regulating the expression of downstream target genes. Recently, several Atf1 orthologues have been characterized in filamentous fungi. One outcome of these studies was that Atf1 share some functions with the stress-activated MAP kinase. Thus, Atf1 may be a putative downstream target of the stress-activated MAP kinase signaling cascade. In *A. nidulans*, AtfA interacts with SakA in the nucleus under oxidative and osmotic stress conditions or during normal conidia development to regulate different antioxidant responses, development and spore functions (Lara-Rojas et al., 2011). The expression of conidial genes such as *catA* and *gfdB* as well as oxidative or heat stress sensitivity of conidia are dependent on AtfA, SskA and HogA in *A. nidulans* (Hagiwara et al., 2008). Hagiwara et al. (2009) published DNA microarray data on fludioxonil and sorbitol-responsive *A. nidulans* genes. The DNA microarray data show that the expression of several genes is both influenced by SakA and AtfA. Based on these observations, they conclude that AtfA acts as a putative downstream target in SakA/AtfA signaling cascade under fludioxonil treatment and osmotic stress. In *N. crassa*, the SAPK (OS-2) expression of genes involved in conidiation, circadian rhythm, and ascospore maturation is also dependent on Atf-1. However, the phenotype of *OS-2* and *Atf-1* deletion mutants is partially different. For example, osmotic sensitivity and fludioxonil resistance are observed in the *OS-2* deletion mutants but not in the *Atf-1* deletion mutants (Yamashita et al., 2008). In *Magnaporthe oryzae*, Atf1 plays a major role in mediating oxidative stress responses and scavenging host derived ROS and is required for full virulence (Min Guo et al., 2010). In the biotrophic grass pathogen *Claviceps purpurea*, the Atf1 homologue Tf1 is

believed to act as a positive regulator of the catalase genes and a repressor of the ROS-generating system (*Nox* genes) (Nathues et al., 2004). In the necrotrophic fungus *B. cinerea*, the Atf1 homologue is essential for normal pathogenicity. Knock-out mutants are hypervirulent towards different host plants (Temme et al., 2012). In *A. oryzae*, conidial germination and stress tolerance are controlled by AtfA and *atfA* deletion mutants are sensitive to oxidative stress (Sakamoto et al., 2009).

Generally, the basic leucine zipper transcription factor Atf1 in fungi is a putative downstream target of the stress-activated MAP kinase. They have common functions and involve several physiological processes in fungal life cycles. However, Atf1 also has distinct functions.

1.6. Aims of this study

Previous studies showed that the stress-activated MAP kinase, the activating transcription factor Atf1 and transmembrane receptors are involved in the diverse physiological processes in fungal life cycles. Atf1 acts as a putative downstream target of the stress-activated MAP kinase. Atf1 shares more functions with the stress-activated MAP kinase but has important-independent features. Transmembrane receptors perceive external signals and communicate them to MAP kinases and cAMP/PKA signaling cascades. However, the signaling crosstalk between TMRs and intracellular signaling cascades in *F. graminearum* remain unclear. A balanced ROS metabolism is crucial for proper fungal development. I hypothesise that the diverse physiological processes in *F. graminearum* controlled by the stress-activated MAP kinase FgOS-2 (*S. cerevisiae* HOG1 orthologue) are executed through the regulation of ROS. In order to understand signaling crosstalk between TMRs and specific FgOS-2 signaling cascade as well as other signaling cascades and ROS metabolism in *F. graminearum*, FgOS-2 and Fgatf1 and seven putative TMRs were indentified from the MIPS *Fusarium graminearum* Genome Database. In the following, the deletion mutants for all genes were generated. Constitutive overexpressing mutants were created for Fgatf1. Subsequently, these mutants were functionally characterized under different growth conditions. The roles of FgOS-2, Fgatf1 and seven putative TMRs in the virulence of *F. graminearum* towards wheat and maize were also examined in plant infection assays. The interaction of FgOS-2 and Fgat1 in the nucleus under stress conditions was proved by bimolecular fluorescence complementation (BiFC) experiment. The results were later analyzed to elucidate FgOS-2, Fgatf1 and seven putative TMRs functions connecting to different signaling cascades and ROS metabolism in *F. graminearum*.

2. Materials and Methods

2.1. Fungal strains and culture conditions

F. graminearum wild-type strain PH1 was used for this study. Conidia water suspensions were stored at -70 °C. Conidiation was induced on SNA agar plates incubated for 2 weeks at 18 °C under near-UV light and white light (both TL 40W-33 RS; Philips, Eindhoven, The Netherlands) with a 12-h photoperiod or in liquid wheat medium incubated for four days at 28 °C in darkness. Perithecia formation was induced on carrot agar plates and detached wheat nodes on water agar plates (double autoclaved wheat parts with a nodium in the middle). Conidia of the wild type, $\Delta FgOS-2$, *Fgatf1* mutants ($\Delta Fgatf1$, *Fgatf1^{oe}* and *Fgatf1^{oe}:: $\Delta FgOS-2$*) and the different TMR deletion mutants were inoculated on carrot agar plates at 28 °C in the dark. After 3 days, the aerial mycelia were knocked down with 1 ml of sterile 2.5% Tween 60 solution, using a sterile glass rod. The carrot agar plates and wheat nodes on water agar plates were further incubated at 18 °C under near-UV light and white light with a 12-h photoperiod for 3-8 weeks. In order to examine whether or not the perithecia that developed contained asci with ascospores, the perithecia were excised using a knife and placed on objective slides. They were then crushed between the slide and a cover slip and analysed for asci and ascospores under a microscope. The growth rates of the wild type and several independent $\Delta FgOS-2$, *Fgatf1* mutants and TMR deletion strains were determined by inoculating 5 mm mycelial plugs taken from the edge of a 3-day-old colony on complete medium (CM) or potato-dextrose agar (PDA) plates on news assay plates. In order to test the effect of several chemical substances on the growth performance of the wild type and the mutant strains, the solid growth media were supplemented with the following agents: D-sorbitol, NaCl, KCl, H₂O₂, fludioxonil, iprodione, azoxystrobin, tebuconazole, catalase, congo red, different carbon and nitrogen sources, respectively at concentrations as indicated in the figure legends. The plates were inoculated at 28 °C for at least 3 days in the dark. For temperature stress conditions, the plates were incubated at 18 °C, 30 °C and 32 °C. For the pH-assays, media were adjusted to certain pH-values indicated in the figure legends. The diameter of the mycelial colonies was measured using a technical ruler or scale. The analyses were performed on two or three independent mutants with at least five replicates. For RNA isolation the strains were cultured in liquid YPD for 3 days. Grown mycelia were harvested using a sieve (200 μ m) and washed with double-distilled water several times. Equal portions of semi-dried mycelia were then shifted in new liquid media containing the stressors NaCl, H₂O₂ and fludioxonil, respectively, in the concentrations shown in the figure legends. Mycelia harvested from the toxin induction media (see below) were also used for the RNA isolation analysis.

Media used for cultivation of the wild type, $\Delta FgOS-2$, the different *Fgatf1* mutants and the different TMR deletion strains in the experiments were prepared as follows:

CM medium (Leach et al., 1982):

- Solution A (100x): 100 g/l $\text{Ca}(\text{NO}_3)_2 \times 4 \text{H}_2\text{O}$.
- Solution B (100x): 20 g/l KH_2PO_4 ; 25 g/l $\text{MgSO}_4 \times 7\text{H}_2\text{O}$; 10 g/l NaCl (sterilized by filtration).
- Solution C: 20% (w/v) Glucose (sterilized by filtration through 0.2 μm filter).
- Suspension D (100x): 60 g/l H_3BO_3 ; 390 mg/l $\text{CuSO}_4 \times 5\text{H}_2\text{O}$; 13 mg/l KI; 60 mg/l $\text{MnSO}_4 \times \text{H}_2\text{O}$; 51 mg/l $(\text{NH}_4)_6\text{Mo}_7\text{O}_{24} \times 4\text{H}_2\text{O}$; 5.48 g/l $\text{ZnSO}_4 \times 7\text{H}_2\text{O}$; 932 mg/l $\text{FeCl}_3 \times 6 \text{H}_2\text{O}$; 2ml Chloroform (added for sterilization of the solution).
- Solution E: 1 g Yeast extract; 0.5 g Casein, hydrolyzed by enzymatic cleavage; 0.5 g Casein, hydrolyzed by acid degradation.

To prepare 1 l CM, 10 ml of solution A was added to 929 ml H_2O and was sterilized in the autoclave. For solid CM media, 16 g/l granulated agar was supplemented before autoclaving. Then 10 ml of the solution B, 50 ml of the solution C, 1 ml of the suspension D and the complete solution E were added. For selection of the transformants, 100-250 $\mu\text{g ml}^{-1}$ Hygromycin B or Geneticin were added to the solid medium, respectively.

MM medium:

- Solution B (100x): 20 g/l KH_2PO_4 ; 25 g/l $\text{MgSO}_4 \times 7\text{H}_2\text{O}$; 10 g/l NaCl (sterilized by filtration).
- Solution C: 20% (w/v) sucrose (sterilized by filtration through 0.2 μm filter).
- Suspension D (100x): 60 g/l H_3BO_3 ; 390 mg/l $\text{CuSO}_4 \times 5\text{H}_2\text{O}$; 13 mg/l KI; 60 mg/l $\text{MnSO}_4 \times \text{H}_2\text{O}$; 51 mg/l $(\text{NH}_4)_6\text{Mo}_7\text{O}_{24} \times 4\text{H}_2\text{O}$; 5.48 g/l $\text{ZnSO}_4 \times 7\text{H}_2\text{O}$; 932 mg/l $\text{FeCl}_3 \times 6 \text{H}_2\text{O}$; 2 ml Chloroform (added for sterilization of the solution).

To prepare 1 l MM medium, 10 ml of solution B, 50 ml of the solution C, and 1 ml of the suspension D were added to 939 ml sterilized H_2O .

YPD medium (Sambrook et al., 1989): 1% Yeast extract; 2% Pepton; 2% Dextrose. To prepare solid agar plate, 2% granulated agar was added before autoclaving.

SNA medium (Nirenberg, 1981): Components of 1 l SNA are as follows: 1 g KH_2PO_4 ; 1 g KNO_3 ; 0.5 g $\text{MgSO}_4 \times 7 \text{H}_2\text{O}$; 0.5 g KCl; 0.2 g Glucose; 0.2 g Saccharose; 1 l H_2O ; 16 g granulated agar (used for solid agar plate).

PDB and PDA media: Components of 1 l PDB are as follows: 4 g Potato; 20 g Dextrose; and add double-distilled water to 1 l. For PDA medium, 20 g granulated agar was added.

Carrot agar (Klittich C and Leslie, 1988): 400 g fresh carrots (cooked for 10 min in 400 ml double-distilled water), 20 g granulated agar and 500 ml double-distilled water. The medium was sterilized for 30 min at 121 °C in the autoclave.

2.2. Oligonucleotide primers

All oligonucleotide primers used in this study were designed by using PrimerSelect program (DNASTAR software, USA). PCRs were performed using non-proofreading Taq DNA Polymerase for the disruption of *FgOS-2*, *Fgatf1* and the TMRs (purchased from Fermentas or 5 prime) whose terminal transferase activity adds extra A nucleotides to the 3'-ends of PCR products. Therefore fusion primers were designed just after T to avoid mismatch mutations at the 3' ends of PCR products (Clark, 1988). PCRs were performed using proofreading Tag DNA Polymerase (Promega, Madison, WI, U.S.A.) for the *Fgatf1* overexpression and bimolecular fluorescence complementation constructs. All primers are listed in 5'-3'-direction, restriction enzyme recognition sites introduced to the primers are underlined. Lower letters are DNA overhang regions between hygromycin resistant cassette and flanking regions of target disrupted genes.

Table 1. Primers for generation of TMR gene replacement constructs: FGSG_05006, FGSG_02655, FGSG_03023, FGSG_07716, FGSG_01861, FGSG_05239 and FGSG_09693.

<i>FGSG_05006</i>	
No. (Fig. 10E)	Sequence (5'→ 3')
1	TCTGTTGGTGAAGTAATTCGT
2	agatccgaccgaacaagactgtcccccTGATGTGACGAGTAAACACC
3	caatgctacatcaccacctcgtccccc GTCAGGTTTGCATTGATAGG
4	CTCAAGCTGGTAGAGTACAC
5	GCGGCGCGCCCAAAGTTTCACCTTCCCTC
6	GCCTCGAGTGGACAAGATGGTAAGTTGG
7	GCTTCACTGGCATTATCGAG
8	ACCAGAGAATCAACCAAGCC
9	GTTGGCGACCTCGTATTGG
10	CTTACCACCTGCTCATCACCT
<i>FGSG_02655</i>	
No. (Fig. 10F)	Sequence (5'→ 3')
1	TCAGGAACGGAAAAAGAA

2 agatgccgaccgaacaagagctgtcccccCGGGAGCGAAGAAAGTA
3 caatgctacatcaccacctcgtcccccGACCTCGAATCAAAAAC
4 CTCTCGCACCAAGCACA
5 GCTCTAGACTAGCGGCCCAAAGAAC
6 GCTCTAGACCAGTGCGTGCGAGTGAG
7 GAGCCTGTCTTATCATGCTG
8 CTTGAGGGTTAATGTGCTCG
9 GTTGGCGACCTCGTATTGG
10 CTTACCACCTGCTCATCACCT

FGSG_03023

No. **Sequence (5'→3')**
(Fig. 10A)

1 TCAAGACAGAAACAAACATC
2 agatgccgaccgaacaagagctgtcccccACGCATCCATGGTCAAAGA
3 caatgctacatcaccacctcgtcccccGGGTTTTCTTTGTCTCG
4 CTGACCTAACTCAAGATATGCT
5 GCACCGGTAGAACCTGGATAAGTAGAGC
6 GCACCGTCGTTTTGTTTTATTATTGTGTAGT
7 CTTATTTGGGATCCAATCCACTG
8 ATTGGGATCGCTTTCATCCAG
9 GTTGGCGACCTCGTATTGG
10 CTTACCACCTGCTCATCACCT

FGSG_07716

No. **Sequence (5'→3')**
(Fig. 10B)

1 TCCTAACTAGTAATGATGCCTGTC
2 agatgccgaccgaacaagagctgtcccccGATTTTGACTTGCTCGTAT
3 caatgctacatcaccacctcgtcccccGCTTTCGGCCACATTTGA
4 TCGGCAGCATCGCAGAC
5 GCAAGCTTCCAGGATGATAAGCCAAAGGAC
6 GCICTAGACCAGTGGCAAAAAGTTCT
7 ATAGCCAGTATCTGCTTCATCC
8 AACCCTTGTAGAGGAAGTACTG

9	GTTGGCGACCTCGTATTGG
10	CTTACCACCTGCTCATCACCT

FGSG_01861

No. (Fig. 10C)	Sequence (5'→ 3')
-------------------	-------------------

1	AAGGGGCGGTTGGTCTGT
2	agatgccgaccgaacaagagctgtcccccAGAGAAGCGGTCGGTTTTA
3	caatgctacatcaccacctcgtcccccGACGTCITTTCTITTTGTIGTTT
4	GGGCTCAATTTCTCCAC
5	<u>GCCTCGAG</u> ATATGGGTGTCCTCCTCTTTCTTC
6	<u>GCCTCGAG</u> GGCAAGCCACCACAGAGATAC
7	AACATGATAGTCAATGTCGG
8	AACAGAATAGACACGGTTGG
9	GTTGGCGACCTCGTATTGG
10	CTTACCACCTGCTCATCACCT

FGSG_05239

No. (Fig. 10D)	Sequence (5'→ 3')
-------------------	-------------------

1	GCAATAATTAAATCGTTGGTGG
2	agatgccgaccgaacaagagctgtccccc AAAGCAAAGAGTGAACAAAGAC
3	caatgctacatcaccacctcgtccccc TATGCTGATGGGATATGTGAC
4	ACATGATGATACCGCTACAC
5	<u>GCGGCGCGCCG</u> TTTCTCATTTTCGTCTCGTC
6	<u>GCCTCGAGA</u> AAGCAAACAGGATCAGTCTC
7	GGATTCTGTTCCGTAAATGGTG
8	TCCCTCTCCAATGTTTCTATACCA
9	GTTGGCGACCTCGTATTGG
10	CTTACCACCTGCTCATCACCT

FGSG_09693

No. (Fig. 11)	Sequence (5'→ 3')
------------------	-------------------

1	TACAACACCCAAATAAAAAG
2	agatgccgaccgaacaagagctgtcccccTGATAGCCATGGCAAGAGACC
3	caatgctacatcaccacctcgtcccccCTGAGGATGCCGAGAAGT

4	TTGGAGCGCGGGTAAGT
5	GCTCTAGATGCCGCAGAAATACAGAGA
6	GCTCTAGACGAGGCCGACGATGTTCTTT
7	TGCTGGATTGGAACCGACTGGA
8	CCTTCCAGCTGGTTGTAAA
9	GTTGGCGACCTCGTATTGG
10	CTTACCACCTGCTCATCACCT

Table 2. Primers for generation of gene replacement construct of *FgOS-2* (FGSG_09612).

No. (Fig. 28)	Sequence (5'→ 3')
1	CGACACTAGACCGACCCAACA
2	agatgccgaccgaacaagagctgtcccccTGGTTGTTGAGCGAGAAGTTTGAG
3	caatgctacatcaccacctcgtcccccATGGACAATAGAAGGGAGAAGTGG
4	TTCGCATGGCCAAAGACAG
5	GCTCTAGAAAAAGTCAACAAAACAACAAACAA
6	GCTCTAGAAAAAGCATATGTAACCTGGGAACC
7	CAACCAAAAATGTCGCCGTCAAG
8	TGTAGGGTCATGGTAGGGAGAAAAG
9	GTTGGCGACCTCGTATTGG
10	CTTACCACCTGCTCATCACCT

Table 3. Primers for generation of gene replacement construct of *Fgatfl* (FGSG_10142), *Fgatfl* overexpression, and bifluorescence complementation experiments.

No. (Fig. 49 and 50)	Sequence (5'→ 3')
1	GTTCTATGGCTCTTCTGTTTTTCA
2	agatgccgaccgaacaagagctgtcccccGCAGAGGCITTCAGTTGTAGTC
3	caatgctacatcaccacctcgtcccccTGTCCAACCAGCAAGTCAT
4	GATGGAGGATTGTGGTTCCG
5	GCTCTAGACTCGCTGCCACAACGTCATCTCT
6	GCTCTAGATCAACAGCAGCGGGAACAAAT
7	ACATCACCATCTTCACTACTACCC

8	GCCACTGCTTCTTCCTTTGA
9	GTTGGCGACCTCGTATTGG
10	CTTACCACCTGCTCATCACCT
11	GCGAGCTCATGGGGACTACAACTGAAGC
12	GCTCTAGACTATGAGAATCGCCTCTGGACAC
13	<u>CCatggccgagttgtacgcgcc</u>
14	<u>GCGGCCGctattgtcattaaactgctct</u>
15	<u>CCatggggactacaactgaagcctc</u>
16	<u>GCGGCCGctatgagaatcgctctgg</u>

Table 4. Primers for semi-quantitative RT-PCR

Name	Sequence (5'→ 3')	Description
β-TubF	TGCTGTTCTGGTCGATCTTG	Forward primer β-tubulin (FGSG_06611)
β-TubR	ATGAAGAAGTGAAGTCGGGG	Reverse primer β-tubulin
NOXAF	AGGTGCTGGTTTAGTTCTC	Forward primer <i>noxA</i> (FGSG_00739)
NOXAR	ATGAAGTGATGGTAAAGGGATGC	Reverse primer <i>noxA</i>
NOXBF	GCCTGACGTGCTCCCTTTTG	Forward primer <i>noxB</i> (FGSG_10807)
NOXBR	GCGAGAAGAAGCGAACGGAACC	Reverse primer <i>noxB</i>
NOXCF	ACGGACCTGAGATTGTGTTT	Forward primer <i>noxC</i> (FGSG_11195)
NOXCR	GGAATCCGAGACCAACAC	Reverse primer <i>noxC</i>
NOXRF	AGCTCTCGCCAACTTCAA	Forward primer <i>noxR</i> (FGSG_04123)
NOXRR	CAGCGGCGTGCGAGTAGTC	Reverse primer <i>noxR</i>
Opsin1F	CGTCTTCTACTTCCTGTCCACCTT	Forward primer <i>Opsin1</i> (FGSG_07554)
Opsin1R	GCAAAGCTCGACAACCAGAA	Reverse primer <i>Opsin1</i>
Opsin2F	ATCTTCCACTACCTCTTCACCATT	Forward primer <i>Opsin2</i> (FGSG_01440)
Opsin2R	CCGAAGGCGAAGAAACC	Reverse primer <i>Opsin2</i>
Opsin3F	TTCATTACCACCCCTCTACTTCTT	Forward primer <i>Opsin3</i> (FGSG_03064)
Opsin3R	CAGGCAATTGGGTAGAGGAT	Reverse primer <i>Opsin3</i>
Vvd1F	ACTGCTCTGTGCCCCTTGTCTG	Forward primer <i>Vvd1</i> (FGSG_08456)
Vvd1R	GATGGTCAGGAGGTTGTTG	Reverse primer <i>Vvd1</i>
FrqF	ACAAACCCTACTACAATCAACTCG	Forward primer <i>Frq</i> (FGSG_06454)

FrqR	CGACGACGTATTGGGAGAT	Reverse primer <i>Frq</i>
------	---------------------	---------------------------

Table 5. Primers for quantitative RT-PCR

Name	Sequence (5'→3')	Description
β-TubqF	TGTCGACGACCAGTTCTCAGC	Forward primer β-tubulin
β-TubqR	CGATGTCGGCGTCTTGGTAT	Reverse primer β-tubulin
CAT1F	GGAAAGCCAGAACCAAACAA	Forward primer <i>cat1</i> (FGSG_06554)
CAT1R	CGTTGACGAGAGTGTAGGTGTTGA	Reverse primer <i>cat1</i>
CAT2.1F	GCTTGGGCTTCTGCTTCTACTTTC	Forward primer <i>cat2.1</i> (FGSG_02974)
CAT2.1R	GCCTTGCCGTTGGACTGA	Reverse primer <i>cat2.1</i>
CAT2.2F	ATCTTATTGTTCTCGGCGGTGTTG	Forward primer <i>cat2.2</i> (FGSG_12369)
CAT2.2R	CGAGCAGTCCCGTGTCCATAGTT	Reverse primer <i>cat2.2</i>
CAT3F	TCAACCGTCCCTCTGTCTCCTATCC	Forward primer <i>cat3</i> (FGSG_06733)
CAT3R	AGCCTTTTCCCTTGTGTCTGGTT	Reverse primer <i>cat3</i>
TF1F	CAAAGATGACCGACGAAGAGAAGC	Forward primer <i>atf1</i> (FGSG_10142)
TF1R	CGAGAAGGAGGGTTTTGAGGTTGA	Reverse primer <i>atf1</i>
NOXCF	CACACGTAACAGCCAAACAGAAG	Forward primer <i>noxC</i> (FGSG_11195)
NOXCR	TCITTATTTCTTGTACTTGTCCCTC	Reverse primer <i>noxC</i>
GIP1F	CCGGAGTTGGAGAGTGGA	Forward primer <i>gip1</i> (FGSG_02338)
GIP1R	TCAAACCACGGATCAAAGTCT	Reverse primer <i>gip1</i>
GIP2F	GCTGCGCATCTTATCCTG	Forward primer <i>gip2</i> (FGSG_02320)
GIP2R	GGCTCACTTCCGTCTTGT	Reverse primer <i>gip2</i>
PKS12F	CAGACTACGCCAATGACTAC	Forward primer <i>pks12</i> (FGSG_02324)
PKS12R	GTCTCCATAAACACCAACCACA	Reverse primer <i>pks12</i>
TRI4F	GAAGCGAACCATCACCAACC	Forward primer <i>tri4</i> (FGSG_03535)
TRI4R	AAGGCACAAAAAGCACCATCAA	Reverse primer <i>tri4</i>
TRI5F	TTTTTGAGGGATGCTGGATTGA	Forward primer <i>tri5</i> (FGSG_03537)
TRI5R	GCCATAGAGAAGCCCCAACAC	Reverse primer <i>tri5</i>
TRI6F	GGCATTACCGGCAACACTTCA	Forward primer <i>tri6</i> (FGSG_16251)

TRI6R	CATTGTTGTCCTTCCTTGTCTT	Reverse primer <i>tri6</i>
TRI10F	ATATGGTGCGAGCTGGATGAA	Forward primer <i>tri10</i> (FGSG_03538)
TRI10R	CTGCGGCGAGTGAGTTTGA	Reverse primer <i>tri10</i>
ZEB2F	TGAGGACCCCAACGAGAG	Forward primer <i>zeb2</i> (FGSG_02398)
ZEB2R	ATTCGACGTTTGGCATTGG	Reverse primer <i>zeb2</i>
ZEB1F	CTCTCGCTGCTCTGGGTCTC	Forward primer <i>zeb1</i> (FGSG_17459)
ZEB1R	GTAGCAAACGTCCACCAAATA	Reverse primer <i>zeb1</i>
PKS13F	GGCAACTCTTCTTCCATCAC	Forward primer <i>zea1</i> (FGSG_15980)
PKS13R	GGCTGGATCACCGACTTTT	Reverse primer <i>zea1</i>
G3PPF	AAACCCGACCCCGCCTGCTAT	Forward primer <i>g3pp</i> (FGSG_07096)
G3PPR	GTCTCGAACAACCCAATCT	Reverse primer <i>g3pp</i>

2.3. Vector construction

2.3.1. Vector construction for deletion of *FgOS-2*, *Fgatf1* and the TMRs

Standard recombinant DNA methods were performed according to Ausubel et al. (2002) and Sambrook et al. (1989). Double homologous recombination constructs were generated for the disruption of *FgOS-2*, *Fgatf1* and the different TMRs in the *F. graminearum* strain PH1 (Fig. 9). For disruption construct of *FgOS-2*, *Fgatf1*, and the TMRs, 5'- and the 3'-flanking regions (from 0.5-1 kb upstream and downstream fragments) were cloned by PCR from genomic DNA (gDNA) using the primers listed in Table 1, Table 2 and Table 3. The PCR was initiated by denaturation at 94 °C for 4 min, followed by 35 cycles of 94 °C for 45 s, 55 °C for 45 s and 72 °C for 60 s. The PCR included a final extension step at 72 °C for 10 min and a cooling step at 4 °C. The replacement vector was constructed using fusion PCR. The PCR amplification was performed using the following parameters: initial denaturation at 94 °C for 4 min, followed by 20 cycles of 94 °C for 45 s, 58 °C for 2 min, 72 °C for 4 min and a final extension step at 72 °C for 10 min. The upstream and downstream fragment (200 ng each), together with the HYG cassette (hygromycin cassette; 1.8 kb) released from the pGEM-HYG vector (Dr A. Löscher, University of Hamburg, Germany) by digestion (400 ng), were used in a 25 µl PCR reaction without the addition of primers as the fragments acted as primers and templates for the elongation. The PCR product was ligated into the pGEM-T vector (Promega, Madison, WI) to generate pGEM-FgOS-2-HYG, pGEM-Fgatf1-HYG and pGEM-TMR-HYG); this was then transformed into XL1-blue *Escherichia coli*-competent cells (DNA Cloning

Services, Biozentrum Klein Flottbek, Hamburg, Germany). Bacteria were cultivated in sterile Luria Bertani (LB) medium (Sambrook et al., 1989) either as a liquid culture or on agar plates. Vector p99II::dsRed was used for the generation of dsRed-fluorescent strains (Ilgen et al., 2009). This vector facilitates the constitutive expression of dsRed under the control of the *gpdA*-promoter of *A. nidulans* and confers geneticin resistance.

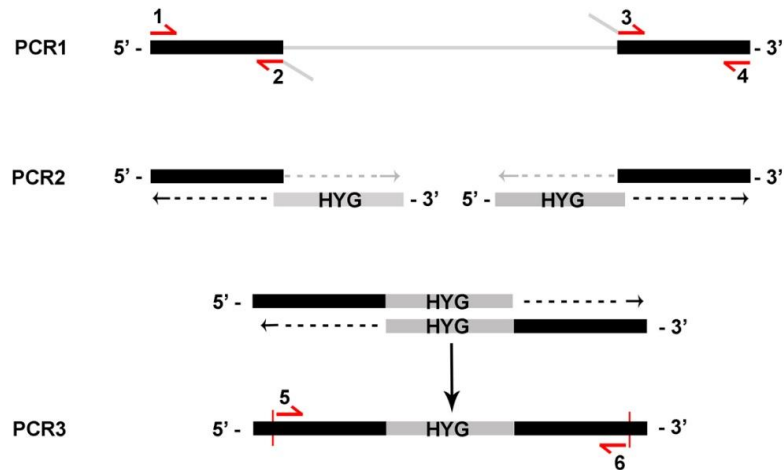


Figure 9. Gene replacement strategy using double homologous recombination method. PCR1: 5'- and the 3'-flanking regions of a target gene are amplified using primer pair 1 and 2. PCR2: Two flanking fragments amplified from PCR1 are fused with the *HYG* fragment in one PCR reaction. In the first PCR cycles, each flanking fragment is fused with the *HYG* fragment, which results in up-*HYG* and *HYG*-do fragments. In the following PCR cycles, the *HYG* fragments anneal and the entire fragment is elongated. PCR3: specific amplification of the disruption constructs by the use of nested primers 5 and 6.

2.3.2. Vector construction for *Fgatf1* overexpression

For constitutive expression of *Fgatf1* controlled by the *gpdA* from *Cochliobolus heterostrophus*, the open reading frame (ORF) of *Fgatf1* was amplified by PCR from gDNA using the *Pfu* proofreading polymerase (Promega, Madison, WI, U.S.A.) primers 11 and 12 (Table 3). The PCR product was ligated into pJET1.2 vector (Fermentas, St. Leon-Rot, Germany) and sequenced. The ORF (1898 bp) was excised from pJET1.2 by restriction enzyme *SacI* and *XbaI* and cloned into pII99 vector, which contains the *gpdA* promoter from *C. heterostrophus*, and a geneticin-resistance cassette. The resulting plasmid, GPD-*Fgatf1*-pII99, was linearized at the unique *ApaI* restriction site which cuts the *Fgatf1* sequence at position 1050 to facilitate single crossover events. The linearized construct was used for fungal transformation (Fig. 50).

2.3.3. Bimolecular fluorescence complementation experiments

For bimolecular fluorescence complementation experiments (BiFC), *FgOS-2* and *Fgatf1* were tagged with separated halves of the yellow fluorescent protein (Hoff and Kück, 2005). To fuse

the N-terminal half of YFP to *FgOS-2*, a 1074 bp *FgOS-2* PCR product was amplified using primers 13 (which introduces an *NcoI* restriction site before the starting ATG) and 14 (which introduces a *NoI* restriction site after the stop codon) (Table 3). To fuse the C-terminal part of YFP to *Fgatf1*, primers 15 (which introduces an *NcoI* restriction site before the starting ATG) and 16 (which introduces a *NoI* restriction site after the stop codon) were used to generate a 1581 bp PCR product (Table 3). Both products were cloned into pJET1.2 plasmids and subsequently released by restriction using enzymes *NcoI* and *NoI*. The fragments were ligated into the vectors YFP-N and YFP-C (Hoff and Kück, 2005) to generate plasmid YFP-N::*FgOS-2* and YFP-C::*Fgatf1*, respectively. Both plasmids were linearized by *EcoRI* (YFP-N::*FgOS-2*) and *XmnI* (YFP-C::*Fgatf1*) and afterward co-transformed into *F. graminearum*.

2.4. Transformation of *F. graminearum*

For the fungal transformation, pGEM-*FgOS-2*-HYG, pGEM-*Fgatf1*-HYG, GPD-*Fgatf1*-pII99 and each pGEM-T vector containing one TMR-knock-out construct were digested with appropriate restriction enzyme underlined in the primers number 5 and 6 of each construct or in Fig. 50 for *Fgatf1* overexpression construct, and BiFC-plasmids were linearized using restriction enzymes *EcoRI* (YFP-N::*FgOS-2*) and *XmnI* (YFP-C::*Fgatf1*), respectively, to release the constructs. A solution of 30-50 μ l containing 10-30 μ g DNA of each construct was used for the transformation. The protoplast transformation method was performed as previously described (Proctor et al., 1995; Jansen et al., 2005), where 100 ml of YEPD medium (0.3% yeast extract, 1% bacto peptone, 2% D-glucose) was inoculated with 1×10^6 conidia and incubated overnight at 28 °C, 150 rpm. The mycelia were collected by filtering with a 200 μ m-diameter sieve and washed by rinsing three times with double-distilled water. Then, 0.5-2 g of mycelia were resuspended in a 20 ml mixture of driselase and lysing enzymes (Invitrogen; 2.5% : 0.5% in 1.2 M KCl or 0.6 M for the retransformation of $\Delta FgOS-2$ mutant for the dsRed tag) and digested for 2-3 h at 30 °C, 80 rpm. Undigested hyphal material was removed from the protoplast suspension by subsequent filtration, first through a 100 μ m Wilson sieve and then through a 40 μ m Wilson sieve or three layers of cheesecloth. The protoplasts were pelleted at room temperature by centrifugation for 10 min at 2000 rpm, washed once with 10 ml STC (20% sucrose, 10 mM Tris-HCl, pH 8.0, 50 mM CaCl₂), centrifuged again and then resuspended and adjusted in STC at 1×10^8 protoplasts per ml. For transformation, 200 μ l of the protoplast suspension was supplemented with the DNA. The samples were mixed and incubated at room temperature for 20 min. Following this, 1 ml PEG (40% polyethylene glycol 4000, 60% STC) was added and incubated at room temperature for 20 min. The protoplast suspension was added to 5 ml TB3 medium (100 g sucrose, 0.3% yeast extract,

0.3% casamino acids) and shaken overnight at room temperature and 100 rpm for cell wall regeneration. After 12-24 h, the regenerated protoplasts were collected by centrifugation at 5000 rpm for 10 min at room temperature and 5 ml of TB3 was removed. The regenerated protoplasts were mixed in 1.5% TB3 agar at 50 °C containing hygromycin B (250 µg ml⁻¹) for *FgOS-2*, *Fgatf1*, all TMR deletion mutants, and the BiFC constructs or geneticin (100 µg ml⁻¹) for *Fgatf1* overexpression and plated out in 92 mm petridishes (10 ml/plate). After 12-24 h, the plates were overlaid with the same amount of 1.5% TB3 agar and double the amount of hygromycin B or geneticin as used the day before. Putative transformants were obtained after 2 days post-transformation. They were transferred to fresh plates of CM medium supplemented with 250 µg ml⁻¹ hygromycin B or 100 µg ml⁻¹ geneticin and incubated at 28 °C. The transformants were purified by single-spore isolation and subsequently checked by diagnostic PCR.

2.5. Southern blot analysis

For southern hybridization analysis, approximately 3 µg of genomic DNA of the wild type, $\Delta FgOS-2$, *Fgatf1* mutants and all TMR deletion mutant strains was isolated and restricted with appropriate restriction enzymes overnight. The digested DNA was then separated on 0.8% agarose gel by electrophoresis at 70 V for 6-7 h. Then, the DNA was transferred by capillary blotting onto a Hybond NX membrane (Amersham Biosciences, Little Chalfont, UK) and then hybridized with a DIG (digoxigenin)-labelled (Roche, Germany) DNA internal probe, which was specifically amplified by PCR (primers number: 7 and 8 of each construct and Table 1, Table 2 and Table 3). Detection and visualization procedures were carried out following the manufacturer's manual (Roche, Germany). In order to confirm single copy integration of the hygromycin cassette, re-hybridization with a hygromycin probe was performed.

2.6. Virulence assays on wheat, maize, and *Brachypodium distachyon*

The susceptible spring wheat cultivar Nandu (Lochow-Petkus, Bergen-Wohlde, Germany) and the partially resistant wheat cultivar Amaretto (Berthold Bauer, Niedertraubling, Germany) were used for wheat virulence assay. Plants were cultivated in a growth room at 20 °C, with a photoperiod of 16 h and 60% relative humidity, and then transferred to infection chambers with optimized conditions. A suspension of 500 conidia (10 µl) of the wild type and all independent mutants was inoculated into each of two central spikelets at the early stages of anthesis (Jenczmionka and Schäfer, 2005). The inoculated spikes were enclosed in small plastic

bags misted with water for the first 3 days and then they were monitored for up to three weeks in the infection chambers. Wheat spikes inoculated with 10 μ l pure water were used as the negative control. The wheat infection assay was performed using the wild type PH1, three independent $\Delta FgOS-2$, the *Fgatf1* mutants and two independent deletion strains of each TMR. All infections were repeated with thirty replicates for $\Delta FgOS-2$ mutants or *Fgatf1* mutants and twenty replicates for each TMR deletion strain. For maize infections, the maize inbred line A188 (Green and Phillips, 1975) was grown in the greenhouse (temperature: 26 °C-30 °C, humidity: 70%-85%, natural daily photoperiod with additional artificial light when required). Before inoculation, the silks were manually pollinated to ensure optimal pollination. Each maize cob was inoculated by injecting conidia suspensions into the silk channel of primary ears using a syringe and cannula (Reid et al., 1995). The infection procedure was performed with 4 ml of conidial suspension at a concentration of 2×10^4 conidia per ml of all strains that were used for wheat infection. Maize cobs inoculated with 4 ml of pure water were used for the negative control. The inoculated cobs were enclosed in plastic bags for the first 3 days and the inoculation lasted for 5 weeks.

Brachypodium distachyon (*B. distachyon*) was cultivated in a growth room at 22 °C, with a 20 hours photoperiod and then transferred to infection chambers at 22 °C, 65% humidity, and a photoperiod of 8 h. A suspension of 50 conidia (1 μ l) was inoculated into the central spikelet of each spike at the early stages of anthesis. The inoculated spikes were enclosed in small plastic bags for the first 2 days and then they were monitored for up to two weeks in the infection chambers.

2.7. Deoxynivalenol (DON) and zearalenone (ZEA) production analysis

For *in vitro* DON production measurement, 5×10^3 conidia of the wild type strain PH1, and the gene disruption mutants or overexpression mutant strains were pre-cultured in yeast-peptone-dextrose medium (YPD) for 3 days. The mycelia were collected by filtering with a 200 μ m diameter sieve, washed by rinsing at least three times with double-distilled water and then dried on sterile Whatman paper. Then, 1 g of semi-dried mycelia was further incubated for 24 and 72 h in minimal medium supplemented with 5 mM $(\text{NH}_4)_2\text{SO}_4$ for DON induction. 50 μ l of each supernatant was taken for DON measurement using a highly sensitive DON ELISA technique (RIDAscreen DON kits, R-Biopharm AG, Germany). For the *in planta* analysis, four wheat spikes were each inoculated with the wild type, $\Delta FgOS-2$, *Fgatf1* mutants and all TMR-deletion strains, respectively. The spikes were inoculated with pure water as the negative control. The inoculated samples were collected after 3 or 7 days post-inoculation (dpi) and 200

mg of the infected spikelets were dried in a vacuum and ground to a powder under liquid nitrogen. Then, 50 mg of ground material was suspended in 500 μ l of double-distilled water. The extract was manually mixed by hand or vortex and centrifuged. 50 μ l of the supernatant was used for the DON quantification assay. The production of DON on the wheat kernels was analysed as follows: 15 g of kernels and 10 ml water were autoclaved in a 300 ml Erlenmeyer flask. Autoclaved kernels were inoculated with 2×10^4 conidia of the wild type and $\Delta FgOS-2$ mutants. Water-inoculated samples served as the negative control. The samples were incubated out at 28 °C in the dark for 7 days. After 7 days, the inoculated wheat kernels were treated as described earlier for the *in planta* DON assay. The production of DON was measured like mentioned above. All measurements were subsequently normalized to the amount of mycelium in the sample using quantitative PCR, as previously described (Voigt et al., 2007). The sample preparation procedure for the *in planta* and *in vitro* ZEA measurements was similar to that for DON measurements, except that YES medium (2% yeast extract, 1.5% sucrose, 0.05% $MgSO_4 \times 7H_2O$, 1 ml trace metal solution; 885 ml Milli Q water; pH 6.5) was used for *in vitro* zearalenone induction. Quantification was performed according to the manual contained in the RIDAScreen zearalenone kit (R-Biopharm AG, Germany).

2.8. Reactive oxygen species (ROS) and catalase activity measurements

The production of ROS was determined via two independent methods. First, O_2^- production in whole fungal colonies was detected by staining with nitro blue tetrazolium (NBT) (Sigma, Germany). The wild type, $\Delta FgOS-2$ and all *Fgatf1* mutant strains were cultured on CM agar plates, which were supplemented with 0.2 M or 0.8M NaCl at 28 °C in the dark for 3 days. Then, each plate was stained with 20 ml 0.2% (w/v) NBT solution (NBT diluted in water) and incubated in the dark at 28 °C for 30-45 min. The supernatant was drained and the plates were washed with 99% ethanol. The plates were re-incubated for 30-45 min in the dark at 28 °C before images of whole colonies were taken.

The production of ROS of the wild type and $\Delta FgOS-2$ mutants was also measured using a sensitive ELISA-based assay. In order to detect the release of H_2O_2 , 40 mg of semi-dried mycelia was incubated in a reaction mixture (50 μ M Amplex red reagent and 0.1 U/ml HRP in Krebs-Ringer phosphate buffer (KRPB) consisting of 145 mM NaCl, 5.7 mM sodium phosphate, 4.86 mM KCl, 0.54 mM $CaCl_2$, 1.22 mM $MgSO_4$, 5.5 mM glucose, pH 7.35). In order to detect the release of H_2O_2 in the osmotic medium, KRPB was supplemented with 0.2 M NaCl. The *in vitro* levels of H_2O_2 were measured using the Amplex red peroxide/peroxidase assay kit (Life Technologies, Germany), according to the manufacturer's instructions.

Extinction at 530-560 nm was measured using the Fluoroskan II fluorescence 96-well microplate reader (Synergy HT, Biotek, Germany).

For catalase activity staining, protein extractions from ground mycelia of the wild type and $\Delta FgOS-2$ mutants were performed using potassium phosphate buffer (KP buffer). Catalase activity staining was performed after native isoelectric focusing (IEF) of the protein extracts following the protocol (Robertson et al., 1987): 7 ml water, 2 ml acrylamide mixture (30% (w/v) acrylamide, 1% (w/v) bis-acrylamide), 2.4 ml 50% (v/v) glycerol and 0.6 ml ampholyte (pH range 3-10). The components were mixed and degassed. Then, 50 μ l of 10% (w/v) ammonium persulphate and 20 μ l TEMED were added. The cathode solution was 25 mM NaOH and the anode solution was 20 mM acetic acid. Up to 100 μ g of each sample was loaded and electrophoresed for 2 h at 100 V, 10 to 13 h at 200 V and 2 h at 500 V. The gels were stained for catalase activity using diaminobenzidine (DAB) as follows (Clare et al., 1984): each gel was incubated in horseradish peroxidase (50 μ g ml⁻¹) in phosphate buffer (50 mM potassium phosphate, pH 7.0) for 45 min. Then, H₂O₂ was added at a concentration of 5.0 mM and the mixture was incubated for a further 10 min. The gel was rinsed twice with water and placed in 0.5 mg ml⁻¹ of diaminobenzidine (in phosphate buffer) until the staining became visible.

For the catalase activity measurement, the wild type, the $\Delta FgOS-2$, and the $\Delta Fgatf1$ strains were cultured in CM with and without 2 h-induction by 0.8 M NaCl, and 10 mM H₂O₂ in a rotary shaker operating at 145 rpm at 28 °C. After 2 hours exposure, mycelia were harvested and ground with liquid nitrogen, and then mixed with extraction buffer (150 mM KCl, 200 mM EDTA, and 50 mM K₂PO₄, pH 7.4). The resulting homogenate was centrifuged at 13,000 rpm, for 20 min at 4 °C, and the supernatant was used for enzyme assay. Total catalase activity was measured using the Amplex red catalase assay kit (Life Technologies, Germany) according to manufacturer's instructions. Catalase activity was normalized to the amount of total protein content determined by Bradford Reagent (Sigma, Germany).

2.9. Detection of extracellular lipolytic activity

In order to measure the lipolytic activity of the wild type and TMR deletion strains, an *F.graminearum* pre-culture was started with 10⁶ conidia in 50 ml YPD and incubated for 3 days at 28 °C and 150 rpm. The mycelia were collected by filtering with 200 μ m diameter sieve and were washed three times with double-distilled water. Subsequently approximately 1.5 g of semi-dried washed mycelia was transferred into flasks containing 50 ml water supplemented with 2% (v/v) wheat germ oil for lipase induction. Lipase induction was carried out for 24

hours at 28 °C and 150 rpm. Samples were taken as indicated in the figure legends. Lipolytic activity of the supernatants of the sample was measured with a lipase assay using para-nitrophenyl palmitate (pNPP, Sigma, St. Louis, MO, USA) as substrate (Winkler and Stuckmann, 1979). A volume of 100 µl of the supernatant was mixed with 900 µl of the reaction solution (2 mM pNPP, 0.1% (w/v) Gum Arabic, 0.1% (v/v) Triton X-100, 50 mM bis-tris-propan HCl pH 8.0) in 1 ml cuvettes and was incubated for 60 min at 37 °C. The para-nitrophenol (pNP) amount was photometrically determined at 410 nm. Under the conditions used, one unit (U) of lipolytic activity was defined as the amount of enzyme that liberated 1 µmol of p-nitrophenol from p-nitrophenyl palmitate per minute. The relative lipolytic activity was calculated following the differences of OD₄₁₀ values between samples and control. All measurements were repeated twice with two replicates.

2.10. cAMP level measurement

Tissues used for steady-state intracellular cAMP levels measurement of the wild type and two independent *FGSG_05006* deletion strains were obtained from liquid minimal-glycerol cultures incubated at 28 °C and 150 rpm for 3 days. Mycelia were lyophilized overnight and ground in liquid nitrogen. 6 mg of ground mycelia was suspended in 200 µl lysis buffer 1B (0.25% solution of Dodecyltrimethylammonium Bromide in assay buffer; supplied with the kit) and incubated on shaker for 15 min at room temperature. The resulting homogenate was centrifuged for 10 min at 13.000 rpm. Then, supernatant was diluted with lysis buffer 1B with ratio: 1:5, 1:10, 1:50 and 1:100 for the assay. 100 µl of diluted supernatant was used for the cAMP quantification assay using the Amersham™ cAMP Enzymeimmunoassay (EIA) kits (GE healthcare-UK) following non-acetylated assay protocol. The assay was performed using two biological and three technical replicates each.

2.11. DAPI-nuclei staining, BiFC assays and microscopy

To stain the nuclei, the wild type and $\Delta FgOS-2$ strains were pre-cultured in a liquid PD medium and a PD medium supplemented with 0.8 M NaCl for 16 h and then centrifuged for 15 min at 13.000 rpm. The pellets were rinsed and diluted again with double-distilled water prior to staining. Samples were placed on glass slides and stained with 1 µg ml⁻¹ DAPI for 10 min before being analysed under a Zeiss microscope Axio Imager Z1 (Carl Zeiss, Germany) equipped with filter sets for excitation at 538 to 562 nm and emission wavelength detection from 570 to 640 nm.

For BiFC assays, conidia of the wild type and BiFC strains were pre-cultured in liquid CM for 16 h and then centrifuged and washed with double-distilled water to remove liquid CM medium. Mycelia were treated with 1.2 M NaCl and examined by confocal laser scanning microscopy with filter sets for excitation at 514 nm (YFP) and 594 nm (dsRed), emission wavelength detection from 519-573 nm (YFP) and 588-740 nm (dsRed). Untreated samples served as the negative control.

2.12. Expression analysis by semi-quantitative and quantitative real-time PCR

In order to study the expression of possible targets of FgOS-2 and Fgatf1 in *F. graminearum* *in vitro* and *in planta*, RNA was isolated using a Nucleospin RNA II Kit (Macherey-Nagel, Germany). Samples were collected from *in vitro* submersed cultures and from wheat spikes at 3 and 7 dpi, respectively, and frozen in liquid nitrogen for subsequent RNA isolation. For RT-PCR, SuperScript II RNase H Reverse Transcriptase (Invitrogen, Germany) was used, according to the manufacturer's instructions. The resulting single-stranded cDNA was later used as a template for quantitative real-time PCR (qRT-PCR) reactions. Transcript levels of the target genes were normalized against β -tubulin gene expression. The qRT-PCR reactions were carried out using gene-specific primers (Table 5), with SYBR Green qPCR SuperMix-UDG (Fermentas, Germany) in a volume of 20 μ l in a light Cycler 480 (Roche, Germany). The PCR program was as follows: incubation for 2 min at 50 °C, then 2 min at 95 °C, followed by up to 40 cycles of denaturation at 94 °C for 30 s, annealing at 55-58 °C for 30 s and extension at 72 °C for 15 s, followed by a melting curve analysis in order to check the specificity of fragment amplification. All of the measurements were repeated twice, each with three replicates and using at least two independent deletion strains and the wild type. Relative changes in gene expression were calculated using the comparative C_p method (using LC 480 software for the light Cycler 480).

To study the expression of NOX genes and genes involved in the perception and transduction of light signals (Opsins, Vvd1, and Frq), semi-quantitative RT-PCR using cDNA obtained from *in planta* or *in vitro* under different conditions were carried out. The PCR reactions were conducted with specific primers (Table 4). The PCR was initiated by denaturation at 94 °C for 4 min, followed by 25 or 30 cycles of 94 °C for 30 s, 58 °C for 30 s and 72 °C for 30 s. The final elongation step was performed at 72°C for 10 min. The level of constitutively expressed β -tubulin mRNA served as reference (β -TubF, β -TubR primers at Table 4 for semi-quantitative RT-PCR and Table 5 for quantitative RT-PCR).

3. Results

3.1. The role of transmembrane receptors in *Fusarium graminearum*

3.1.1. Identification of transmembrane receptors from *F. graminearum*

Transmembrane receptors (TMRs) perceive external signals and communicate them to intracellular signaling cascades such as MAP kinase pathway. Consequently, the cells respond to external stimuli by changing the expression of downstream target effectors. In this section, I present data on functional characterization of seven TMRs in *F. graminearum* in order to understand their functions as well as related signaling cascades.

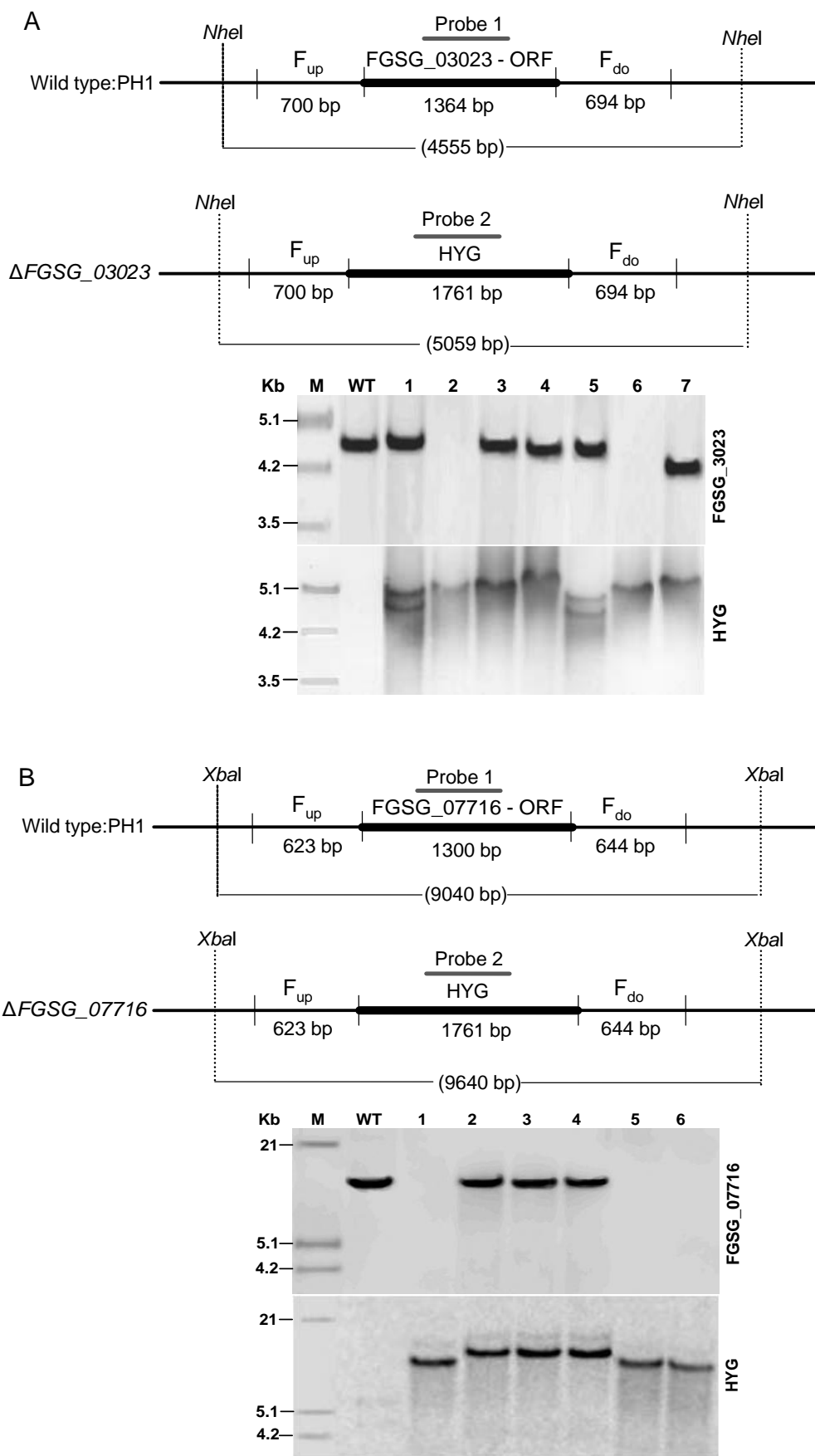
The pheromone receptor *pre2* (FGSG_02655) was shown to be important for sexual reproduction. Deletion of *pre2* and of the corresponding pheromone precursor gene *ppg1* in *F. graminearum* leads to a reduced perithecia maturation rate and ascospore formation (Lee et al., 2008). In contrast, Kim and co-workers (2008) found out that *pre2* is not essential for the sexual development in *F. graminearum*. Sometimes, Deletion of *pre2* leads to an increased numbers of immature perithecia (Kim et al., 2008). In order to confirm the roles of *pre2* in sexual reproduction and find out further functions of *pre2*, this TMR was chosen for functional characterization. The sequence of this TMR was sought in MIPS *F. graminearum* Genome Database with its number. FGSG_02655 contains 386 amino acids (aa) and six transmembrane domains. Plant cell walls are composed predominantly of carbon sources and these might be important growth substrates for fungal plant pathogens (Gilbert, 2010). Recent studies have revealed molecular mechanism that how fungi sense nutrients including nitrogen and carbon sources such as glucose, mannitol and amino acids. In *S. cerevisiae* and *C. albicans*, GPCR carbon receptors senses glucose, sucrose and methionine and activates cAMP signaling through Gpa2 (Lemaire et al., 2004; Maidan et al., 2005). In *N. crassa*, carbon sensor Gpr-4 associates with G_α subunit GNA-1 in cAMP/PKA signaling pathway. They play an important role in poor carbon source utilization and a normal cAMP signal upon addition of glucose. The functions of carbon sensor in *F. graminearum* are not known so far. Therefore, carbon sensor was chosen for functional characterization. The putative carbon sensor sequence from *F. graminearum* was identified using *N. crassa* Gpr-4 genomic sequence as query for a BlastX search against MIPS *F. graminearum* Genome Database. The putative carbon sensor in *F. graminearum* is FGSG_05006 containing 576 aa and five transmembrane domains. Disruption of GPCR *gpr1* (a cAMP receptor-like GPCR) in *N. crassa* causes deficiency in perithecial development and ascospore discharge. Perithecia are frequently ruptured and generally did not reach maturity (Krystofova and Borkovich, 2006). Using a BlastX search against MIPS *F. graminearum* Genome Database with *N. crassa* Gpr1 genomic sequence as query, five

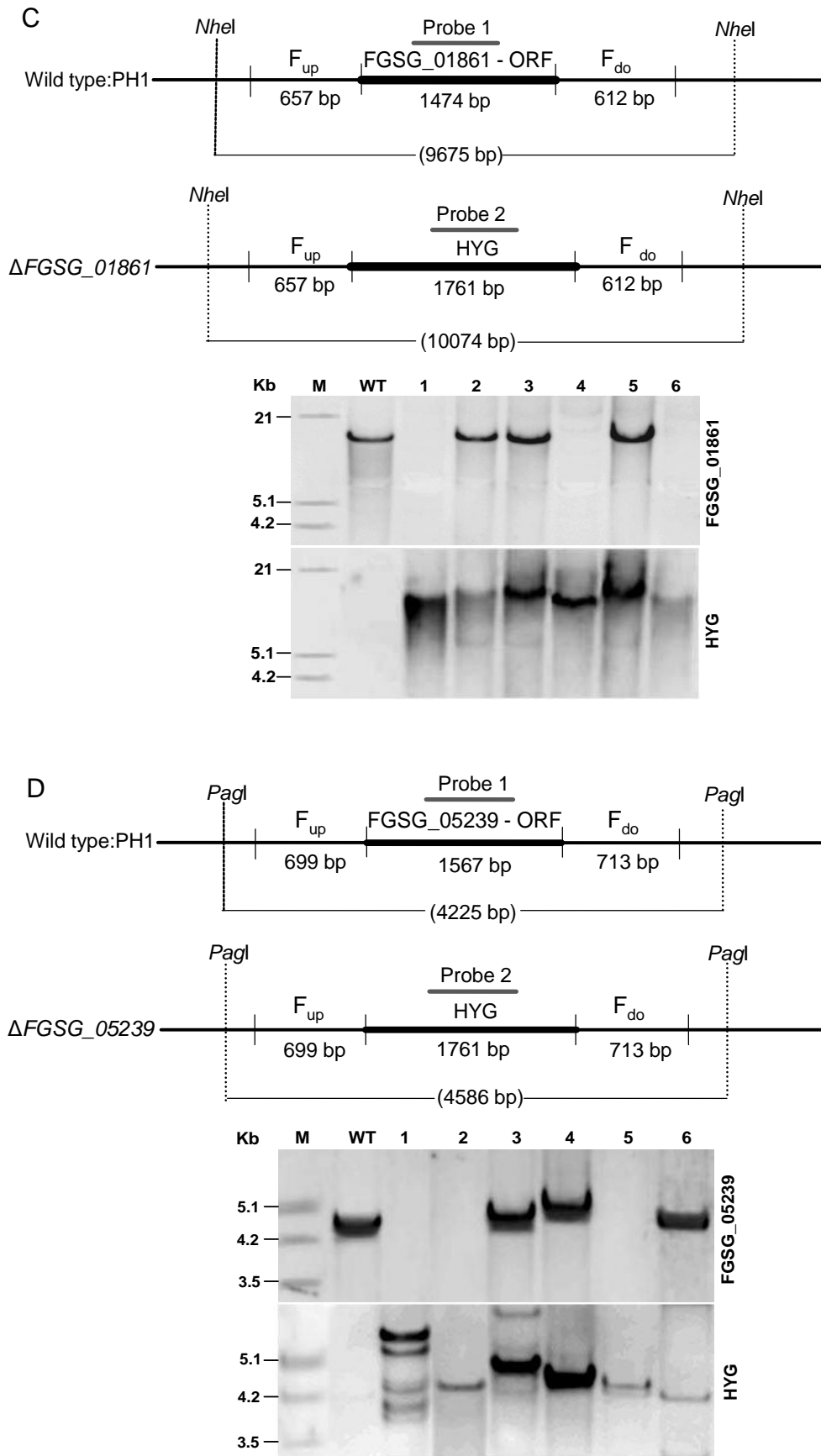
homologous transmembrane receptors were found including: FGSG_03023, FGSG_07716, FGSG-01861, FGSG_05239 and FGSG_09693. Each of these transmembrane receptors contains seven transmembrane domains.

In this study seven TMR-knock-out constructs for double homologous recombination method were created for the following: *FGSG_05006*, *FGSG_02655*, *FGSG_03023*, *FGSG_07716*, *FGSG-01861*, *FGSG_05239* and *FGSG_09693*.

3.1.2. Generation of TMR deletion mutants

In order to study the function of transmembrane receptors in the life cycle of *F. graminearum* the gene of each TMR was deleted using double homologous recombination method (Fig. 9, Fig. 10 and Fig. 11). 5'- and the 3'-flanking regions were amplified by PCR and subsequently fused to a hygromycin resistance cassette. The replacement fragments were excised by appropriate restriction enzymes (restriction enzyme recognition sites for each TMR-knock-out construct were introduced to the primers: 5 and 6, Table 1) and used for fungal transformation as described in materials and methods. Primary transformants were screened in a diagnostic PCR with primers amplifying a gene-internal fragment. The length of flanking regions and internal primers of each TMR-knock-out construct are indicated in the Fig. 10 and primers number 7 and 8, Table 1. Transformants with a low internal signal were used for single conidia isolation to obtain homokaryotic deletion mutants. Several mutants and strain with ectopic integration of each TMR-knock-out approach, and the wild type were subsequently analysed in Southern blot experiments. When probed for the integration of the hygromycin gene (Probe 2, Probe 2 was amplified by PCR with the use of primers number: 9 and 10, Table 1 and pGEM-HYG as template), some mutants, but not the wild type, showed a single integration of the fragment. The other mutants showed multiple integration of fragment (Fig. 10A-F). When hybridized with a probe amplified from the TMR gene (Probe 1, Probe 1 was synthesized by PCR with the use of primers number: 7 and 8 of each TMR-knock-out construct, Table 1 and wild type DNA as template), all mutants except for ectopic strains showed no signal. Also in the wild type a signal was visible (Fig. 10A-F).





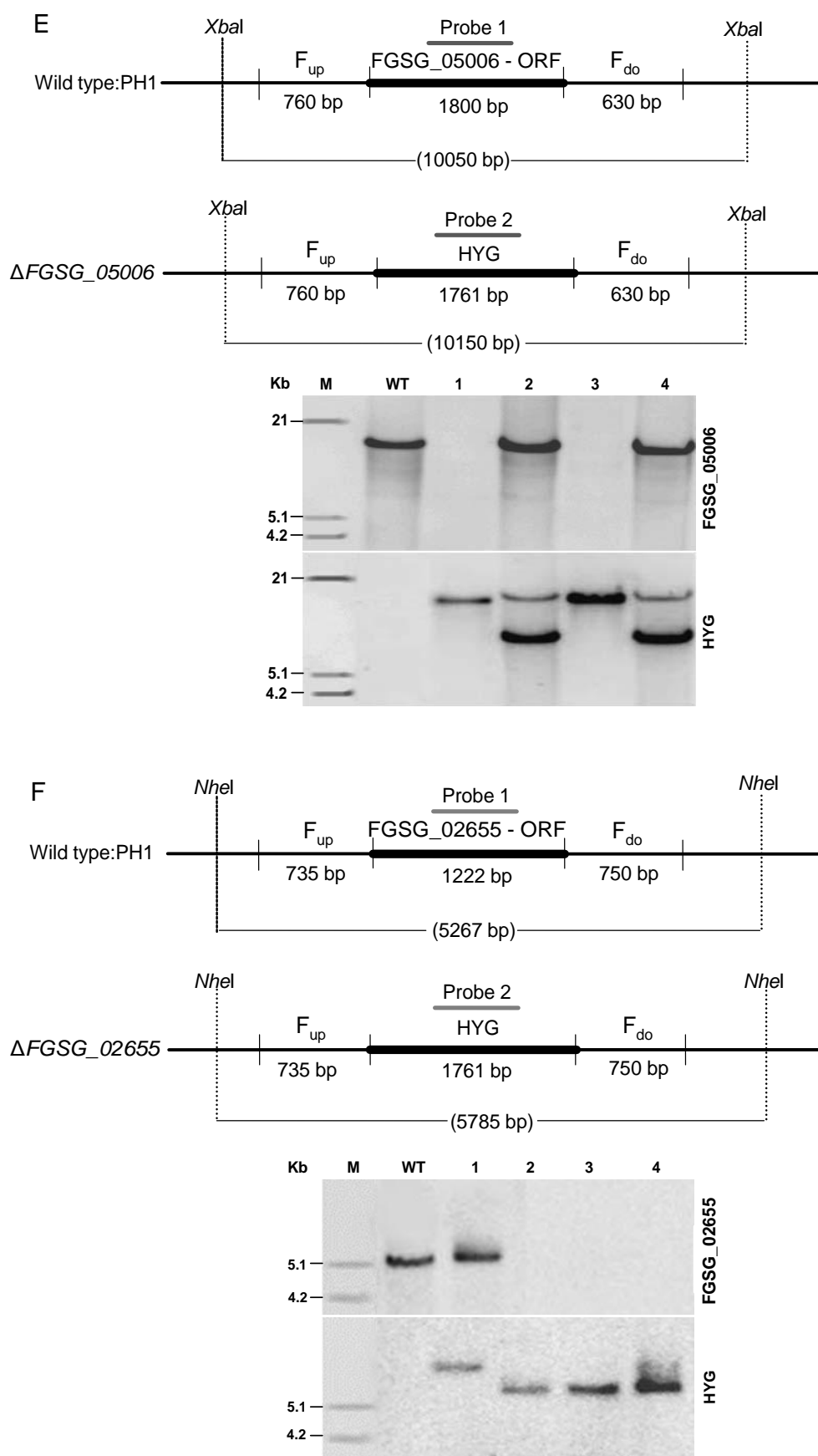


Figure 10. Gene replacement strategies and Southern analysis of TMR deletion. DNA of the mutant and ectopic of each TMR-knock-out construct, and the wild type was digested with appropriate restriction enzymes indicated in the figure, separated on agarose gel, blotted on a membrane and

Figure 10 continuance

probed with DIG-labelled probes for hygromycin (Probe 2) and a fragment of each TMR gene (Probe 1), respectively. A, $\Delta FGSG_{03023}$; B, $\Delta FGSG_{07716}$; C, $\Delta FGSG_{01861}$; D, $\Delta FGSG_{05239}$; E, $\Delta FGSG_{05006}$ and F, $\Delta FGSG_{02655}$. The disruption mutants of each TMR lacked a signal when probed with probe1 and showed a signal at the expected location with Probe 2. Both probes had a signal in the ectopic strain. The wild type only showed a signal with probe 1.

For *FGSG_09693*-knock-out construct, fifteen primary transformants were used for single conidia isolation. Then, transformants were screened in a diagnostic PCR with primers 7 and 8 (Table 1) amplifying the *FGSG_09693* internal fragment (Fig. 11A). Homologous integration of the replacement fragment was checked by PCR with primers 1 and 10 (l: left flank, 2328 bp) and 4 and 9 (r: right flank, 2332 bp; Fig. 11A). Two independent *FGSG_09693* deletion mutants were PCR-positive for the flank-spanning, but not for the *FGSG_09693* internal fragment. The wild type and ectopic strains were only PCR-positive for the *FGSG_09693* internal fragment (Fig. 11B and C).

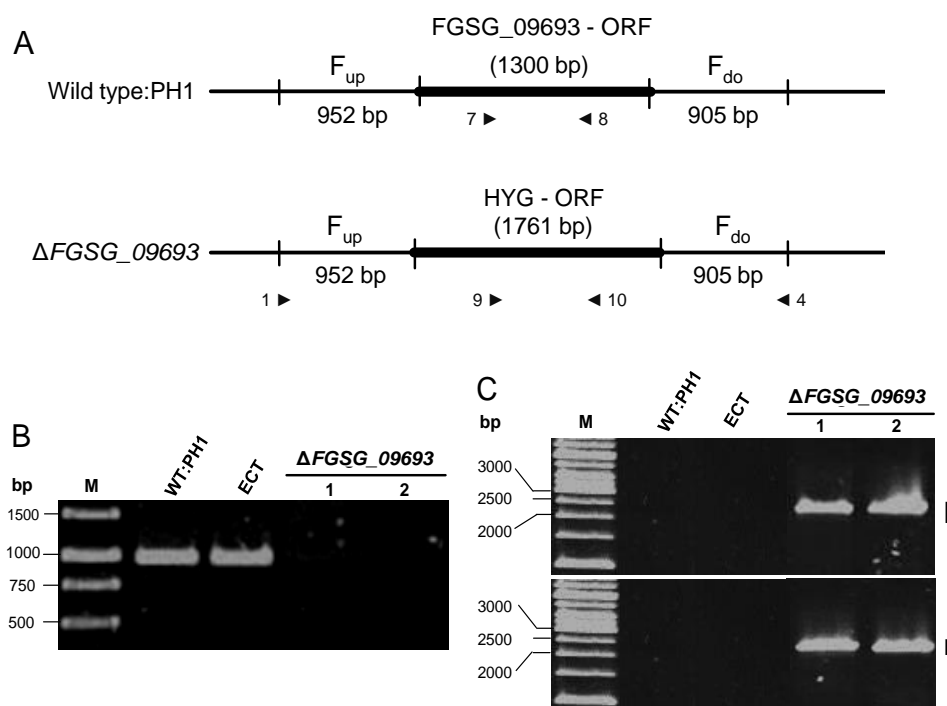


Figure 11. Gene replacement strategy and PCR analysis of *FGSG_09693* deletion. A. Gene replacement strategy. B. PCR analysis of $\Delta FGSG_{09693}$ and the wild type (WT:PH1). Deletion of *FGSG_09693* was verified in two independent mutants using primers 7 and 8 (787 bp). C. Homologous integration of the replacement fragment was checked by PCR with primers 1 and 10 (l: left flank, 2328 bp) and 4 and 9 (r: right flank, 2332 bp). The wild type and ectopic strains were PCR-positive for the gene internal fragment, but not for the flank-spanning PCR.

Two $\Delta FGSG_{03023}$, three $\Delta FGSG_{07716}$, three $\Delta FGSG_{01861}$, three $\Delta FGSG_{05239}$, two $\Delta FGSG_{09693}$, two $\Delta FGSG_{05006}$ and three $\Delta FGSG_{02655}$ mutants were obtained in this study. Phenotypic characterization in terms of vegetative growth on different media (i.e.

conferring salt, oxidative and fungicide stress; different C- and N-sources), perithecia formation, conidia germination, DON production, cAMP production, lipase secretion and pathogenicity towards wheat and maize was performed using two independent disruption mutants of each TMR.

In the following, I will present results on a comprehensive functional characterization of these seven putative TMRs. Two TMRs are involved in pathogenicity, DON production and lipase secretion. One TMR is necessary for utilization of poor carbon sources. One TMR negatively regulates stress tolerance. Three TMRs do not provoke any obvious function.

3.1.3. Putative carbon sensor FGSG_05006 is necessary for utilization of poor carbon sources but not for virulence toward wheat and maize

Since FGSG_05006 is homologous to putative carbon sensor receptors found in yeast, growth assays were performed in the presence of different poor carbon sources. Poor carbon sources are nutrients such as sugars comprising a low number of carbon atoms in chemical structures. When grown on poor carbon sources (100 mM glycerol, 100 mM manitol, 100 mM arabinose), $\Delta FGSG_{05006}$ mutants produced less aerial hyphae compared to the wild type. This defect was most severe on glycerol, where the dry mass of $\Delta FGSG_{05006}$ mutants was approximately one-third that of the wild type (Fig. 12A, B and Table 6). Moreover, $\Delta FGSG_{05006}$ mutants showed a reduced radial growth on these media compared to the wild type. However, $\Delta FGSG_{05006}$ mutants did not exhibit defects during asexual growth and development (colony morphology, growth rate, dry mass) on medium containing sucrose as a sole carbon source (Fig. 12A, B and Table 6). Surprisingly, supplementation of 1 mM cAMP partially restored the growth defect of $\Delta FGSG_{05006}$ mutants on minimal-glycerol agar plates (Fig. 12A). No differences in growth performance between the wild type and other TMR deletion strains were observed on agar plates supplemented with poor carbon sources after 3 days post-incubation.

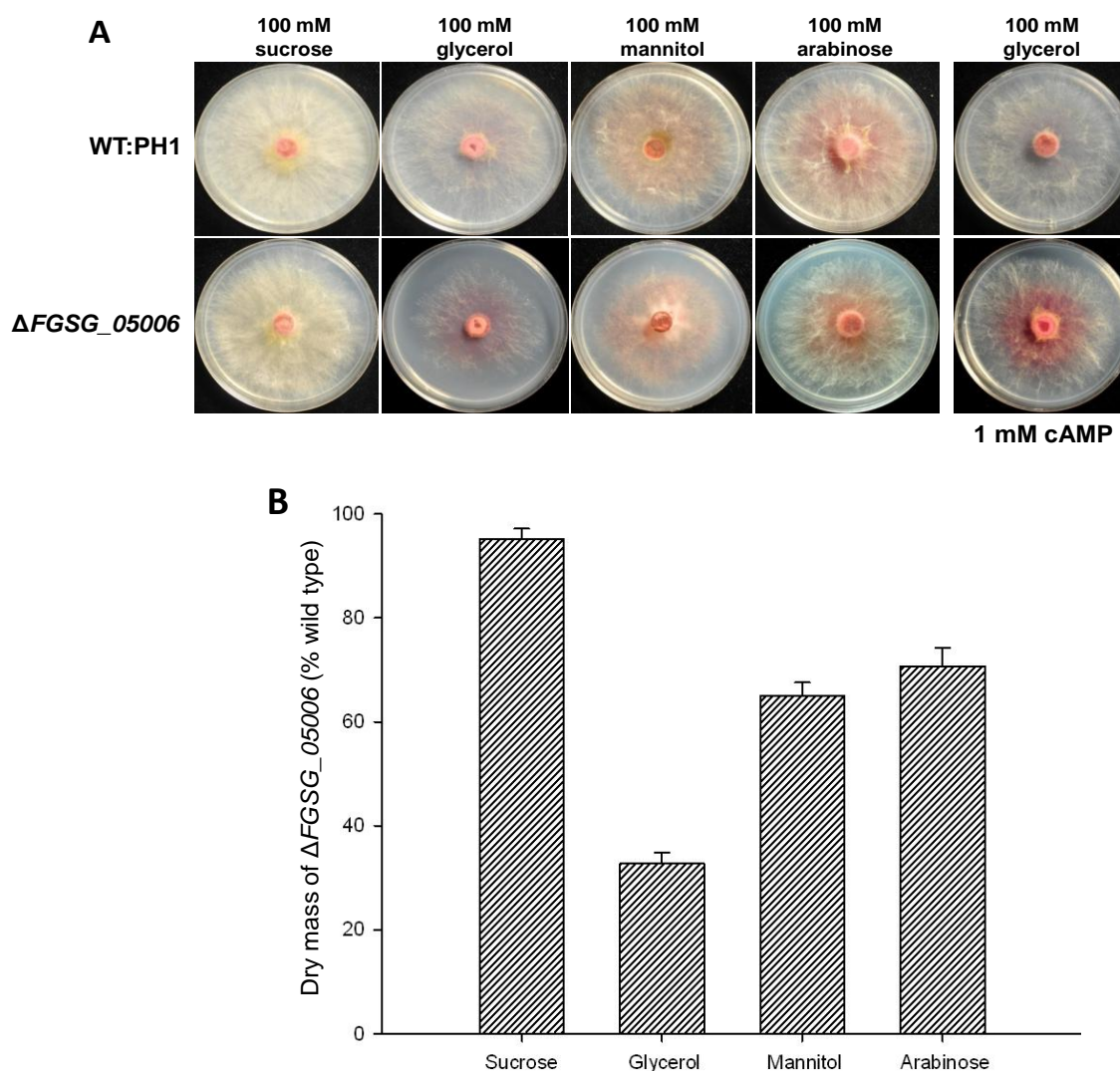


Figure 12. Vegetative growth of the wild type and $\Delta FGSG_05006$ mutant strains on different poor carbon sources. **A.** Colony morphology of the wild type (WT:PH1) and $FGSG_05006$ deletion strains after 3 days on agar plates containing minimal medium (MM) supplemented with 100 mM sucrose, glycerol, mannitol and arabinose as a sole carbon source, respectively. The $FGSG_05006$ deletion strain showed a reduction in growth and less aerial hyphae formation on poor carbon sources. On agar plates supplemented with 100 mM sucrose, the mutant exhibited no difference in growth compared to the wild type. In the presence of 1 mM cAMP in MM-glycerol medium, the wild type phenotype was partially restored in the $\Delta FGSG_05006$ mutant. **B.** Dry mass of the $\Delta FGSG_05006$ mutants compared the wild type. 10^5 conidia of each the wild type strain and the $\Delta FGSG_05006$ mutants were inoculated in 50 ml MM liquid medium containing a single carbon source as indicated. Mycelia were harvested, lyophilized and measured after 3 dpi on a shaker at 150 rpm and 28 °C. The dry mass accumulation of the mutant was about 30, 65 and 70% of the wild type on glycerol, mannitol and arabinose, respectively.

Table 6. Dry mass of and the wild type (WT:PH1) and *FGSG_05006* deletion strains after 3 dpi in MM liquid medium supplemented with 100 mM sucrose, glycerol, mannitol and arabinose as a sole carbon source, respectively. Experiments were repeated twice with triplicates.

MM medium supplemented with	Dry mass (mg)	
	WT:PH1	$\Delta FGSG_{05006}$
100 mM sucrose	54.00±2.64	51.33±2.08
100 mM glycerol	37.67±1.52	12.34±1.04
100 mM mannitol	54.33±3.05	35.45±2.52
100 mM arabinose	62.66±2.08	44.52±3.51

As shown in Figure 12A, B and Table 6, the biomass accumulation of $\Delta FGSG_{05006}$ mutants was significantly reduced on MM-glycerol medium compared to the wild type in the absence of cAMP. The addition of cAMP increased the aerial hyphae formation of both the wild type and $\Delta FGSG_{05006}$ mutant strains, but it had the greatest effect on $\Delta FGSG_{05006}$ mutants. In the presence of 1 mM cAMP, the aerial hyphae of the mutants were nearly the same like the wild type. Thus, the addition of cAMP partially rescued this defect of $\Delta FGSG_{05006}$ mutants on MM-glycerol medium and implicates this TMR in cAMP-related signaling cascade. Steady-state intracellular cAMP level measurements in the wild type and $\Delta FGSG_{05006}$ mutant strains grown on MM-glycerol medium were conducted (see materials and methods). The steady-state intracellular cAMP level of $\Delta FGSG_{05006}$ mutants was strongly reduced to about 14% compared to the wild type (Fig. 13). This implicates *FGSG_05006* in the regulation of the steady-state intracellular cAMP levels in cAMP/PKA signaling cascade in *F. graminearum*.

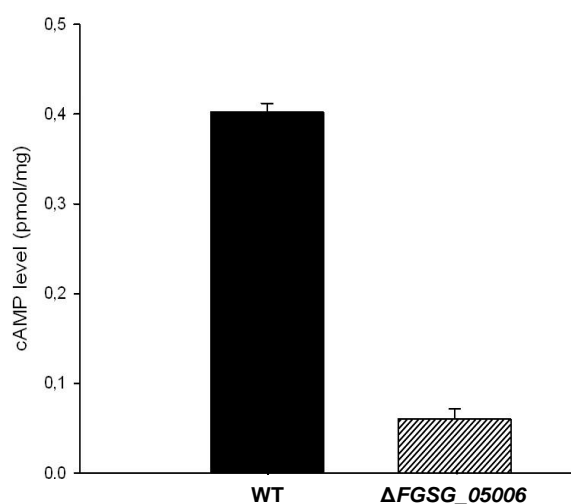


Figure 13. Steady-state intracellular cAMP level measurements of the wild type (WT:PH1) and $\Delta FGSG_{05006}$ mutant strains on minimal-glycerol medium. *FGSG_05006* deletion mutants

Figure 13 continuance

displayed severe reduction in steady-state intracellular cAMP level compared to the wild type. The assay was performed using two biological and three technical replicates each.

To figure out the role of *FGSG_05006* in the pathogenic development of *F. graminearum*, pathogenicity assays on wheat and maize were performed. Deletion of *FGSG_05006* did not cause a reduction in virulence towards the susceptible wheat cultivar Nandu compared to the wild type (Fig. 14A). The same applies for the infection on maize cobs (Fig. 14B). These results indicate that *FGSG_05006* is dispensable for fungal virulence at least under the conditions tested. DON measurements in the wild type and $\Delta FGSG_05006$ infected spikes were carried out using a highly sensitive ELISA test. The result revealed no significant difference in DON contents between the wild type and $\Delta FGSG_05006$ mutant strains in wheat heads after 7 dpi (Fig. 14C).

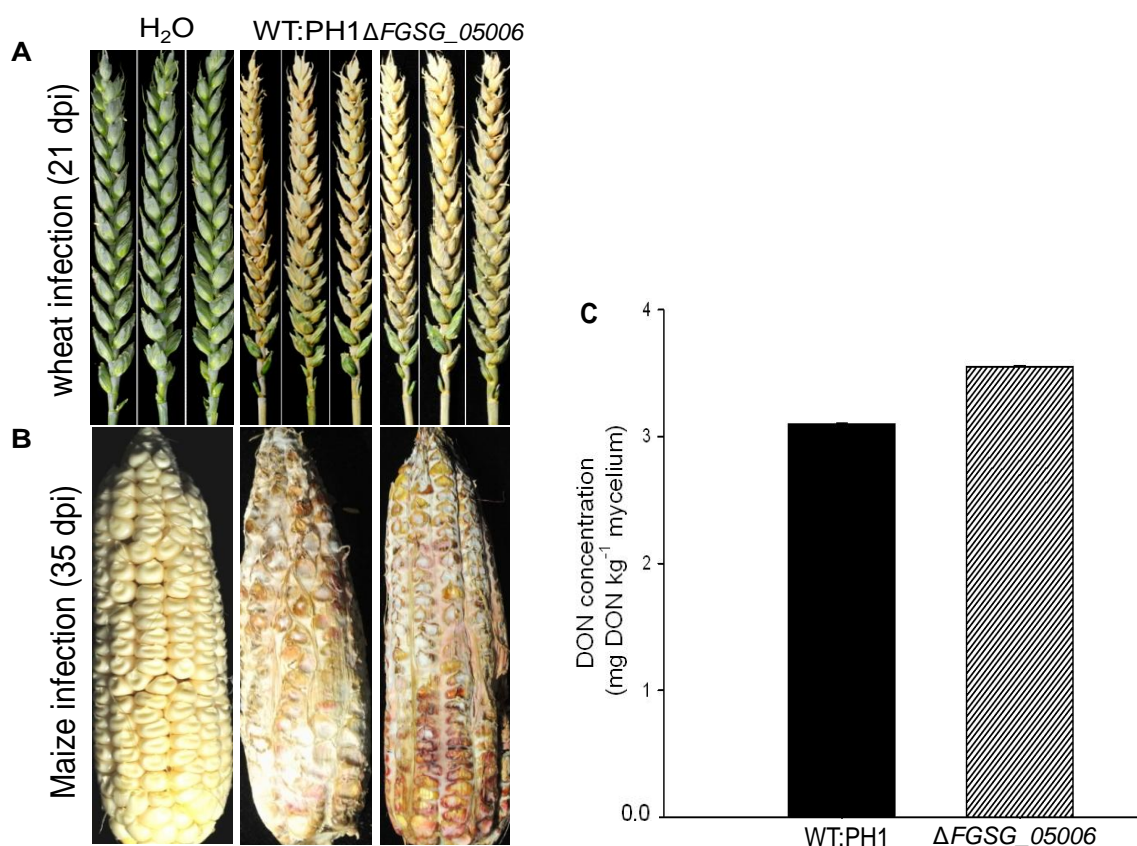


Figure 14. Pathogenicity assay on wheat and maize and DON concentrations measurement in wheat heads. Pathogenicity on wheat heads (A, upper) and maize (B, lower) infected with conidia of the wild type (WT:PH1) and *FGSG_05006* deletion strains and inoculated for 21 (wheat) and 35 (maize) days. Water was used as the control. The *FGSG_05006* deletion mutant showed no reduction in virulence towards wheat (cv. Nandu) and maize compared to the wild type. The wheat infections were performed 20 times, the maize infections were repeated 3 times. C. DON-quantification in infected wheat heads. No significant difference was found in the DON contents between the wild type and $\Delta FGSG_05006$ mutant strains. Toxin measurements were performed using two biological and three technical replicates.

Thus, FGSG_05006 is necessary for utilization of poor carbon sources and the regulation of the steady-state intracellular cAMP levels in cAMP/PKA signaling cascade but dispensable for virulence towards wheat and maize.

3.1.4. The pheromone receptor FGSG_02655 is involved in sexual reproduction and virulence

To investigate whether TMRs are involved in sexual reproduction, all TMR deletion mutants and the wild type were screened for perithecia formation on both detached wheat nodes and carrot agar plates. After 3 weeks post-inoculation, the wild type produced several clusters of perithecia which contained numerous asci and ascospores. In contrast, gene disruption of the pheromone receptor (Δ FGSG_02655) led to a significant reduction in perithecia maturation on both detached wheat nodes and carrot agar plates. Perithecia of Δ FGSG_02655 mutants were also crushed to examine their asci and ascospores. Mature perithecia contained normal asci and ascospores, however, the amount of ascospores was strongly reduced compared to the wild type. Immature perithecia had fewer asci and no ascospore compared to the wild type (Fig. 15). Intriguingly, the wild type and Δ FGSG_02655 mutant strains produced equal amounts of conidia. There was no difference in perithecia formation and conidia production between the wild type and the other TMR deletion mutant strains.

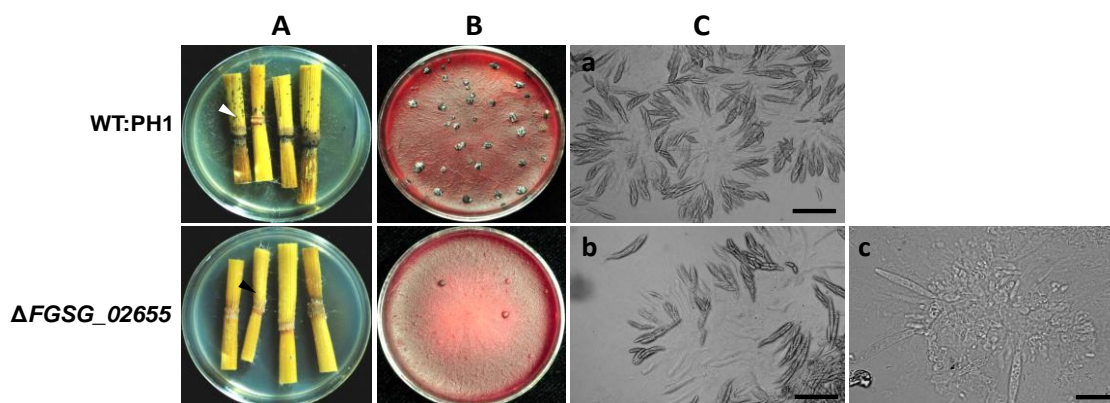


Figure 15. Assay for perithecia formation. Conidia of the wild type (WT:PH1) and *FGSG_02655* deletion strains were placed on wheat nodes (**A**) and carrot agar (**B**). After 21 days of incubation, the wild type had produced numerous clusters of perithecia (white arrows on wheat nodes). Squeezing these clusters released the asci containing ascospores (**C-a**). The amount of mature perithecia (**A, B**) and ascospores (**C-b**) of the *FGSG_02655* deletion mutant was significant reduced both on detached wheat nodes and carrot agar plates. The immature perithecia (black arrows on wheat nodes) of the Δ FGSG_02655 mutant contained no ascospore (**C-c**). Scale bar 20 μ m (**C-a, b**) and Scale bar 10 μ m (**C-c**).

To determine if the TMR FGSG_02655 is involved in pathogenicity towards wheat and maize, pathogenicity assays were conducted. Water was used as the control. Disruption of

FGSG_02655 attenuated virulence towards wheat and maize compared to the wild type. On wheat spikes (cv. Nandu) inoculated with $\Delta FGSG_02655$ mutants, infection was reduced to about 70% of the wild type after 21 dpi (Fig. 16A). Similar to wheat infections, $\Delta FGSG_02655$ mutants also showed a reduced virulence towards maize after five weeks post-inoculation. Cobs infected by the mutants still had uninfected cob parts with normal kernel development (Fig. 16B). In contrast, the wild type completely rotten the cobs. The cobs and spikes inoculated with water remained symptomless.

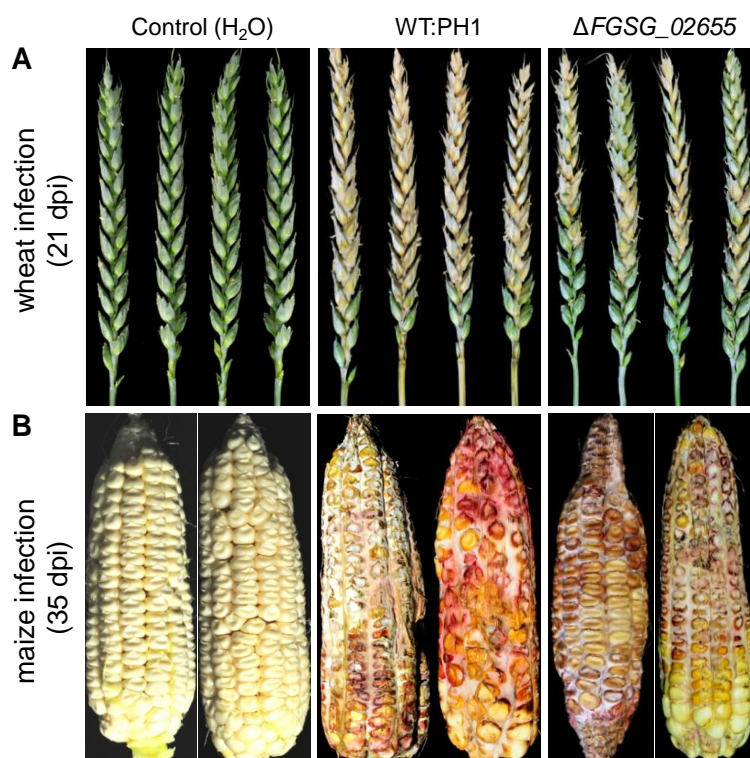


Figure 16. Pathogenicity assay on wheat and maize. Wheat heads (A, upper) and maize (B, lower) were infected with conidia of the wild type (WT:PH1) and *FGSG_02655* deletion strains and inoculated for 21 (wheat) and 35 (maize) days. The mutant caused attenuated virulence towards wheat (cv. Nandu) and maize. The wild type infection caused typical symptoms for maize cob rot and *Fusarium* head blight disease. The wheat infections were performed 20 times, the maize infections were repeated 3 times.

The reduced virulence of $\Delta FGSG_02655$ mutants towards wheat may be due to a reduction in DON production during infection. To answer this question, DON contents in the wild type and $\Delta FGSG_02655$ infected spikes were measured using a highly sensitive ELISA test. The result showed that spikelets inoculated with $\Delta FGSG_02655$ mutants only accumulated approximately 30% of the wild-type DON level after 7 dpi (Fig. 17A and Table 7). The DON contents produced by $\Delta FGSG_02655$ mutants during growth in induction medium containing ammonium sulphate as the sole nitrogen source (Ilgen et al., 2009) were also measured. It was found that *FGSG_02655* deletion strains produced less DON levels compared to the wild

type in this medium. After an incubation period of 1 day, the supernatant of $\Delta FGSG_02655$ mutant cultures contained about 45% less DON compared to the wild type culture (Fig. 17B and Table 7).

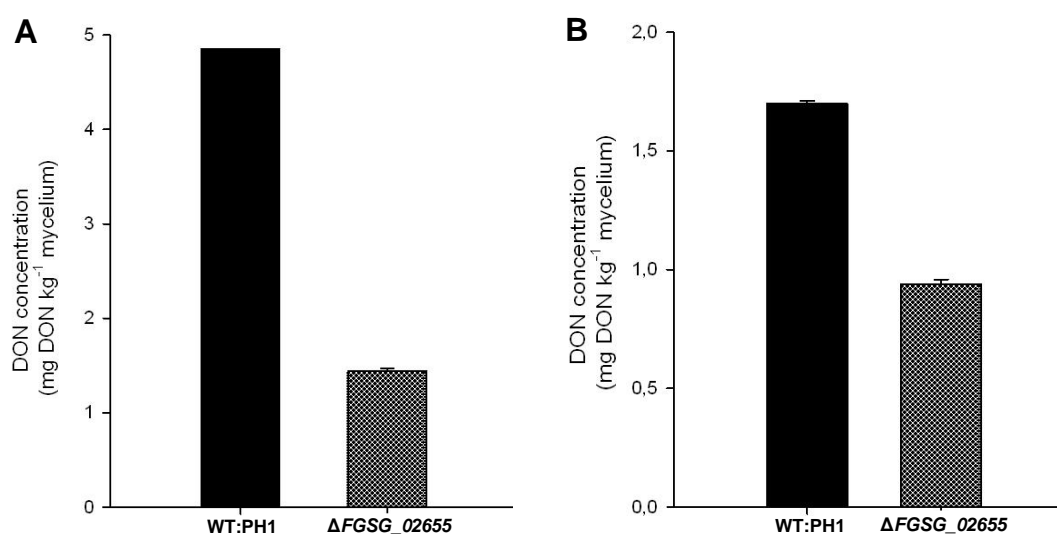


Figure 17. DON concentrations of the wild type (WT:PH1) and $FGSG_02655$ deletion strains in wheat heads (A) and submerged culture (B). The DON contents in wheat spikelets inoculated with the $\Delta FGSG_02655$ mutants were lower compared to the wild type after 7 dpi. *In vitro*, DON production was induced using 5 mM $(NH_4)_2SO_4$. After 24 hpi, the mutants produced less DON in this medium compared to the wild type. The DON concentrations were normalized against the amount of fungal mycelium per kilogram of substrate, determined by quantitative PCR. Toxin measurements were performed using two biological and three technical replicates each.

Table 7. ELISA analysis of DON production under different growth conditions in the wild type (WT:PH1) and $FGSG_02655$ deletion strains. All values were normalized against the amount of fungal material in the sample using qPCR (see Material and Methods).

Strains	DON (mg kg ⁻¹ mycelium)	
	<i>in vitro</i> (1 dpi)	<i>in planta</i> (7 dpi)
WT:PH1	1.699±0.013	4.85±0.0035
$\Delta FGSG_02655$	0.94±0.019	1.445±0.025

F. graminearum is able to secrete a variety of hydrolytic enzymes in appropriate growth conditions and during plant infection (Wanjiru et al., 2002; Phalip et al., 2005; Paper et al., 2007). Besides endoglucanase, xylanolytic, proteolytic, and cellulosic enzymes, lipolytic enzymes are also detected in the presence of lipid substrates such as wheat germ oil (Jenczmionka and Schäfer, 2005). Previously, it has been shown that secreted lipases of *F. graminearum* are important enzymes for virulence toward wheat and maize (Jenczmionka and

Schäfer, 2005; Voigt et al., 2005; Nguyen et al., 2010). $\Delta FGSG_02655$ mutants showed a reduction in virulence. It is possible that $FGSG_02655$ is involved in secretion of lipases in *F. graminearum* during plant infection. To address with this question, the lipase activity of the supernatant of the wild type and $\Delta FGSG_02655$ mutant strains induced by 2% (v/v) wheat germ oil was tested. It was found that the extracellular lipase activity at early time points of induction was slightly reduced in the mutants compared to the wild type. Lipase activity of $\Delta FGSG_02655$ mutants was reduced to 50, 80 and 82 % after 2, 4 and 6 hours of induction, respectively compared to the wild type (Fig. 18 and Table 8). The lipase activity of $\Delta FGSG_02655$ mutants was restored to wild type lipase activity level after 24 h of induction (Table 8). These data suggest that $FGSG_02655$ are involved in the regulation of lipase secretion in *F. graminearum*.

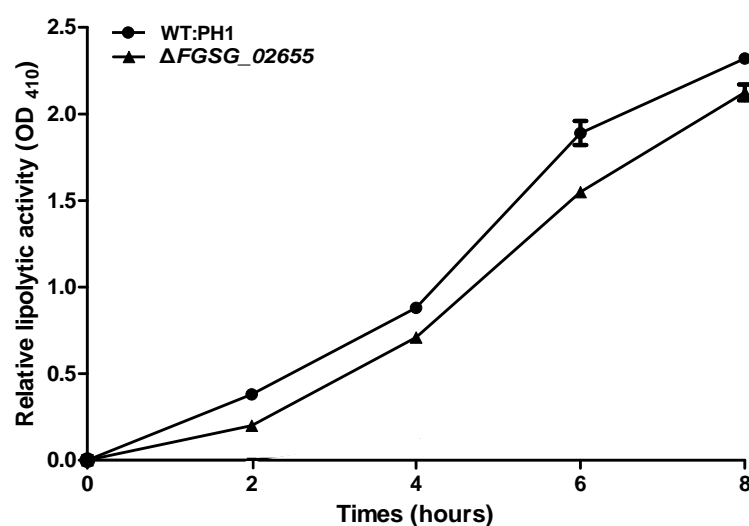


Figure 18. Extracellular lipolytic activity of the wild type and $FGSG_02655$ deletion mutant strains after induction by 2% (v/v) wheat germ oil. Lipase activity in the supernatants of the induced cultures of the wild type (WT:PH1), and $\Delta FGSG_02655$ mutant strains at different time points was assayed using para-nitrophenyl palmitate as the substrate. The $\Delta FGSG_02655$ mutants showed a slightly reduction in lipase activity compared to the wild type. The assay was performed using two biological and three technical replicates each.

Table 8. Extracellular lipolytic activity of the wild type and $FGSG_02655$ deletion strains after induction by 2% wheat germ oil at different time points. The assay was performed using two biological and three technical replicates each.

Lipolytic activity	2 h	4 h	6h	8 h	24 h
WT:PH1	0.38 (± 0.028)	0.88 (± 0.027)	1.89 (± 0.098)	2.32 (± 0.03)	2.87 (± 0.035)
$\Delta FGSG_02655$	0.2 (± 0.014)	0.71 (± 0.042)	1.55 (± 0.028)	2.15 (± 0.06)	2.79 (± 0.028)

In summary, the pheromone receptor *FGSG_02655* is involved in sexual development, virulence, DON production and lipase secretion.

3.1.5. Deletion of *FGSG_01861* enhances stress tolerance towards oxidative, osmotic, fungicide, temperature and cell wall stress

In order to test the vegetative growth on different media, plate assays were conducted using all TMR deletion mutants and the wild type. No differences in growth performance between the wild type and the TMR deletion mutant strains were observed on CM agar plates or agar plates containing different nitrogen sources (NaNO_3 , $(\text{NH}_4)_2\text{SO}_4$, each 5 mM and medium buffered to certain pH values (pH 4, 5, 6 and 9). However, on plates incubated at different temperatures (18 and 30 °C) as well as plates supplemented with 0.2 mg ml⁻¹ congo red, $\Delta FGSG_01861$ mutants grew better than the wild type (Fig. 19). To test the response of the mutants to oxidative stress, CM plates were supplemented with 10 and 20 mM H₂O₂. At concentration of 10 mM H₂O₂, growth of the wild type was strongly reduced compared to growth on CM, whereas growth of $\Delta FGSG_01861$ mutants was only slightly inhibited (Fig. 19). On plates supplemented with 20 mM H₂O₂, the wild type was significantly reduced in growth compared to the $\Delta FGSG_01861$ mutants.

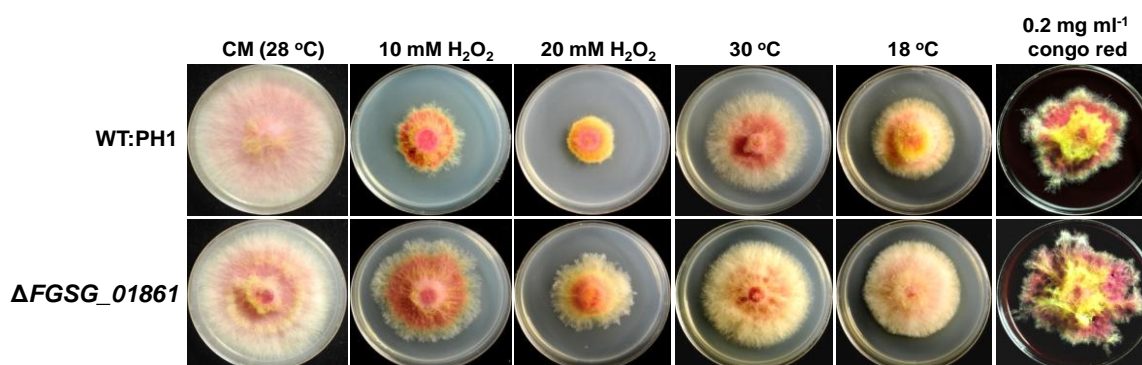


Figure 19. Colony morphology of the wild type (WT:PH1) and *FGSG_01861* deletion strains after 3 days of growth under different stress conditions. The basic medium was complete medium (CM) inoculated with mycelial plugs from 3-day-old cultures. Media were supplemented with 10 and 20 mM H₂O₂, or 0.2 mg ml⁻¹ congo red. No growth differences between the wild type and $\Delta FGSG_01861$ mutant strains could be detected on agar plates at normal culture temperature (28 °C) and without H₂O₂ or congo red after 3 days post-incubation. On plates supplemented with 10 and 20 mM H₂O₂ or 0.2 mg ml⁻¹ congo red as well as at 18 °C and 30 °C, the mutant grew better than the wild type.

Similarity, under high osmotic stress conditions (1.2 and 2 M NaCl), growth of $\Delta FGSG_01861$ mutants was better compared to the wild type (Fig. 20).

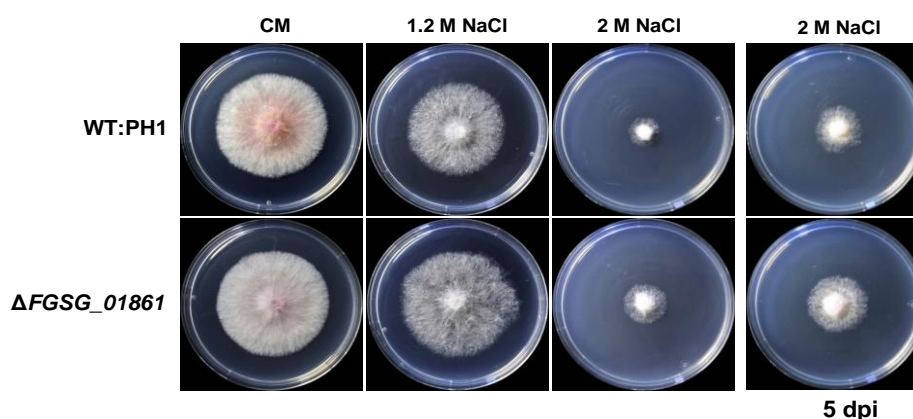


Figure 20. Colony morphology of the wild type (WT:PH1) and *FGSG_01861* deletion strains after 3 days and 5 days of growth under osmotic conditions. The basic medium was complete medium (CM) inoculated with mycelial plugs from 3-day-old cultures. Media were supplemented with 1.2 and 2 M NaCl. No obvious difference in growth was apparent between the wild type and $\Delta FGSG_01861$ mutant strains on CM without osmotic agent after 3 days post-inoculation. On plates supplemented with 1.2 M or 2 M NaCl, the mutant grew better than the wild type.

In order to examine the susceptibility of all TMR deletion mutants to antifungal drugs, the growth of the TMR deletion mutants was screened on CM plates containing 0.2 and 0.4 $\mu\text{g ml}^{-1}$ tebuconazole. At concentration of 0.2 $\mu\text{g ml}^{-1}$ tebuconazole, growth of $\Delta FGSG_01861$ mutants was nearly the same like on CM plates. The mutants were still able to grow on plates supplemented with 0.4 $\mu\text{g ml}^{-1}$ tebuconazole. In contrast, the wild type growth was strongly reduced at concentration of 0.2 $\mu\text{g ml}^{-1}$ tebuconazole and nearly abolished in the presence of 0.4 $\mu\text{g ml}^{-1}$ tebuconazole. Besides tebuconazole resistance, $\Delta FGSG_01861$ mutants exhibited a partial resistance against the phenylpyrrolic fungicide fludioxonil (Fig. 21).

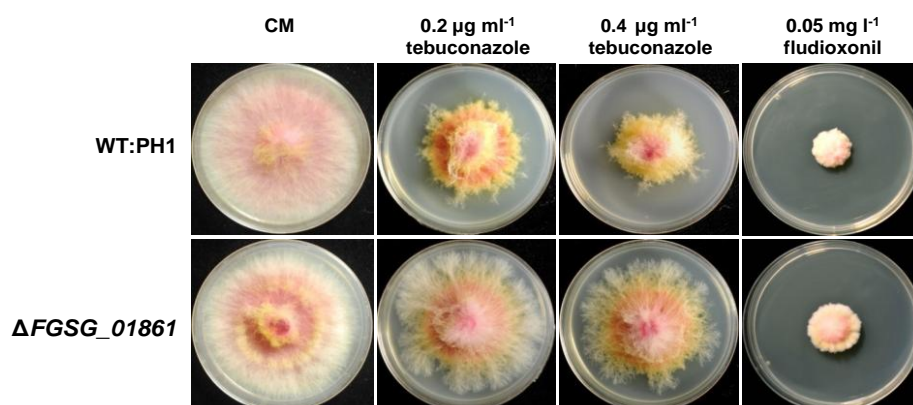


Figure 21. Fungicide sensitivity assay. Colony morphology of the wild type (WT:PH1) and *FGSG_01861* deletion strains after 3 days of growth on agar plates. The basic medium was complete medium (CM) inoculated with mycelial plugs from 3-day-old cultures. In order to test growth behaviour, the medium was supplemented with the antibiotics tebuconazole (0.2 $\mu\text{g ml}^{-1}$ or 0.4 $\mu\text{g ml}^{-1}$) and fludioxonil (0.05 mg l⁻¹). Growth of the mutant was similar compared to the wild type on CM plates. On CM plates containing tebuconazole, the growth of the wild type significantly decreased compared to the mutant. The mutant showed partial resistance towards fludioxonil compared to the wild type.

The germination rate of the wild type conidia was reduced to about 57% and 42 % compared to $\Delta FGSG_01861$ mutants at concentration of 0.2 and 0.4 $\mu\text{g ml}^{-1}$ tebuconazole, respectively. Interestingly, the germination rate of the $\Delta FGSG_01861$ conidia were also reduced in liquid CM containing tebuconazole compared to that in CM without tebuconazole. It was reduced to about 89 % and 76 % at concentration of 0.2 and 0.4 $\mu\text{g ml}^{-1}$ tebuconazole, respectively (Fig. 22A). Microscopic analysis of the germinating conidia on 0.4 $\mu\text{g ml}^{-1}$ tebuconazole revealed an abnormal morphology of the wild type germ tubes. Starting at the conidial compartments the hyphae were swollen and frequently burst. In contrast, hyphae of the $\Delta FGSG_01861$ mutants appeared unaffected (Fig. 22B). On the non-tebuconazole medium, no obvious difference in conidial germination or initial mycelial growth was apparent between the wild type and $\Delta FGSG_01861$ mutant strains. All other TMR deletion mutants showed a similar sensitivity towards fungicides like the wild type.

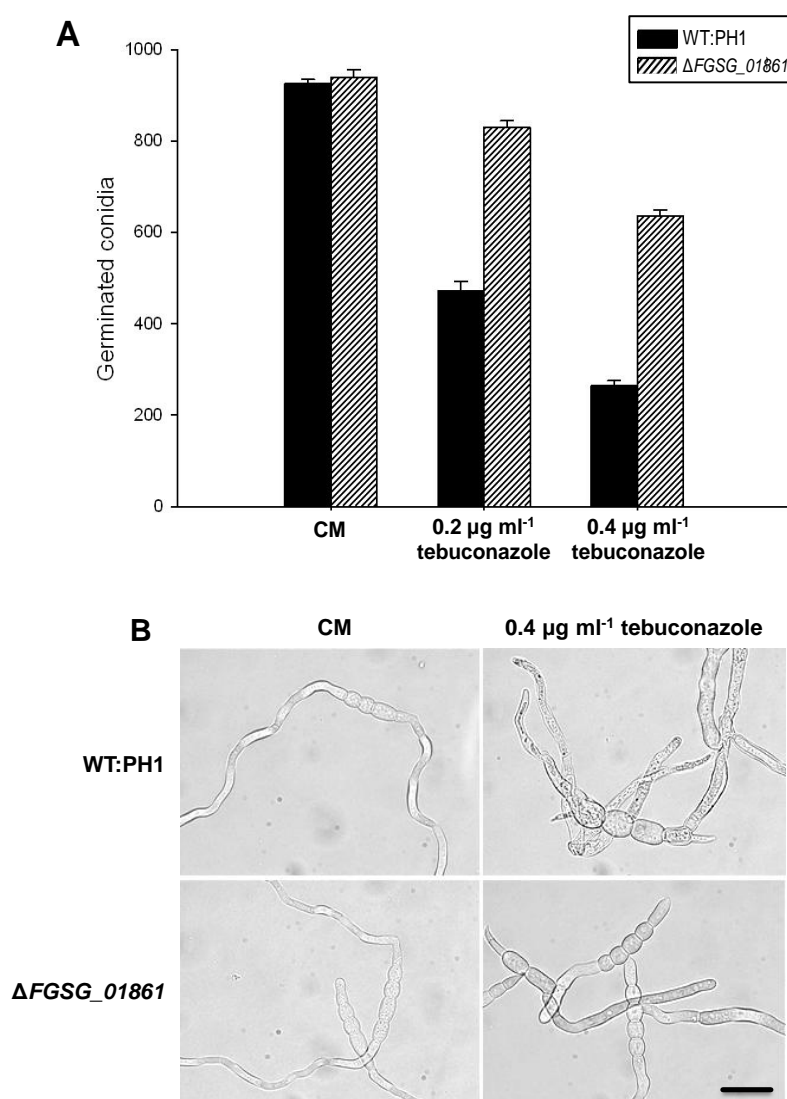


Figure 22. Conidia germination assay. **A.** Approximately 1000 conidia of the wild type and $\Delta FGSG_01861$ deletion strains were plated onto CM and CM supplemented with tebuconazole (0.2 μg

Figure 22 continuance

ml⁻¹ or 0.4 µg ml⁻¹). The number of germinated conidia was counted. The germination rate of the wild type conidia was significantly reduced on tebuconazole plates compared to the $\Delta FGSG_01861$ mutant ($P = <0.001$, *t*-test). Error bars indicate the standard deviation ($n=6$). **B.** Conidia of the wild type and $\Delta FGSG_01861$ mutant strains were germinated on CM and CM containing 0.4 µg ml⁻¹ tebuconazole. Pictures were taken 16-h post-inoculation. Both strains showed a normal germination pattern on CM. For the wild type on 0.4 µg ml⁻¹ tebuconazole, the conidial compartments and hyphae emerging from the conidia appeared to be swollen and they frequently burst. Germination of mutant conidia was not affected. Scale bar: 10 µm

Deletion of *FGSG_01861* did not reduce virulence towards the wheat cultivar Nandu (21 dpi) and maize (35 dpi) compared to the wild type (Fig. 23). Thus, *FGSG_01861* is dispensable for virulence towards wheat and maize.

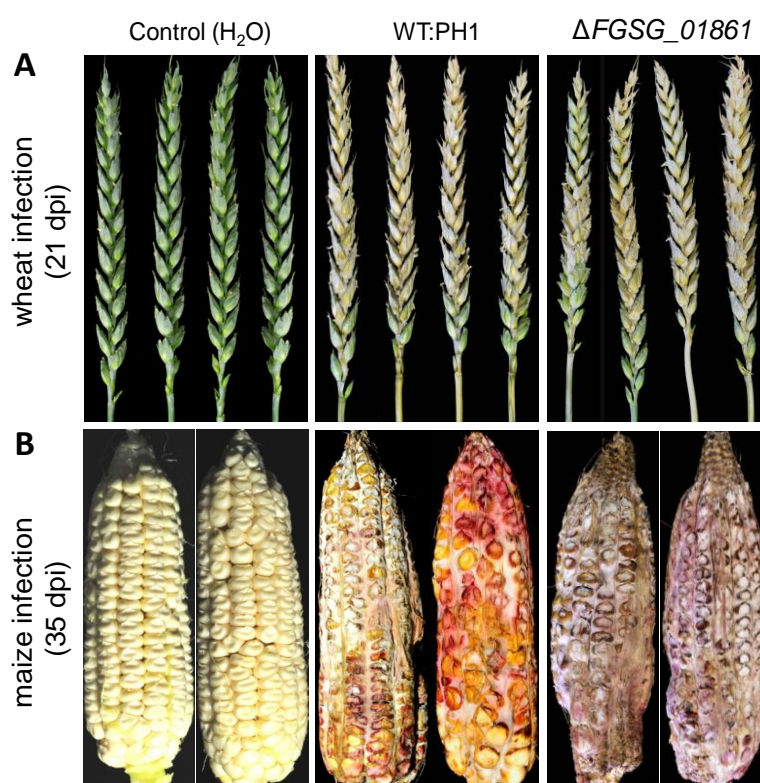


Figure 23. Pathogenicity assay on wheat and maize. Wheat heads (**A**, upper) and maize (**B**, lower) were infected with conidia of the wild type (WT:PH1) and *FGSG_01861* deletion strains and inoculated for 21 (wheat) and 35 (maize) days. Water was used as the control. Deletion of *FGSG_01861* did not lead to a reduction in virulence towards wheat (cv. Nandu) and maize compared to the wild type. The wheat infections were performed 20 times, the maize infections were repeated 3 times.

In summary, the TMR *FGSG_01861* negatively regulates stress tolerance towards oxidative, osmotic, fungicide and temperature stress as well as the cell wall stressor congo red.

3.1.6. Deletion of *FGSG_03023* attenuates virulence towards wheat and maize

Deletion of *FGSG_03023* led to a severe reduction in virulence towards wheat compared to the wild type. Infection of $\Delta FGSG_03023$ mutants stopped at the inoculated spikelet, while the wild type successfully colonized the whole spike (Fig. 24A). $\Delta FGSG_03023$ mutants were also reduced in virulence towards maize. All maize cobs inoculated with $\Delta FGSG_03023$ mutants still had uninfected cob parts with normal kernel development. The wild type colonized the complete maize cobs after 35 days of incubation (Fig. 24B). The cobs and spikes inoculated with water remained symptomless.

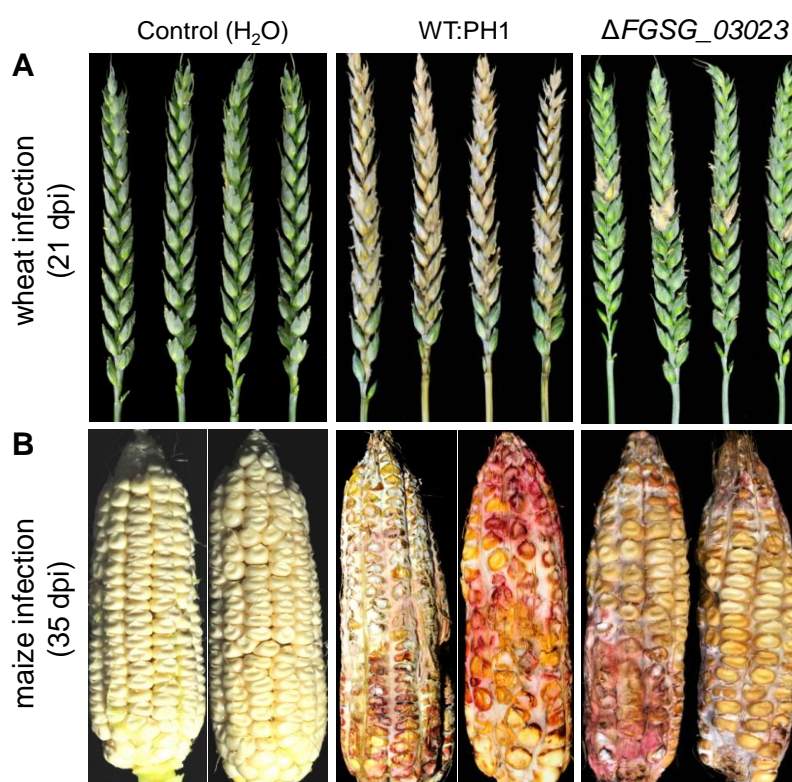


Figure 24. Pathogenicity assay on wheat and maize. Wheat heads (**A**, upper) and maize (**B**, lower) were infected with conidia of the wild type (WT:PH1) and *FGSG_03023* deletion strains and inoculated for 21 (wheat) and 35 (maize) days. Disruption of *FGSG_03023* attenuated virulence towards wheat (cv. Nandu) and maize. The wild type infection caused typical symptoms for maize cob rot and *Fusarium* head blight disease. The wheat infections were performed 20 times, the maize infections were repeated 3 times.

The $\Delta FGSG_03023$ mutants showed a reduction in DON production during wheat infection and *in vitro*. Spikelets inoculated with $\Delta FGSG_03023$ mutants accumulated approximately 33% of the wild-type DON level after 7 dpi (Fig. 25A and Table 9). The DON contents produced by the $\Delta FGSG_03023$ mutants during growth in induction medium containing ammonium sulphate as the sole nitrogen source were also measured. *FGSG_03023* deletion strains produced less DON levels compared to the wild type strain in this medium. After an

incubation period of 1 day, the supernatant of $\Delta FGSG_03023$ mutant cultures contained about 76% less DON compared to the wild type culture (Fig. 25B and Table 9).

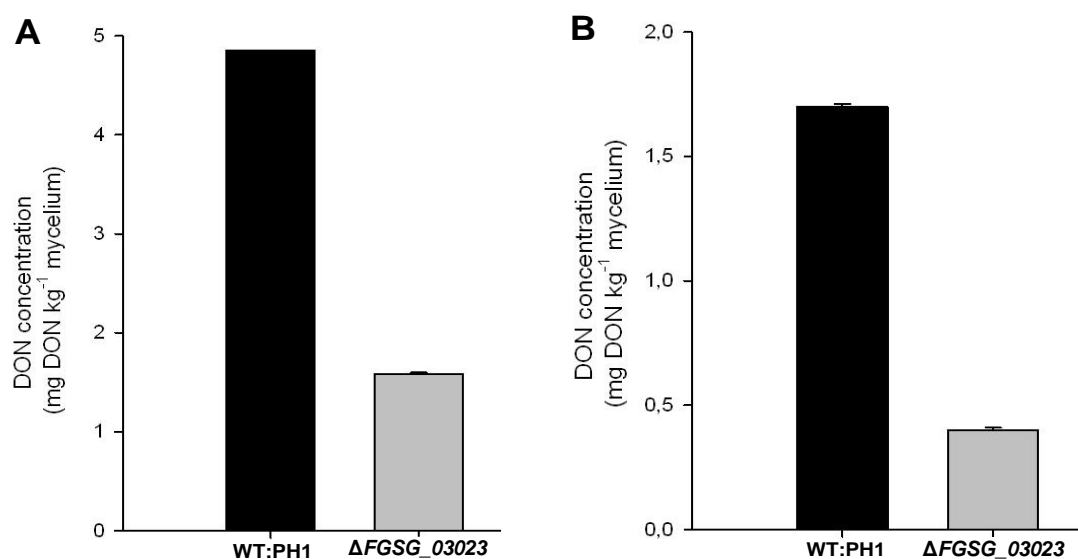


Figure 25. DON concentrations of the wild type (WT:PH1) and $FGSG_03023$ deletion strains in wheat heads (A) and submerged culture (B). The DON contents in wheat spikelets inoculated with the $\Delta FGSG_03023$ mutants were lower compared to the wild type after 7 dpi. *In vitro*, DON production was induced using 5 mM $(NH_4)_2SO_4$. After 24 hpi, the mutants produced less DON in this medium compared to the wild type. The DON concentrations were normalized against the amount of fungal mycelium per kilogram of substrate, determined by quantitative PCR. Toxin measurements were performed using two biological and three technical replicates each.

Table 9. ELISA analysis of DON production under different growth conditions in the wild type (WT:PH1) and $FGSG_03023$ deletion strains. All values were normalized against the amount of fungal material in the sample using qPCR (see Material and Methods).

Strains	DON (mg kg ⁻¹ mycelium)	
	<i>in vitro</i> (1 dpi)	<i>in planta</i> (7 dpi)
WT:PH1	1.699±0.013	4.85±0.0035
$\Delta FGSG_03023$	0.399±0.011	1.583±0.014

The lipase activity of the supernatant of the wild type and $\Delta FGSG_03023$ mutant strains induced by 2% (v/v) wheat germ oil was tested. Lipase activity of $\Delta FGSG_03023$ strains was strongly reduced compared to the wild type at early time points of induction. It was not detected after 2 hours of induction and decreased from 72% to 68% and 50% after 4, 6 and 8

hours of induction, respectively (Fig. 26 and Table 10). The lipase activity of the mutants was nearly the same like wild type lipase activity level after 24 h of induction (Table 10).

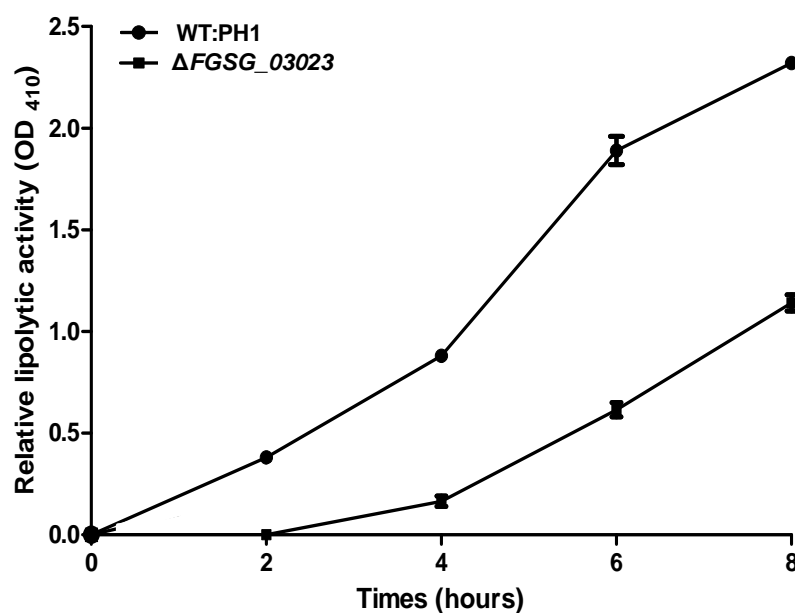


Figure 26. Extracellular lipolytic activity of the wild type and $\Delta FGSG_03023$ mutant strains after induction by 2% (v/v) wheat germ oil. Lipase activity in the supernatants of the induced cultures of the wild type (WT:PH1) and $\Delta FGSG_03023$ mutant strains at different time points was assayed using para-nitrophenyl palmitate as the substrate. Lipase activity of the $\Delta FGSG_03023$ mutants was drastically reduced compared to the wild type at early time points. The assay was performed using two biological and three technical replicates each.

Table 10. Extracellular lipolytic activity of the wild type and $FGSG_03023$ deletion strains after induction by 2% wheat germ oil at different time points. The assay was performed using two biological and three technical replicates each.

Lipolytic activity	2 h	4 h	6h	8 h	24 h
WT:PH1	0.38 (± 0.028)	0.88 (± 0.027)	1.89 (± 0.098)	2.32 (± 0.03)	2.87 (± 0.035)
$\Delta FGSG_03023$	0.0	0.165 (± 0.035)	0.615 (± 0.049)	1.14 (± 0.056)	2.65 (± 0.098)

These results indicate that the TMR $FGSG_03023$ is involved in pathogenicity towards wheat and maize. It furthermore influences DON biosynthesis and lipase secretion in *F. graminearum*.

In summary, transmembrane receptors are involved in several physiological processes in *F. graminearum* such as vegetative growth, sexual development, pathogenicity, secondary metabolite products (DON, lipase secretion) and stress response.

3.2. The role of FgOS-2 in *Fusarium graminearum*

3.2.1. Identification of FgOS-2 from *F. graminearum*

The OS-2 gene from *F. graminearum* FGSG_09612 was identified using a BlastX search against MIPS *Fusarium graminearum* Genome Database and has a high homology to putative osmolarity MAP kinases of other fungi (Fig. 27). It is published in the NCBI genebank under accession no. XM389788.1. It has a length of 1641 bp and a translated sequence of 357 aa. The coding sequence has nine exons: 56 bp, 48 bp, 30 bp, 44 bp, 111 bp, 357 bp, 79 bp, 184 bp and 73 bp. Figure 27 showed an alignment of the predicted amino acid sequence of OS-2 from *F. graminearum* and several fungal MAP kinases. The protein kinase domains of the yeast/fungi stress-activated protein kinase subgroup comprises of 11 domains (Hanks et al., 1991) and the conserved TGY-sequence which is required for kinase activation (Kültz, 1998).

	I	II		
SAPK	MAEFVRAQIFGTTFEITSRYTDLQPVGMGAFLVCSAKDQLTSQAVAIKKIMKPFSTPVL	60		
SRM	MAEFVRAQIFGTTFEITSRYTDLQLVGMGAFLVCSAKDQLTNQAVAVKKIMKPFSTPVL	60		
HOG1P	MAEFVRAQIFGTTFEITSRYTDLQPVGMGAFLVCSAKDQLTSQAVAVKKIMKPFSTPVL	60		
FpHOG1	MAEFVRAQIFGTTFEITSRYSDLQPVGMGAFLVCSARDQLTNQNVAVKKIMKPFSTPVL	60		
FgOS-2	MAEFVRAQIFGTTFEITSRYSDLQPVGMGAFLVCSARDQLTNQNVAVKKIMKPFSTPVL	60		
OSM1	MAEFVRAQIFGTTFEITSRYSDLQPVGMGAFLVCSARDQLTNQNVAIKKIMKPFSTPVL	60		
NcOS-2	MAEFIRAQIFGTTFEITSRYSDLQPVGMGAFLVCSAKDQLTNQNVAVKKIMKPFSTPVL	60		
BcSak1	MAEFVRAQIFGTTFEITSRYSDLQPVGMGAFLVCSAKDNLTGSNVAVKKIMKPFSTPVL	60		
SAKA	MAEFVRAQIFGTTFEITSRYTDLQPVGMGAFLVCSARDQLTAQPVAVKKIMKPFSTPVL	60		
	****:*****:*** *****:*** . ** :*****			
	III	IV	V	
SAPK	SKRTYRELKLLKHLRHENIISLSDIFISPLEDIYFVTELLGTDLHRLLLTSRPLEKQFIQY	120		
SRM	SKRTYRELKLLKHLRHENIISLSDIFISPLEDIYFVTELLGTDLHRLLLTSRPLEKQFIQY	120		
HOG1P	SKRTYRELKLLKHLRHENIICLSDFISPLEDMYVTELLGTDLHRLLLTSRPLEKQFIQY	120		
FpHOG1	AKRTYRELKLLKHLKHENVISLSDIFISPLEDIYFVTELLGTDLHRLLLTSRPLEKQFIQY	120		
FgOS-2	AKRTYRELKLLKHLKHENVISLSDIFISPLEDIYFVTELLGTDLHRLLLTSRPLEKQFIQY	120		
OSM1	AKRTYRELKLLKHLKHENVISLSDIFISPLEDIYFVTELLGTDLHRLLLTSRPLEKQFIQY	120		
NcOS-2	AKRTYRELKLLKHLRHENVISLSDIFISPLEDIYFVTELLGTDLHRLLLTSRPLEKQFIQY	120		
BcSak1	SKRTYRELKLLKHLKHENVISLSDIFISPLEDIYFVTELLGTDLHRLLLTSRPLEKQFIQY	120		
SAKA	SKRTYRELKLLKHLRHENIISLSDIFISPLEDIYFVTELLGTDLHRLISSRPLEKQFIQY	120		
	:*****:***:*. *****:*. *****:*****			
	VI	VII	VIII	IX
SAPK	FLYQILRGLKYVHSAGVVHDXDLKPSNILVNENCDLKICDFGLARIQDPQMTGYVSTRYYR	180		
SRM	FLYQILRGLKYVHSAGVVHRDLKPSNILVNENCDLKICDFGLARIQDPQMTGYVSTRYYR	180		
HOG1P	FLYQILRGLKYVHSAGVVHRDLKPSNILINENCDLKICDFGLARIQDPQMTGYVSTRYYR	180		
FpHOG1	FLYQIMRGLKYVHSAGVVHRDLKPSNILVNENCDLKICDFGLARIQDPQMTGYVSTRYYR	180		
FgOS-2	FLYQIMRGLKYVHSAGVVHRDLKPSNILVNENCDLKICDFGLARIQDPQMTGYVSTRYYR	180		
OSM1	FLYQIMRGLKYVHSAGVVHRDLKPSNILVNENCDLKICDFGLARIQDPQMTGYVSTRYYR	180		
NcOS-2	FLYQIMRGLKYVHSAGVVHRDLKPSNILVNENCDLKICDFGLARIQDPQMTGYVSTRYYR	180		
BcSak1	FLYQILRGLKYVHSAGVVHRDLKPSNILVNENCDLKICDFGLARIQDPQMTGYVSTRYYR	180		
SAKA	FLYQIMRGLKYVHSAGVVHRDLKPSNILINENCDLKICDFGLARIQDPQMTGYVSTRYYR	180		
	*****:***** *****:*****			
	X	XI		
SAPK	APEIMLTWQKYDVEVDIWSAGCIFAEMLEGKPLFPGKDHVNQFSIITELLGAPPDDVIQT	240		
SRM	APEIMLTWQKYDVEVDIWSAGCIFAEMLEGKPLFPGKDHVNQFSIITELLGTPDDVIQT	240		
HOG1P	APEIMLTWQKYDVEVDIWSAGCIFAEMLEGKPLFPGKDHVNQFSIITELLGTPDDVIAT	240		
FpHOG1	APEIMLTWQKYDVEVDIWSAGCIFAEMLEGKPLFPGKDHVNQFSIITELLGTPDDVINT	240		
FgOS-2	APEIMLTWQKYDVEVDIWSAGCIFAEMLEGKPLFPGKDHVNQFSIITELLGTPDDVINT	240		
OSM1	APEIMLTWQKYDVEVDIWSAGCIFAEMLEGKPLFPGKDHVNQFSIITELLGTPDDVINT	240		
NcOS-2	APEIMLTWQKYDVEVDIWSAGCIFAEMLEGKPLFPGKDHVNQFSIITELLGTPDDVINT	240		
BcSak1	APEIMLTWQKYDVEVDVWSAGCIFAEMLEGKPLFPGKDHVNQFSIITELLGTPDDVIHT	240		
SAKA	APEIMLTWQKYDAKVDVWSAACIFAEMLLGAPLFPKGDHVNQFSIITELLGTPDDVIQT	240		
	***** .**.* ** ***** * *****			

SAPK	ICSENTLRFVQSLPKRERQPLS-----NKFKNAEP---QAVDLENMLVFDPKK	286
SRM	ICSENTLRFVQSLPKRERQPLA-----NKFKNAEP---DAVDLENMLVFDPRK	286
HOG1P	ICSENTLRFVQSLPKRERQPLK-----NKFKNADP---QAIELLERMLVFDPRK	286
FpHOG1	IASENTLRFVKSLSLPRERQPLR-----NKFKNADD---SAIDLLERMLVFDPKK	286
FgOS-2	IASENTLRFVKSLSLPRERQPLR-----NKFKNADD---SAIDLLERMLVFDPKK	286
OSM1	IASENTLRFVKSLSLPRERQPLK-----NKFKNADP---SAIDLLERMLVFDPKK	286
NcOS-2	IASENTLRFVKSLSLPRERQPLK-----NKFKNADS---SAVDLLERMLVFDPKK	286
BcSak1	IASENTLRFVQSLPKRERQPLA-----SKFTQADP---LAIDLLEKMLVFDPPRA	286
SAKA	ICSENTLRFVKSLSLPRERQDLAKLPLKFLALVHPDKKPEEDEDYKNTINLLKAMLVYNPKD	300
	*.*****:***** * * . * : : : : ** : ** : * :	
SAPK	RVRAEQALAHPYLAPYHDPXDEPIAEEKFDWSFNDADLPVDTWKIMMYSEILDYHNVDAA	346
SRM	RVRAEQALAHAYLAPYHDPTDEPVAEEKFDWSFNDADLPVDTWKIMMYSEILDYHNVDAA	346
HOG1P	RVKAGEALADPYLAPYHDPTDEPVAEEKFDWSFNDADLPVDTWKIMMYSEILDYHNVDAN	346
FpHOG1	RITATEALSHDYLSPYHDPTDEPVAEEKLDWSFNDADLPVDTWKIMMYSEILDYHNVEA-	345
FgOS-2	RITATEALAHDYLSPYHDPTDEPVAEEKFDWSFNDADLPVDTWKIMMYSEILDYHNVEA-	345
OSM1	RITATEALAHEYLTPYHDPTDEPIAEEKFDWSFNDADLPVDTWKIMMYSEILDYHNVEA-	345
NcOS-2	RITATEALSHEYLAPYHDPTDEPVAEEKFDWSFNDADLPVDTWKIMMYSEILDYHNVEAS	346
BcSak1	RIKAAEGLAHEYLSPYHDPTDEPAAEERFDWSFNDADLPVDTWKIMMYSEILDYHNVIN-	345
SAKA	RISAEAAALAPYLAPYHDETDEPVAEEKFDWSFNDADLPVDTWKIMMYSEILDFHNIDQG	360
	*: * .*: **:**** *** *:*: :*****:*****:***	
SAPK	AQEQENNGS-----	355
SRM	VQEQEN-GS-----	354
HOG1P	AEQAAHNDTVAG-----	359
FpHOG1	GVTNMEEPFNGQ-----	357
FgOS-2	GVTNMEEQFNGQ-----	357
OSM1	GMQQMDDQFTGQ-----	357
NcOS-2	GQMMFQEDVPPQ-----	358
BcSak1	DAQNLTESQ-----	354
SAKA	GDINPALVEGAGLNQQGFQ	379

Figure 27. Alignment of the predicted amino acid sequence of the putative osmolarity MAP kinase from *F. graminearum* and several fungal MAP kinases. The alignment was performed using the CLUSTAL W program. Identical amino acids are marked with “*”, similar amino acids are marked with dots. Gaps introduced for the alignment are indicated by hyphens. The protein kinase domains of the yeast/fungi stress-activated protein kinase subgroup are indicated by roman numerals (according to Hanks and Quinn 1991). The TGY-sequence required for kinase activation is highlighted in bold black letters (see Kültz, 1998). Genbank accession numbers for *N. crassa* osmotic sensitive-2 MAP kinase NcOS-2, *M. grisea* Osm1, *B. oryzae* SRM, *F. proliferatum* FpHOG1, *B. cinerea* BcSak1, *S. cerevisiae* HOG1P, *A. alternate* SAPK, *A. nidulans* SAKA, and *F. graminearum* FgOS-2 are AF297031.1, AF184980.1, AB242845.1, EF467357.1, AM236311.1, AAM64214.1, GU556629.1, AF282891.1, and XP_389788.1, respectively.

The high sequence similarity leads to the conclusion that FGSG_09612 (FgOS-2) encodes a stress-activated MAP kinase in *F. graminearum*. Ochiai et al. (2007a) described that *FgOS-2* deletion mutants were sensitive to osmotic and oxidative stresses but not to fungicide fludioxonil. $\Delta FgOS-2$ mutants exhibited an up-regulation of red pigment aurofusarin synthesis and a drastic reduction in DON production in *FgOS-2* deletion strains under *in-vitro* conditions (Ochiai et al., 2007a). In this study I describe new aspects of the stress-activated protein kinase signaling in *F. graminearum*.

3.2.2. Generation of *FgOS-2* deletion mutants

In order to study the impact of *FgOS-2* on the pathogenicity and development of *F. graminearum* the gene was deleted using a gene replacement approach (Fig. 28). For this purpose the 5'- and the 3'-flanking regions (1.34 kb upstream and 1.32 kb downstream fragments) were amplified by PCR and subsequently fused to a hygromycin resistance cassette. The excised replacement fragment was used to transform protoplasts of *F. graminearum* strain PH1. Hygromycin-resistant colonies were screened by diagnostic PCR (Fig. 28B and D): 6 out of 45 independent transformants showed homologous integration of the replacement fragment. All transformants showed amplification of the wild-type sequence, indicating that these strains were heterokaryotic. Single-spore isolations were performed to obtain homokaryotic deletion mutants, from which four stable homokaryotic deletion mutants were selected. One mutant was selected which showed the intact wild-type gene and ectopic integration of the vector (Fig. 28B and D). All of the selected mutants and the wild type were analysed in a Southern blot experiment. When hybridized with a probe for the hygromycin gene, all mutants showed a single integration of the fragment. No signal was obtained for the wild type (Fig. 28C). A probe amplified from the wild-type allele of *FgOS-2* generated a signal in the wild type and in one mutant, confirming this strain as being an ectopic strain (Fig. 28C). Four mutants showed no signal. Phenotypic characterization in terms of vegetative growth on different media (i.e. conferring salt, oxidative and fungicide stress), perithecia formation, conidia germination, and pathogenicity towards wheat and maize was performed using at least three independent mutants. Expression analysis was done using two independent mutants. Since all of the transformants showed a similar phenotype, one mutant (named $\Delta FgOS-2-1$) was chosen to illustrate the respective results in the figures (herein referred to as the $\Delta FgOS-2$ mutant). This $\Delta FgOS-2$ mutant was subsequently selected for fluorescent labelling using the red fluorescent protein dsRed.

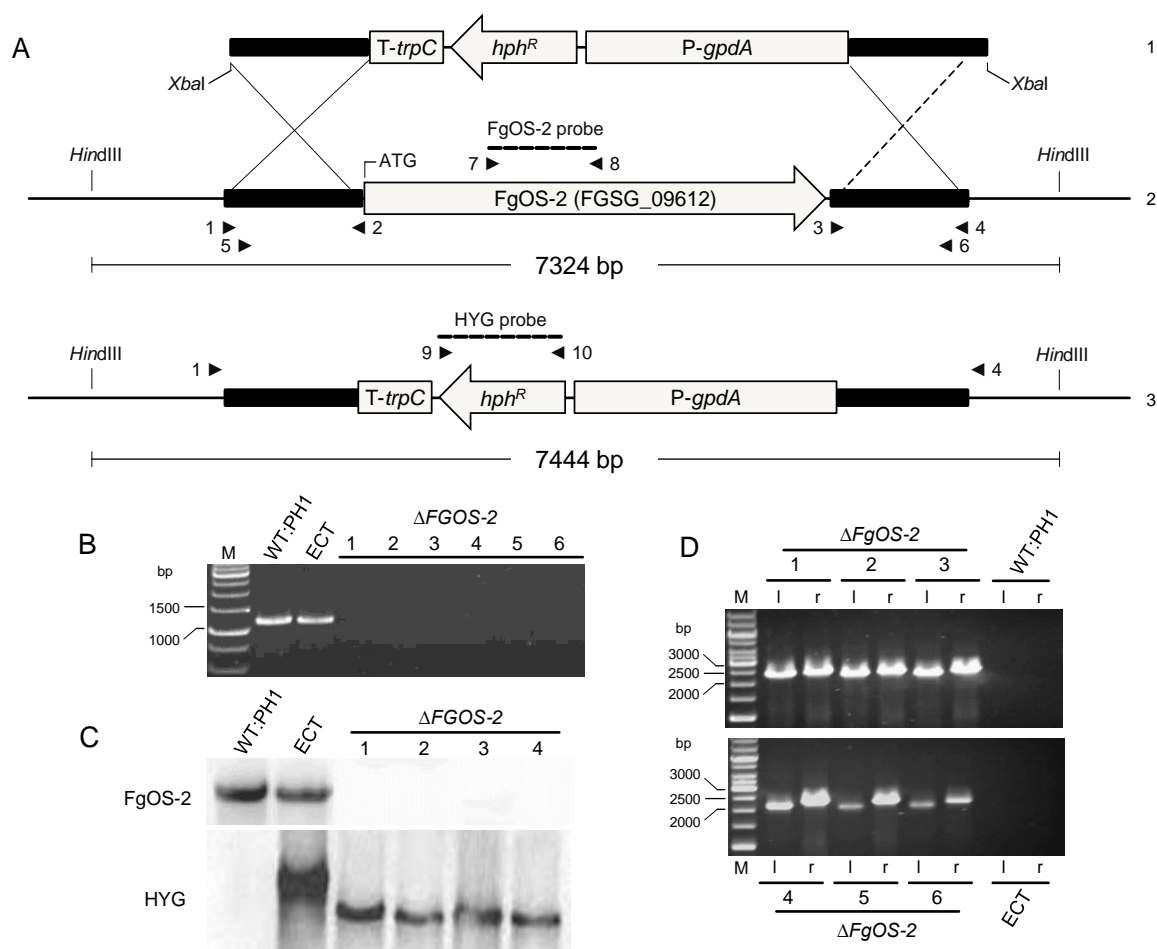


Figure 28. Replacement and Southern hybridization strategy for *FgOS-2*. **A.** Deletion of *FgOS-2* (2) by homologous recombination using a replacement fragment excised from pGEM-*FgOS-2*-HYG using restriction enzyme *Xba*I (1) (3: genotype of disrupted strains). Flanking regions are indicated as bold black lines. The gene flanks were fused to a hygromycin resistance cassette, consisting of the resistance gene (hygromycin B phosphotransferase, *hph*) and the *gpdA* promoter (*P-gpdA*) and *trpC* terminator (*T-trpC*) of *A. nidulans*. Primer binding sites for the fusion and diagnostic PCR are indicated as small arrows (numbering refers to Table 2). The regions used as probes for Southern analysis are represented by the dashed lines. Scheme is not to scale. **B, D.** PCR analysis of $\Delta FgOS-2$ and the wild type (WT:PH1). Deletion of *FgOS-2* was verified in six independent mutants using primers 7 and 8 (1.178 kb; **B**). Homologous integration of the replacement fragment was checked by PCR with primers 1 and 10 (l: left flank, 2.384 kb) and 4 and 9 (r: right flank, 2.498 kb; **D**). The wild type and ectopic strains were PCR-positive for the gene internal fragment, but not for the flank-spanning PCR. **C.** Southern analysis of $\Delta FgOS-2$ and the wild type. DNA of the mutant and wild type strains was digested using *Hind*III, separated on agarose gel, blotted on a membrane and probed with DIG-labelled probes for hygromycin (HYG) and a fragment of *FgOS-2*, respectively. Four disruption mutants lacked a signal when probed with the *FgOS-2* probe. The hygromycin probe hybridized both with wild-type and ectopic-strain DNA. Both probes had a signal in the ectopic strain only.

In the following, I will present results on the functional characterization of the stress-activated MAP kinase *FgOS-2* in *F. graminearum*. It is involved in the diverse physiological processes in *F. graminearum* life cycle.

3.2.3. *FgOS-2* deletion mutants are sensitive to osmotic stress but not to oxidative stress or fungicides

To test the vegetative growth on different media a plate assay was conducted using three independent deletion mutants, one ectopic strain and the wild type, respectively. When grown on agar plates containing basic medium (e.g. PDA), the mutant strains showed slightly retarded growth compared to the wild type (Fig. 29). Growth of the mutant strains completely ceased on agar plates supplemented with osmotic stress agents (0.3 M NaCl and KCl or 0.6 M sorbitol), whereas the wild type and ectopic strain showed no growth retardation (Fig. 29).

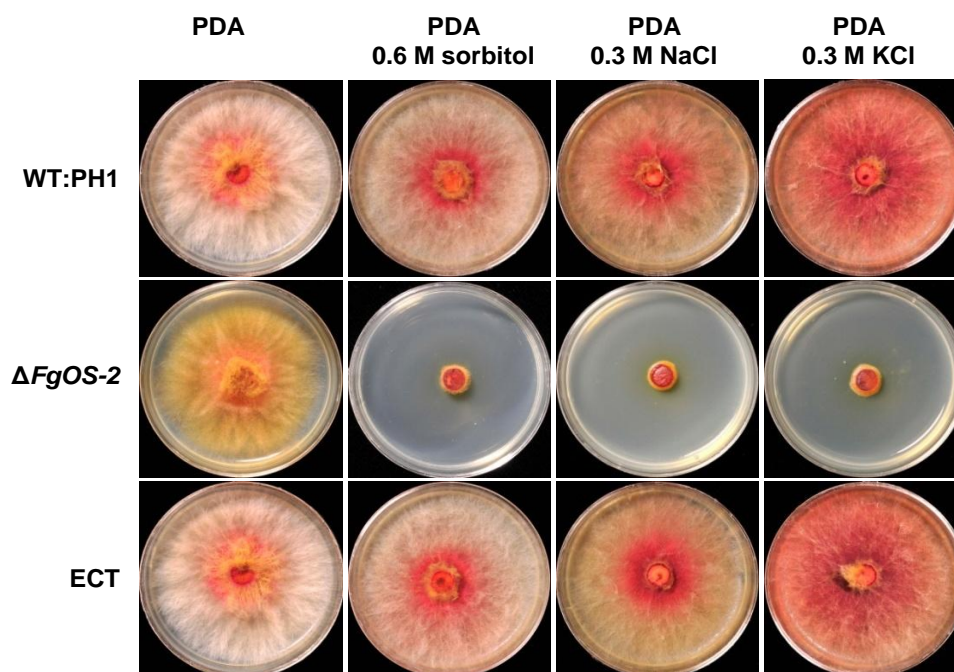


Figure 29. Colony morphology of the wild type (WT:PH1), ectopic (ECT) and *FgOS-2* deletion strains after 3 days of growth on the osmotic stress medium. The basic medium used was potato dextrose agar (PDA) inoculated with mycelial plugs from 3-day-old cultures. In order to test growth behaviour, this medium was supplemented with the osmotic agents: Sorbitol (0.6 M), NaCl (0.3 M) and KCl (0.3 M). Growth of the mutant was slightly retarded on the PDA with no supplement and nearly abolished on osmotic media. The wild type and ectopic strains showed no growth inhibition on all media tested.

The germination of the mutant's conidia in the presence of 0.8 M NaCl was different compared to the wild type: The characteristic swelling of the conidial compartments immediately before and during germination (Seong et al., 2008) was not observed in the mutants (Fig. 30B and C). Also, the germination rate was reduced to about 65% (Fig. 30A). Conidia of the $\Delta FgOS-2$ strains always germinated out of one compartment close to the centre of the spore, whereas the wild type conidia germinated out of 2-3 compartments (Fig. 30B and C). The germ tubes of the deletion mutants were malformed and growth ceased after only a few micrometres of growth (Fig. 30B and C). 4',6-diamidino-2-phenylindole (DAPI) staining

revealed that the germ tube of the deletion mutants was polyenergid (>10 nuclei) and not septated, whereas in the wild type one compartment contained 2-3 nuclei (Fig. 30C). On the non-osmotic medium no obvious difference in conidial germination or initial mycelial growth was apparent.

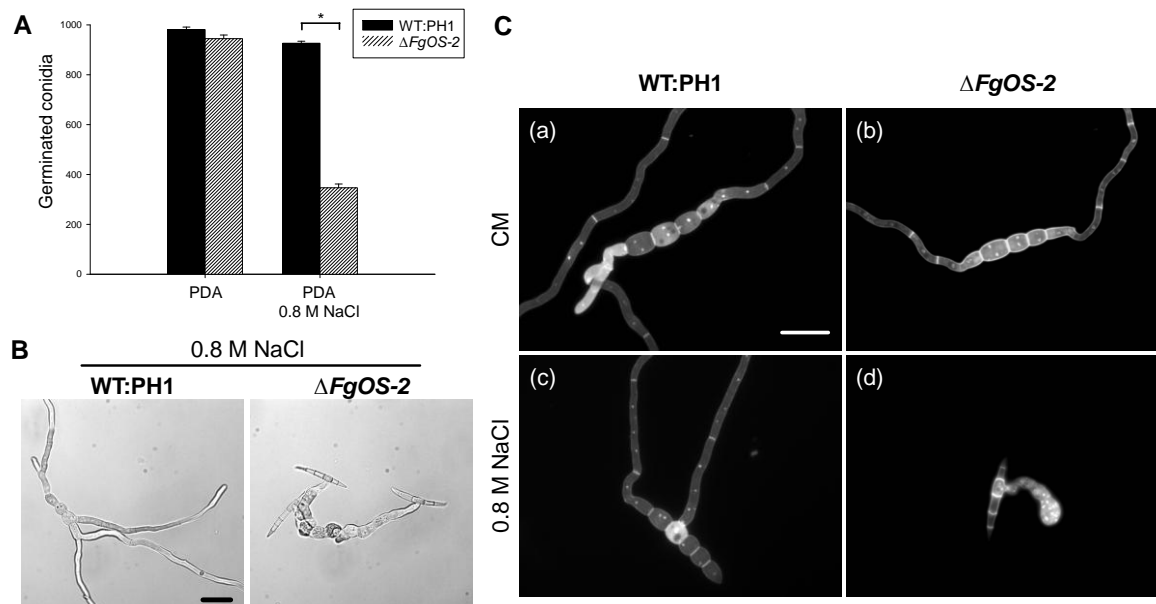


Figure 30. Conidia germination assay. **A.** Approximately 1000 conidia of the wild type and *FgOS-2* deletion strains were plated onto potato dextrose agar (PDA) and PDA supplemented with NaCl (0.8 M). The number of germinated conidia was counted. The germination rate of mutant conidia was significantly reduced ($P = <0.001$, *t*-test). Error bars indicate the standard deviation ($n=6$). The experiments were performed in triplicate. **B.** Bright-field microscopy of germinating conidia on the osmotic medium (0.8 M NaCl). The wild-type conidia formed multiple normally shaped germ tubes. The $\Delta FgOS-2$ germ tubes generally emerged from one conidial compartment and were malformed. **C.** Fluorescence microscopy of germinating conidia on PDA and PDA containing 0.8 M NaCl. The nuclei were stained with DAPI. Germ tubes emerging from wild-type conidia on the osmotic medium (**c**) and from wild type and mutant conidia on non-osmotic media (**a** and **b**), normally containing 2-3 nuclei. Malformed germ tubes of the $\Delta FgOS-2$ mutant contained numerous nuclei (**d**). Scale bar: 10 μm .

In order to test the response to oxidative stress, CM plates were supplemented with 0, 10, 15 and 20 mM H_2O_2 . With increasing concentrations of H_2O_2 in the media, growth of the wild type diminished, whereas growth of the mutant strains was only slightly inhibited. On plates supplemented with 20 mM H_2O_2 for 4 days the wild type was significantly reduced in growth compared to $\Delta FgOS-2$ mutants (Fig. 31). Thus, the mutants grew better than the wild type under oxidative stress conditions. This result contradicts previous findings, that *FgOS-2* mutants are more sensitive towards oxidative stress (Ochiai et al. 2007a).

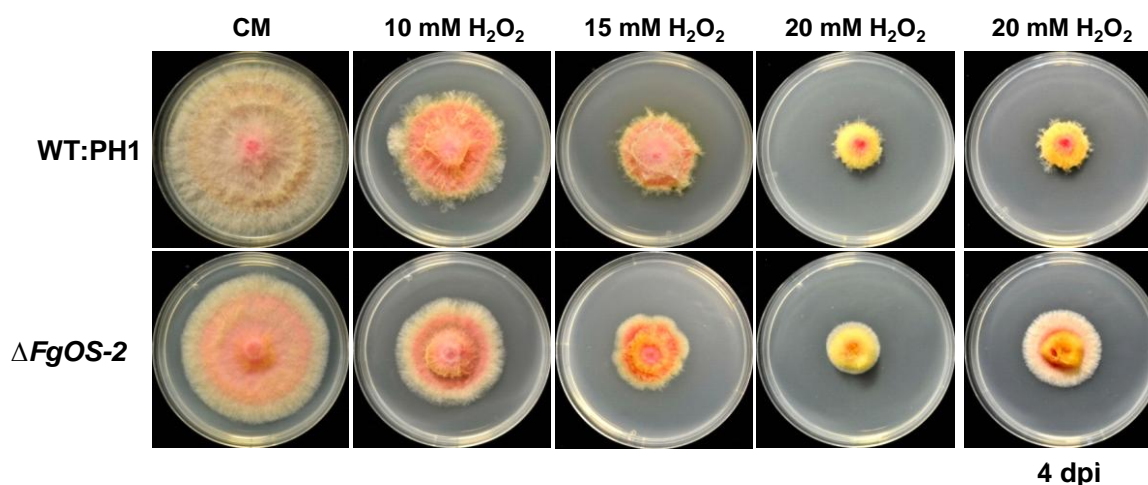


Figure 31. Agar plate assay for oxidative stress. Colony morphology of the wild type (WT:PH1) and *FgOS-2* deletion strains after 3 days or 4 days of growth on agar plates. The basic medium was complete medium (CM) inoculated with mycelial plugs from 3-day-old cultures. Media were supplemented with H_2O_2 as indicated.

No differences in growth performance between the wild type and $\Delta FgOS-2$ mutants were observed on agar plates containing different nitrogen sources ($NaNO_3$, $(NH_4)_2SO_4$, and Glutamin each 5 mM; Fig. 32).

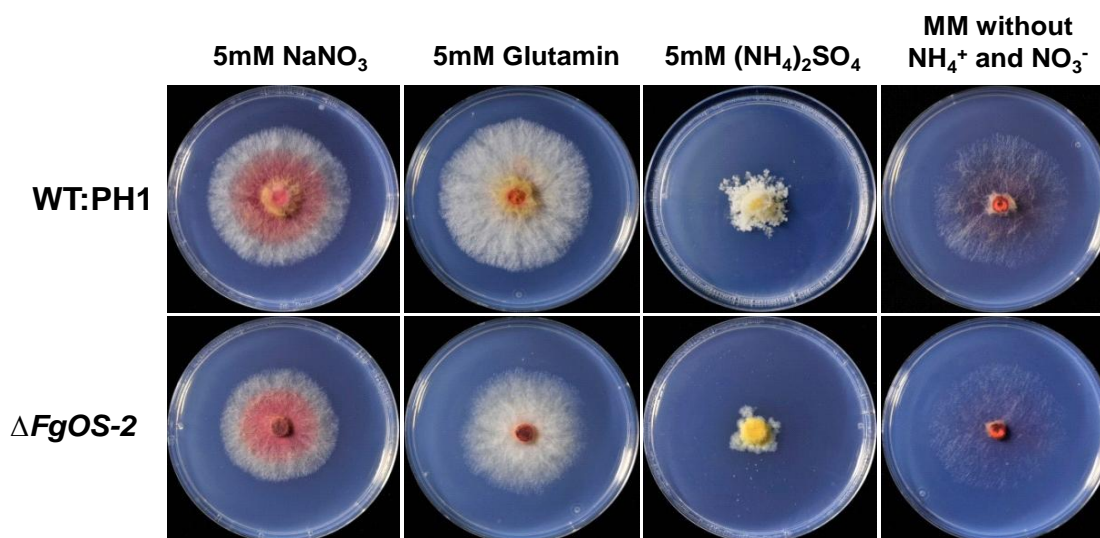


Figure 32. Agar plate assay for different nitrogen sources. Colony morphology of the wild type (WT:PH1) and *FgOS-2* deletion strains after 3 days of growth on agar plates. The basic medium was minimal medium (MM) inoculated with mycelial plugs from 3-day-old cultures. Media were supplemented with nitrogen sources as indicated.

On medium buffered to certain pH values (pH 5, 7 and 9; Fig. 33) and on plates incubated at different temperatures (18, 30 and 32 °C; Fig. 34), the wild type and $\Delta FgOS-2$ mutant strains also showed no difference in growth.

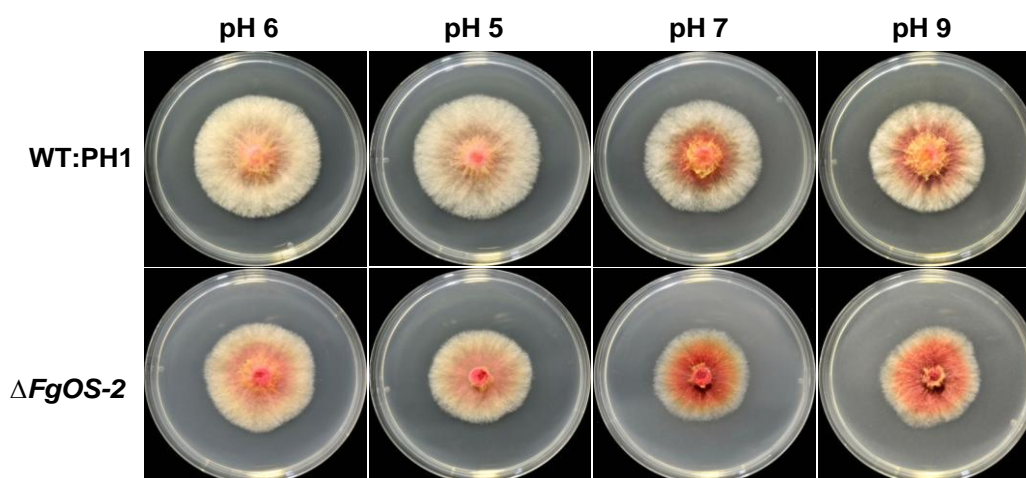


Figure 33. Agar plate assay for different pH values. Colony morphology of the wild type (WT:PH1) and *FgOS-2* deletion strains after 3 days of growth on agar plates. The basic medium was complete medium (CM) inoculated with mycelial plugs from 3-day-old cultures. Media were adjusted to certain pH values as indicated.

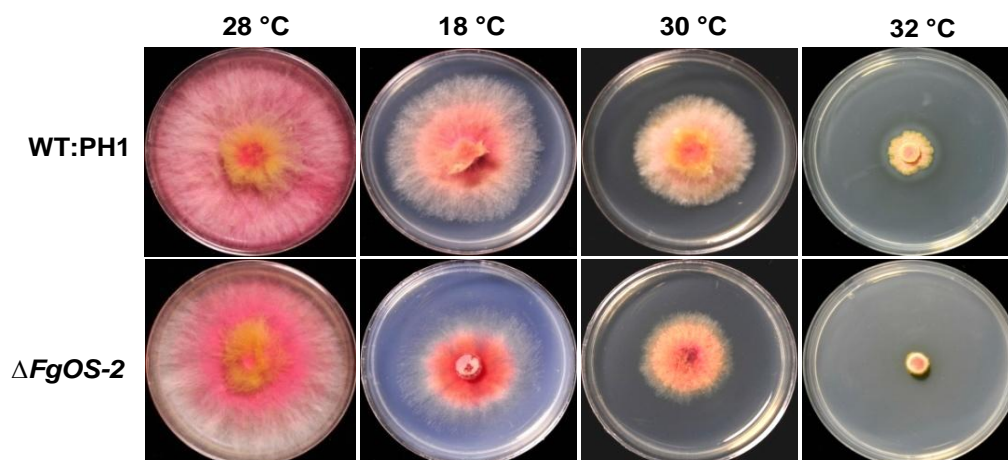


Figure 34. Agar plate assay for different temperatures. Colony morphology of the wild type (WT:PH1) and *FgOS-2* deletion strains after 3 days of growth on complete medium (CM) agar plates inoculated with mycelial plugs from 3-day-old cultures.

Previous results obtained for other fungi showed that HOG1 contribute to resistance against antibiotics. Strains defective in the HOG1-homologue of *C. lagenarium*, *Osc1*, showed partial resistance towards fludioxonil (Kojima et al., 2004) and knock-out mutants in different isolates of *B. cinerea* showed distinct degrees of resistance towards fludioxonil and iprodione (Segmüller et al., 2007; Liu et al., 2008). Strains defective in *FgRrg1* are also partially resistant towards fludioxonil (Jiang et al., 2011). *F. graminearum* wild type and three independent *FgOS-2* knock-out mutants were assayed on plates containing fludioxonil (phenylpyrrole), iprodione

(dicarboximide) and azoxystrobin (aromatic carbon hydrates; Fig. 35A). The absence of *FgOS-2* led to a strongly increased resistance towards fludioxonil. Growth of the wild type completely ceased at a concentration of 0.5 mg l⁻¹, while the mutants were able to grow almost as well as it did on CM control plates. Microscopic analysis of the germinating conidia on 0.5 mg l⁻¹ fludioxonil revealed an abnormal morphology of wild-type hyphae. Starting at the conidial compartments the hyphae were swollen and frequently burst. In contrast, hyphae of the mutants appeared to be unaffected (Fig. 35B). Expression analysis using quantitative real time polymerase chain reaction (qRT-PCR) revealed an up-regulation in the transcript level of the glycerol-3-phosphate phosphatase (G3PP) gene in the wild type under fludioxonil stress (Fig. 35C), indicating an increased production of glycerol. In $\Delta FgOS-2$ mutants, G3PP expression remained unchanged on fludioxonil compared to CM. These *in vitro* experiments demonstrated, that proper response to oxidative, osmotic, and fungicide stress in *F. graminearum* depends on FgOS-2 function. This applies both for hyphal growth and for conidia germination.

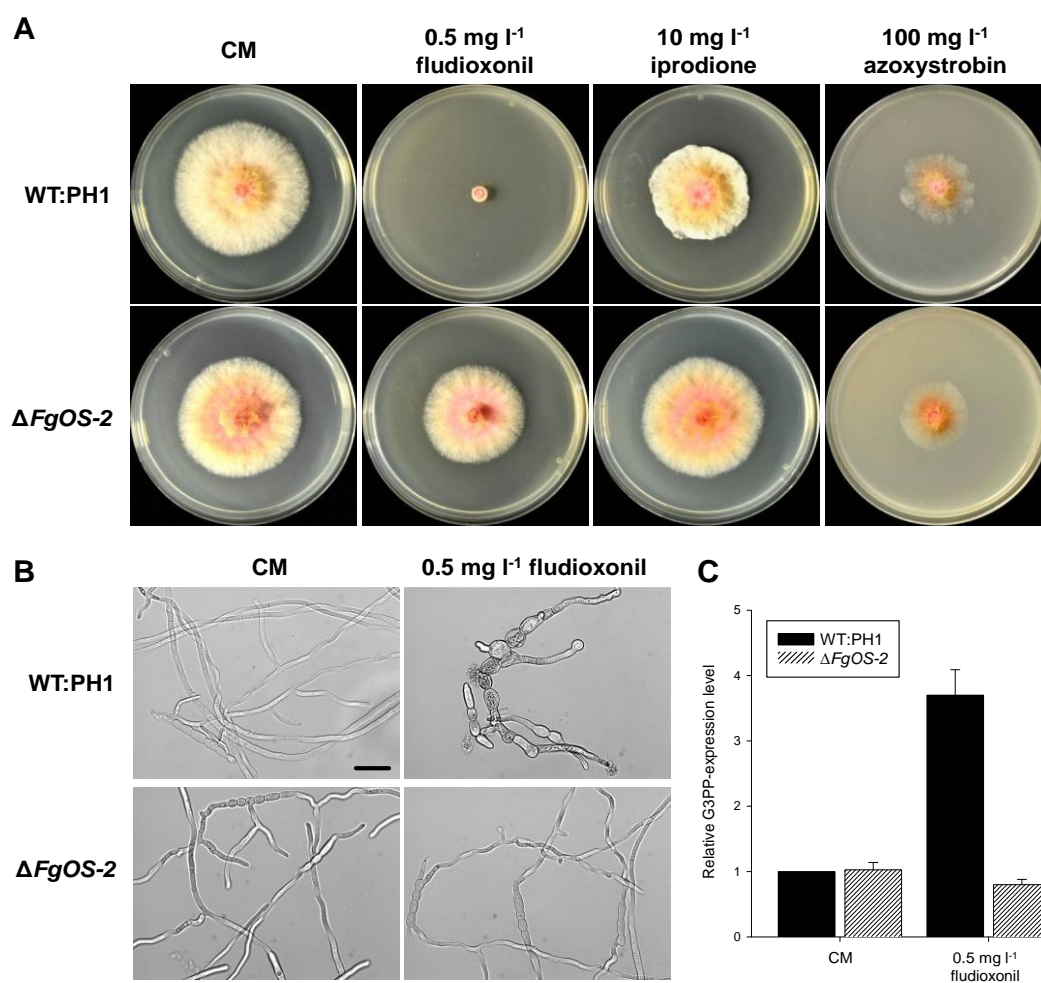


Figure 35. Fungicide sensitivity assay. **A.** Colony morphology of the wild type (WT:PH1) and *FgOS-2* deletion strains after 3 days of growth on agar plates. The basic medium was complete medium (CM) inoculated with mycelial plugs from 3-day-old cultures. In order to test growth behavior, the

Figure 35 continuance

medium was supplemented with the antibiotics fludioxonil (0.5 mg l^{-1}), iprodione (10 mg l^{-1}), and azoxystrobin (100 mg l^{-1}). Growth of the mutant was slightly retarded on the CM medium with no supplement. On media containing fludioxonil and iprodione, the growth of the mutant strain increased compared to that of the wild type, which was not able to grow at all on 0.5 mg l^{-1} fludioxonil. The mutant and the wild types showed a similar sensitivity towards azoxystrobin. **B.** Conidia germination assay. Conidia of the wild type and $\Delta FgOS-2$ mutant strains were germinated on CM and CM containing 0.5 mg l^{-1} fludioxonil, respectively. Pictures were taken 16 hpi. Both strains showed a normal germination pattern on CM. For the wild type on fludioxonil, the conidial compartments and hyphae emerging from the conidia appeared to be swollen and often burst. Germination of mutant conidia was not affected. Scale bar: $10 \mu\text{m}$. **C.** Gene expression analysis. Quantitative RT-PCR of the gene encoding a putative glycerol-3-phosphate phosphatase (G3PP). G3PP expression was higher in the wild type in medium containing 0.5 mg l^{-1} fludioxonil compared to $\Delta FgOS-2$ mutant. On CM, the expression of G3PP in both strains was equal. Error bars indicate the standard deviation. QRT-PCR was performed in triplicate.

3.2.4. FgOS-2 is involved in sexual but not asexual reproduction

F. graminearum is able to complete its entire life cycle in axenic culture. Perithecia formation, representing sexual reproduction, can be induced on wheat nodes (Guenther and Trail, 2005) or on carrot agar (Leslie and Summerell, 2006). The wild type produces perithecia on both substrates after 3-4 weeks of incubation (Fig. 36A). Inside the perithecia are numerous asci with eight four-celled ascospores (Fig. 36B). In two independent $\Delta FgOS-2$ mutants the formation of perithecia was completely abolished (Fig. 36A, lower panel). This indicates that FgOS-2 plays a major role in sexual reproduction. Interestingly, the deletion mutants and the wild type produced nearly equal amounts of conidia.

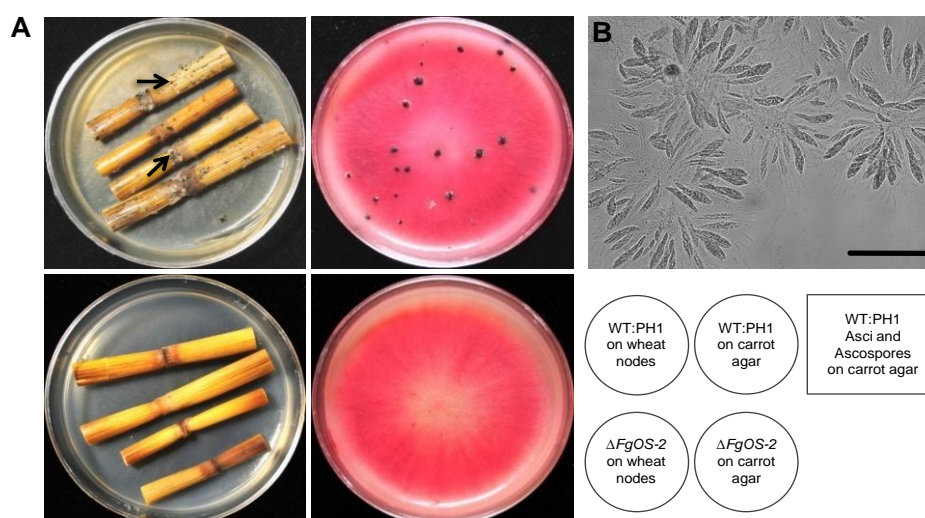


Figure 36. Assay for perithecia formation. Conidia of the wild type (WT:PH1) and *FgOS-2* deletion strains were placed on detached wheat nodes (on water agar) and on carrot agar (**A**). After 21 days of incubation, the wild type had produced numerous clusters of perithecia (arrows on wheat nodes and black dots on carrot agar) on both substrates. Squeezing these clusters released the asci (**B**). The mutant strain completely failed to produce perithecia on both substrates tested. Scale bar $20 \mu\text{m}$.

3.2.5. The deletion of *FgOS-2* leads to reduced virulence towards wheat and maize

Deletion mutants of HOG1 homologues in *M. oryzae* and *B. cinerea* showed opposite phenotypes regarding their pathogenic potential. Whereas *M. oryzae* strains remained fully virulent (Dixon et al., 1999), *B. cinerea* mutants failed to colonize unwounded plant tissues (Segmüller et al., 2007). In order to address this question in $\Delta FgOS-2$ strains, we performed infection assays on both wheat heads and maize cobs using three independent $\Delta FgOS-2$ strains, one ectopic strain, the wild type and water as the negative control. Maize infection was evaluated 35 days post inoculation (dpi) according to the disease severity rating (dsr) proposed by Reid et al. (1996). The wild type almost infected the entire maize cob (Fig. 37A; dsr: 7), whereas the cobs inoculated with the mutant strains showed no or only marginal disease symptoms (Fig. 37A; dsr: 1). Maize cobs inoculated with water remained completely symptomless. In order to determine whether or not *FgOS-2* is also involved in pathogenicity towards wheat, we performed point-inoculation infection assays on the highly susceptible wheat cultivar Nandu. For this experiment, the wild type, three independent $\Delta FgOS-2$ strains and one ectopic strain were assayed on 30 wheat heads. All infected wheat ears showed typical FHB-disease symptoms (bleaching, reduced kernel formation) when infected with the wild type (Fig. 37A) and the ectopic strain. The infection symptoms became visible approximately 5 dpi, starting in the inoculated spikelet and propagating throughout the entire wheat head within 21 dpi, when the infection assay was finally evaluated (Fig. 37A). Spikes infected with *FgOS-2* deletion strains showed a severe reduction in disease symptoms during the infection assay. The infection never spread to the spikelets adjacent to the point-infected ones (Fig. 37B).

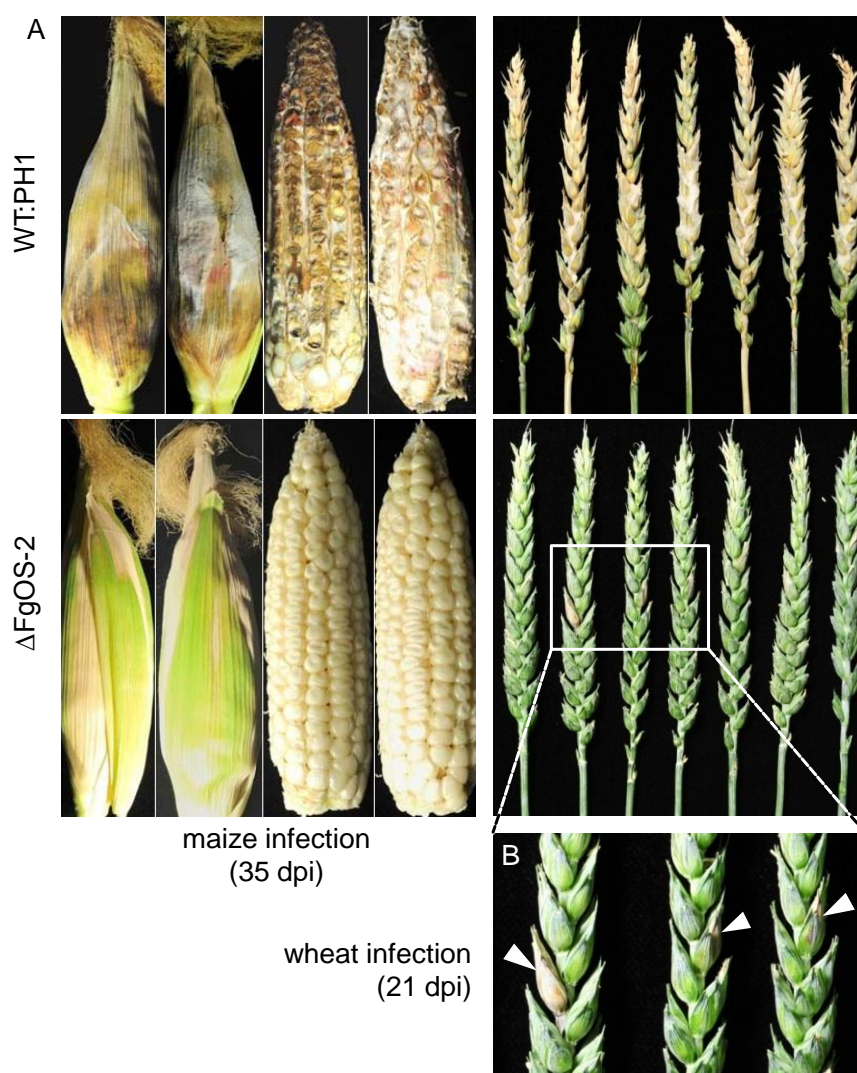


Figure 37. Pathogenicity assay on wheat and maize. Maize cobs (A, left) and wheat heads (A, right) were infected with conidia of the wild type and *FgOS-2* deletion strains and incubated for 35 (maize) and 21 (wheat) days. The mutant strain caused nearly no disease symptoms on maize and the infection of wheat stopped in the inoculated spikelet (arrow heads in B). The wild-type strain infection caused symptoms typical for maize cob rot and *Fusarium* head blight (FHB) disease. The maize infections were repeated six times, the wheat infections were performed 30 times.

In order to further analyse the infection process *in planta*, one deletion mutant and the wild type strains that constitutively expressed the red fluorescent protein dsRed in the cytosol were constructed. Using these strains I again infected wheat spikelets. After 5 dpi the mycelium of the strain derived from the wild type was observed in the infected spikelet and, after 7 dpi, it was also observed in the adjacent spikelet (Fig. 38), indicating that the hyphae successfully crossed the transition zone between the rachis node and the rachis, which was previously shown to be critical for the spread of infection to occur (Jansen et al., 2005; Voigt et al., 2007). After 5 dpi disease symptoms and dsRed-fluorescence were hardly detectable in the spikelets inoculated with the strain derived from the $\Delta FgOS-2$ -strain (Fig. 38). At 7 dpi, the inoculated spikelet was partially colonized by the $\Delta FgOS-2$ -dsRed-strain (Fig. 38). However, no

fluorescence and thus no growth of this strain were detectable within or beyond the rachis node (Fig. 39).

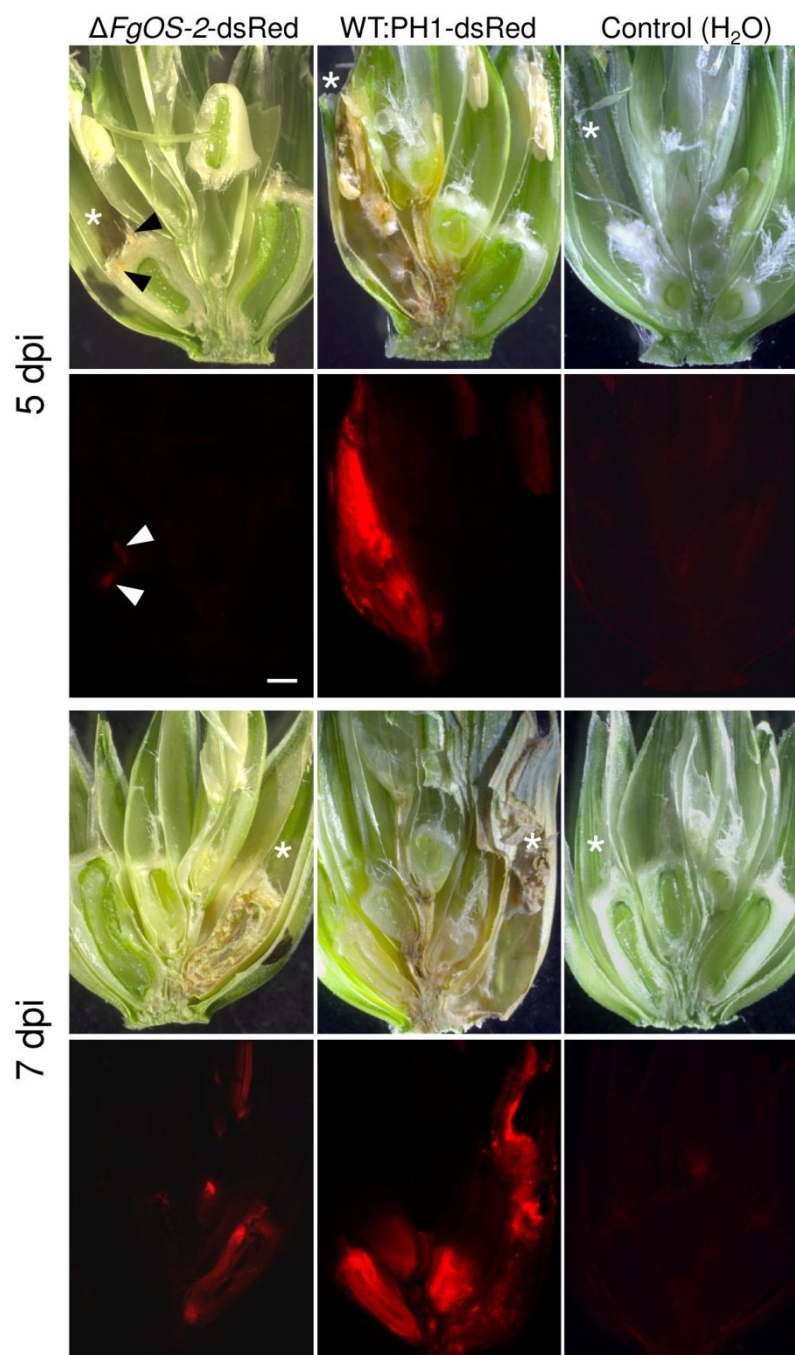


Figure 38. Infection assay. Cross-sections of inoculated wheat spikelets. The spikelets were infected with strains that constitutively expressed dsRed in the cytosol and that were derived from the wild type and a $\Delta FgOS-2$ -strain. Water was used as the control. Overview cross-section including the inoculated spikelet and adjacent tissues (rachis node, rachis and adjacent spikelets), 5 and 7 dpi, respectively. The inoculation points are indicated with white asterisks. The $\Delta FgOS-2$ strain weakly infected the inoculated spikelet, beginning at the stigmatic hairs (arrowheads). Bright-field microscopy revealed small necrotic lesions at the infection site at 5 dpi and complete colonization of the caryopse at 7 dpi. The dsRed-expressing wild-type derivative strain showed complete necrosis of the infected spikelet after 5 dpi. DsRed-fluorescence was evenly distributed throughout the spikelet. Scale bar 1 mm.

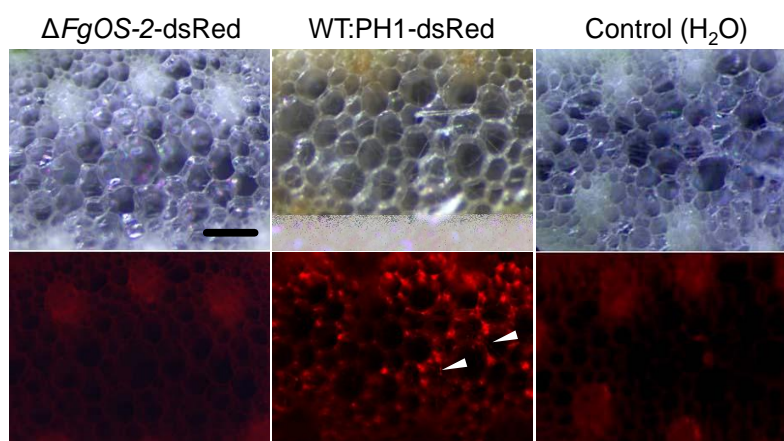


Figure 39. Infection assay. Cross-sections of wheat rachis nodes inoculated with dsRed-expressing wild type (WT:PH1) and $\Delta FgOS-2$ mutant strains, and water (at a time point of 7 dpi). No dsRed fluorescence was detectable in the samples inoculated with the $\Delta FgOS-2$ mutant strain and in the water control. In the wild-type derivative strain, hyphae can be seen inside the vascular system and in the apoplast between the cells. Scale bar 0.1 mm.

3.2.6. Secondary metabolism is controlled by FgOS-2

When grown on CM plates, the colonies of the mutant strains produced more red pigmentation compared to the wild type, indicating an up-regulation of aurofusarin production (Fig. 40A). This observation was already made by Ochiai and co-workers (2007a). This result was verified by qRT-PCR analysis on genes involved in the regulation of aurofusarin production. The expression of *gip1* (putative laccase gene; (Kim et al., 2005a), *gip2* (transcription factor; (Kim et al., 2006) and *pks12* (type 1 polyketide synthase; (Kim et al., 2005a); (Malz et al., 2005) was drastically up-regulated in the mutant compared to the wild type both *in vitro* and during wheat infection (Fig. 40B and Table 11).

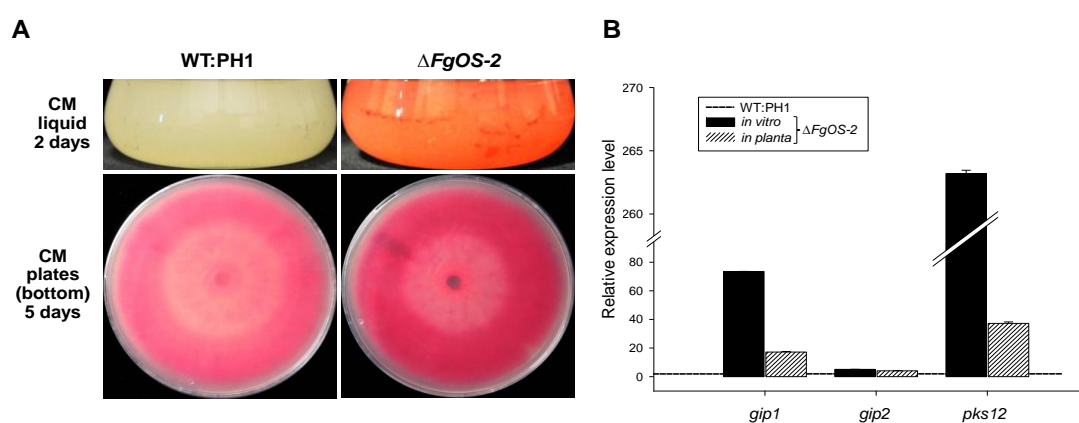


Figure 40. Pigmentation assay and corresponding gene expression analysis. **A.** Aurofusarin production in liquid CM medium and on CM agar plates. Aurofusarin biosynthesis was up-regulated in the $\Delta FgOS-2$ strain compared to the wild type (WT:PH1). **B.** Quantitative RT-PCR on genes involved in aurofusarin biosynthesis, *gip1* (encoding a putative laccase), *gip2* (transcription factor) and *pks12* (polyketide synthase). Expression of *gip1* and *pks12* was massively up-regulated in the $\Delta FgOS-2$ strain compared to the wild type (expression level set at 1) *in planta* and *in vitro*. Error bars indicate the standard deviation. QRT-PCR was performed in triplicate.

Table 11. Gene expression analysis of genes involved in aurofusarin biosynthesis. Quantitative real-time PCR results indicate up or down regulation in the $\Delta FgOS-2$ mutant compared to the wild type (set at 1). Expression analysis was performed using two biological and three technical replicates. Gene expression was normalized against β -tubulin gene expression.

Aurofusarin biosynthesis	<i>gip1</i>	<i>gip2</i>	<i>pks12</i>
CM	73,5167±0,072	5,098 ±0,066	263,197±0,267
<i>in planta</i>	17,1743±0,434	4,1045±0,085	37,2439±1,004

In contrast to aurofusarin, DON production is important for full virulence (Proctor et al., 1995) towards wheat. Mutants defective in the key enzyme of trichothecene biosynthesis, Tri5, failed to cross the transition zone between the rachis and the rachis node and thus failed to propagate from one spikelet to the next (Jansen et al., 2005). Since the pathogenicity assay using $\Delta FgOS-2$ mutants revealed the same phenotype, it is feasible that the mutants were impaired in DON production during infection and in the axenic culture. In this study, spikes inoculated with the wild type and $\Delta FgOS-2$ mutant strains were tested for toxin production using a highly sensitive ELISA test. Spikelets inoculated with the deletion strains only accumulated approximately 9% and 2% of the wild-type level of DON after 3 and 7 days, respectively, normalized to the amount of fungal material (Fig. 41a and Table 12). Interestingly, DON production was also reduced by about 60% on inoculated wheat kernels in the mutant strains compared to the wild type (Table 12 and Fig. 41c). In a third assay, in which DON production was induced in liquid induction medium (Harris et al., 2007) the deletion strains, surprisingly showed a relatively higher DON production compared to the wild type. After an incubation period of 1 day, the supernatant of the wild-type culture contained about 30% less DON than the mutant culture. After 3 days, the deletion mutants accumulated around 50% more DON than the wild type (Table 12 and Fig. 41b). All toxin measurements were performed on two independent mutants and in four replicates and normalized to the amount of fungal material in the sample determined by quantitative PCR (Voigt et al., 2007). The ELISA measurements were substantiated by expression analyses of genes related to toxin production (Fig. 41d-f, Table 13). Table 13 gives an overview on the relative expression levels (wild type level is set at 1). Surprisingly, although DON production was greater in the mutant strains in axenic culture, trichodiene synthase (*tri5*) and cytochrome P450 monooxygenase (*tri4*) gene expression was reduced compared to the wild type (Fig. 41e and Table 13). However, expression of the regulatory gene *tri10* and transcription factor *tri6*

was up-regulated in the mutant strains (Fig. 41e and Table 13) compared to the wild type. During plant infection (7 dpi) the expression of *tri4*, *tri5*, *tri6* and *tri10* was reduced in the mutant strains compared to the wild type (Fig. 41d and Table 13).

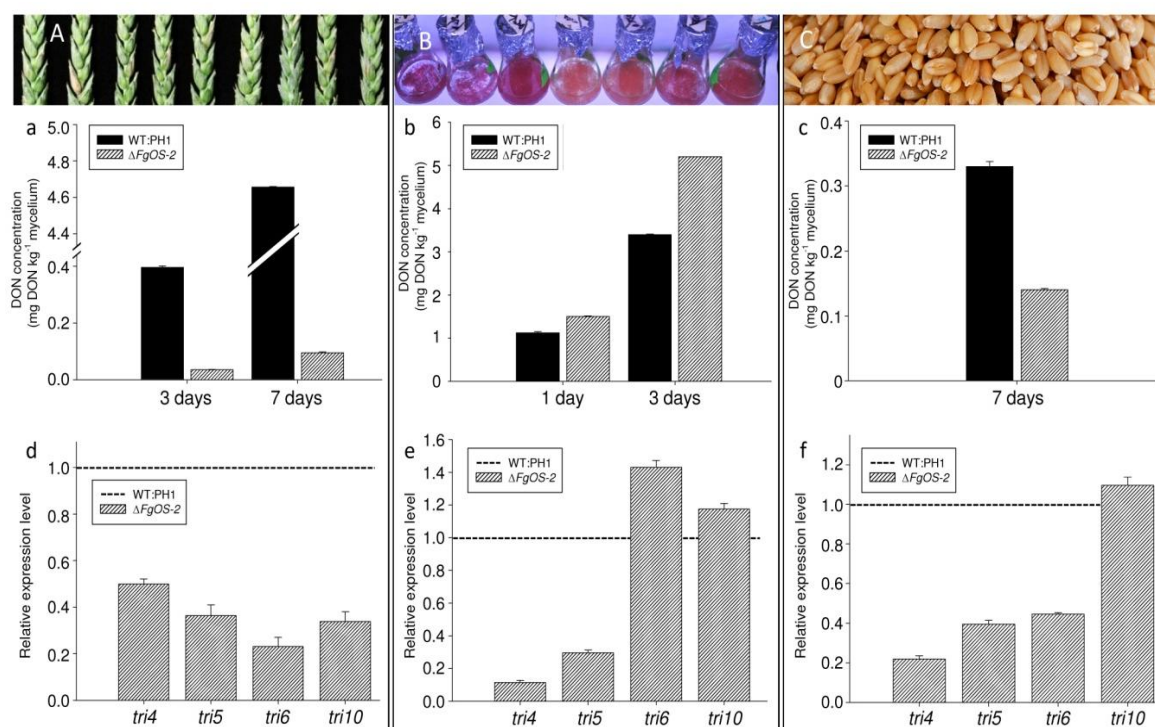


Figure 41. DON concentration and gene expression analysis of the wild type and *FgOS-2* deletion strains in wheat heads (A), submerged culture (B) and wheat kernels (C). a-c. The DON concentration was determined by ELISA. The DON contents in wheat spikelets and kernels inoculated with the Δ*FgOS-2*-mutant were lower compared to the wild type (WT:PH1) at the time points tested. *In vitro*, DON production was induced using (NH₄)₂SO₄ as the sole nitrogen source. The mutant produced more DON in this medium compared to the wild type. The DON concentration was normalized against the amount of fungal mycelium per kilogram of substrate, determined by quantitative PCR. d-f. Quantitative RT-PCR analysis of the wild type and *FgOS-2* deletion strains during the colonization of wheat florets (7 dpi; d), *in-vitro* culture (3 dpi; e), and wheat kernels (7 dpi; f). Gene expression data were generated for the genes *tri4* (encoding a P450 monooxygenase), *tri5* (trichodiene synthase), *tri6* and *tri10* (both transcription regulators) and normalized to β-tubulin expression (primer list: Table. 4). The expression of *tri4* and *tri5* was lower in the mutant strain in all samples assayed when compared to the wild type. The expression of *Tri6* was higher under *in vitro* DON-inducing conditions. Except for the wheat head sample, the expression of *tri10* was slightly up-regulated in the mutant strain compared to the wild type. Quantitative RT-PCR was performed twice, with three replicates each. Wild-type expression was set at 1. DON production measurements were repeated twice with four replicates each. Error bars indicate the standard deviation.

Table 12. ELISA analysis of DON production under different growth conditions in the wild type and $\Delta FgOS-2$ mutant strains. All values were normalized against the amount of fungal material in the sample using qPCR (see Materials and Methods).

	DON (mg kg ⁻¹ mycelium)				
	<i>in vitro</i>		wheat kernels	<i>in planta</i>	
	1 dpi	3 dpi	7 dpi	3 dpi	7 dpi
WT:PH1	1.1 (±0.026)	3.4 (±0.012)	0.33 (±0.008)	0.4 (±0.0028)	4.66 (±0.0113)
$\Delta FgOS-2$	1.5 (±0.012)	5.2 (±0.0042)	0.14 (±0.002)	0.04 (±0.0374)	0.09 (±0.0284)

Table 13. Gene expression analysis of genes involved in DON biosynthesis. Quantitative real-time PCR results indicate up or down regulation in the $\Delta FgOS-2$ mutant compared to the wild type (set at 1). Expression analysis was performed using two biological and three technical replicates. Gene expression was normalized against β -tubulin gene expression.

DON biosynthesis	<i>tri4</i>	<i>tri5</i>	<i>tri6</i>	<i>tri10</i>
Toxin induction medium	0,4777±0,025	0,7795±0,038	1,2202±0,088	1,5814±0,329
wheat kernel	0,2189±0,016	0,3940±0,020	0,4454±0,008	1,0961±0,042
<i>in planta</i>	0,5±0,0208	0,3643±0,046	0,2311±0,040	0,3392±0,041

The third secondary metabolite under investigation is ZEA. Also ZEA biosynthesis *in vitro* was different from that *in planta*. The ELISA analyses revealed no significant difference in the ZEA contents between the deletion strains and the wild type (Table 14 and Fig. 42b) when grown in YES medium (Gaffoor et al., 2005). However, the production of ZEA was found to be significantly reduced to approximately 20% of the wild-type level in wheat heads inoculated with the mutant strains (Table 14 and Fig. 42a). All toxin measurements were performed on two independent mutants and in four replicates and normalized to the amount of fungal material in the sample determined by quantitative PCR (Voigt et al. 2007). Accordingly, genes involved in the regulation of ZEA production were screened by qRT-PCR. Although ZEA production *in planta* was significantly lower in $\Delta FgOS-2$ mutants, expression of the regulatory transcription factor (*zeb2*) was higher in the mutant compared to the wild type. However, expression of the isoamyl alcohol oxidase *zeb1* and of the non-reducing polyketide synthase

zea1 was reduced *in planta* compared to the wild type (Fig. 42c and Table 15). Under *in-vitro* conditions the expression of all of the genes was almost the same in both strains (Fig. 42d and Table 15). To the best of our knowledge, these results describe, for the first time, the signalling cascade of ZEA production and underline the key role of FgOS-2 in the regulation of mycotoxin production in *F. graminearum* during plant infection. Furthermore, these results emphasize the differences in the regulation of mycotoxin biosynthesis between *in-vitro* and *in-planta* growth conditions.

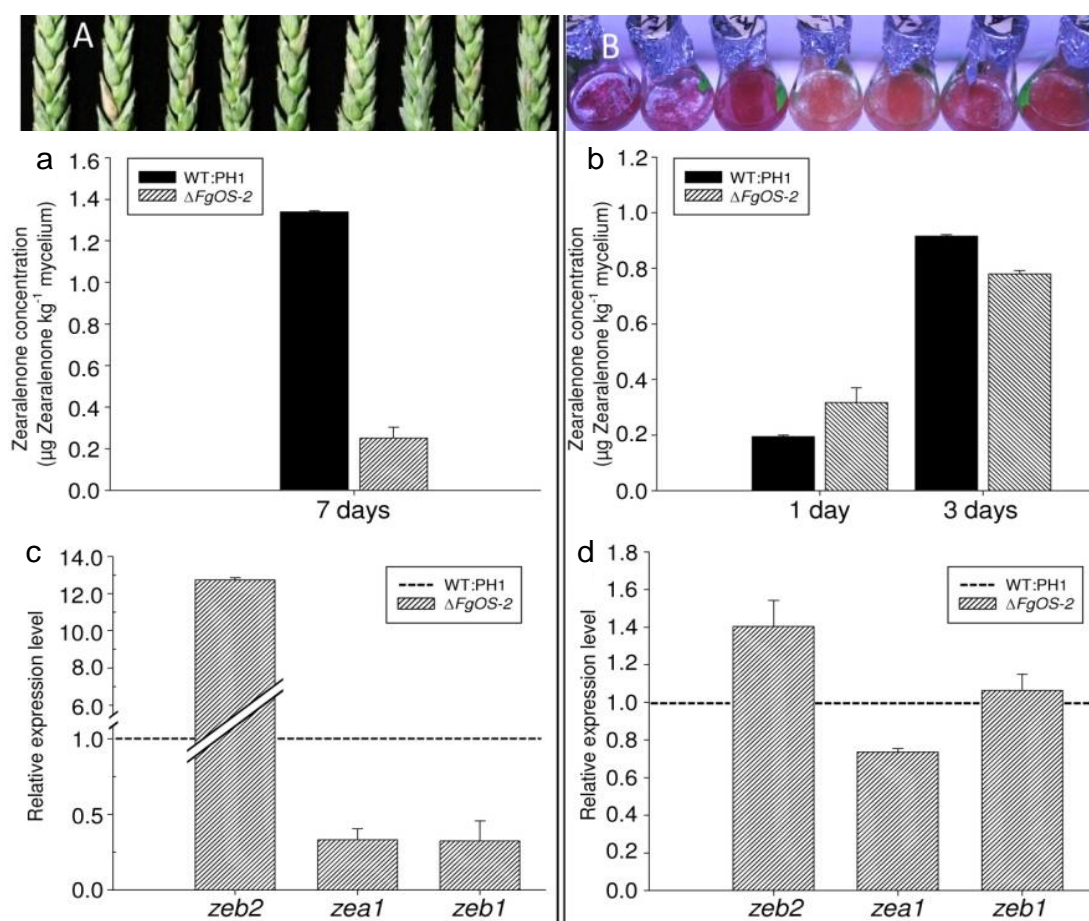


Figure 42. ZEA concentration and gene expression analysis of the wild type and *FgOS-2* deletion strains in wheat heads (A), submerged culture (B). a, b. ZEA production in the wild type and *FgOS-2* deletion strains was measured in inoculated wheat heads (a) and in submerged cultures of YES medium (see Materials and Methods; b) and normalized against the fungal mycelium as described above. No significant difference was found in ZEA contents between the wild type and mutant strains under *in-vitro* conditions. The ZEA concentration was lower in the inoculated wheat florets. c, d. Quantitative RT-PCR on genes involved in ZEA production. The expression of *zeb2* (encoding a regulatory transcription factor), *zea1* (polyketide synthases) and *zeb1* (isoamyl alcohol oxidase) was determined from cDNA derived from both strains after 7 dpi (*in planta*; c) and 3 dpi (*in vitro*; d). In the *in-planta* samples, *zeb2* expression was induced in the mutant strain while the expression of *zeb1* and *zea1* was repressed. No significant differences in gene expression were detectable under *in-vitro* conditions. Quantitative RT-PCR was performed twice, with three replicates each. Wild-type expression was set at 1. ZEA content measurements were repeated twice with four replicates each. Error bars indicate the standard deviation.

Table 14. ELISA analysis of ZEA production under different growth conditions in the wild type and $\Delta FgOS-2$ mutant strains. All values were normalized against the amount of fungal material in the sample using qPCR (see Materials and Methods).

	ZEA ($\mu\text{g kg}^{-1}$ mycelium)		
	<i>in vitro</i>		<i>in planta</i>
	1 dpi	3 dpi	7 dpi
WT:PH1	0.19 (± 0.006)	0.92 (± 0.005)	1.34 (± 0.006)
$\Delta FgOS-2$	0.33 (± 0.053)	0.78 (± 0.011)	0.25 (± 0.053)

Table 15. Gene expression analysis of genes involved in ZEA biosynthesis. Quantitative real-time PCR results indicate up or down regulation in the $\Delta FgOS-2$ mutant compared to the wild type (set at 1). Expression analysis was performed using two biological and three technical replicates. Gene expression was normalized against β -tubulin gene expression.

ZEA biosynthesis	<i>zeb1</i>	<i>zeb2</i>	<i>zea1</i>
Toxin induction medium	1,0629 \pm 0,088	1,4043 \pm 0,138	0,7358 \pm 0,018
<i>in planta</i>	0,3250 \pm 0,131	12,730 \pm 0,128	0,3310 \pm 0,073

3.2.7. Osmotic stress leads to a strongly increased oxidative burst in FgOS-2-mutants

Previous studies showed that oxidative stress modulates DON production under *in-vitro* conditions (Ponts et al., 2006). In order to determine whether or not FgOS-2 is involved in ROS metabolism, nitro blue tetrazolium (NBT)-staining of the wild type and $\Delta FgOS-2$ -mutant colonies grown on agar plates containing a mild osmotic stress medium (0.2 M NaCl) was performed. These experiments demonstrated a massive release of reactive oxygen species (ROS) in the deletion strains (Fig. 43A). Quantification using a ROS-sensitive ELISA showed an approximate 1.6-fold increase in H_2O_2 production in $\Delta FgOS-2$ mutants compared to the wild type under osmotic stress conditions (Fig. 43B).

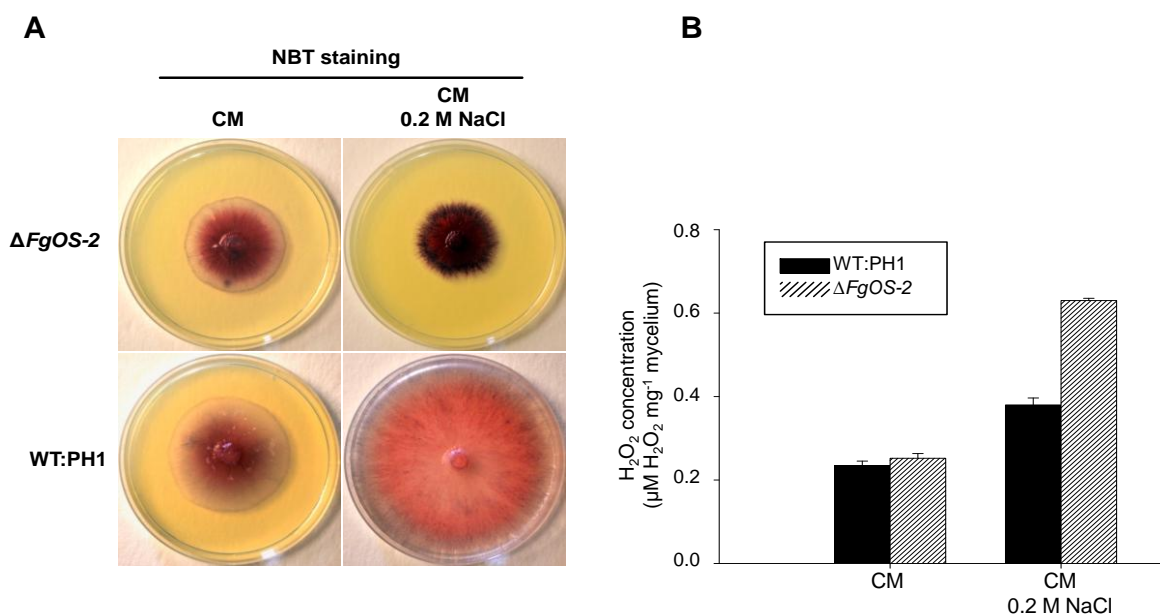


Figure 43. ROS production assay in the wild type (WT:PH1) and *FgOS-2* deletion strains. A. Nitroblue tetrazolium (NBT) staining for reactive oxygen species (ROS) production in cultures of the wild type (WT:PH1) and $\Delta FgOS-2$ mutant strains on CM and CM supplemented with 0.2 M NaCl after 3 days of growth. The dark colour indicates ROS production. The mutant showed a greater production of ROS upon osmotic stress compared to the wild type. **B.** Quantitative analysis of H₂O₂ production in both strains using samples obtained from NaCl-supplemented cultures (0.2 M). Amplex red peroxide/peroxidase assay (Invitrogen, Germany) revealed a higher level of H₂O₂ in the mutant under osmotic stress conditions. Error bars indicate the standard deviation (n=6).

The higher H₂O₂ production might be either due to an enhanced production or a decreased capability for decomposition. I therefore tested the gene expression of H₂O₂-producing enzymes, i.e. NADPH-oxidases (NOX), in a semi-quantitative reverse-transcription PCR (primers number refers to Table 4). Expression level of *noxA*, *noxB* and the regulator gene *noxR* was nearly the same between $\Delta FgOS-2$ mutants and the wild type in all conditions tested (H₂O₂, NaCl, *in planta*; Fig. 44). Only the expression of a putative calcium-dependent NADPH-oxidase *noxC* was drastically down-regulated *in planta* in the deletion strains at 7 dpi (Fig. 44) but like in the wild type under *in-vitro* conditions.

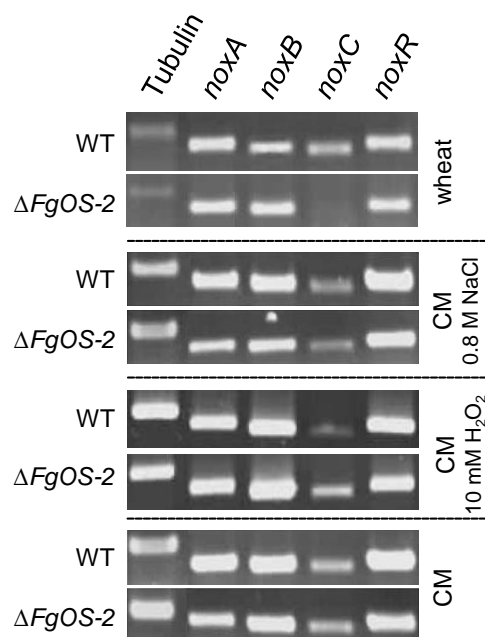


Figure 44. NADPH-oxidase (Nox) expression assay in the wild type (WT:PH1) and *FgOS-2* deletion strains. A semi-quantitative RT-PCR assay (30 PCR cycles, primer list: Supplementary Table 1) was performed on different putative Nox-related genes. CDNA was obtained from the samples as indicated after 3 dpi (*in vitro*) and 7 dpi (*in planta*). The expression of putative *noxA*, *noxB* and the regulatory gene *noxR* remained unchanged between the conditions and strains. The expression of a putative *noxC* gene was down-regulated during wheat infection in the mutant strain.

Quantitative real-time PCR verified this result and revealed a 218-fold down-regulation of *noxC* expression (Fig. 45B and Table 16) during plant infection. These results suggest that, under *in-vitro* conditions, the regulation of *nox* gene expression is independent of *FgOS-2*. Maybe, however, regulation might occur through regulation of enzyme activity. In order to determine how *FgOS-2* is involved in regulation of ROS decomposition, expression analysis and activity assays on fungal catalases were performed. Table 16 summarized the results and provides the relative expression levels (the wild-type expression level is set at 1). Under oxidative stress conditions induced by exogenous H_2O_2 (10 mM), catalase gene expression (Fig. 46B) and enzyme activity (Fig. 46D) and *atf1* (Fig. 45A) gene expression was greater in *FgOS-2* mutants than in the wild type. This might explain the increased growth observed for the mutants on agar plates supplemented with H_2O_2 (Fig. 31). However, expression of all catalase genes tested (*cat1*, *cat2.1*, *cat2.2*, *cat3*) and of the putative transcriptional regulator of catalase gene expression, *atf1*, was strongly down-regulated *in planta* and in the osmotic stress medium (0.8 M NaCl) in $\Delta FgOS-2$ mutants (Fig. 46A, C and Fig. 45A). In order to determine whether or not this would lead to a decrease of individual catalase enzymes activity, I used 0.8 M NaCl-stressed mycelium and measured catalase activity in a native PAGE. Figure 46E clearly showed a complete loss of *cat2.2*-activity and a drastic down-regulation of *cat1*. Also the highly sensitive fluorometric catalase activity assay certified the overall decrease in catalase

activity in $\Delta FgOS-2$ -mutants compared to the wild type (Fig. 46D). Thus, FgOS-2 is involved in ROS catabolism under salt stress.

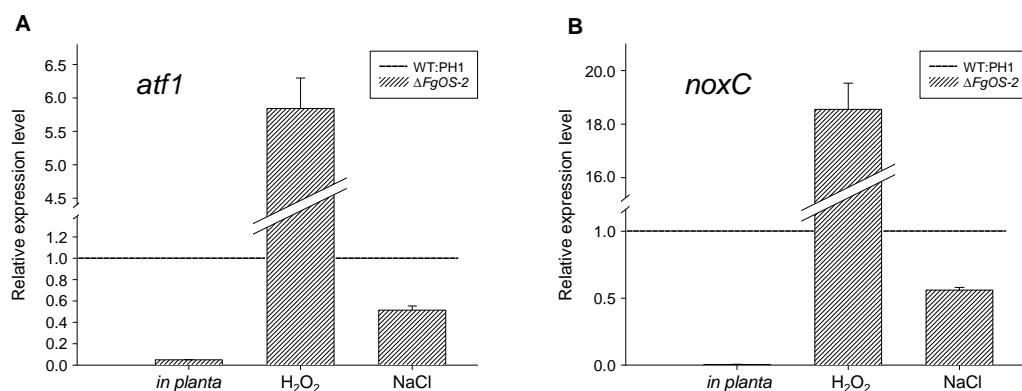


Figure 45. Gene expression analysis of the putative transcriptional regulator of ROS metabolic genes, *atf1* (A) and the putative calcium-responsive NADPH-oxidase *noxC* (B) using cDNA obtained from inoculated wheat spikelets (7 dpi), H_2O_2 supplemented (10 mM) and NaCl-supplemented samples (0.8 M). Gene expression was assayed in the wild type and $\Delta FgOS-2$ mutant strains (primer list: Table 5). The wild-type expression level was set at 1. The *atf1* and *noxC* gene expression in the $\Delta FgOS-2$ mutant was reduced during the infection of wheat and under salt stress and was massively induced in the samples supplemented with H_2O_2 . Error bars indicate the standard deviation. QRT-PCR was performed in triplicate.

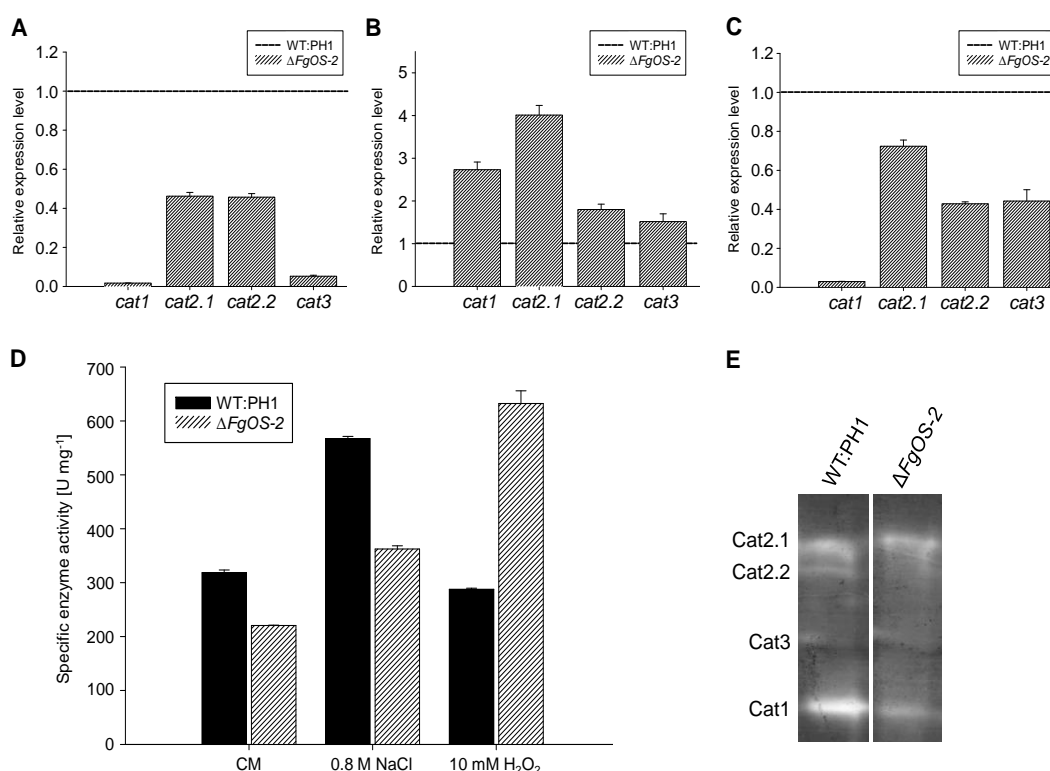


Figure 46. Catalase expression and activity assay. A-C. Quantitative RT-PCR using cDNA obtained from inoculated wheat spikelets (7 dpi, A), H_2O_2 supplemented (10 mM, B) and NaCl-supplemented samples (0.8 M, C). Expression of four different, putative catalase genes was assayed in the wild type and $\Delta FgOS-2$ mutant strains (primer list: Table 5). The wild-type expression level was set at 1. Catalase expression in the $\Delta FgOS-2$ mutant was reduced during the infection of wheat and in the

Figure 46 continuance

medium supplemented with NaCl, but not in the samples supplemented with H₂O₂. Error bars indicate the standard deviation. QRT-PCR was performed in triplicate. **D.** Catalase activity assay using protein extract obtained from mycelium raised in CM with and without 2h-induction by 0.8 M NaCl and 10 mM H₂O₂, respectively. Total catalase activity was reduced in the $\Delta FgOS-2$ mutant under no-stress and osmotic-stress conditions and elevated under oxidative stress conditions. The assay was performed using two biological and three technical replicates. **E.** Catalase activity staining using native protein extract from the wild type and the mutant strains cultures supplemented with NaCl (0.8 M). Activity of all catalases was reduced in the mutant.

Table 16. Gene expression analysis of genes involved in ROS metabolism. Quantitative real-time PCR results indicate up or down regulation in the $\Delta FgOS-2$ deletion strain compared to the wild type (set at 1). Expression analysis was performed using two biological and three technical replicates. Gene expression was normalized against β -tubulin gene expression.

ROS metabolism	<i>cat1</i>	<i>cat2.1</i>	<i>cat2.2</i>	<i>cat3</i>	<i>atf1</i>	<i>noxC</i>
NaCl	0,0296 ($\pm 0,001$)	0,7236 ($\pm 0,032$)	0,4286 ($\pm 0,01$)	0,4426 ($\pm 0,058$)	0,5150 ($\pm 0,038$)	0,5601 ($\pm 0,020$)
H ₂ O ₂	2,7323 ($\pm 0,179$)	4,0107 ($\pm 0,226$)	1,8003 ($\pm 0,124$)	1,5177 ($\pm 0,181$)	5,8421 ($\pm 0,455$)	18,5494 ($\pm 0,98$)
<i>in planta</i>	0,0171 ($\pm 0,006$)	0,4623 ($\pm 0,019$)	0,4570 ($\pm 0,018$)	0,0523 ($\pm 0,005$)	0,0492 ($\pm 0,001$)	0,0046 ($\pm 0,001$)

Interestingly, supplementation of CM containing 0.2 M NaCl with up to 50 $\mu\text{g ml}^{-1}$ of purified catalase partially restored the usually observed growth defect of $\Delta FgOS-2$ mutants on osmotic medium (Fig. 47).

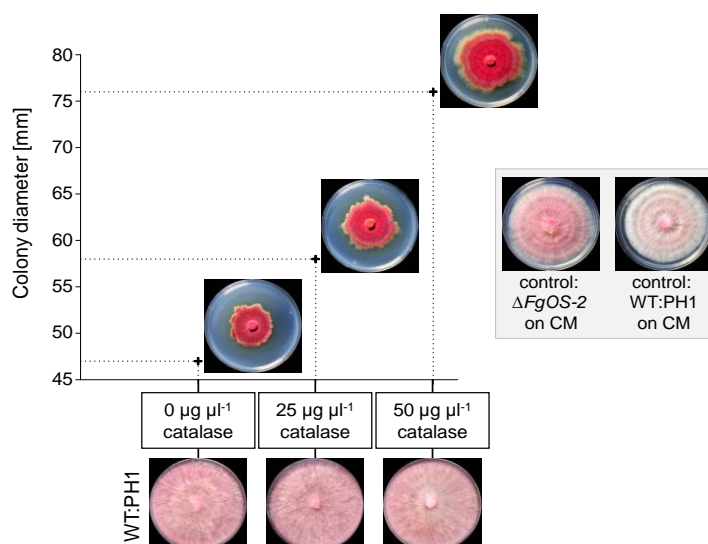


Figure 47. Growth performance of the *FgOS-2* deletion and wild type (WT:PH1) strains on CM agar plates containing 0.2 M NaCl and increasing concentrations of purified catalase. After 5 days of growth pictures were taken and the diameter of the colonies was measured. The wild type colonized the whole plate. Growth of the mutant enhanced with increasing concentrations of catalase in the medium.

Taken together, FgOS-2 is a central regulator of all steps in the life cycle of *F. graminearum*. It is involved in nearly all developmental processes, such as perithecia formation, oxidative and osmotic stress tolerance, fungicide resistance, virulence, ROS metabolism and secondary metabolite production, including mycotoxins.

3.3. The role of the Activating Transcription Factor Atf1 in *Fusarium graminearum*

3.3.1. Computer-based identification of transcription factor Atf1 from *F. graminearum*

The putative *atf1* gene from *F. graminearum* FGSG_10142 was identified using *Neurospora crassa* *atf1* genomic sequence as query for a BlastX search against MIPS *F. graminearum* Genome Database. The gene is published in NCBI genebank as a hypothetical protein under the accession no. XP_390318.1. According to the MIPS *Fusarium graminearum* Genome Database, the protein consists of 526 amino acids including a basic-leucine zipper (bZIP) domain for DNA binding ranging from amino acid E411–H474 (Fig. 48), an osmotic stress activation (OSA) region, a homologous recombination activation (HRA) region, and a homologous recombination repression (HRR) region, located within residues 43-94, 116-188 and 194-282, respectively.



Figure 48. Protein alignment (CLUSTALW) of the basic-leucine zipper (bZIP) domain for DNA binding of *F. graminearum* Atf1 (Genebank accession number XP_390318.1) and other (putative) Atf1 orthologues from *Claviceps purpurea* (CAD21519.1), *Aspergillus fumigatus* (XP_754486.2), *Emericella nidulans* (AAN75015.1), *Neurospora crassa* (XP_961431.2) and *Schizosaccharomyces pombe* (BAA12194.1). Identical amino acids are highlighted in yellow, conserved amino acids are highlighted in cyan and blocks of similar amino acids are highlighted in green.

3.3.2. Generation of *Fgatf1* deletion mutants

In order to study the function of the Atf1 protein in the life cycle of *F. graminearum* the gene was deleted using a gene replacement approach (Fig. 49). 5'- and the 3'-flanking regions (1.054 kb upstream and 1.056 kb-downstream fragments) were amplified by PCR and subsequently fused to a hygromycin resistance cassette. The replacement fragment was excised by restriction enzyme *Xba*I and used for fungal transformation. Fifty primary transformants were screened in a diagnostic PCR (Fig. 49B): Five independent transformants showed homologous integration of the replacement fragment. Single conidia of those mutants were used to obtain homokaryotic deletion mutants. One additional mutant was chosen which

showed amplification of the wild type gene even after repetitive single spore isolation indicating an ectopic integration of the vector (Fig. 49B and D). All of the selected mutants and the wild type were analysed in a Southern blot experiment. When probed for the integration of the hygromycin gene, all mutants, but not the wild type, showed a single integration of the fragment (Fig. 49D). When hybridized with a probe amplified from the *Fgatf1* gene, all mutants except the one expected to have an ectopic integration of the replacement construct showed no signal. In the wild type a signal was visible (Fig. 49D). Unless otherwise mentioned, phenotypic characterization in terms of vegetative growth on different media (i.e. conferring salt, oxidative and fungicide stress), perithecia formation, conidia germination, and pathogenicity towards wheat and maize was performed using at least three independent knock-out mutants. Expression analysis was done using two independent mutants. Since all of the transformants showed a similar phenotype, one mutant (named $\Delta Fgatf1$ -45.5) was chosen to illustrate the respective results in the figures (herein referred to as the $\Delta Fgatf1$ mutant). This $\Delta Fgatf1$ mutant was subsequently selected for fluorescent labelling using the red fluorescent protein dsRed.

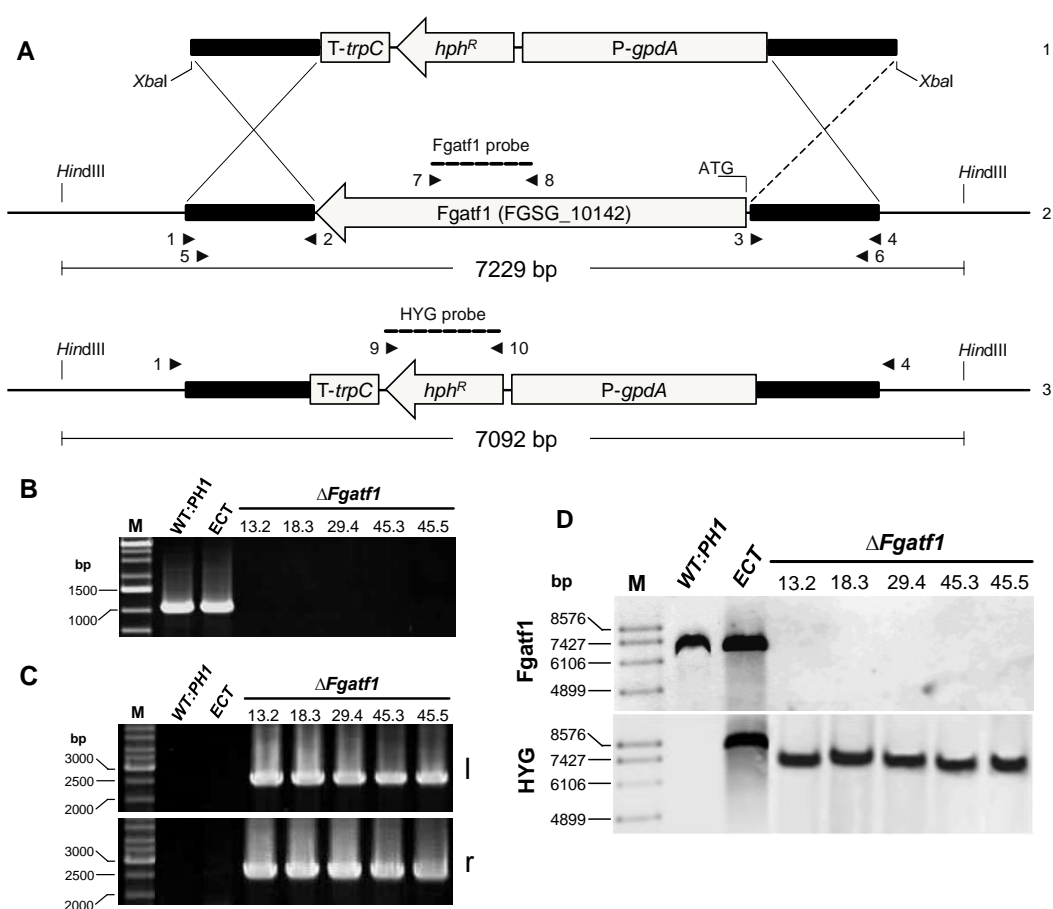


Figure 49. Gene replacement and Southern hybridization strategy for *Fgatf1*. A. Deletion of *Fgatf1* (2) by homologous recombination using a replacement fragment excised from pGEM-*Fgatf1*-HYG using restriction enzyme *XbaI* (1) (3: genotype of disrupted strains). Flanking regions are

Figure 49 continuance

indicated as bold black lines. The gene flanks were fused to a hygromycin resistance cassette, consisting of the resistance gene (hygromycin B phosphotransferase, *hph*) and the *gpdA* promoter (*P-gpdA*) and *trpC* terminator (*TtrpC*) of *A. nidulans*. Primer binding sites for the fusion and diagnostic PCR are indicated as small arrows (numbering refers to Table. 3). The regions used as probes for Southern analysis are represented by the dashed lines. Scheme is not to scale. **B, C.** PCR analysis of $\Delta Fgatf1$ mutants and the wild type. Deletion of *Fgatf1* was verified in five independent mutants using primers 7 and 8 (991 bp; **B**). Homologous integration of the replacement fragment was checked by PCR with primers 1 and 10 (l: left flank, 2.468 kb) and 4 and 9 (r: right flank, 2.453 kb; **C**). The wild type and ectopic strains were PCR-positive for the gene internal fragment, but not for the flank-spanning PCR. **D.** Southern analysis of $\Delta Fgatf1$ mutants and the wild type. DNA of the mutant and wild type strains was digested using *HindIII*, separated on agarose gel, blotted on a membrane and probed with DIG-labelled probes for hygromycin (HYG) and a fragment of *Fgatf1*, respectively. Five disruption mutants lacked a signal when probed with the *Fgatf1* probe. The hygromycin probe hybridized both with wild-type and ectopic-strain DNA. Both probes had a signal in the ectopic strain only.

3.3.3. Generation of *Fgatf1* overexpressing mutants (*Fgatf1^{oe}*)

In order to generate mutants that constitutively express *Fgatf1*, the open reading frame (ORF) of *Fgatf1* was amplified by PCR from gDNA and then ligated into the pJET1.2 vector. The ORF was excised from pJET1.2 by restriction using enzymes *SacI* and *XbaI* and cloned into pII99 vector which contains the constitutive glyceraldehyde-3-phosphate dehydrogenase promoter (*gpdA*), the tryptophan synthase C terminator (*trpC*) from *Cochliobolus heterostrophus*, and a geneticin-resistance cassette (M. Woriedh, University of Hamburg, Germany). The resulting plasmid, GPD-*Fgatf1*-pII99, was linearized at the unique *ApaI* restriction site to facilitate single crossover events. The linearized construct was used for fungal transformation (Fig. 50A and B). Five transformants were obtained and single-spore isolations were performed. Southern blot analysis was conducted with DIG-labelled *Fgatf1* probe. Two independent transformants (number 1.2 and 4.4) showed a single integration event in the right locus with approximately 12337 bp hybridization signal. Three mutants (number 2.2, 3.1 and 3.3) showed hybridization signals with other sizes, indicating a random integration of the transformation vector in the genome. The wild type showed 4537 bp hybridization signal (Fig. 50C). Phenotypic characterization was conducted using both mutants. One of them (named *Fgatf1^{oe}*-1.2) was chosen to illustrate the respective results in the figures (herein referred to as the *Fgatf1^{oe}* mutant).

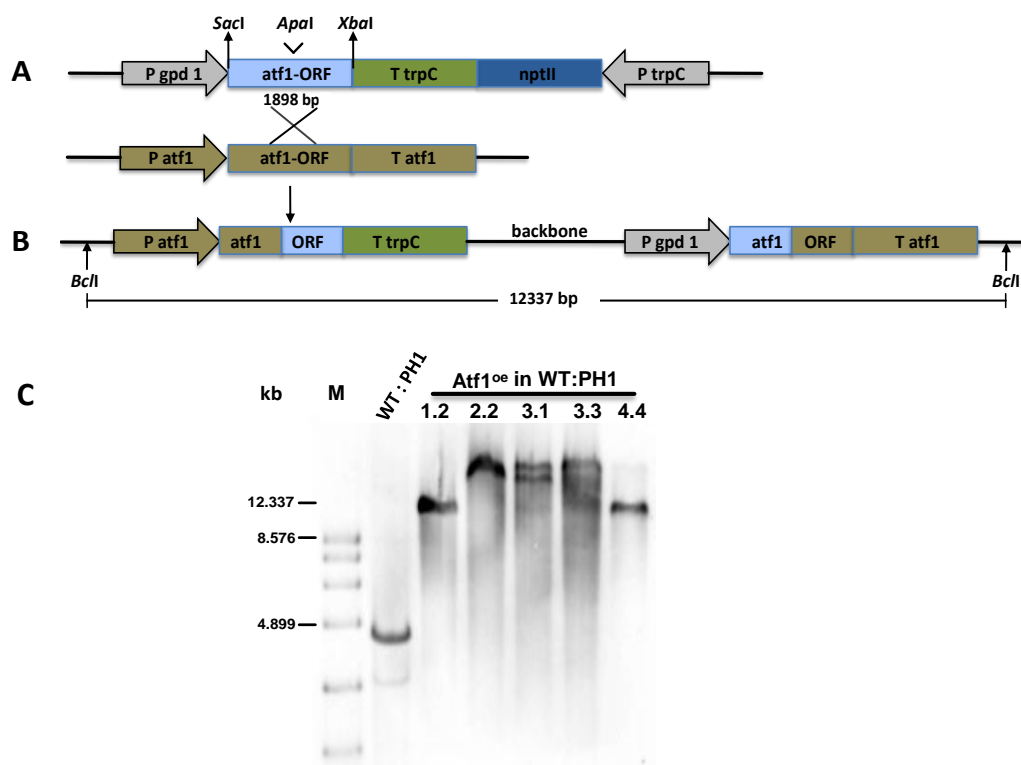


Figure 50. Scheme representation for the generation of the *Fgatf1* overexpression construct. A. The *Fgatf1* open reading frame was excised from pJET1.2 and ligated into the pII99 vector after digestion with *SacI* and *XbaI* site (upper panel). The genomic *Fgatf1* locus is demonstrated in lower panel. **B.** Panel describes the genomic structure of the *Fgatf1* locus after integration of the *Fgatf1* overexpression construct by single homologous recombination. The expression vector was linearized at the unique *ApaI* restriction site for single homologous recombination. Arrows indicate the enzymes that were used for molecular cloning and Southern blot. **C.** Southern analysis of the *Fgatf1* overexpression mutants. DNA of the five independent transformants and the wild type was digested using *BclI*, separated on agarose gel, blotted on a membrane and probed with DIG-labelled *Fgatf1* probe. Two independent transformants named 1.2 and 4.4 were considered *Fgatf1* overexpression mutants by single crossover events.

3.3.4. Generation of *FgOS-2* deletion mutants in a *Fgatf1* overexpression mutant (*Fgatf1^{oe}::ΔFgOS-2*)

Fgatf1^{oe} mutant number 1.2 was chosen for *FgOS-2* deletion. The construct and method for *FgOS-2* deletion is described as 3.2.2 (Fig. 28). Deletion of *FgOS-2* in the *Fgatf1^{oe}* mutant was also verified using primers 7 and 8 (1.178 kb; B), primers 1 and 10 (l: left flank, 2.384 kb) and 4 and 9 (r: right flank, 2.498 kb; C). The *Fgatf1^{oe}* and ectopic strains were PCR-positive for the gene internal fragment, but not for the flank-spanning. Seven independent transformants showed homologous integration of the replacement fragment, indicating deletion of *FgOS-2* (Fig 51B and C). All of the selected mutants and the *Fgatf1^{oe}* were analysed in a Southern blot experiment. When probed for the integration of the hygromycin gene, all mutants, but not the *Fgatf1^{oe}*, showed a single integration of the fragment (Fig. 51D). When hybridized with a probe

amplified from the *FgOS-2* gene, seven mutants except ectopic integration strain showed no signal. In the *Fgatf1^{oe}* a signal was visible (Fig. 51D).

Phenotypic characterization was carried out using at least three independent mutants. Since all of the transformants showed a similar phenotype, one mutant (*Fgatf1^{oe}::ΔFgOS-2*.8.1) was chosen to illustrate the respective results in the figures (herein referred to as the *Fgatf1^{oe}::ΔFgOS-2* mutant).

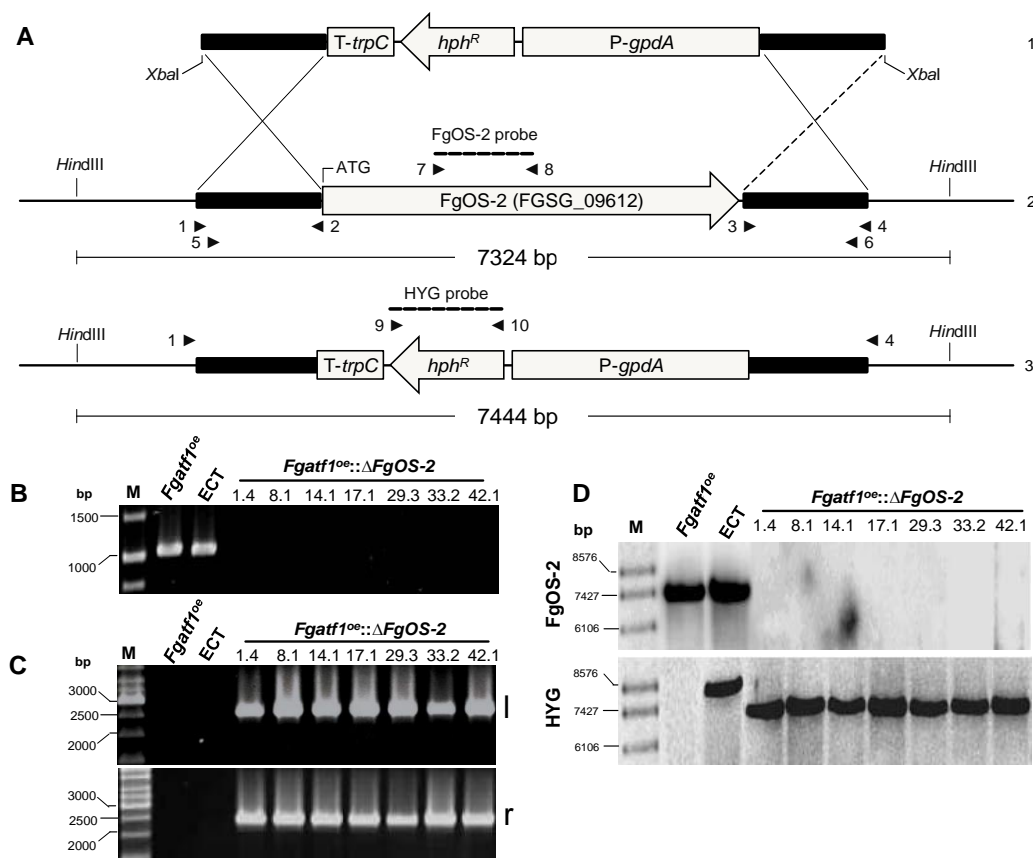


Figure 51. Replacement and Southern hybridization strategy for *FgOS-2*. **A.** Deletion of *FgOS-2* (2) by homologous recombination using a replacement fragment excised from pGEM-*FgOS-2*-*HYG* using restriction enzyme *XbaI* (1) (3: genotype of disrupted strains). Flanking regions are indicated as bold black lines. The gene flanks were fused to a hygromycin resistance cassette, consisting of the resistance gene (hygromycin B phosphotransferase, *hph*) and the *gpdA* promoter (*P-gpdA*) and *trpC* terminator (*TtrpC*) of *A. nidulans*. Primer binding sites for the fusion and diagnostic PCR are indicated as small arrows (numbering refers to Table 2). The regions used as probes for Southern analysis are represented by the dashed lines. Scheme is not to scale. **B, C.** PCR analysis of $\Delta FgOS-2$ and *Fgatf1^{oe}* strains. Deletion of *FgOS-2* was verified in 7 independent mutants using primers 7 and 8 (1.178 kb; **B**). Homologous integration of the replacement fragment was checked by PCR with primers 1 and 10 (l: left flank, 2.384 kb) and 4 and 9 (r: right flank, 2.498 kb; **C**). The *Fgatf1^{oe}* and ectopic strains were PCR-positive for the gene internal fragment, but not for the flank-spanning PCR. **D.** Southern analysis of $\Delta FgOS-2$ and the *Fgatf1^{oe}* strains. DNA of the mutants and *Fgatf1^{oe}* strain was digested using *HindIII*, separated on agarose gel, blotted on a membrane and probed with DIG-labelled probes for hygromycin (*HYG*) and a fragment of *FgOS-2*, respectively. Seven disruption mutants lacked a signal when probed with the *FgOS-2* probe. The hygromycin probe hybridized both with *Fgatf1^{oe}* and ectopic-strain DNA. Both probes had a signal in the ectopic strain only.

In section 3.2, the stress-activated MAP-kinase FgOS-2 was presented as a central regulator in the life cycle of the cereal pathogen *F. graminearum*. Here, I present data on the functional characterization of a putative downstream regulator, the ATF/CREB activating transcription factor Fgatf1.

3.3.5. Functional Fgatf1 is necessary for proper vegetative growth and interacts with FgOS-2 under osmotic stress conditions

To test the influence of Fgatf1 on vegetative growth, plate assays on different media were conducted. When grown on CM agar plates, *Fgatf1* deletion strains were slightly reduced in growth compared to the wild type (Fig. 52). On agar plates supplemented with osmotic agents the growth reduction was more pronounced. However, in contrast to *FgOS-2* deletion strains, growth is still possible on plates containing 0.8 M NaCl and KCl, respectively or 1.2 M sorbitol (Fig. 52). *Fgatf1^{oe}* mutants also showed a slightly reduced growth rate on the osmotic stress media but grew better than the deletion strains. Interestingly, *Fgatf1^{oe}::ΔFgOS-2* mutants, grew much better than $\Delta FgOS-2$ mutants on medium conferring osmotic stress (Fig. 52).

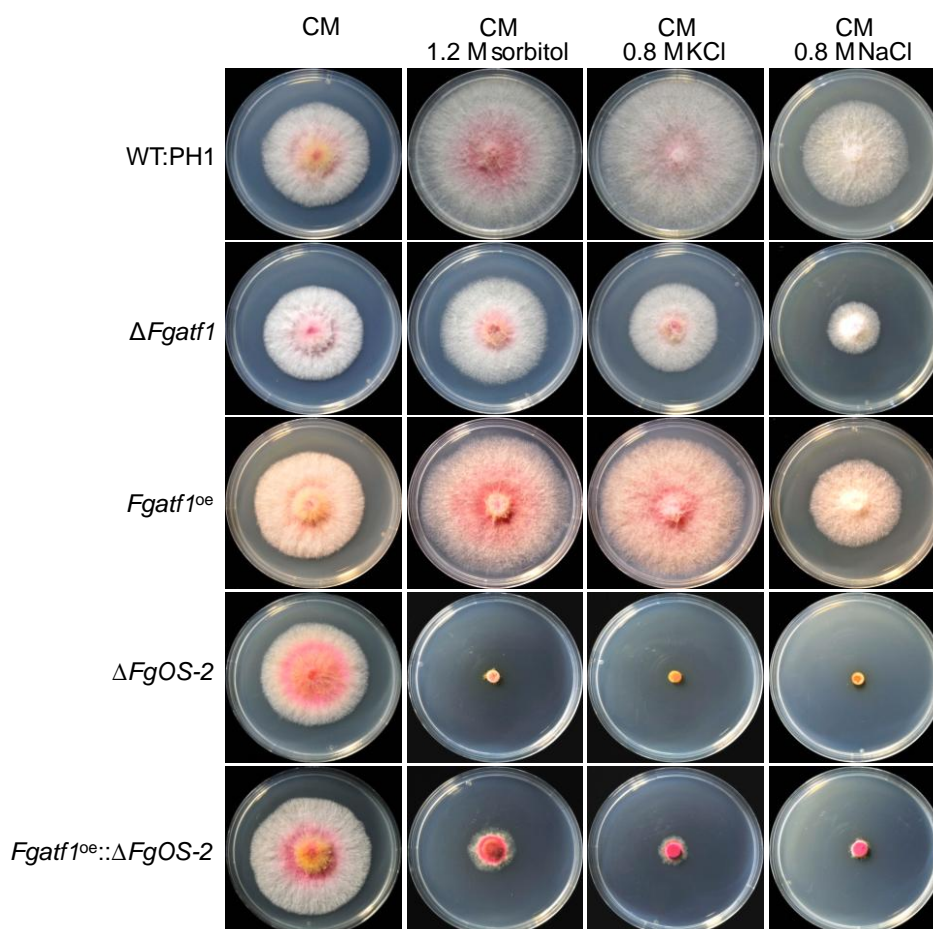


Figure 52. Colony morphology of the wild type (WT:PH1) and the mutants $\Delta Fgatf1$, *Fgatf1^{oe}*, $\Delta FgOS-2$ and *Fgatf1^{oe}::ΔFgOS-2* after 3 days of growth on the osmotic stress media. Complete

Figure 52 continuance

medium (CM) inoculated with mycelial plugs from 3-day-old cultures. In order to test growth behavior, this medium was supplemented with the osmotic agents: Sorbitol (1.2 M), NaCl (0.8 M) and KCl (0.8 M). Growth of the $\Delta Fgatf1$ mutant was slightly retarded on the CM without osmotic stress agent and drastically reduced on osmotic media. In contrast to *FgOS-2* deletion strain, growth of the *Fgatf1^{oe}:: $\Delta FgOS-2$* mutant was still possible on plates containing 0.8 M NaCl and KCl, respectively or 1.2 M sorbitol. The *Fgatf1^{oe}* mutant also showed a slightly reduced growth rate on the osmotic stress medium but grew better than the *Fgatf1* deletion strain.

On medium conferring mild osmotic stress, overexpression of *Fgatf1* led to an almost full restoration of growth in the $\Delta FgOS-2$ mutant background (Fig. 53).

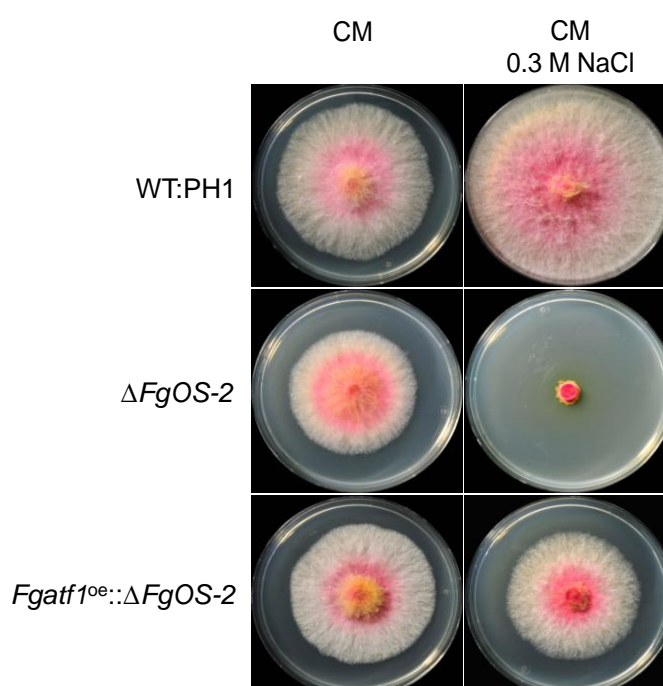


Figure 53. Colony morphology of the wild type (WT:PH1), $\Delta FgOS-2$ and *Fgatf1^{oe}:: $\Delta FgOS-2$* strains after 3 days of growth on the mild osmotic stress medium. The basic medium used was complete medium (CM) inoculated with mycelial plugs from 3-day-old cultures. To test sensitivity towards osmotic stress, medium was supplemented with 0.3 M NaCl. Constitutive expression of *Fgatf1* led to a pronounced complementation of the growth defect caused by the *FgOS-2* deficiency.

The germination of the wild type and the mutant's conidia in non-osmotic and osmotic media was tested. In the presence of 0.8 M NaCl, germ tubes usually emerged at one apical compartment of $\Delta Fgatf1$ -conidia. The wild type in contrast usually germinated at two places. Moreover, on medium containing 0.8 M NaCl, the germ tubes of *Fgatf1* deletion strains were delayed in growth compared to the wild type after 16 hours of incubation. Under non-stress conditions conidial germination was similar between the strains (Fig. 54).

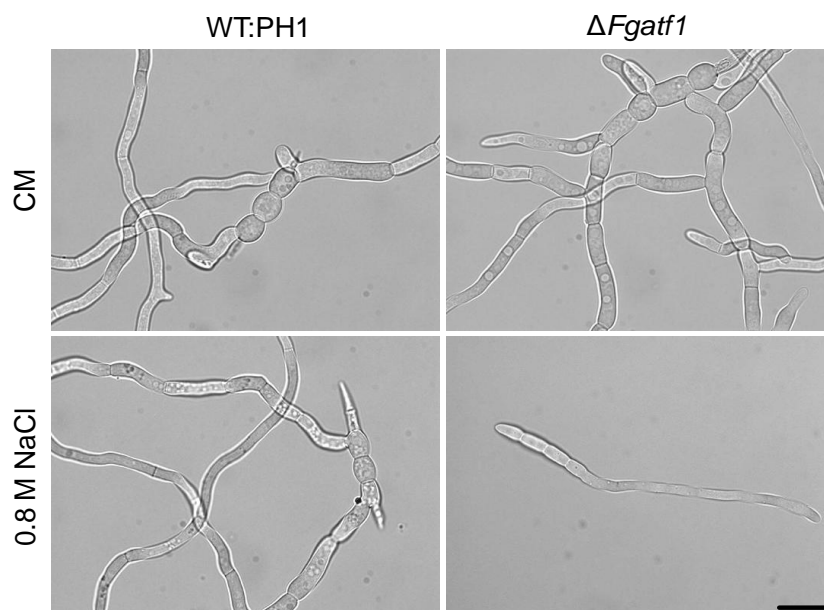


Figure 54. Bright-field microscopy of germinating conidia of the wild type and $\Delta Fgat1$ mutant strains in liquid CM and liquid CM supplemented with 0.8 M NaCl after 16 hours of incubation. In non-osmotic medium, the wild-type and $\Delta Fgat1$ mutant conidia formed multiple normally shaped germ tubes. In osmotic medium, the wild type conidia germination was similar to non-osmotic medium. The $\Delta Fgat1$ germ tubes generally emerged at one apical compartment of $\Delta Fgat1$ -conidia and were delayed in the development compared to the wild type. The wild type and $\Delta Fgat1$ mutant strains showed comparable conidial germination rates in both osmotic and non-osmotic media. Scale bar: 10 μm .

Like *FgOS-2* deletion strains, also $\Delta Fgat1$ mutants exhibited a partial resistance against the phenylpyrrolic fungicide fludioxonil (Fig. 55). These results indicate that *Fgat1* is a downstream target of *FgOS-2* under osmotic and fungicide stress conditions and that activation of *Fgat1* is necessary for proper vegetative growth. Surprisingly, *Fgat1^{oe}::ΔFgOS-2* mutants exhibited the highest resistance against fludioxonil.

Fgat1 deletion strains, but not the overexpression mutants, grew much better on medium supplemented with H_2O_2 compared to the wild type (Fig. 55). I could demonstrate that deletion of *FgOS-2* also led to an increased resistance towards oxidative stress. This observation substantiates the assumption that the *FgOS-2*/*Fgat1*-cascade is the central trigger of ROS metabolism in *F. graminearum* (see also 3.2.3 and 3.2.7).

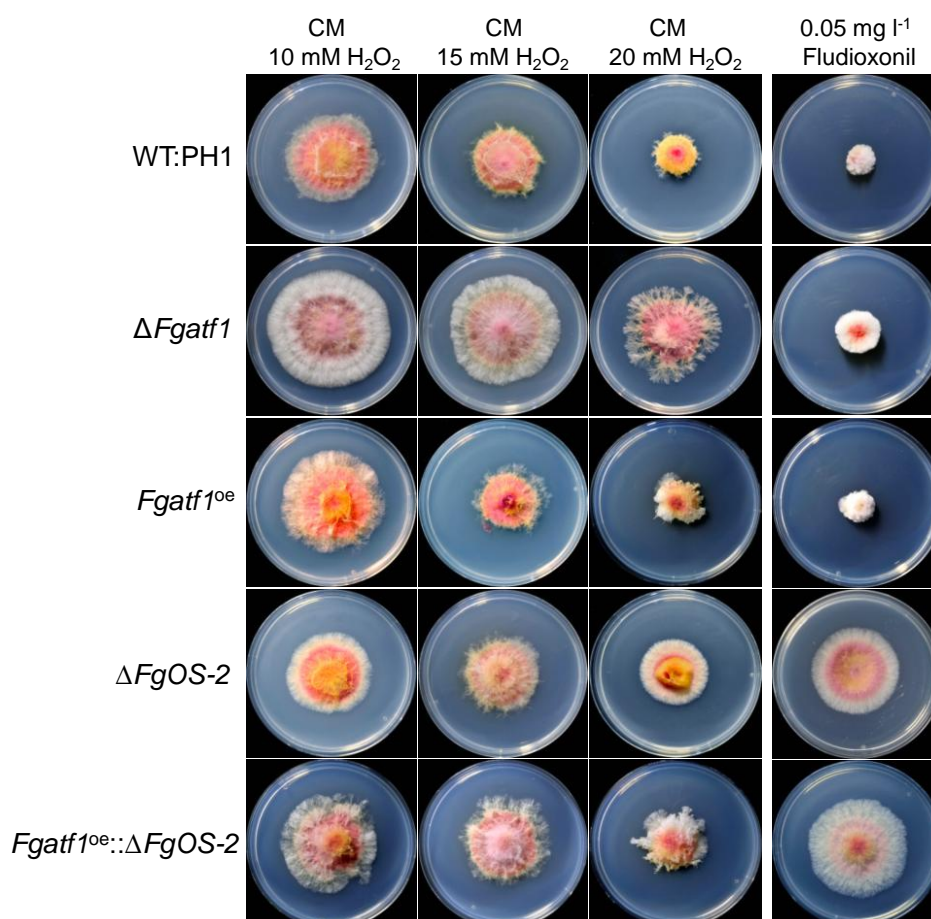


Figure 55. Colony morphology of the wild type (WT:PH1) and the mutants $\Delta FgOS-2$, $\Delta Fgatf1$, $Fgatf1^{oe}$ and $Fgatf1^{oe}::\Delta FgOS-2$ after 4 days of growth on oxidative stress and fungicide agar plates. The basic medium was complete medium (CM) inoculated with mycelial plugs from 3-day-old cultures. Media were supplemented with 10, 15 and 20 mM H_2O_2 or 0.05 mg l^{-1} fludioxonil. No differences in growth performance between the wild type and $FgOS-2$ deletion mutant strains were observed on agar plates supplemented with 10, 15 mM H_2O_2 . On plates supplemented with 20 mM H_2O_2 , the $\Delta FgOS-2$ mutant grew even better than the wild type after 4 days post-incubation. The $Fgatf1$ deletion strain, but not $Fgatf1^{oe}$ and $Fgatf1^{oe}::\Delta FgOS-2$ mutants, grew much better on medium supplemented with H_2O_2 compared to the wild type. On plates containing 0.05 mg l^{-1} fludioxonil, growth of the $FgOS-2$ deletion and $Fgatf1^{oe}::\Delta FgOS-2$ mutant strains were similar to CM control plates, while growth of the wild type and $Fgatf1^{oe}$ mutant strains nearly ceased. The $\Delta Fgatf1$ mutant displayed a partial resistance against the phenylpyrrolic fungicide fludioxonil.

To further proof the interaction of FgOS-2 and Fgat1 under stress conditions I performed a bimolecular fluorescence complementation assay (BiFC; Hoff and Kück, 2005). For this purpose, the open reading frame (ORF) of FgOS-2 was fused to the N-terminus of the yellow fluorescent protein (YFP) and the ORF of Fgatf1 was fused to the C-terminus of YFP. A strain expressing a histon-1-mCherry fusion which facilitates detection of nuclei (A. L. Martínez-Rocha, unpublished results), was used as recipient for both plasmids. Strains obtained from co-transformation of both plasmids were initially analysed by PCR. Mutants positive for both plasmids were subsequently analysed by confocal laser scanning microscopy

(see material and methods). Unstressed mycelia of the mutant and the wild type strains did not emit YFP-fluorescence when excited with a 514 nm laser line. Application of 1.2 M NaCl, mutants evoked fluorescence inside the nucleus of fungal hyphae within 30 minutes (Fig. 56). This result provides further evidence for an interaction of *Fgatf1* and *FgOS-2* under osmotic stress conditions.

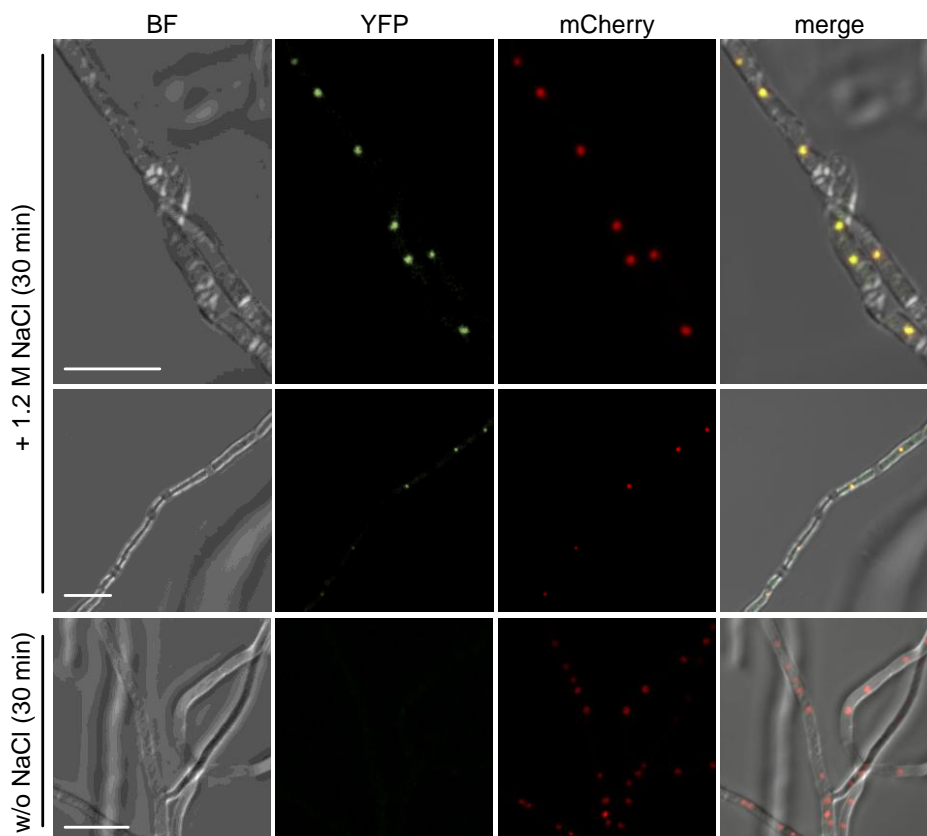


Figure 56. Bimolecular fluorescence complementation assay. *FgOS-2* was fused to the N-terminus and *Fgatf1* to the C-terminus of YFP, respectively. Both constructs were co-transformed into *F. graminearum* wild type. 24h after germination of conidia osmotic stress mediated by 1.2 M NaCl was applied and hyphae were subsequently imaged using confocal laser scanning microscopy. Scale bar: 10 μ m.

3.3.6. Overexpression of *Fgatf1* restores sexual reproduction in *FgOS-2* deletion strains

As shown in 3.2.4, *FgOS-2* is necessary for sexual reproduction in *F. graminearum*. To test the importance of *Fgatf1* in this process, I analysed three independent *Fgatf1* deletion strains for perithecia formation both on carrot agar and on detached wheat nodes. On both substrates *Fgatf1* deletion strains were delayed in perithecia formation. While the wild type produced mature perithecia containing numerous asci and ascospores after three weeks, it took 7 (wheat nodes) and 8 (carrot agar) weeks in $\Delta Fgatf1$ mutants. However, once matured, also these perithecia contained asci and ascospores. Interestingly, overexpression of *Fgatf1* restored the ability of an *FgOS-2* deletion strain to produce perithecia. $\Delta FgOS-2$ deletion strains completely

failed to produce perithecia, *Fgatl1^{oe}::ΔFgOS-2* mutants produced mature asci and ascospores after 7 (wheat nodes) and 8 (carrot agar) weeks (Fig. 57 and Fig. 58). However, the clusters of perithecia appeared much smaller compared to the wild type. Intriguingly, the *Fgatl1* mutants and the wild type produced nearly equal amounts of conidia.

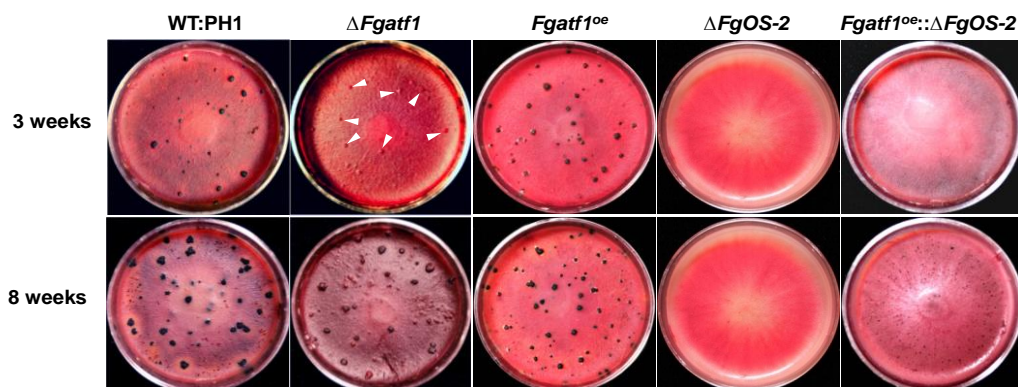


Figure 57. Assay for perithecia formation. Conidia of the wild type, the mutants $\Delta Fgatl1$, $Fgatl1^{oe}$, $\Delta FgOS-2$ and $Fgatl1^{oe}::\Delta FgOS-2$ were placed on carrot agar plates. After 21 days of incubation, the wild type and the $Fgatl1^{oe}$ mutant strains had produced numerous clusters of perithecia. The $\Delta Fgatl1$ mutant produced immature perithecia clusters (arrowheads), which mature after 56 days of incubation. Whilst the $\Delta FgOS-2$ mutant failed to produce clusters of perithecia, the $Fgatl1^{oe}::\Delta FgOS-2$ mutant produced numerous small clusters. Immature perithecia are indicated with white arrows.

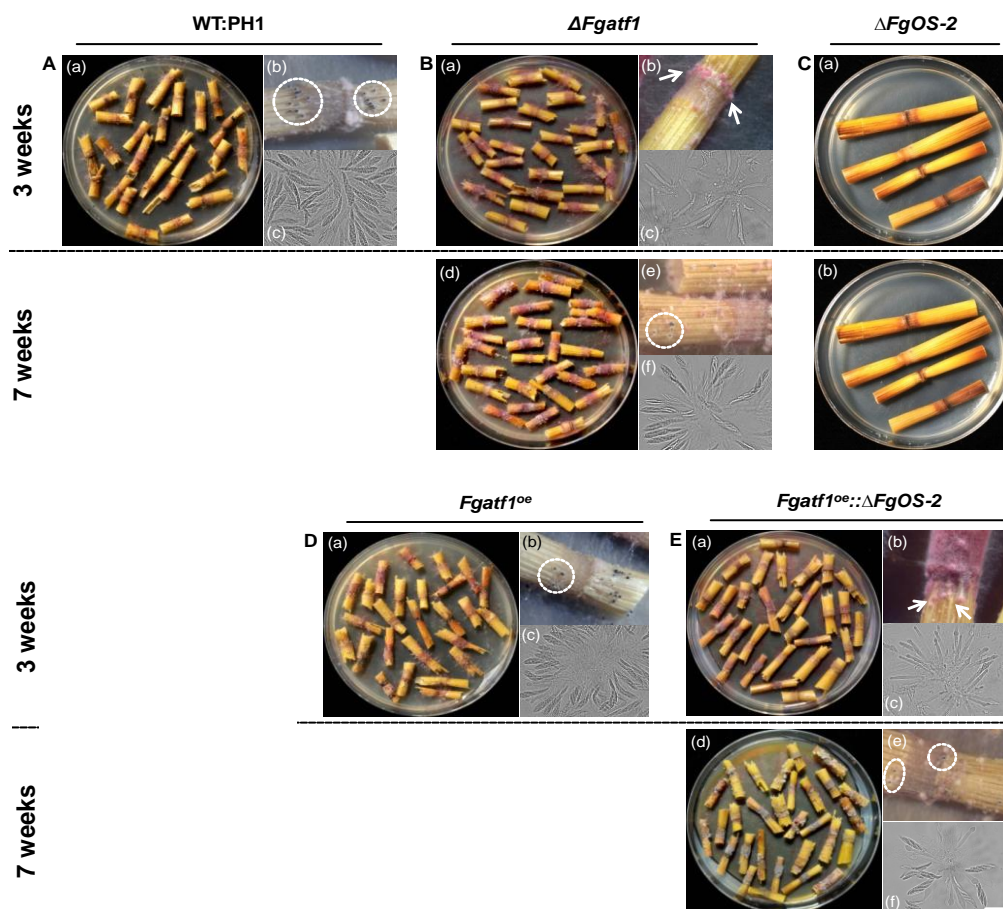


Figure 58. Perithecia and ascospore development on detached wheat nodes. Conidia of the wild type (A), the mutants $\Delta Fgatl1$ (B), $\Delta FgOS-2$ (C), $Fgatl1^{oe}$ (D), and $FgOS-2$ deletion in the $Fgatl1^{oe}$ mutant

Figure 58 continuance

(E) were assayed. Clusters of perithecia are indicated by the dotted circles in **A** (b), **B** (e), **D** (b) and **E** (e). Squeezing these clusters released the asci (**A** (c); **B** (c) and (f); **D** (c) and **E** (c) and (f)). The $\Delta Fgatf1$ mutant produced immature perithecia clusters (arrows in B (b) and (c)), which mature after 56 days of incubation (B (f)). Whilst the $\Delta FgOS-2$ mutant failed to produce perithecia clusters (**C** (a) and (b)), the $FgOS-2$ deletion strain in the $Fgatf1^{oe}$ produced numerous clusters containing mature asci (**E** (d) and (f)) after 56 days of incubation.

3.3.7. Deletion of *Fgatf1* attenuates virulence towards wheat and maize

The *FgOS-2* signaling cascade is involved in virulence towards two important hosts of *F. graminearum*, wheat and maize (Jiang et al., 2011; Nguyen et al., 2012). Deletion of *Fgatf1* led to a strong reduction in virulence towards wheat and maize compared to the wild type. Nevertheless, the disease symptoms caused by $\Delta Fgatf1$ mutants were more apparent compared to the $\Delta FgOS-2$ mutants. On wheat (cv. Nandu), the spikes infected with *Fgatf1* deletion strains showed a significantly reduced virulence compared to the wild type. The inoculated spikelets got fully colonized by $\Delta Fgatf1$ mutants within 21 dpi. However, they were defective in growth from the inoculated spikelets to the adjacent spikelets through rachis (Fig. 59). $\Delta Fgatf1$ mutants were also reduced in virulence towards maize. All maize cobs inoculated with $\Delta Fgatf1$ mutants were only superficially colonized and still had uninfected cob parts with normal kernel development. The wild type colonized the complete maize cobs after 35 dpi (Fig. 59).

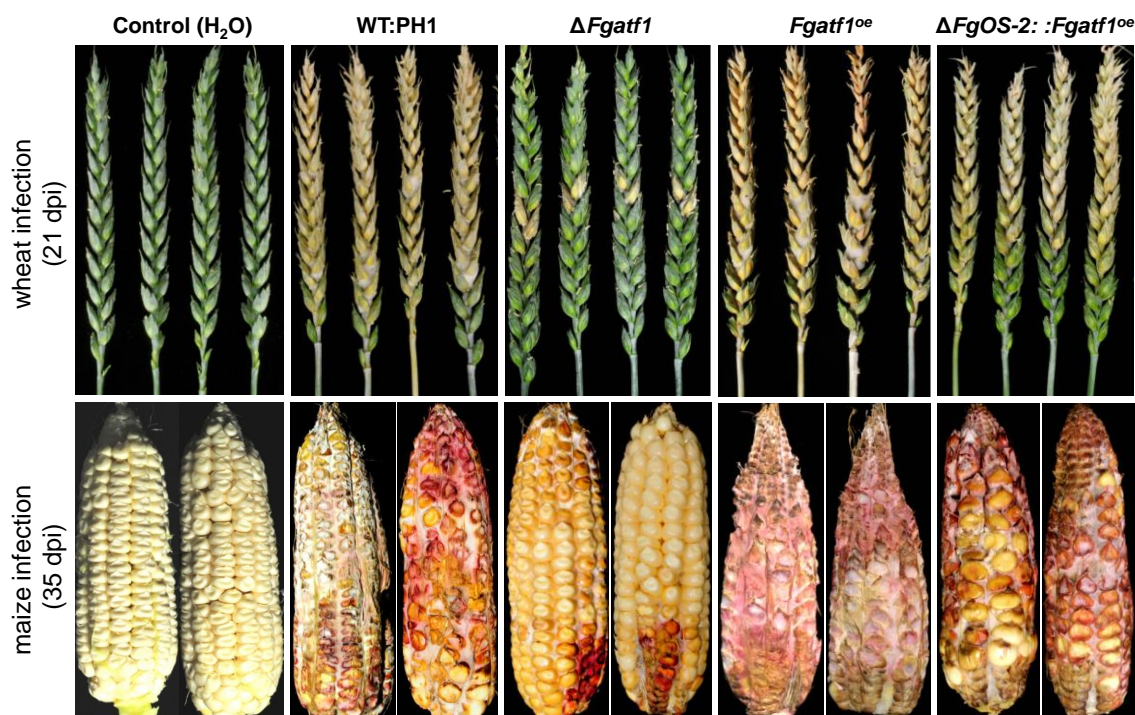


Figure 59. Pathogenicity assay on wheat and maize. Wheat heads (cv. Nandu; upper panel) and maize cobs (lower panel) were infected with conidia of the wild type (WT:PH1) and the mutants

Figure 59 continuance

$\Delta Fgatf1$, $Fgatf1^{oe}$, and $Fgatf1^{oe}::\Delta FgOS-2$ and then incubated for 21 (wheat) and 35 (maize) days. Inoculation with water served as the control. The $\Delta Fgatf1$ mutant showed a strong reduction in virulence towards maize and wheat. The $Fgatf1^{oe}$ mutant comprised an increased virulence towards wheat compared to the wild type. Constitutive expression of $Fgatf1$ partially restored the reduced virulence towards wheat and maize of the $\Delta FgOS-2$ mutant. The wild type infection caused typical symptoms for maize cob rot and *Fusarium* head blight (FHB) disease. The maize infections were repeated six times, the wheat infections were performed 30 times.

Intriguingly, the constitutive overexpression of $Fgatf1$ partially complements the apathogenicity towards wheat and maize caused by the deletion of $FgOS-2$ (Fig. 59 and Fig. 37). This phenotype is related to the observation that constitutive overexpression of $Fgatf1$ increased the virulence. On the susceptible wheat cultivar Nandu, infection proceeded faster compared to the wild type (Fig. 59). This accelerated infection became more obvious on the more resistant wheat cultivar Amaretto. The average infection of overexpression mutants proceeded faster and spread further compared to the wild type infection (Fig. 60).

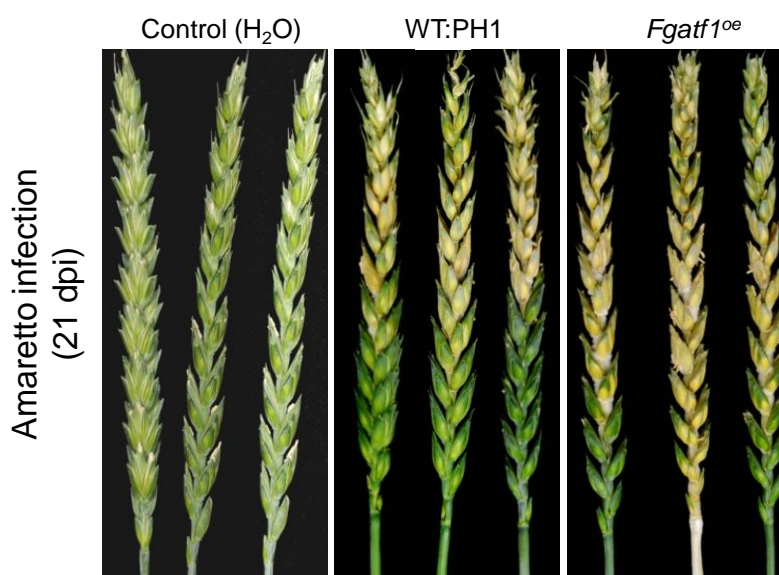


Figure 60. Pathogenicity assay on wheat cultivar Amaretto. Wheat heads were infected with conidia of the wild type (WT:PH1) and $Fgatf1^{oe}$ mutant strains and incubated for 21 days. The average infection of the $Fgatf1^{oe}$ mutant proceeded faster and spread further compared to the wild type infection. The infections were performed 20 times.

The reduction in virulence towards wheat of $\Delta Fgatf1$ mutants was certified by histological observations in longitudinal sections of whole spikes and also the rachis infected with red-fluorescent strains derived from one $\Delta Fgatf1$ strain and the wild type strain (Fig. 61 and Fig. 62). After 7 dpi, the $\Delta Fgatf1$ -dsRed strain partially colonized the inoculated spikelets but its growth towards the rachis node was attenuated. No dsRed fluorescence was detectable within or beyond the rachis nodes (Fig. 61A). After 21 dpi, inoculated spikelets were completely colonized by the $\Delta Fgatf1$ -dsRed-strain but not the adjacent spikelets (Fig. 61B and 62). In

contrast, the fluorescence of the strain derived from the wild type was observed in the infected spikelets and the adjacent spikelets after 7 dpi and propagating throughout the entire wheat heads within 21 dpi (Fig. 61 and Fig. 62).

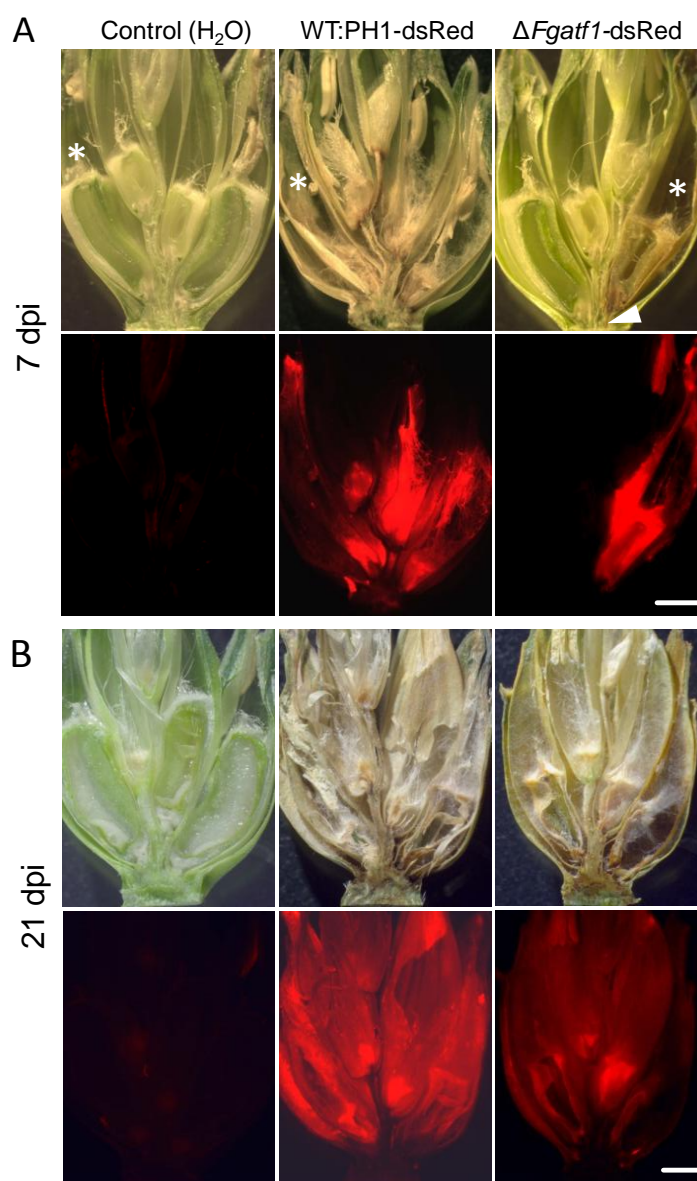


Figure 61. Infection assay. Cross-sections of inoculated wheat spikelets. The spikelets were infected with strains that constitutively express dsRed in the cytosol and that were derived from the wild type (WT:PH1) and a $\Delta Fgatf1$ strain. Water was used as the control. The inoculation points are indicated with white asterisks. **A.** Cross-sections of inoculated wheat spikelets after 7 dpi. The $\Delta Fgatf1$ -dsRed strain partially colonized the inoculated spikelet but growth towards the rachis node was attenuated (arrow head). The dsRed-expressing wild-type derivative strain showed complete necrosis of the infected spikelet after 7 dpi. DsRed-fluorescence was evenly distributed throughout the spikelet. **B.** Cross-sections of inoculated wheat spikelets after 21 dpi. The $\Delta Fgatf1$ -dsRed strain completely colonized the spikelet but no dsRed fluorescence was detected within or beyond the rachis node. The dsRed fluorescence of the WT:PH1-dsRed was observed in the entire spike. Scale bar 1 mm.

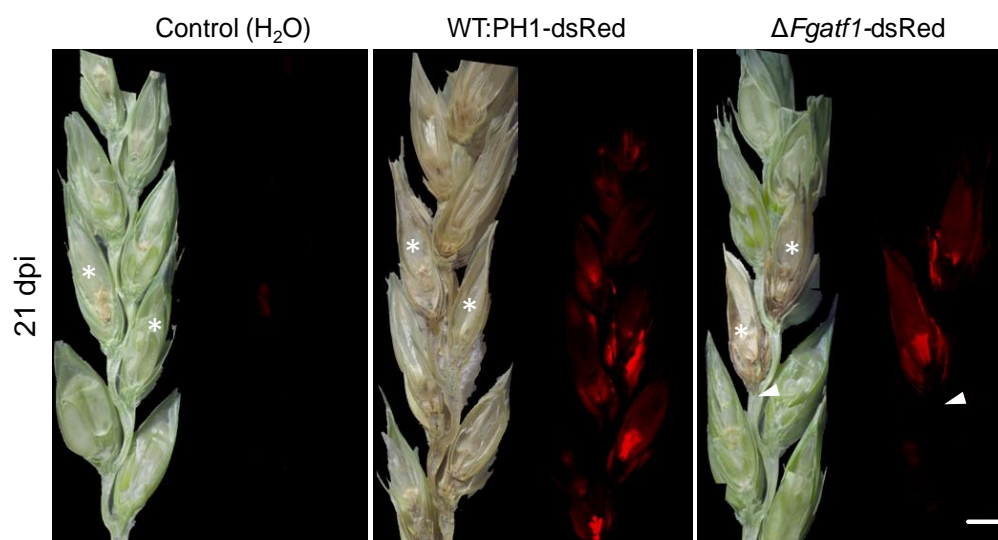


Figure 62. Infection assay. Longitudinal sections of the inoculated and adjacent spikelets. The spikelets were infected with strains that constitutively expressed dsRed in the cytosol and that were derived from the wild type (WT:PH1) and a $\Delta Fgatf1$ mutant. Water was used as the control. The inoculation points are indicated with white asterisks. Longitudinal sections of the entire spikes revealed that the $\Delta Fgatf1$ -dsRed strain colonized completely the inoculated spikelet but its growth stopped at the rachis node. No dsRed-fluorescence was detected in the rachis node (arrow heads), the rachis and the adjacent spikelets. The wild type successfully colonized the entire spike. Composite picture. Scale bar 2 mm.

Constitutive overexpression of *Fgatf1* also increased the virulence towards the close relative to cereal grain species, *B. distachyon*. When inoculated with the wild type, infection usually stops in the point-inoculated spikelets (Fig. 63). However, the average infection of the *Fgatf1* overexpressing mutants proceeded beyond inoculated spikelets (Fig. 63). These results suggest that the transcript level of *Fgatf1* plays a pivotal role in proper pathogenic development of *F. graminearum* on different hosts.

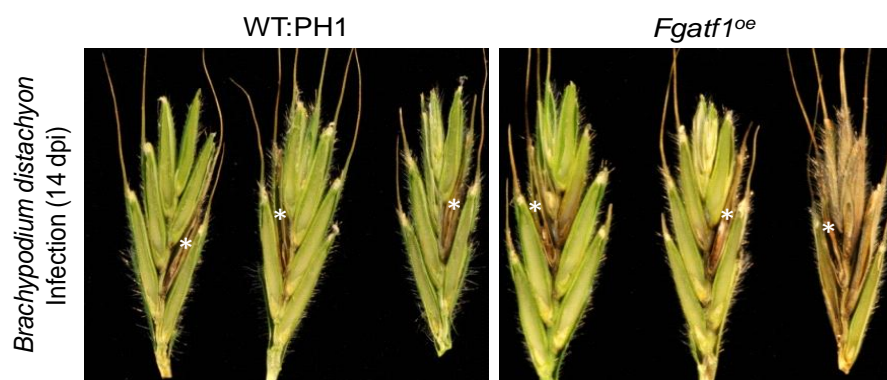


Figure 63. Pathogenicity assay on *Brachypodium distachyon*. *B. distachyon* was infected with conidia of the wild type (WT:PH1) and *Fgatf1^{oe}* mutant strains and incubated for 14 days. The inoculation points are indicated with white asterisks. Infection usually stops in the point-inoculated spikelet when inoculated with the wild type. The *Fgatf1^{oe}* mutant showed increases in virulence towards *B. distachyon* compared to the wild type. The infection of the *Fgatf1^{oe}* mutant spread beyond the inoculated spikelet. The infections were performed 20 times.

3.3.8. *Fusarium graminearum* Atf1 orchestrates secondary metabolite production

As shown previously, the ability to produce the trichothecenous mycotoxin deoxynivalenol and virulence towards wheat correlates (Proctor et al., 1995; Maier et al., 2006). Mutants deficient in the gene encoding a trichodien synthase are unable to bridge the rachis node. Deletion of *FgOS-2* also led to a reduced DON-production *in planta* and thus to a reduced virulence (see 3.2.5 and 3.2.6). The question if *Fgatf1* regulates DON-production, highly sensitive ELISA-measurements were conducted using infected wheat spikelets and samples obtained from liquid toxin-induction cultures. Spikelets inoculated with $\Delta Fgatf1$ mutants accumulated approximately 40 % of the amount of DON the wild type accumulated after 7 days of infection (Fig. 64a and Table 17). However, under *in-vitro* conditions, $\Delta Fgatf1$ mutants produced much more DON than the wild type. The mutant's DON-production was approximately 4 times higher after 1 day and 2 times higher after 3 days of incubation in DON-induction medium (Fig. 64b and Table 17). All measurements are normalized to the amount of fungal material in the sample using qPCR (Voigt et al., 2007). During plant infection expression of four genes involved in DON-production (*tri4*, encoding a P450 monooxygenase; *tri5*, trichodiene synthase; *tri6* and *tri10*, both transcription regulators) was lower in the $\Delta Fgatf1$ mutant compared to the wild type (Fig. 64c and Table 18). Under *in vitro* DON-inducing condition the expression of four *tri* genes was drastically up-regulated in the $\Delta Fgatf1$ mutant compared to the wild type (Fig. 64d and Table 18).

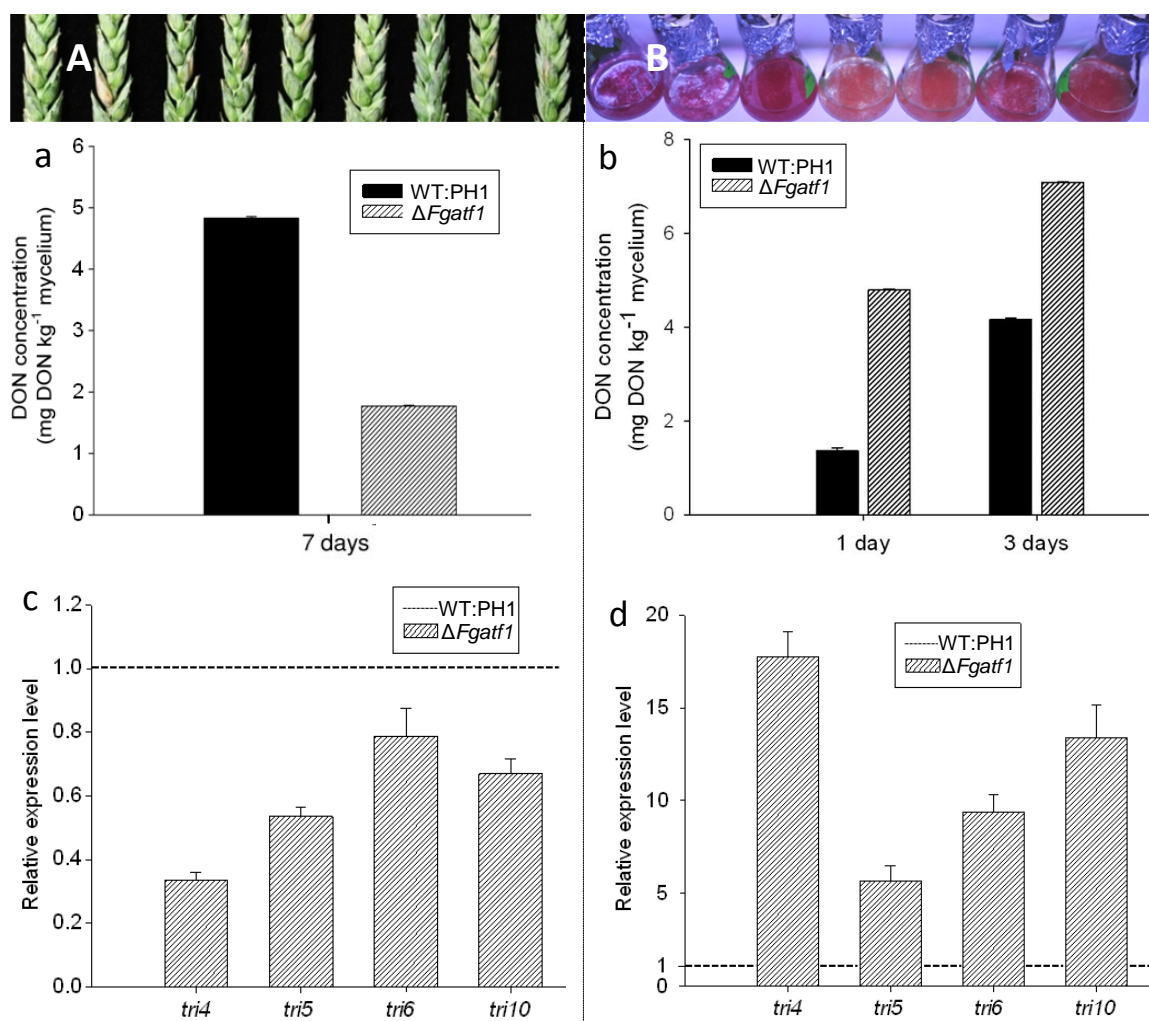


Figure 64. DON concentrations and gene expression analysis of the wild type and *Fgaf1* deletion strains in wheat heads (A) and submerged culture (B). a, b. The DON concentration was determined by ELISA. The DON contents in wheat spikelets inoculated with the $\Delta Fgaf1$ mutant were lower compared to the wild type (WT:PH1). *In vitro*, DON production was induced using $(\text{NH}_4)_2\text{SO}_4$ as the sole nitrogen source. The mutant produced much more DON in this medium compared to the wild type. The DON concentrations were normalized against the amount of fungal mycelium per kilogram of substrate, determined by quantitative PCR. c, d. Quantitative RT-PCR analysis. Transcriptional profiling of the wild type and *Fgaf1* deletion strains after the colonization of wheat florets (7 dpi; c) and after *in-vitro* culture (1 dpi; d). Gene expression data were generated for the genes *tri4* (encoding a P450 monooxygenase), *tri5* (trichodiene synthase), *tri6* and *tri10* (both transcription regulators) and normalized to β -tubulin expression (primer list: Table 5). The expression of four *tri* genes was lower in the $\Delta Fgaf1$ mutant *in planta* assayed when compared to the wild type. Under *in vitro* DON-inducing condition the expression of four *tri* genes was drastically up-regulated in the $\Delta Fgaf1$ mutant compared to the wild type. Quantitative RT-PCR was performed twice, with three replicates each. Wild-type expression was set at 1. Toxin measurements were repeated twice with four replicates each. Error bars indicate the standard deviation.

Table 17. ELISA analysis of DON production under different growth conditions in the wild type (WT:PH1) and *Fgatf1* deletion strains. All values were normalized against the amount of fungal material in the sample using qPCR (see Materials and Methods). The assay was performed using two biological and four technical replicates.

	DON (mg kg ⁻¹ mycelium)		
	<i>in vitro</i>		<i>in planta</i>
	1 dpi	3 dpi	7 dpi
WT:PH1	1,367 (±0.062)	4,169 (±0.026)	4.83 (±0.0249)
$\Delta Fgatf1$	4,793 (±0.0143)	7,092 (±0.0095)	1,77 (±0.0139)

Table 18. Gene expression analysis of genes involved in DON biosynthesis. Quantitative real-time PCR results indicate up or down regulation in the *Fgatf1* deletion strain compared to the wild type (WT:PH1) (set at 1). Expression analysis was performed using two biological and three technical replicates. Gene expression was normalized against β -tubulin gene expression.

DON biosynthesis	<i>tri4</i>	<i>tri5</i>	<i>tri6</i>	<i>tri10</i>
Toxin induction medium	17,7572±1,3205	5,6795±0,8125	9,3880±0,9085	13,3796±0,1,7432
<i>in planta</i>	0,3365±0,0236	0,5355±0,0301	0,7871±0,0886	0,6691±0,0470

The other mutants (*FgOS-2*, *Fgatf1^{oe}* and *Fgatf1^{oe}:: $\Delta FgOS-2$*) were also assayed for DON production *in planta*. Interestingly, the $\Delta Fgatf1$ DON level ranges in between the wild type and the $\Delta FgOS-2$ DON level. $\Delta Fgatf1$ mutants produced approximately 40 % of the amount of DON the wild type and 19 times more than $\Delta FgOS-2$ mutants produced after 7 days of infection (Fig. 65 and Table 19). *Fgatf1^{oe}* mutants produced 1.5 times more DON production compared to the wild type after 7 of wheat infection. Interestingly, overexpression of *Fgatf1* drastically increased the DON production in $\Delta FgOS-2$ mutants. Spikelets inoculated with *Fgatf1^{oe}:: $\Delta FgOS-2$* mutants accumulated approximately 75% of the amount of DON in the wild type and 47 times more than $\Delta FgOS-2$ mutants (Fig. 65 and Table 19). This substantiates a previous finding that *FgOS-2*, in concert with the downstream transcriptional regulator *Fgatf1*, is the central trigger for growth-conditions dependent regulatory networks for DON-production. Furthermore, these results indicate a dominant inhibitory effect of *Fgatf1* on the production of DON under *in-vitro* conditions. Whether this is an effect of direct regulation or due to pleiotropic effects demands further investigation.

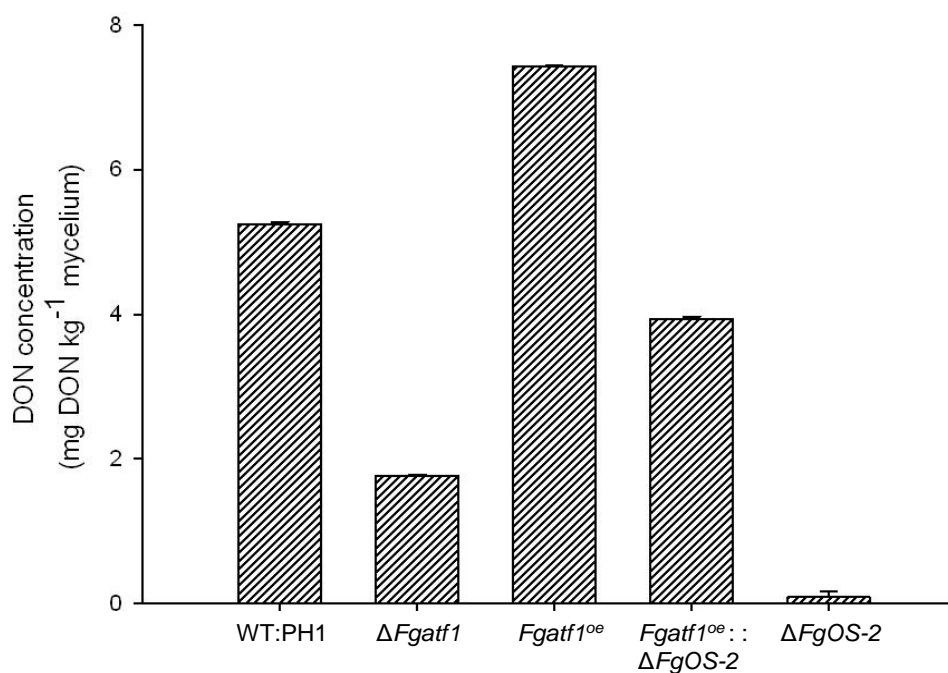


Figure 65. DON concentrations of the wild type (WT:PH1) and the mutants $\Delta Fgatf1$, $Fgatf1^{oe}$ and $Fgatf1^{oe}::\Delta FgOS-2$ and $\Delta FgOS-2$ in wheat heads after 7 dpi. The DON concentration was determined by ELISA. The DON contents in wheat spikelets inoculated with the $\Delta FgOS-2$ mutant were approximately 59 times lower compared to the wild type (WT:PH1). The $\Delta Fgatf1$ DON level was in-between the wild type and the $\Delta FgOS-2$ DON levels. The mutant $Fgatf1^{oe}$ produced more DON compared to the wild type. The constitutive expression of $Fgatf1$ restored DON-deficiency resulting from the deletion of $FgOS-2$. The DON concentrations were normalized against the amount of fungal mycelium per kilogram of substrate, determined by quantitative PCR. Toxin measurements were repeated twice with four replicates each. Error bars indicate the standard deviation.

Table 19. ELISA analysis of mycotoxin production *in planta* of the wild type (WT:PH1) and the mutants $\Delta Fgatf1$, $\Delta FgOS-2$, $Fgatf1^{oe}$ and $Fgatf1^{oe}::\Delta FgOS-2$. All values were normalized against the amount of fungal material in the sample using qPCR (see Materials and Methods). The assay was performed using two biological and four technical replicates.

	DON (mg kg ⁻¹ mycelium)
WT:PH1	5,2501±0,0318
$\Delta FgOS-2$	0,0838±0,0777
$\Delta Fgatf1$	1,77±0.0139
$Fgatf1^{oe}$	7,4316±0,0156
$Fgatf1^{oe}::\Delta FgOS-2$	3,9351±0.0359

A second predominant mycotoxin, Zearalenone (ZEA), accumulates in infected grains and is also produced in axenic culture (Gaffoor et al., 2005). After 7 dpi on wheat spikes, $\Delta Fgatf1$ mutants synthesised approximately 3 times less ZEA compared to the wild type (Fig. 66a and

Table 20). Like already observed for $\Delta FgOS-2$ mutants (see 3.2.6), transcript level of the putative regulatory transcription factor ($zeb2$) was higher in $Fgatf1$ deletion mutants compared to the wild type at 7 dpi. Expression of genes encoding an isoamyl alcohol oxidase ($zeb1$) and a non-reducing polyketide synthase ($zea1$) was reduced *in planta* compared to the wild type (Fig. 66c and Table 21). Under *in-vitro* induction conditions there was no difference in ZEA production (and the regulation of gene expression) between $\Delta Fgatf1$ mutants and the wild type (Fig. 66b, d; Table 20 and 21).

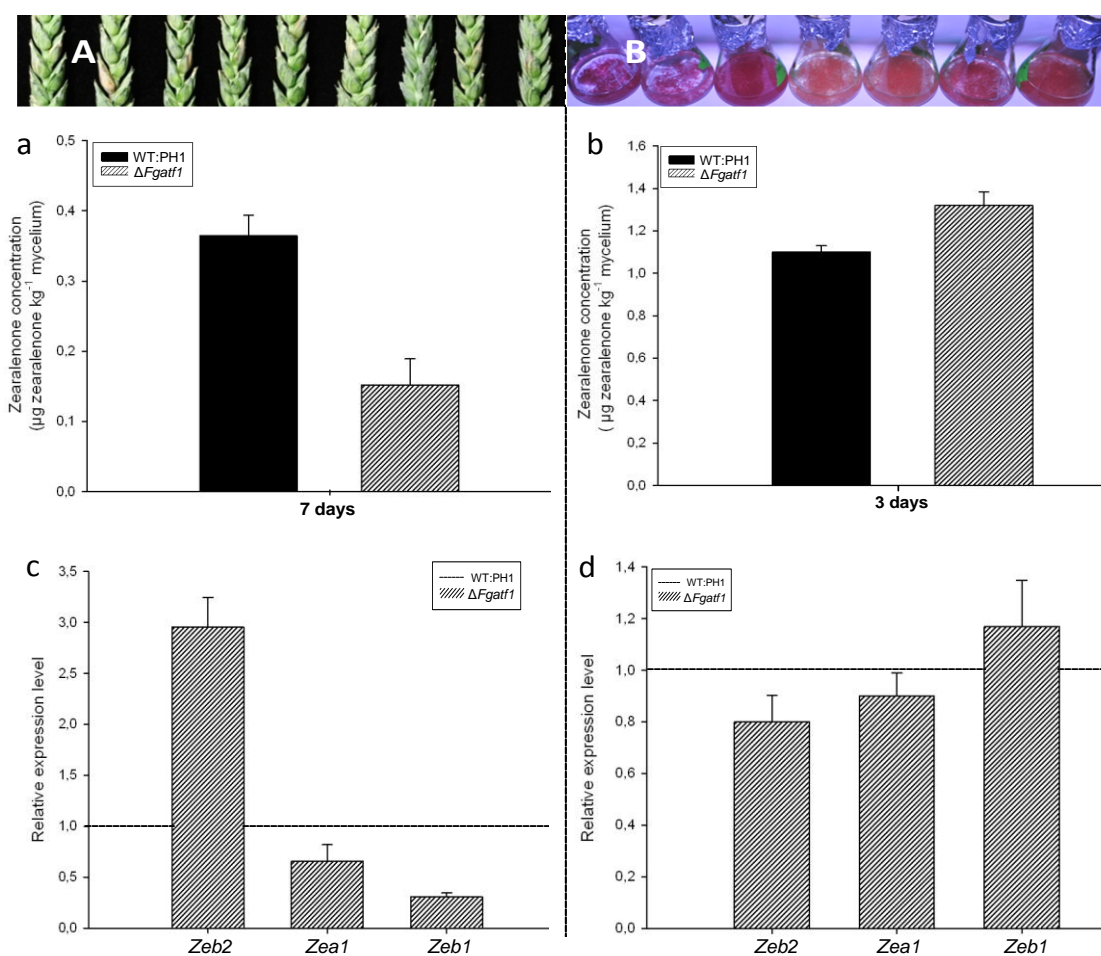


Figure 66. ZEA concentrations and gene expression analysis of the wild type and $Fgatf1$ deletion strains in wheat heads (A), submerged culture (B). ZEA production in the wild type (WT:PH1) and $Fgatf1$ deletion strains was measured in inoculated wheat heads (a) and in submerged cultures of YES medium (see Materials and Methods; b) and normalized against the fungal mycelium as described above. No significant difference was found in ZEA contents between the wild type and $\Delta Fgatf1$ mutant strains under *in-vitro* conditions. The ZEA concentration in wheat spikelets inoculated with the $\Delta Fgatf1$ mutant was lower compared to the wild type. c, d. Quantitative RT-PCR on genes involved in ZEA production. The expression of $zeb2$ (encoding a regulatory transcription factor), $zea1$ (polyketide synthases) and $zeb1$ (isoamyl alcohol oxidase) was determined from cDNA derived from both strains after 7 dpi (*in planta*; c) and 3 dpi (*in vitro*; d). In the *in-planta* samples, $zeb2$ expression was induced in the mutant strain while the expression of $zeb1$ and $zea1$ was repressed. No significant differences in gene expression were detectable under *in-vitro* conditions. Quantitative RT-PCR was performed twice, with three replicates each. Wild-type expression was set at 1. Toxin measurements were repeated twice with four replicates each. Error bars indicate the standard deviation.

Table 20. ELISA analysis of ZEA production under different growth conditions in the wild type (WT:PH1) and *Fgatf1* deletion strains. All values were normalized against the amount of fungal material in the sample using qPCR (see Materials and Methods). The assay was performed using two biological and four technical replicates.

	ZEA ($\mu\text{g kg}^{-1}$ mycelium)	
	<i>in vitro</i>	<i>in planta</i>
	3 dpi	7 dpi
WT:PH1	1,1 (± 0.0302)	0,3645 (± 0.0292)
$\Delta Fgatf1$	1,32 (± 0.0636)	0,152 (± 0.0372)

Table 21. Gene expression analysis of genes involved in ZEA biosynthesis. Quantitative real-time PCR results indicate up or down regulation in the *Fgatf1* deletion strain compared to the wild type (WT:PH1) (set at 1). Expression analysis was performed using two biological and three technical replicates. Gene expression was normalized against β -tubulin gene expression.

ZEA biosynthesis	<i>zeb1</i>	<i>zeb2</i>	<i>zea1</i>
Toxin induction medium	1,1688 \pm 0,1798	0,8 \pm 0,1026	0,9 \pm 0,0884
<i>in planta</i>	0,3040 \pm 0,0439	2,953 \pm 0,2959	0,36585 \pm 0,1603

A third prominent secondary metabolite of *F. graminearum* is the red pigment aurofusarin. When grown on CM plates, the colonies of the $\Delta Fgatf1$ mutants produced more red pigmentation compared to the wild type, indicating an up-regulation of aurofusarin production (Fig. 67A). Regulation of aurofusarin production was shown previously to be regulated in an FgOS-2 dependent manner (see 3.2.6). This regulation partially takes place via *Fgatf1*-signaling since pigment production and expression of genes involved in aurofusarin biosynthesis (*gip1*, encoding a putative laccase; *gip2*, transcription factor; *pks12*, polyketide synthase) were up-regulated in $\Delta Fgatf1$ mutants compared to the wild type (Fig. 67B).

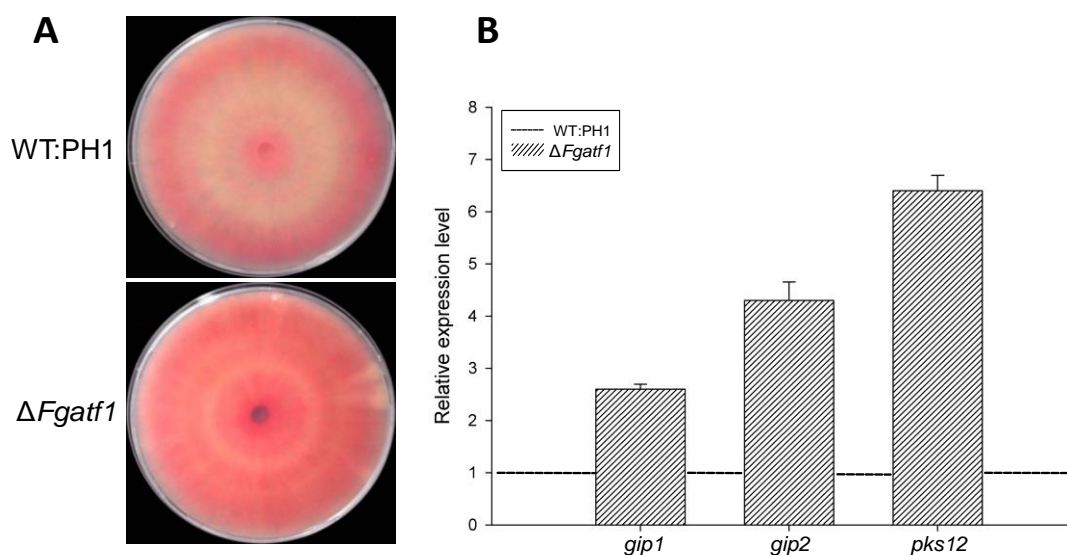


Figure 67. Pigmentation assay and corresponding gene expression analysis. **A.** Aurofusarin production on CM agar plates after 5 dpi. Aurofusarin biosynthesis was up-regulated in the $\Delta Fgatf1$ mutant compared to the wild type (WT:PH1). **B.** Quantitative RT-PCR on genes involved in aurofusarin biosynthesis (primer list: Table. 5), *gip1* (encoding a putative laccase), *gip2* (transcription factor) and *pks12* (polyketide synthase). Expression of *gip1*, *gip2* and *pks12* was up-regulated in the $\Delta Fgatf1$ mutant compared to the wild type (expression level set at 1) *in vitro*. Error bars indicate the standard deviation. QRT-PCR was performed using two biological and three technical replicates.

Taken together these results underline the pivotal role of the FgOS-2/Fgatf1-signaling cascade in the regulation of secondary metabolite production.

3.3.9. *Fusarium graminearum* Atf1 is involved in regulation of ROS metabolism and catalase gene expression

The stress-activated protein kinase FgOS-2 is a key regulator in the life cycle of the cereal pathogen *F. graminearum*. The diverse physiological functions controlled by FgOS-2 are executed through the regulation of ROS; these include perithecia formation, the production of secondary metabolites and virulence. FgOS-2 may regulate catalase expression and activity through its putative downstream target Atf1. FgOS-2 may act as a positive or negative regulator of Atf1 and catalase genes depending on growth conditions (see 3.2.7). One assumption is that the global ROS-metabolism is synchronized by the FgOS-2/FgAtf1 signaling machinery, probably by regulation of catalase expression. In order to determine whether or not Fgatf1 is involved in ROS metabolism, nitro blue tetrazolium chloride (NBT)-staining of the wild type and the $\Delta FgOS-2$, $\Delta Fgatf1$, *Fgatf1^{oe}* and *Fgatf1^{oe}:: $\Delta FgOS-2$* mutant colonies grown on agar plates containing osmotic stress agent (0.2 M NaCl or 0.8 M NaCl) were performed. Gene expression of four putative catalase genes (Primer list: Table 5) in the

wild type, $\Delta FgOS-2$ and $Fgatf1$ mutants under different stress conditions and *in planta* were also tested.

Detection of ROS using NBT revealed no remarkable coloration of $\Delta Fgatf1$ mutant colonies on CM containing 0.2 M NaCl compared to the wild type like it was detectable for the $\Delta FgOS-2$ mutants (Fig. 68A). Hence, there was no accumulation of ROS under mild osmotic stress conditions. Interestingly, on high osmotic stress (0.8 M NaCl), ROS production in $Fgatf1^{oe}$ mutants was higher compared to $\Delta Fgatf1$ mutants but lower compared to the wild type (Fig. 68B). NBT staining also confirmed the previous result that the $\Delta FgOS-2$ mutant showed a greater ROS production upon mild osmotic stress compared to the wild type. $Fgatf1^{oe}::\Delta FgOS-2$ mutants exhibited a lower accumulation in ROS production compared to $\Delta FgOS-2$ mutants (Fig. 68A).

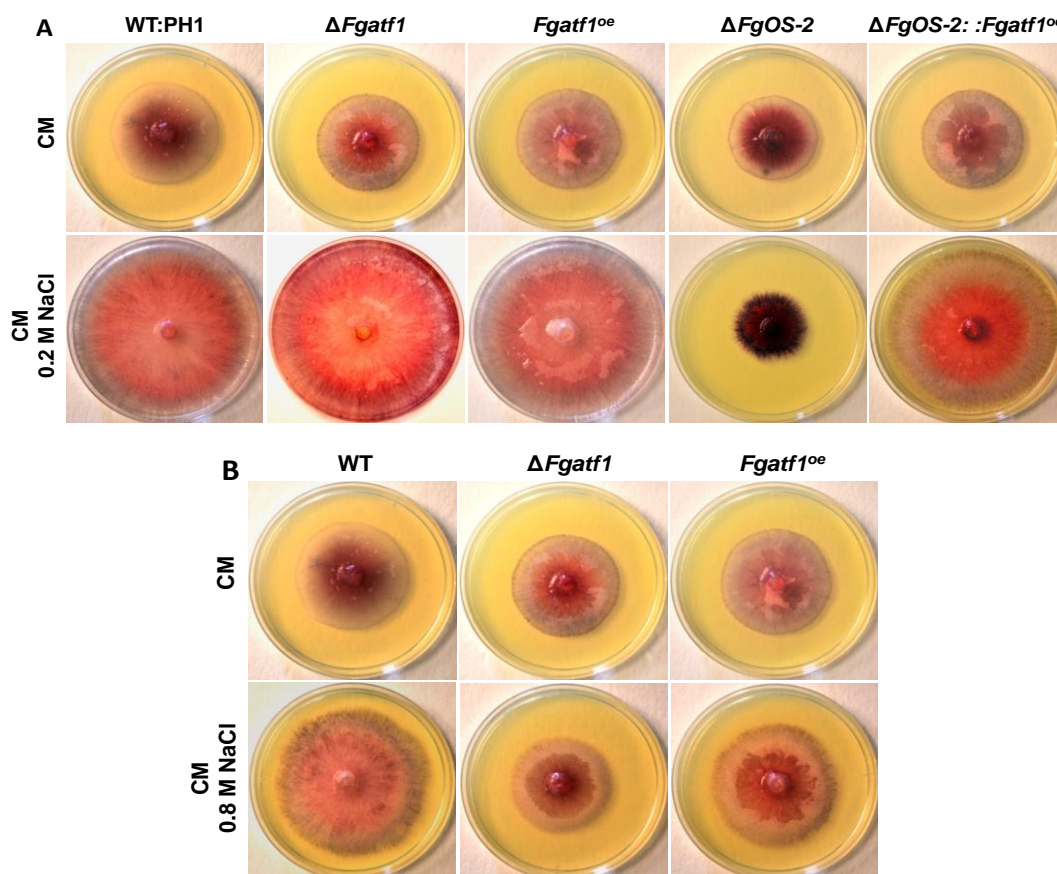


Figure 68. Nitroblue tetrazolium (NBT) staining for reactive oxygen species (ROS) production of the wild type (WT:PH1), $\Delta FgOS-2$ mutant and the $Fgatf1$ mutants on CM and CM supplemented with 0.2 M NaCl (A) and 0.8 M NaCl (B) after 3 days of growth. The dark color indicates ROS production. On CM plates supplemented with 0.2 M NaCl, the $FgOS-2$ deletion strain showed a greater production of ROS upon osmotic stress compared to the wild type. The $Fgatf1^{oe}::\Delta FgOS-2$ mutant exhibited a lower ROS production on osmotic stress compared to the $FgOS-2$ deletion strain. No remarkable difference in ROS production was visible between the $\Delta Fgatf1$, $Fgatf1^{oe}$ and the wild type strains on this medium. On CM plates supplemented with 0.8 M NaCl, the wild type exhibited a higher production of ROS compared to the $Fgatf1^{oe}$ and the $\Delta Fgatf1$ mutants.

In order to investigate the regulation of four putative catalase genes on the transcriptional level, mycelia of the wild type and $\Delta Fgatf1$ mutant strains were raised in liquid CM and subsequently shifted to induction media containing 0.8 M NaCl and 10 mM H_2O_2 , respectively. Induction with 0.8 M NaCl led to a 2-3-fold up regulation of all catalase genes, except for *cat2.1* which transcript level remained stable compared to the wild type (Fig. 69C and Table 22). Under oxidative stress condition the expression of all catalase genes was greater in $\Delta Fgatf1$ mutants compared to the wild type (Fig. 69B and Table 22). During infection of wheat heads (7dpi) transcript levels of *cat1* and *cat3* were nearly the same between the wild type and *Fgatf1* deletion mutant strains. However, two catalase-encoding genes *cat2.1* and *cat2.2* were up-regulated approximately 1.5 times in the *Fgatf1* deletion mutants compared to the wild type (Fig. 69A and Table 22). The influence of *Fgatf1* on catalase expression levels under osmotic stress and oxidative stress conditions is also reflected by the results of an enzyme activity assay. As shown in Figure 69D, catalase activity was unremarkably increased in *Fgatf1* deletion strains compared to the wild type under osmotic stress conditions. However, under oxidative stress conditions, catalase activity in $\Delta Fgatf1$ mutants was elevated compared to the wild type.

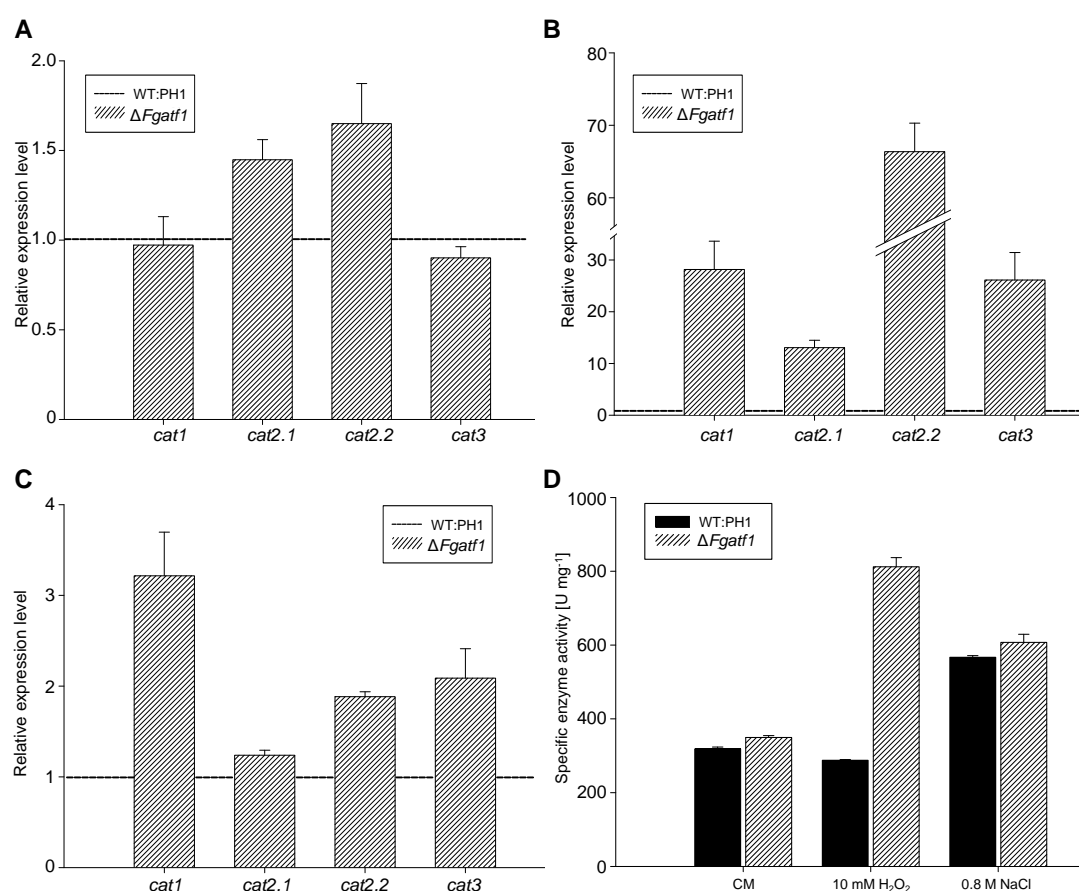


Figure 69. Catalase expression and activity assay. A-C. Quantitative RT-PCR using cDNA obtained from inoculated wheat spikelets (7 dpi, **A**), H_2O_2 supplemented (10 mM, **B**) and NaCl-

Figure 69 continuance

supplemented samples (0.8 M, **C**). Expression of four different, putative catalase genes was assayed in the wild type and $\Delta Fgatf1$ mutant strains. The wild type expression level was set at 1. Expression of all catalase genes except *cat2.1* were up-regulated in the $\Delta Fgatf1$ mutant compared to the wild type under osmotic conditions (**C**). During infection of wheat heads (7dpi) in the $\Delta Fgatf1$ mutant, transcript levels of *cat1* and *cat3* were similar to the wild type. *Cat2.1* and *cat2.2* expression levels were up-regulated in the $\Delta Fgatf1$ mutant compared to the wild type. Under oxidative stress conditions gene expression of all catalase genes is drastically up in the $\Delta Fgatf1$ mutant compared to the wild type. Error bars indicate the standard deviation. QRT-PCR was performed twice in triplicate. **D**. Catalase activity assay using protein extract obtained from mycelium raised in CM with and without 2 h-induction by 0.8 M NaCl and 10 mM H₂O₂, respectively. Total catalase activity of the $\Delta Fgatf1$ mutant was slightly higher compared to the wild type under no-stress and osmotic-stress conditions and drastically elevated under oxidative stress conditions. The assay was performed using two biological and three technical replicates.

Table 22. Gene expression analysis of putative catalase genes. Quantitative real-time PCR results indicate up or down regulation in the $\Delta Fgatf1$ mutant compared to the wild type (WT:PH1) (set at 1). Expression analysis was performed using two biological and three technical replicates. Gene expression was normalized against β -tubulin gene expression.

	<i>cat1</i>	<i>cat2.1</i>	<i>cat2.2</i>	<i>cat3</i>
NaCl	3,2161±0,4806	1,2383±0,0555	1,8842±0,0534	2,0880±0,3238
H₂O₂	28,1526±5,4778	13,0572±1,4254	66,3641±3,9346	26,1159±5,3194
<i>in planta</i>	0,9721±0,1587	1,4482±0,1121	1,6498±0,2237	0,9012±0,0620

The expression analysis of four catalase genes in the mutants $\Delta FgOS-2$, $Fgatf1^{oe}$, $Fgatf1^{oe}::\Delta FgOS-2$ under osmotic stress conditions and *in planta* was also performed by qRT-PCR. Expression of *cat1*, *cat2.1* and *cat2.2* were up-regulated in the $Fgatf1^{oe}$ mutants compared to the wild type. Only *cat3* expression level was down-regulated compared to the wild type after a 2-h induction in 0.8 M NaCl. The expression levels of the four catalase genes (in particular catalase 1 gene expression) were down-regulated in the $FgOS-2$ -deletion strains compared to the wild type (Fig. 70 and Table 23).

Intriguingly, overexpression of *Fgatf1* partially restored the expression levels of the four catalases in the $\Delta FgOS-2$ mutant background. Catalase1 expression level in $Fgatf1^{oe}::\Delta FgOS-2$ mutants was 15-fold up-regulated compared to the $\Delta FgOS-2$ mutants (Fig. 70 and Table 23).

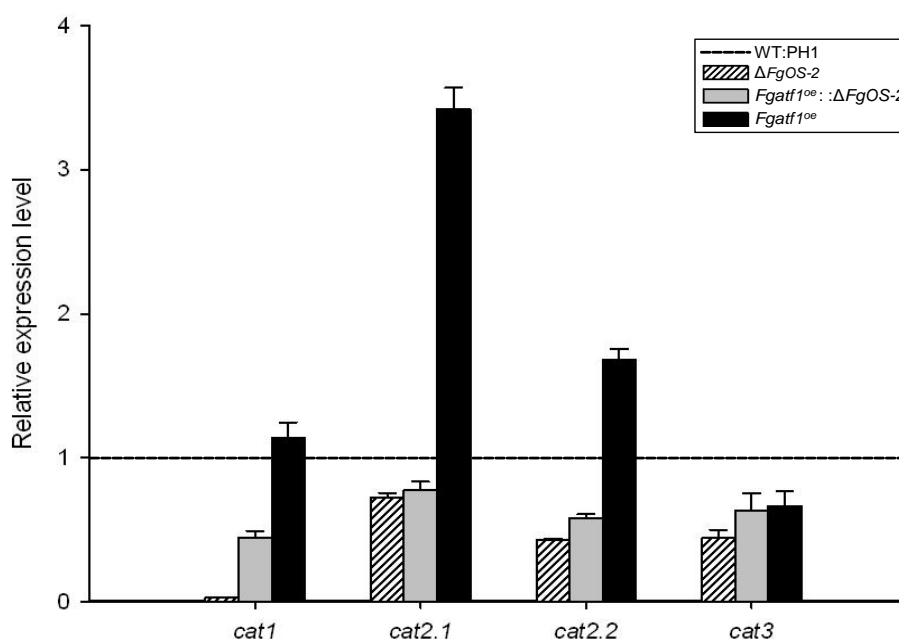


Figure 70. Catalase gene expression analysis. Quantitative RT-PCR using cDNA obtained from induction medium containing 0.8 M NaCl after a 2-h induction. Expression of four different, putative catalase genes was assayed in the wild type and the mutants $\Delta FgOS-2$, $Fgatf1^{oe}::\Delta FgOS-2$ and $Fgatf1^{oe}$ mutants. The wild-type expression level was set at 1. The $Fgatf1^{oe}$ mutant showed an increase in *cat1*, *cat2.1* and *cat2.2* expression levels. *Cat3* expression level was down-regulated compared to the wild type. All catalase genes were down-regulated in the $FgOS-2$ -deletion strain compared to the wild type. Overexpression of *Fgatf1* led to a partially restoration of the expression levels of all catalases in the $\Delta FgOS-2$ mutant background. Error bars indicate the standard deviation. QRT-PCR was performed twice with triplicate each.

Table 23. Gene expression analysis of putative catalase genes in osmotic stress medium (0.8 M NaCl). Quantitative real-time PCR results indicate up or down regulation in the mutants $\Delta FgOS-2$, $Fgatf1^{oe}::\Delta FgOS-2$ and $Fgatf1^{oe}$ compared to the wild type (WT:PH1) (set at 1). Expression analysis was performed using two biological and three technical replicates. Gene expression was normalized against β -tubulin gene expression.

	<i>cat1</i>	<i>cat2.1</i>	<i>cat2.2</i>	<i>cat3</i>
$\Delta FgOS-2$	0,0296±0,00109	0,7236±0,032	0,4286±0,0098	0,4426±0,0582
$Fgatf1^{oe}::\Delta FgOS-2$	0,4471±0,0451	0,7785±0,0576	0,5844±0,0231	0,634±0,1206
$Fgatf1^{oe}$	1,1399±0,1077	3,42±0,153	1,6786±0,079	0,6674±0,1006

In planta, the expression levels of *cat2.1* and *cat2.2* were up-regulated in $Fgatf1^{oe}$ mutants as well as $Fgatf1^{oe}::\Delta FgOS-2$ mutants compared to the wild type, respectively. On the other hand, expression levels of *cat1* and *cat3* were down-regulated. However, the expression levels of *cat1*

and *cat3* genes in *Fgatf1^{oe}* as well as *Fgatf1^{oe}::ΔFgOS-2* were about 10 and 5 times higher compared to *FgOS-2* deletion strains, respectively (Fig. 71 and Table 24).

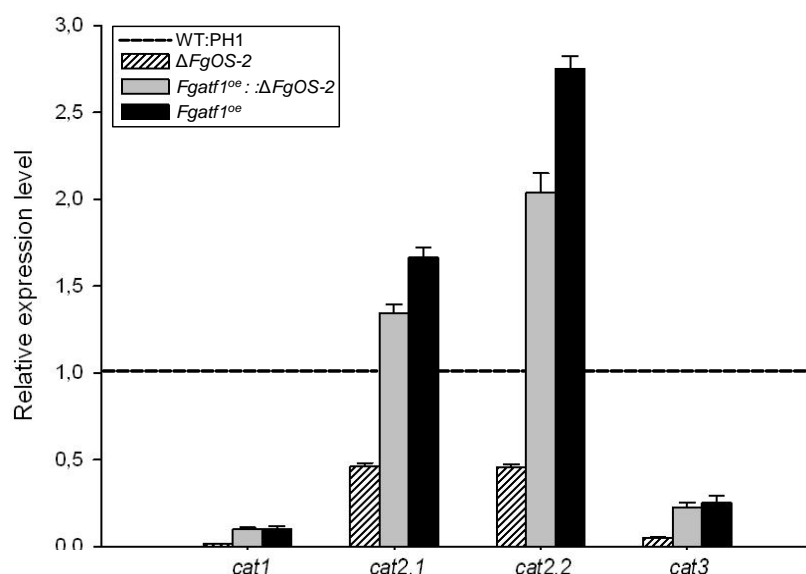


Figure 71. Catalase gene expression analysis. Quantitative RT-PCR using cDNA obtained from inoculated wheat spikelets (7 dpi). Expression of catalase genes was assayed in the wild type (WT:PH1) and the mutants $\Delta FgOS-2$, *Fgatf1^{oe}* and *Fgatf1^{oe}::ΔFgOS-2*. The wild-type expression level was set at 1. Expression analysis was performed using two biological and three technical replicates. Gene expression was normalized against β -tubulin gene expression.

Table 24. Gene expression analysis of putative catalase genes of *F. graminearum* during wheat infection. Quantitative real-time PCR results indicate up or down regulation in the mutants *Fgatf1^{oe}*, $\Delta FgOS-2$ and *Fgatf1^{oe}::ΔFgOS-2* compared to the wild type (WT:PH1) (set at 1). Expression analysis was performed using two biological and three technical replicates. Gene expression was normalized against β -tubulin gene expression.

	<i>cat1</i>	<i>cat2.1</i>	<i>cat2.2</i>	<i>cat3</i>
$\Delta FgOS-2$	0,0171±0,00066	0,4623±0,019	0,457±0,0182	0,0523±0,0051
<i>Fgatf1^{oe}::ΔFgOS-2</i>	0,109±0,00985	1,3426±0,0498	2,0377±0,1138	0,2227±0,0302
<i>Fgatf1^{oe}</i>	0,104±0,01339	1,664±0,0593	2,75±0,0764	0,253±0,0418

These results substantiate the assumption that the FgOS-2/Fgatf1-cascade is the central trigger of ROS metabolism via catalase gene expression in *F. graminearum*.

3.3.10. *Fusarium graminearum* Atf1 is involved in the regulation of light-dependent processes

Numerous developmental processes in fungi are regulated in a light- and circadian-clock dependent manner (reviewed in Dunlap and Loros 2004 , Rodriguez-Romero et al. 2010). In

addition, there are indications for a connection between the SAPK-signaling cascade and the light-dependent regulation. To check if –in *F. graminearum*– the light perception and the regulation of light dependent genes are influenced by Atf1, we conducted plate assays under different light conditions. First, CM plates were inoculated with the wild type and the mutants $\Delta FgOS-2$, $\Delta Fgatf1$, $Fgatf1^{oe}$ and $Fgatf1^{oe}::\Delta FgOS-2$, respectively. Second, these plates were incubated at 28°C under permanent light, permanent darkness, and with a 6-hours-light/6-hours-darkness rhythm, respectively. Figure 72 shows the colonies morphology after 4 days of incubation. The wild type, $\Delta FgOS-2$ and $\Delta Fgatf1$ strains developed pericentric rings of yellowish and reddish regions when they were incubated in the light-darkness rhythm. In both *Fgatf1* over-expressing mutants the red colour was evenly distributed in the centre of the colonies. The growing edge of colonies of all strains was uniformly yellowish. Under permanent darkness condition, the formation of rings was weaker in the wild type and $\Delta FgOS-2$ mutant strains and absent in $\Delta Fgatf1$ as well as $Fgatf1^{oe}$ mutants (Fig. 72). Finally, under permanent light condition, none of the strains produced coloured rings. Interestingly, $\Delta FgOS-2$ mutants were strongly affected in the formation of aerial hyphae under permanent light condition.

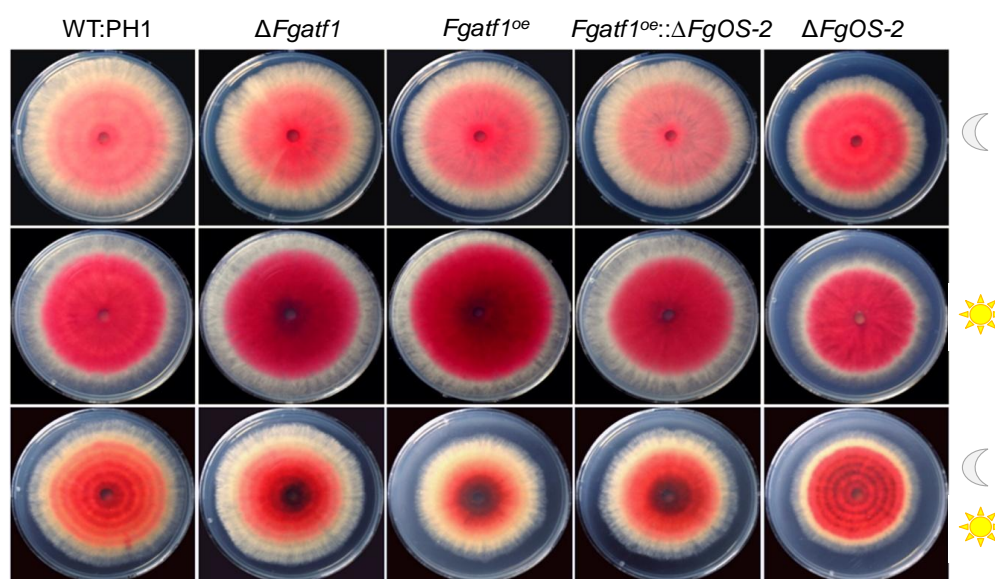


Figure 72. Growth assay in different light conditions. The wild type (WT:PH1) and the mutants $\Delta FgOS-2$, $\Delta Fgatf1$, $Fgatf1^{oe}$ and $Fgatf1^{oe}::\Delta FgOS-2$ were inoculated on CM plates and then incubated at 28°C for 4 days under permanent light, permanent darkness, and with a 6-hours-light/6-hours-darkness rhythm, respectively.

To proof if genes involved in the perception and transduction of light signals are influenced by *Fgatf1* and *FgOS-2*, respectively, RT-PCR using cDNA obtained from liquid cultures raised under permanent darkness and permanent light conditions, respectively, were conducted. Three different putative green light receptors (opsins; FGSG_07554,

FGSG_01440 and FGSG_03064), the putative blue light receptor VIVID (Vvd1; FGSG_08456) and the putative circadian clock regulator protein, Frequency (Frq; FGSG_06454) were analyzed. In summary, *Fgatf1* has a dominant influence on the expression of the *ops2*, *frq1* and *vvd1*. Upon *Fgatf1* deletion, the induction of *ops2* expression in the light was absent. In the wild type, *frq1* and *vvd1* expression were induced in darkness and repressed under light conditions. This regulation pattern was inverted in $\Delta Fgatf1$, *Fgatf1*^{oe} and $\Delta FgOS-2$ mutants. Interestingly, in *Fgatf1*^{oe}:: $\Delta FgOS-2$ mutants, *frq1* and *vvd1* transcript level were elevated both in darkness and in permanent light. In $\Delta FgOS-2$ mutants under light conditions, *ops2* and *ops3* expression were strongly induced compared to the wild type. *Ops1* expression was independent from light conditions and the genetic background (Fig. 73).

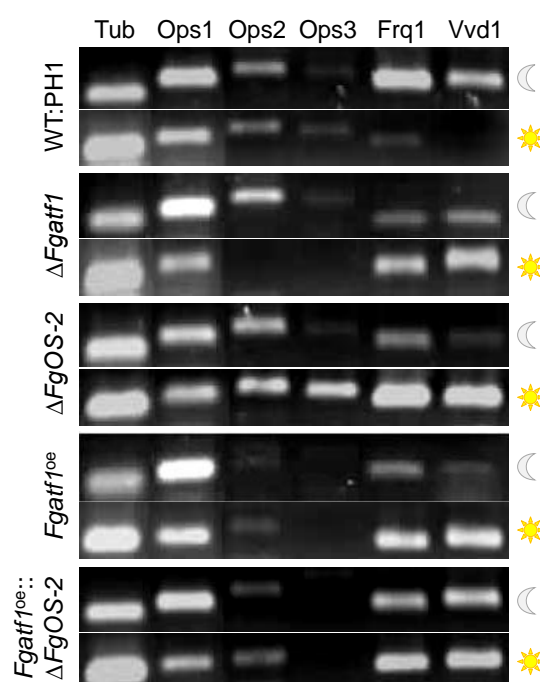


Figure 73. Expression analysis of genes encoding for putative light receptors and putative circadian clock receptor proteins in the wild type (WT:PH1) and the mutants $\Delta FgOS-2$, $\Delta Fgatf1$, *Fgatf1*^{oe} and *Fgatf1*^{oe}:: $\Delta FgOS-2$. A RT-PCR (35 PCR cycles, primer list: Table. 4) using cDNA obtained from liquid cultures raised under permanent darkness and permanent light conditions, respectively. Expression analysis was performed using two biological and three technical replicates.

These results indicate that genes involved in the perception and transduction of light signals are influenced by *Fgatf1* and *FgOS-2*.

Taken together, *Fgatf1* is the main downstream target of *FgOS-2*. *Fgatf1* plays important roles in stress adaptation, secondary metabolism including mycotoxin production, sexual reproduction and virulence towards wheat and maize.

4. Discussion

Functional characterization of FgOS-2, Fgatf1 and several TMRs provides insight into a complex and interactive signaling network in the unique pathosystem *F. graminearum*. It became apparent that FgOS-2 is a central regulator of all steps in the life cycle of this pathogen. It is involved in nearly all developmental processes, such as perithecia formation, oxidative and osmotic stress tolerance, fungicide resistance, virulence and secondary metabolite production, including mycotoxins. Fgatf1 acts as a putative downstream target of the stress-activated MAP kinase. Fgatf1 shares more functions with the stress-activated MAP kinase but has important-independent features. In the following the hypothesis, that FgOS-2 and Fgatf1 regulate several of the diverse phenotypes by modulating ROS levels will be developed (summarized in Fig. 82). Some of the observed phenotypes suggest overlapping functions of some TMRs with the stress-MAPK-cascade. Deletion of *FGSG_01861* enhances stress tolerance towards oxidative, osmotic, fungicide, temperature stresses and cell wall stress. TMRs *FGSG_03023* and *FGSG_02655* are required for pathogenicity, DON production, lipase secretion and sexual reproduction. TMR *FGSG_05006* is necessary for utilization of carbon sources and steady-state intracellular cAMP levels in the cAMP/PKA signaling pathway. TMRs are proposed to be associated with a network of signaling proteins, most important of which are heterotrimeric G-proteins, MAP kinases, and cyclic AMP dependent protein kinase PKA (summarized in Fig. 82).

4.1. Osmotic stress and altered ROS metabolism influences spore development, germination and mycelial growth in different mutants

In *A. nidulans*, the central transcriptional regulator Atf1/AtfA downstream of HOG1/SakA orchestrates the fungal response to oxidative stress, mainly by the positive regulation of catalase genes (Lara-Rojas et al., 2011). The Atf1 homologue of the biotrophic grass pathogen *C. purpurea*, Tf1, is believed to act as a positive regulator of catalase genes and a repressor of *nox*-genes (Nathues et al., 2004). The results in this study also indicate a FgOS-2 dependent regulation of catalase and *NoxC* gene expression through Atf1. The scheme in Figure 74 provides an overview of the putative regulatory pathways. Under oxidative stress conditions, deletion of *FgOS-2* led to a massive up regulation of *atf1* expression. In consequence, catalase and *noxC* gene expression was higher in $\Delta FgOS-2$ mutants compared to the wild type (Fig. 45 and 46B). Thus, FgOS-2 seems to act as a repressor of *atf1* expression under oxidative stress conditions. Under osmotic stress conditions, catalase and *noxC* gene expression and activity was lower in $\Delta FgOS-2$ mutants compared to the wild type, although gene expression of *atf1*

was only slightly reduced in the deletion strains (Fig. 45 and 46C). During the infection of wheat florets, the interplay between FgOS-2/Atf1 seems to be most important: *atf1* gene expression is drastically reduced in the $\Delta FgOS-2$ mutants in course of infection. Accordingly, catalase and *noxC* gene expression was also reduced in the mutant strains but not in the wild type (Fig. 45 and 46A).

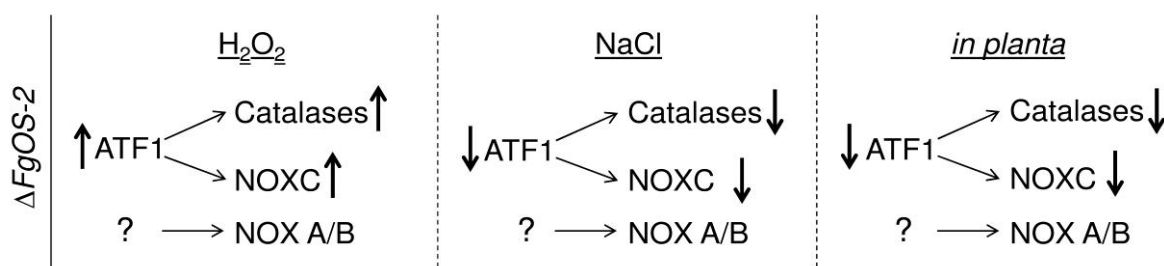


Figure 74. Hypothetical regulation network of ROS metabolic genes. The results highlight the central role of FgOS-2 and the putative downstream transcription factor Atf1 in the regulation of ROS metabolism. Conclusions: in the deletion mutant background under oxidative stress conditions *atf1*, catalase and *noxC* gene expressions are drastically up-regulated. Under osmotic stress conditions *atf1*, *noxC* and catalase gene expression decreases. Finally, during *in planta* growth, the expression of catalases, *noxC* and *atf1* is massively down-regulated. Intriguingly, the regulation of other *nox* genes seemed to be independent of FgOS-2/Atf1 and regulated by an unknown factor. Bold arrows indicate the regulation pattern, narrow arrows indicate a putative signaling connection.

The growth of $\Delta FgOS-2$ mutants completely ceased on agar plates supplemented with osmotic stress agents (Fig. 29). Catalase expression and activity was lower compared to the wild type in cultures induced with NaCl (Fig. 46C, D). Thus, the observed reduction in growth may be connected to the missing ROS-detoxification capabilities of the mutants due to the down-regulated catalase genes. The NBT staining revealed a strong formation of ROS at the growing edges of the mutant colonies on agar containing 0.2 M NaCl (Fig. 43A) and the results of the ROS ELISA indicated an accumulation of ROS in the mutant strains under osmotic stress (Fig. 43B). Furthermore, addition of purified catalase to the medium partially restores the growth defect of the mutants under mild salt stress (Fig. 47). However, since it was not possible to fully complement the growth defect, it seems likely that the growth defect is due to pleiotropic effects of FgOS-2. These results suggest that the proper growth is regulated by FgOS-2 through ROS metabolism. Not only vegetative growth but also conidia germination is defective under osmotic stress conditions. The abnormal conidia germination under osmotic stress conditions was observed in $\Delta FgOS-2$ mutants (Fig. 30), while the wild type showed a normal germination pattern consisting of spore swelling, germination tube emergence and elongation from conidia, and hyphal branching (Seong et al., 2008). It is feasible that a defective phosphorelay system during conidia germination leads to this phenotype. In *N. crassa* SakA de-phosphorylation is necessary in order to break spore dormancy and thus for the

transition between non-growing and growing mycelia (Lara-Rojas et al., 2011). Furthermore, Egan and co-workers (2007) observed a significant accumulation of ROS in non-germinated conidia of *M. oryzae*. In germinating conidia a tip-high gradient of ROS was observed. However, under normal growth conditions *F. graminearum* genes involved in the oxidative stress response are slightly down-regulated during spore swelling, germination and germ-tube formation (data obtained from supplemental material of Seong et al. 2008), which indicates that the germinating spore does not face imminent ROS stress. The ROS measurements indicated increased H₂O₂ production under osmotic stress conditions in the *FgOS-2* deletion mutants. This increase could interfere with physiological processes, leading to spore germination and germ tube formation. Thus, it is likely that the defective spore germination in the $\Delta FgOS-2$ mutants is due to a disturbed ROS metabolism.

Deletion of *Fgatf1* also altered ROS metabolism. However, unlike the *FgOS-2* deletion strains, $\Delta Fgatf1$ mutants exhibited a reduction in ROS accumulation when exposed to osmotic stress (Fig. 68B). The catalase expression and activity were higher in $\Delta Fgatf1$ mutants compared to the wild type (Fig. 69C). Therefore, growth of $\Delta Fgatf1$ mutants is still possible on medium containing osmotic stress agents (Fig. 52). The expression levels of four catalase genes in *Fgatf1^{oe}*: $\Delta FgOS-2$ mutants were much higher compared to $\Delta FgOS-2$ mutants under osmotic stress conditions. The full restoration of growth in the $\Delta FgOS-2$ mutant background on mild osmotic stress medium by constitutive overexpression of *Fgatf1* might be due to restoration of ROS-detoxification capabilities.

On the other hand, the $\Delta FgOS-2$ and $\Delta Fgatf1$ mutants grew better than the wild type on plates containing up to 20 mM H₂O₂ (Fig. 55). This was also observed in both *Epichloë festucae SakA* (Eaton et al., 2008) and in *M. oryzae Osm1* deletion strains (Dixon et al. 1999). Lara-Rojas and co-workers (2011) found out that conidia but not mycelia of *A. nidulans SakA* deletion strains are sensitive towards oxidative stress. In *B. cinerea* $\Delta bcatf1$ mutants show no increased sensitivity towards oxidative stress mediated by H₂O₂ (Temme et al. 2012). Analyses of catalase transcription levels and enzyme activities in *F. graminearum* cultures induced with H₂O₂ clearly showed a higher transcript level and enzyme activity of all catalases in $\Delta FgOS-2$ -mutants and elevated in $\Delta Fgatf1$ mutants compared to the wild-type cultures (Fig. 46B and D, and Fig. 69B and D). This up-regulation might increase the ability of the mutants to decompose ROS and thus lead to the observed higher resistance to oxidative stress. Deletion of the *M. oryzae* Atf1 orthologue (*Moatf1*) in contrast leads to hypersensitivity against oxidative stress (Guo et al., 2010). The authors connect this phenotype to the mutant's disability to detoxify ROS. Deletion strains in the upstream SAPK, *BcSak1* (the *FgOS-2* orthologue in *B.*

cinerea) lose elevation of catalase B expression upon H₂O₂-treatment and are hypersensitive towards oxidative stress (Segmüller et al., 2007; Heller et al., 2012).

So far the contribution of FgOS-2 and Fgatf1 to ROS metabolism in *F. graminearum* remained unclear. Deletion of *Fgatf1* led to a significantly decreased ROS production through an up-regulated catalase gene expression under osmotic stress conditions, whereas disruption of *FgOS-2* led to a drastically enhanced ROS production through down-regulated catalase gene expression under osmotic conditions. The difference in regulation of ROS production between *FgOS-2* and *Fgatf1* deletion mutants under osmotic stress conditions may have three reasons: first, FgOS-2 regulates not only Fgatf1 but also other transcription factors that participate in the regulation of ROS production. In *S. cerevisiae*, the Hog1 MAP kinase regulates at least four transcription factors, namely Msn2, Msn4, Hot1, and Sko1 (Hohmann, 2002). Second, Fgatf1 is not only activated by FgOS-2 but also from other signaling pathways. Even a repressing function of the FgOS-2 on Fgatf1 depending on growth conditions is feasible. In *N. crassa*, Atf-1 is a major regulator of cat-1 expression; however, the expression of cat-1 is different under stress conditions and during conidiation. The authors hypothesized that, under stress conditions, Atf-1 is probably regulated by OS-2 MAP kinase. Nonetheless, during conidiation, Atf-1 is regulated by other factors (Yamashita et al., 2008). The Sko1 of *S. cerevisiae* and Atf1 of *S. pombe* are known to be negatively regulated by the cAMP-dependent protein kinase (PKA) and positively regulated by a MAP kinase (Pascual-Ahuir et al., 2001; Davidson et al., 2004). In *S. pombe*, Atf1 is a downstream target of PMK1 MAP kinase and thereby involved in cell wall integrity signaling (Takada et al., 2007). Third, Fgatf1 acts as a repressor of catalase gene expression. Therefore, deletion of *Fgatf1* leads to an enhanced ROS decomposition under different conditions. In contrast, FgOS-2 is a positive regulator of catalase genes under osmotic conditions. Consequently, disruption of *FgOS-2* leads to increase oxidative burst under osmotic conditions. Under oxidative stress conditions, the expression and activity of four catalase genes were higher in $\Delta FgOS-2$ and $\Delta Fgatf1$ mutants compared to osmotic stress conditions. It seems likely that FgOS-2 acts as a repressor of catalase gene expression and Fgatf1 regulates catalase gene expression via other factors under oxidative stress conditions.

The $\Delta FGSG_{01861}$ mutants showed a partially resistance against osmotic stress. $\Delta FGSG_{01861}$ mutants grew better than the wild type strain on CM plates containing 1.2 and 2 M NaCl (Fig. 20). It is possible that FGSG_01861 interferes with the FgOS-2 signaling pathway in *F. graminearum*. FGSG_01861 might be a repressor of FgOS-2 and Fgatf1 under osmotic stress conditions. Furthermore, it is feasible that FGSG_01861 acts as an osmosensor for both the FgOS-2 signaling pathway and the MGV1-signaling pathway that is responsible

for proper hyphal growth. Maybe, for the cross talk between the FgOS-2 signaling pathway and the MGV1-MAP kinase signaling pathway under osmotic conditions, the TMR FGSG_01861 is essential. The FgOS-2 signaling pathway might have a negative feedback regulation on the MAP kinase MGV1 signaling pathway via TMR FGSG_01861. In *S. cerevisiae*, Sho1 is not only an osmosensor for the HOG signaling pathway but also a receptor for pseudohyphal growth and pheromone response signaling pathways. Under osmotic conditions, Hog1 and Pbs2 mutants activate the pheromone response and pseudohyphal growth signaling pathways through the osmosensor Sho1. Moreover, the HOG signaling has another unknown osmosensor distinct from Sho1 and Sln1. The unknown osmosensor is also required for the cross talk between the HOG signaling pathway and other signaling pathway (O'Rourke and Herskowitz, 1998).

The *FGSG_01861* -deletion strains grew better than the wild type on plates containing 20 mM H₂O₂ (Fig. 19). As mentioned above, it was possible to connect the higher resistance to oxidative stress to a higher expression and activity of catalases. Thus, maybe, the catalase and peroxidase transcription levels in $\Delta FGSG_01861$ mutants may also be higher compared to the wild type under oxidative stress conditions. Therefore, the observed increase in growth under oxidative stress conditions may be due to the increasing ROS-detoxification capabilities of $\Delta FGSG_01861$ mutants. Deletion of two nox genes ($\Delta bcnoxA$, $\Delta bcnoxB$ and $\Delta\Delta bcnoxAB$ mutants) involved in ROS generation in *B. cinerea* leads to a significant reduction in growth rate under oxidative stress conditions, particularly in the double deletion mutant $\Delta\Delta bcnoxAB$ (Segmüller et al., 2008). These results suggest that FGSG_01861 may act as a positive regulator of the FgOS-2/Fgatf1 signaling cascade and involve in ROS metabolism under oxidative stress conditions. In *M. oryzae* $\Delta des1$ and $\Delta ap1$ mutants are sensitive to H₂O₂ because the expression levels and activity of peroxidases and laccases are down-regulated compared to the wild type (Chi et al., 2009; Guo et al., 2010). *Skn7* plays an important role in oxidative stress resistance. *Skn7* deletion mutants are sensitive to oxidative stresses (Krems et al., 1996; Singh et al., 2004). *F. graminearum* $\Delta Gpmk1$ mutants are also more sensitive to oxidative stress compared to the wild type. The NBT staining revealed very high ROS accumulation at the growing edges of the mutant colonies on CM agar plates. These results lead to the hypothesis that FGSG_01861 may be involved in ROS metabolism via different signaling pathways. FGSG_01861 may act as a positive regulator of the FgOS-2/Fgatf1 signaling cascade but a repressor of the MAP kinase PMK1 and the Skn7/Des1/AP1 oxidative signaling cascades under oxidative stress conditions.

In summary, FgOS-2 and the putative downstream transcription factor Fgatf1 are involved in ROS metabolism. The altered ROS metabolism influences spore development, germination

and mycelial growth in the $\Delta FgOS-2$ and $\Delta Fgatf1$ mutants under osmotic conditions. TMR FGSG_01861 may be also involved in ROS metabolism through different signaling cascades (Fig. 75).

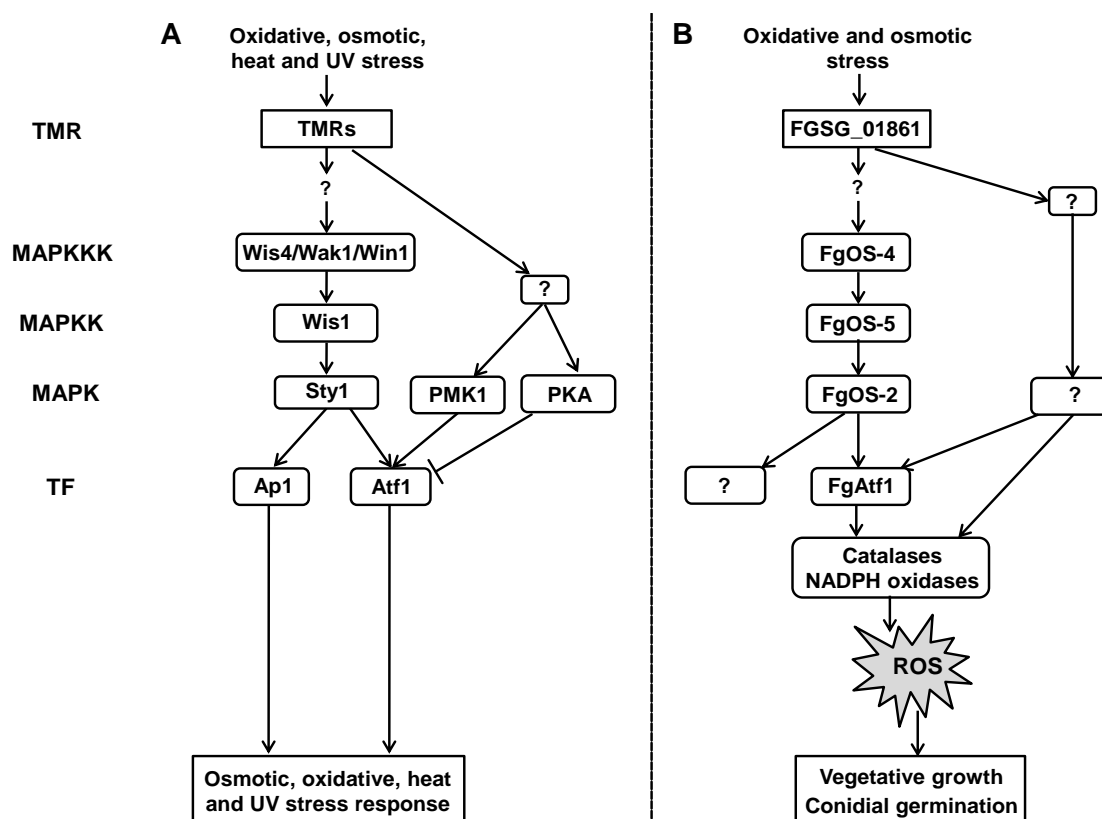


Figure 75. Model for the *S. pombe* Sty1 signaling pathway and hypothesized model for ROS metabolism-mediated signaling pathway in *F. graminearum*. **A.** Model for the *S. pombe* Sty1 signaling pathway. The Sty1 MAPK regulates not only the transcription factor (TF) Ap1 but also Atf1. The transcription factor Atf1 is downstream target of the Sty1, PMK1 and PKA MAP kinases. Reproduced from Hohmann et al. (2002). **B.** Hypothesized model for ROS metabolism-mediated signaling pathway in *F. graminearum*. Atf1 acts as a downstream target of FgOS-2 and is involved in regulation of ROS metabolism. TMR FGSG_01861 may be also involved in ROS metabolism through different signaling cascades. Altered ROS metabolism influences conidial germination and vegetative growth.

4.2. Deletion of *FgOS-2*, *Fgatf1* and TMR *FGSG_01861* alters the fungal sensitivity towards the phenylpyrrolic fungicide

Disruption of *FgOS-2* led to a strongly increased resistance towards fludioxonil. Growth of the wild type completely ceased at a concentration of 0.5 mg l⁻¹ while the mutant was able to grow almost as well as it did on CM control plates (Fig. 35A). Conidial germination of the wild type is also defective in response to fludioxonil (Fig. 35B). The question, if this phenotype is connected to an abnormal ROS homeostasis remains open. It is assumed that fludioxonil triggers an abnormal accumulation of glycerol via a fungicide-mediated de-regulation of the osmoregulatory pathway (Pillonel and Meyer, 1997). Furthermore, an *A. nidulans* microarray

study published by Hagiwara et al. (2009) revealed a large number of genes simultaneously regulated by HogA and its putative downstream target Atf1 after fludioxonil treatment. Among them was a gene encoding glycerol-3-phosphate dehydrogenase, an enzyme that is also involved in glycerol biosynthesis. A massive up-regulation of the gene encoding a glycerol-3-phosphate phosphatase was observed (Fig. 35C) in the wild type when exposed to fludioxonil; this enzyme catalyses the de-phosphorylation of glycerol-3-phosphate to glycerol and phosphate. This hyper-accumulation of glycerol increases cellular turgor and leads to cell rupture. $\Delta FgOS-2$ mutants exhibited no up regulation of the glycerol-3-phosphate phosphatase gene, avoiding the hyper-accumulation of glycerol and allowing normal growth. Also the *Fgatf1* and *FGSG_01861* deletion mutants were slightly more resistant against fludioxonil (Fig. 21 and Fig. 55). These results underline the close signaling connection between FgOS-2, *Fgatf1* and *FGSG_01861*. *FGSG_01861* is a positive regulator of FgOS-2 and *Fgatf1* after fludioxonil treatment. *FGSG_01861* may be associated with other sensor histidine kinases in FgOS-2 signaling pathway in response to fludioxonil. In *N. crassa*, Atf1 and OS-2 share some functions in response to fludioxonil, although *Atf1* deletion mutants were as susceptible to this fungicide as the wild type (Yamashita et al., 2008). Deletion of the sensor histidine kinases *Tco1* and *Tco2* in *C. neoformans* leads to a resistance to fludioxonil. The single mutants, $\Delta Tco1$ or $\Delta Tco2$, display a partial resistance to fludioxonil. The double deletion mutant $\Delta\Delta Tco1Tco2$ exhibits complete resistance to fludioxonil (Bahn et al., 2006).

In summary, the *FGSG_01861*/*FgOS-2*/*Fgatf1* signaling pathway control fludioxonil antifungal sensitivity in *F. graminearum*. TMR *FGSG_01861* may interact with other histidine kinases in the *FgOS-2*/*Fgatf1* signaling pathway in response to fludioxonil (Fig. 76).

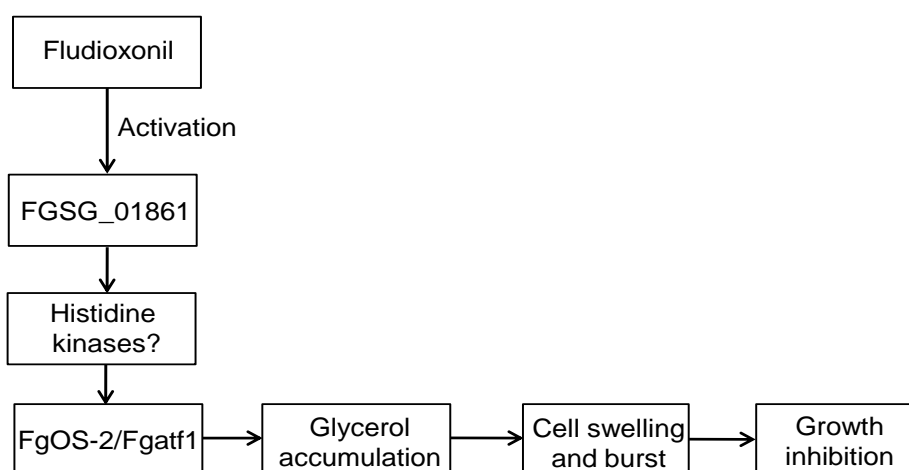


Figure 76. Proposed model for the FgOS2/Fgatf1 signaling pathway in response to fludioxonil in *F. graminearum*. Fludioxonil treatment activates the FgOS-2 signaling pathway through TMR *FGSG_01861* by rapid dephosphorylation of FgOS-2. FgOS-2 activation contributes to hyper-accumulation of glycerol, causing cell swelling, burst and growth inhibition.

4.3. Cell wall integrity and ergosterol biosynthesis relies on the activation of MAP-kinase cascades by FGSG_01861

In *C. neoformans*, $\Delta bog1$ mutants show a resistance against fludioxonil, whereas $\Delta mpk1$ mutants exhibit fludioxonil hypersensitivity. Therefore, the *C. neoformans* sensitivity to fludioxonil is not only positively controlled by the HOG signaling pathway, but also negatively controlled by the calcineurin/PKC1/MPK1 signaling pathways, which are involved in maintaining cell wall integrity (Kojima et al., 2006). $\Delta FGSG_01861$ mutants exhibited partially resistant against fludioxonil. This result suggests that FGSG_01861 is also involved in the calcineurin/PKC1/MPK1 signaling pathways. Therefore, the sensitivity of $\Delta FGSG_01861$ mutants to the cell wall damaging agent, congo red and to heat stress was tested. $\Delta FGSG_01861$ mutants showed a resistance to congo red and heat stress compared to the wild type (Fig. 19). Congo red inhibits fungal cell wall assembly by binding 1,4-glucans (Wood and Fulcher, 1983). In *C. albicans*, *C. neoformans*, *S. cerevisiae* and *F. graminearum*, the PKC1/MPK1, cAMP/PKA, MGVI and HOG signaling pathways are involved in maintaining cell wall integrity (Verna et al., 1997; Hou et al., 2002; Kojima et al., 2006; Lenardon et al., 2010). These results suggest that FGSG_01861 is a receptor of the different signaling cascades and involved in maintaining cell wall integrity. FGSG_01861 may function upstream of G_α subunit or the small GTPase Ras in the cAMP/PKA, PKC1/MPK1, MGVI and FgOS-2 signaling pathways. Deletion of G_α subunit GPA2 in *F. graminearum* leads to higher chitin accumulation compared to the wild type (Yu et al., 2008). The absence of *MGV1* in *F. graminearum* leads to a drastic reduction in vegetative growth on solid media and cell wall defects (Hou et al., 2002). Thus, FGSG_01861 may associate with G_α subunit GPA2 in the MAP kinase MGVI signaling to maintain cell wall integrity. In *S. cerevisiae*, the genes *Wsc1*, *Wsc2*, and *Wsc3* encode predicted integral membrane proteins that maintain cell wall integrity under heat stress conditions in the calcineurin/PKC1/MPK1 signaling pathways. *Wsc* deletion mutants are sensitive to heat stress. *Wsc* proteins also interact with the Ras/cAMP/PKA pathway. The Ras/cAMP/PKA pathway is necessary for cell cycle progression and the heat shock response. Deletion of *Ras2* rescues the heat shock resistance of triple *Wsc1Wsc2Wsc3* deletion mutants. Constitutive overexpression of *Wsc1* suppresses the heat shock sensitivity of $\Delta\Delta Ras1Ras2$ mutants (Verna et al., 1997). In *N. crassa*, deletion of the G_α subunit *gna-1* in the cAMP/PKA signaling pathway causes pleiotropic defects in asexual and sexual development (Ivey et al., 1996; Yang and Borkovich, 1999). However, $\Delta gna-1$ mutants are more resistant to heat and oxidative stress compared to the wild type (Yang and Borkovich, 1999). These results suggest that FGSG_01861 may function upstream of the small GTPase Ras or G_α subunit in

the PKC1/MPK1, MGV1 and FgOS-2 signaling pathways or the cAMP/PKA signaling pathway in maintaining cell wall integrity and heat stress response (Fig. 77).

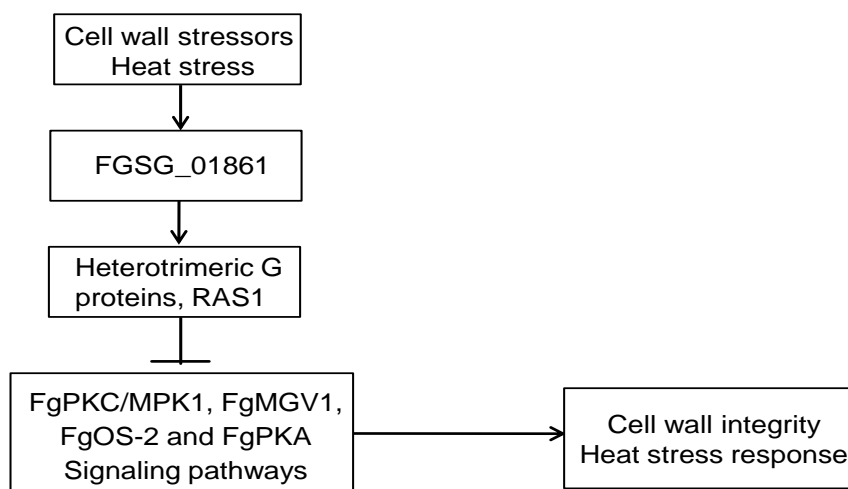


Figure 77. Proposed signaling pathway mediating cell wall integrity and heat stress response in *F. graminearum*. TMR FGSG_01861 associates with heterotrimeric G proteins or the small GTPase RAS1 in the MAPK signaling pathways or the cAMP/PKA signaling pathway to negatively regulate cell wall integrity and heat stress response.

The *FGSG_01861* mutants grew much better on CM agar plates containing 0.2 or 0.4 $\mu\text{g ml}^{-1}$ tebuconazole compared to the wild type (Fig. 21). In the presence of 0.4 $\mu\text{g ml}^{-1}$ tebuconazole, germinating conidia of the wild type revealed an abnormal germ tube morphology. In contrast, hyphae of $\Delta FGSG_01861$ appeared unaffected (Fig. 22B). The ergosterol biosynthesis pathway is the target of azole fungicides. These compounds obstruct the ergosterol biosynthesis pathway via inhibiting the enzyme 14- α -demethylase encoded by the *cyp51* gene. This enzyme is crucial for ergosterol biosynthesis. Consequently, fungal membrane integrity is disturbed under azole fungicide treatments (Buchenauer, 1987; De Backer et al., 2001). Several studies pointed out some factors that affect azole fungicide susceptibility. The following modifications lead to an increase resistance against azole fungicides: target-site mutagenesis in the CYP51 gene (Wyand and Brown, 2005; Leroux et al., 2007), the expression of azole fungicide resistant target genes was elevated (Godet and Limpert, 1998; Schnabel and Jones, 2001), sterol biosynthesis and cellular sterol composition were disturbed with a reduction in desmethyl sterols and an increased accumulation of 14 α -methyl sterols (Joseph-Horne et al., 1995; Joseph-Horne et al., 1996), enhanced energy-dependent efflux transport of the toxic compounds (Nakaune et al., 1998; Reimann and Deising, 2005), and copy numbers of the target gene and a transcriptional regulator of drug efflux pumps were increased (Selmecki et al., 2008). Liu et al. (2010) showed that expression of a large number of genes in *F. graminearum* respond to tebuconazole. Among these target genes, the expression levels of two putative *cyp51* homologs are drastically up-regulated after tebuconazole treatment (Liu et al., 2010). In

C. albicans and *Trichophyton rubrum*, the expression level of *erg6* is strongly up-regulated under azole fungicide treatments (De Backer et al., 2001; Yu et al., 2007). Disruption of *erg6* gene leads to loss of ergosterol synthesis in *C. albicans* (Jensen-Pergakes et al., 1998). The reduced azole fungicide susceptibility of $\Delta FGSG_01861$ mutants suggests that FGSG_01861 is a receptor of the ergosterol biosynthesis pathway.

4.4. The putative transmembrane receptor FGSG_05006 regulates vegetative growth and intracellular cAMP levels on poor carbon sources via the cAMP-PKA or MAP kinase signaling pathways

Deletion of *FGSG_05006* in *F. graminearum* led to a reduced biomass accumulation compared to the wild type on poor carbon sources like glycerol. The steady-state intracellular cAMP levels in $\Delta FGSG_05006$ mutants were lower compared to the wild type on glycerol-minimal medium (Fig. 12 and Fig. 13). The addition of exogenous cAMP to glycerol-minimal medium partially reversed the biomass and growth defects of $\Delta FGSG_05006$ mutants (Fig. 12A). These results suggest that the putative carbon sensor TMR FGSG_05006 is necessary for utilization of carbon sources and steady-state intracellular cAMP levels in the cAMP/PKA signaling pathway or MAP kinase pathways in *F. graminearum*. When a carbon source indicating a poor carbon source binds to FGSG_05006, FGSG_05006 may activate a heterotrimeric G protein or the small GTPase Ras. Then the signal activates the downstream target genes to regulate vegetative growth and steady-state intracellular cAMP levels (Fig. 78).

The functions of carbon sensors and its downstream heterotrimeric G proteins in the cAMP/PKA signaling pathway have been demonstrated by previous studies in many fungi. In *S. cerevisiae*, TMR Gpr1 is a carbon sensor of glucose and sucrose. Gpr1 activates the cAMP/PKA signaling pathway through Gpa2 (Yun et al., 1997; Xue et al., 1998; Yun et al., 1998; Lorenz et al., 2000; Lemaire et al., 2004a). In *C. albicans*, a homolog of the *S. cerevisiae* Gpr1 receptor senses low concentrations of glucose and methionine. Gpr1 is associated with the heterotrimeric G_x subunit Gpa2 to regulate filamentous growth in cAMP/PKA signaling pathway (Maidan et al., 2005). In *N. crassa*, GPCR-4 and its downstream G_x subunit GNA-1 in the cAMP/PKA signaling pathway are required for utilization of poor carbon sources (Li and Borkovich, 2006). The putative carbon sensor TMR FGSG_05006 may also be associated with small GTPase proteins Ras in different signaling pathways to regulate vegetative growth on poor carbon sources. In *S. cerevisiae*, the small GTPase protein Ras2 activates both the MAP kinase and cAMP/PKA signaling pathways to regulate filamentous growth on media containing different carbon sources (Mösch et al., 1996).

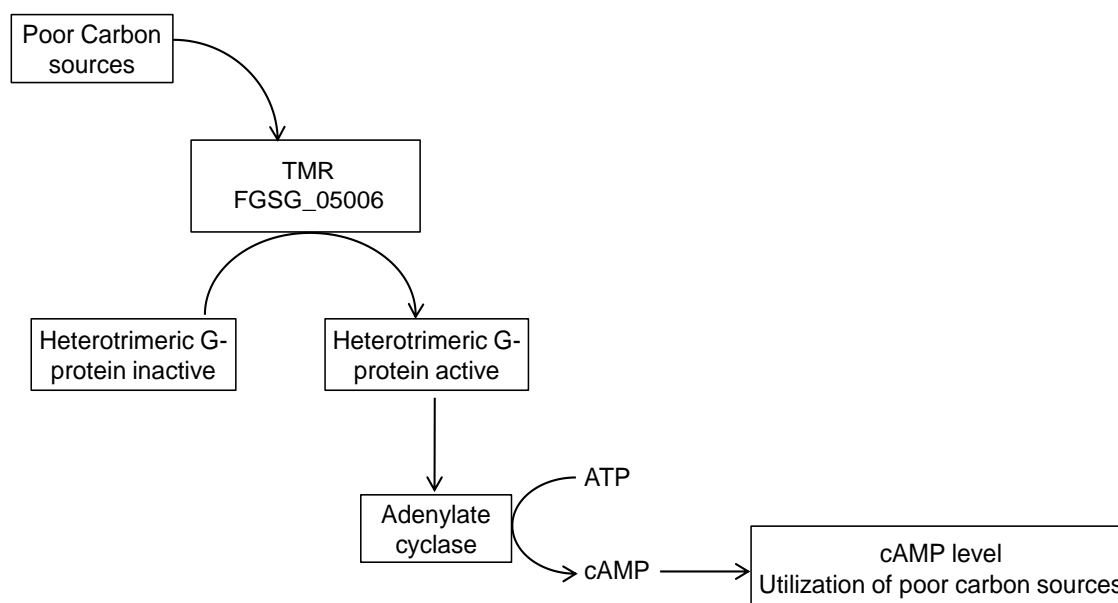


Figure 78. Hypothesized model for the putative carbon sensor TMR FGSG_05006 -mediated signaling cascade in *F. graminearum*. When a ligand indicating a poor carbon source binds to TMR FGSG_05006, it leads to a dissociation of a heterotrimeric G-protein. This activation finally leads to changes in target gene expression. The changing expression of these target genes is essential for regulating cAMP level and utilization of poor carbon sources in *F. graminearum*.

4.5. The activating transcription factor Fgatf1 and the TMR FGSG_02655 are prerequisite for sexual reproduction

FgOS-2 deficiency led to a complete loss of sexual reproduction. Interestingly, deletion of *Fgatf1* in *F. graminearum* also negatively influenced formation of reproductive structures. Development of perithecia was delayed in $\Delta Fgatf1$ mutants compared to the wild type on carrot agar and on detached wheat nodes. Intriguingly, the inability of the $\Delta FgOS-2$ mutants to produce perithecia and ascospores could be restored by constitutive overexpression of *Fgatf1* (Fig. 57 and 58). These results indicate that FgAtf1 is the major regulator of sexual reproduction in *F. graminearum*. The balanced *Fgatf1* transcript level is prerequisite for sexual reproduction. *B. cinerea atf1* deletion mutants are completely unable to produce perithecia (Temme et al., 2012). The authors speculate about a disturbed light-dependent regulation in the mutants. It has been described previously that especially blue light induces sexual reproduction, i.e. in *N. crassa* (Degli Innocenti et al., 2008). In this study the ability of the wild type and the mutants to form perithecia was analyzed both in light and in darkness. Carrot agar plates and detached wheat nodes inoculated with conidia were incubated under conditions of 12h darkness and 12h light. On both substrates the phenotypes were comparable. This indicates that, in *F. graminearum*, the development of perithecia is independent of light. Deletion of *FgOS-2* or *Fgatf1* led to an altered ROS metabolism. Perithecia formation of *F. graminearum* might depend on a tight regulation of ROS metabolism

by FgOS-2 and Fgatf1. Many previous studies reported the linking between sexual development and the local formation of ROS. Deletion of the H₂O₂-producing NADPH oxidase *NoxA* in *A. nidulans* leads to reduced ROS production and the complete loss of fruiting body formation (Lara-Ortiz et al., 2003). *NoxA* deletion in other filamentous fungi such as *Podospora anserina* (Malagnac et al., 2004) and *N. crassa* (Cano-Dominguez et al., 2008) also blocked fruiting body development. Disruption of *FGSG_02655* (*pre2*) also led to a significant reduction in perithecia maturation on both wheat nodes and carrot agar (Fig. 15A and B). It is possible to hypothesize that TMR FGSG_02655 is a receptor of the FgOS-2/Fgatf1 signaling pathway in regulation of sexual reproduction. Deletion of the small GTPase *Ras1*, the heterotrimeric G_α *GPA1* and of the MAP kinase genes *Gpmk1* and *MGV1*, respectively, also leads to a significant defect in sexual development in *F. graminearum*. These mutants were infertile, the ability of perithecia formation in these mutants was completely abolished on carrot agar plates and detached wheat nodes (Hou et al., 2002; Jenczmionka et al., 2003; Bluhm et al., 2007; Yu et al., 2008). These phenotypic overlaps indicate that the pheromone receptor FGSG_02655 functions upstream of the small GTPase *Ras1* or heterotrimeric G_α in the different MAP kinase signaling pathways or the cAMP/PKA signaling pathway to regulate sexual development in *F. graminearum*. However, one cannot exclude that these phenotypic overlaps might due to a cross talk regulation between the FgOS-2/Fgatf1 signaling pathway with other MAP kinase signaling pathways as well as the cAMP/PKA signaling pathway in sexual reproduction. When *F. graminearum* responds to ligands such as mating pheromones, FGSG_02655 activates *Ras1* or heterotrimeric G proteins and a signal is transmitted to the different MAP kinase pathway or the cAMP/PKA signaling pathway to regulate sexual development (Fig. 79). In *S. cerevisiae* the pheromone response pathway consists of the peptide pheromones α-factor and a-factor, the pheromone receptors Ste2p and Ste3p, a heterotrimeric G_α subunit Gpa1p and a G_{βγ} dimer Ste4p/Ste18p, and the MAP kinase cascade (Ste11, Ste7, and Fus3/Kss1). Upon binding of pheromones, the pheromone receptors undergo conformational changes and activate G_α subunit Gpa1p and the MAP kinase cascade via the Ste20 kinase (Leberer et al., 1997; O'Rourke and Herskowitz, 1998). The *A. nidulans* genome has two pheromone receptors, *gprA* and *gprB*. Deletion of either *gprA* or *gprB* results in the production of fewer and smaller cleistothecia that contain less ascospores. Double-receptor mutants completely fail to produce cleistothecia (Seo et al., 2004). No G_α protein has been linked to these pheromone receptors. However, the G_{βγ} dimer SfaD-GpgA and PhnA phosphatase are associated with these pheromone receptors and are required for formation of cleistothecia. The Δ *phnA*, Δ *sfaD* and Δ *gpgA* mutants are not able to form cleistothecia (Rosen et al., 1999; Seo et al., 2005; Seo and Yu, 2006). These results

suggest that the pheromone receptor FGSG_02655 may function upstream not only heterotrimeric G_α but also G_β in the different signaling cascades to regulate sexual reproduction. The *C. neoformans* genome has two pheromone receptors $CPR\alpha$ and $CPR\beta$. Deletion of $CPR\alpha$ decreases mating efficiency and the ability to sense to the MAT α pheromone. The absence of $CPR\beta$ increases mating ability (Chang et al., 2003). Also in *C. neoformans*, Deletion of G_α gene *gpa1* leads to decrease basidiospore production. The supplementation of exogenous cAMP can restore basidiospore production (Alspaugh et al., 1997). Disruption of G_β *gpb1* causes completely deficiency in mating. The addition of exogenous cAMP does not rescue this phenotype. However, constitutive overexpression of the *cpk1* MAPK gene can restore the mating ability of the *gpb1* deletion mutant (Wang et al., 2000). These results suggest that G_β Gpb1 regulates the MAPK signaling cascade during pheromone signaling and Gpa1 functions upstream of the cAMP/PKA signaling pathway regulates sexual development. These results also implicate pheromone receptors in different signaling cascades in *C. neoformans*.

In summary, FgOS-2 and Fgatf1 play a major role in sexual reproduction in *F. graminearum*. The pheromone receptor FGSG_02655 may function upstream of the different MAP kinase signaling pathways or the cAMP/PKA signaling pathway to regulate sexual reproduction. It is possible to have a cross talk regulation between the FgOS-2/Fgatf1 signaling pathway with other MAP kinase signaling pathways as well as the cAMP/PKA signaling pathway in sexual reproduction in *F. graminearum* (Fig. 79).

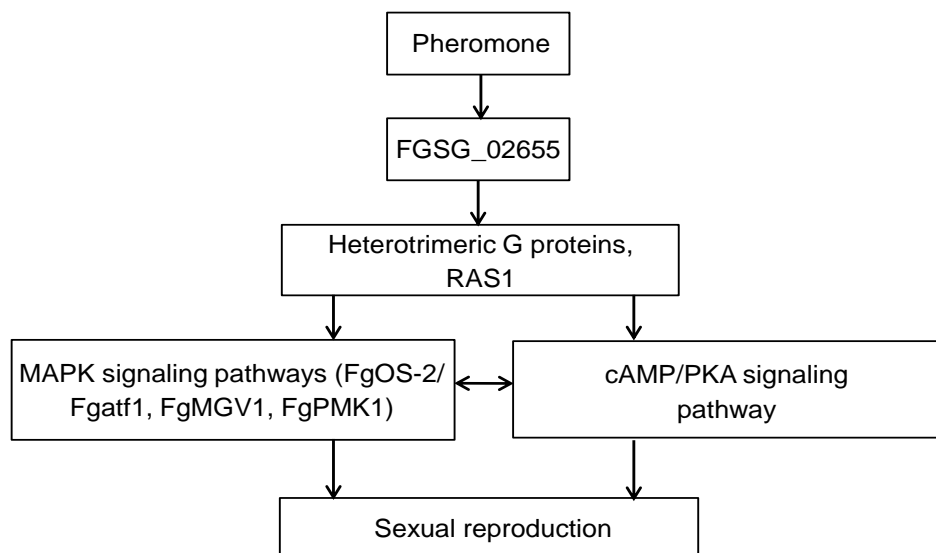


Figure 79. Hypothesized model for the pheromone receptor FGSG_02655 -mediated signaling cascades in *F. graminearum*. FGSG_02655 perceives environmental signals such as pheromones and then activates heterotrimeric G proteins or the small GTPase RAS1 in the MAPK signaling pathways or the cAMP/PKA signaling pathway to regulate sexual reproduction. There might be a cross-talk regulation between the MAPK signaling pathways and the cAMP/PKA signaling pathway in sexual reproduction.

4.6. Virulence of *F. graminearum* relies on FgOS-2 and Fgatf1 in concert with the function of the TMRs FGSG_03023 and FGSG_02655

Pathogenicity assays on wheat and maize revealed a drastically reduced virulence of *FgOS-2* deficient strains compared to wild type (Fig. 37). The HOG1 homologues in phytopathogenic fungi contribute to virulence at different degrees. While the *M. oryzae* homologue Osm1 is dispensable for appressorium formation and pathogenicity towards rice, *B. cinerea* BcSak1 is necessary for the colonization of unwounded plant tissue (Dixon et al., 1999; Segmüller et al., 2007). *F. graminearum* OS-2 seems to be an “intermediate” regarding its importance for pathogenic development on wheat: the protein is not needed for cuticle penetration or initial colonization of the wheat plant. However, infection is restricted to the inoculated spikelet since it never proceeds beyond the rachis node. Deletion of *Fgatf1* from the genome led to a severe reduction in virulence. Constitutive overexpression, on the other hand, results in a greater aggressiveness against wheat and maize. Strikingly, constitutive overexpression of *Fgatf1* restored virulence of *FgOS-2* deletion strains (Fig. 59). Two TMR-deletion mutants, $\Delta FGSG_03023$ and $\Delta FGSG_02655$, also showed a reduction in virulence towards wheat and maize (Fig. 16 and Fig. 24). The phenotypic overlaps in pathogenicity of $\Delta FGSG_03023$, $\Delta FGSG_02655$, $\Delta FgOS-2$ and $\Delta Fgatf1$ mutants suggest that TMRs FGSG_03023 and FGSG_02655 may function upstream of the *FgOS-2*/*Fgatf1* signaling cascade. In *F. graminearum*, the production of DON is prerequisite for successful colonization of wheat. Wheat head infection of deficient mutants (Proctor et al., 1995; Maier et al., 2006; Jiang et al., 2011) or markedly reduced (Hou et al., 2002; Jonkers et al., 2012) in DON production was always restricted to the point-inoculated spikelet. In this study, a reduction in DON production by the $\Delta Fgatf1$, $\Delta FgOS-2$, $\Delta FGSG_03023$ and $\Delta FGSG_02655$ mutants was observed. Hence, it is feasible that the reduced virulence towards wheat is due to the reduced DON level. In this regard, it seems likely, that the increased DON production observed in the *Fgatf1*^{oe} mutants compared to the wild type (Fig. 65) has a positive impact on the pathogenic potential. This overproduction of DON also elevates the DON accumulation in the $\Delta FgOS-2$ strains. Therefore, constitutive overexpression of *Fgatf1* increased virulence towards wheat compared to the wild type. The increased virulence of *Fgatf1*^{oe} mutants towards *B. distachyon* might also be due to the increased DON production. DON functions as a virulence factor in *B. distachyon* as it does in wheat (Peraldi et al., 2011). The drastic reduced virulence of *FgOS-2* deficient strains and partially restored virulence of the $\Delta FgOS-2$ mutant also might be explained by an altered ROS balance in the interaction between wheat and the mutant strains. Gene expression analysis on infected wheat spikes revealed a down-regulation of all catalase genes in the *FgOS-2* deletion strains compared to the wild type and an up-regulation in

Fgat1^{oe}:: $\Delta FgOS-2$ mutants compared to $\Delta FgOS-2$ mutants (Fig. 71). The tight regulation of the equilibrium between ROS generation and degradation facilitates normal host-pathogen interactions (Nathues et al., 2004; Tanaka et al., 2006; Kim et al., 2009). *E. festucae* mutants defective in ROS producing NADPH-oxidase 1 (NoxA) showed a drastic switch in lifestyle: instead of mutualistic symbiosis (wild type) the NoxA-deletion strains strongly affected the viability of colonized plants (Tanaka et al., 2006). The NoxA-deletion strains of *C. purpurea* also showed severely a reduced virulence towards rye (Giesbert et al., 2008). Deletion mutants of the *M. oryzae atf1* orthologue are severely attenuated in virulence on rice (Guo et al. 2010). The mutant is able to cause small restricted lesions on spray inoculated rice leaves. Staining experiments using 3,3'-diaminobenzidine (DAB) revealed an enhanced ROS production upon penetration of the plant surface by the mutant indicating a disturbed ROS-balance. The same applies for *atf1*-deficient mutants of *C. purpurea* (Nathues et al., 2004). For the deletion strains which were attenuated in virulence towards rye, the authors could observe an increased ROS-accumulation along the interface between the fungus and the host plant. This accumulation might be due to a transcriptional down regulation of catalase 1. In *F. graminearum*, an altered *in-planta* catalase gene expression level upon *Fgat1* deletion was not observed (Fig. 69A). Thus, the misbalance in the ROS level might not be that drastic in the $\Delta Fgat1$ /wheat interaction. Recently, Temme et al. (2012) published results on *atf1* deletion in the necrotrophic fungus *B. cinerea*. Apparently, in this fungus, *atf1* deletion leads to an enhanced virulence towards several hosts. On inoculated host plants, vigorous hyphal growth is accompanied by a disability to produce conidia. A greater aggressiveness in parasitic growth was also observed in *F. graminearum*, however, only upon constitutive expression of *Fgat1*. This indicates that, during evolution, *Fgat1* orthologues in different organisms gain divergent gene repressing and activating capacities, respectively.

The reduced virulence towards maize caused by of $\Delta FgOS-2$, $\Delta Fgat1$, $\Delta FGSG_03023$ and $\Delta FGSG_02655$ mutants cannot be explained by DON production since DON is no virulence factor for maize infection (Maier et al., 2006). Another important secreted virulence factor of *F. graminearum*, a lipase (FGL1), was important for both wheat and maize infection. Deletion of *FGL1* leads to reduced extracellular lipase activity in culture and reduced virulence towards wheat and maize (Voigt et al., 2005).

Lipase activity of $\Delta FGSG_03023$ and $\Delta FGSG_02655$ mutants was reduced compared to the wild type at early time points of induction (Fig. 18 and Fig. 26). Therefore, the reduced virulence of $\Delta FGSG_03023$ and $\Delta FGSG_02655$ mutants towards wheat and maize might be due to the impaired secretion of lipases. These results also suggest that *FGSG_03023* and *FGSG_02655* may be receptors of the PMK1 signaling cascade. In *F. graminearum* the MAP

kinase PMK1 is responsible for the induction of secreted lipase activity (Jenczmionka and Schäfer, 2005).

As mentioned above, FGSG_05006 is essential for utilization of poor carbon sources and regulate vegetative growth through steady-state intracellular cAMP levels in the cAMP/PKA signaling pathway. The hypothesis that $\Delta FGSG_05006$ mutants would be severely affected in virulence was not verified. Unexpectedly, deletion of *FGSG_05006* did not attenuate virulence toward wheat and maize compared to the wild type. The missing influence of FGSG_05006 on virulence may arise from two reasons: first, plant cell wall is composed of not only poor carbon sources but also rich carbon sources (Félix and Edivaldo, 2010). Therefore, during wheat and maize infections, the growth of $\Delta FGSG_05006$ mutants was the same like the wild type and caused full virulence towards wheat and maize. Second, it is possible that other pathways involved in morphogenesis may be activated by external signals and they may overcome the absence of *FGSG_05006*. In *C. albicans*, GPCR Gpr1 regulates filamentous growth in the cAMP/PKA signaling pathway. Deletion of *Gpr1* leads to a severe defect in hyphal formation during growth on solid media containing low concentrations of glucose and methionine. However, Gpr1 plays a minor role in virulence and invasion in human tissue (Maidan et al., 2005). There is also evidence that the function of the *C. albicans* Gpr1 receptor diverged from the function of the homologous receptor in *S. cerevisiae*. Deletion of the *S. cerevisiae* GPR1 receptor leads to the absence of a cAMP signal after addition of glucose (Lemaire et al., 2004). In *C. albicans*, deletion mutants in *Gpr1* still have a normal cAMP signal upon addition of glucose (Maidan et al., 2005). This indicates that the *C. albicans* cAMP/PKA pathway can be activated independently from Gpr1. However, constitutive overexpression of *Gpa2* or the catalytic protein kinase A subunit *TPK1* restores the wild-type phenotype of *Gpr1* deletion strains (Maidan et al., 2005). So it seems that Gpr1 may activate more than one pathway. The same observation can be made for Gpa2. Recently, it has been shown that Gpa2 not only functions in the cAMP/PKA pathway but also plays an important role in the mating pathway in *C. albicans* (Bennett and Johnson, 2006). In *C. neoformans*, GPCR Gpr4 interacts with downstream G_α subunit Gpa1 to regulate cAMP levels and mating in the cAMP/PKA signaling cascade on medium containing methionine. However, Gpr4 is not essential for virulence in mice. The authors hypothesize that virulence is controlled by several factors such as melanin production, capsule formation and growth at body temperature. The author also hypothesize that *C. neoformans* may have many signaling pathways, multiple sensors and G proteins related to the cAMP/PKA signaling pathway (Xue et al., 2006).

F. graminearum is able to resist azole fungicide in the field and *in vitro* (Klix et al., 2007). Adapted strains showed higher virulence and nivalenol (NIV) levels than non-adapted strains

(Becher et al., 2010). $\Delta FGSG_{01861}$ mutants exhibited a strongly increased resistance towards azole fungicide tebuconazole. Therefore, mycotocxin NIV levels or even DON levels *in planta* produced by $\Delta FGSG_{01861}$ mutants might be higher compared to the wild type. Consequently, $\Delta FGSG_{01861}$ mutants were fully pathogenic on wheat and maize or higher virulence compared to the wild type.

In summary, virulence of *F. graminearum* relies on FgOS-2 and Fgatf1 in concert with the function of the TMRs FGSG_03023 and FGSG_02655. TMRs FGSG_03023 and FGSG_02655 may function upstream of FgOS-2/Fgatf1 signaling pathway or other MAPK signaling pathways and involve in DON production and lipase secretion. Pathogenic development of *F. graminearum* also depends on tight regulation of ROS metabolism by FgOS-2 (Fig. 80).

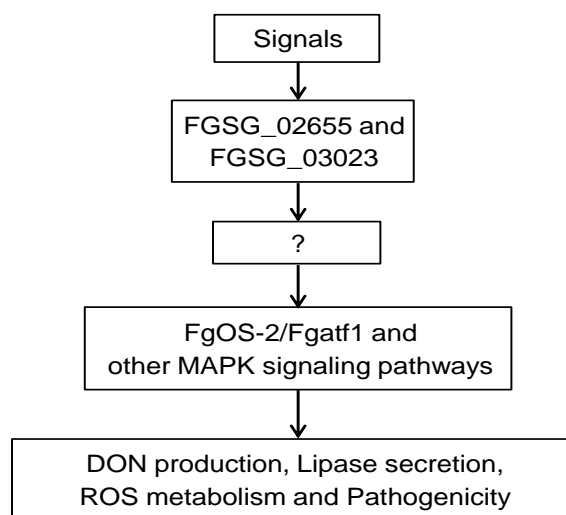


Figure 80. Hypothesized model for TMRs FGSG_03023 and FGSG_02655-mediated signaling pathways involved in pathogenesis of *F. graminearum*. During interaction between *F. graminearum* and its host plants, the TMRs FGSG_03023 and FGSG_02655 can be activated by various signals such as nutrients or host signals. The TMRs FGSG_03023 and FGSG_02655 then activate downstream target proteins in the FgOS2/Fgatf1 signaling pathway or other MAPK pathways which control DON production, lipase secretion, ROS metabolism and pathogenicity in *F. graminearum*.

4.7. Normal secondary metabolite production depends on functional FgOS-2 and Fgatf1

The DON levels *in planta* of $\Delta FgOS-2$ and $\Delta Fgatf1$ mutants were drastically reduced compared to the wild type. The $\Delta FgOS-2$ DON level on wheat kernels was also lower compared to the wild type. However, under *in-vitro* liquid culture induction conditions, DON accumulation of $\Delta FgOS-2$ and $\Delta Fgatf1$ mutants was higher than in the wild type. These results indicate an ambivalent role of FgOS-2 and Fgatf1 in the regulation of DON production. It has to be assumed that DON production is regulated through different and independent signaling

pathways whose activation depends on culture conditions. Under the experimental conditions used in this study, FgOS-2 and Fgatf1 represses DON production *in vitro*, whereas they activate DON production *in planta*. By demonstrating that the *in-vitro* induction of DON is different from *in-planta* induction, the necessity of searching for conditions that induce DON production during plant infection is once again highlighted. There are good indications for a pivotal role of ROS in this regulatory process. H₂O₂ is a potent inducer of DON production *in vitro* (Ponts et al. 2006) and fungal secretion of H₂O₂ is altered in Δ FgOS-2 and Δ Fgatf1 mutants depending on the growth conditions could be demonstrated (Fig. 46 and Fig. 69). Of course, the situation during plant infection might be more sophisticated. DON elicits PCD as a result of ROS production when injected into wheat leaves (Desmond et al., 2008). Since the FgOS-2 and Fgatf1 deletion mutants produce less DON during wheat infection, it is possible that the decrease in PCD-related ROS release leads to the missing DON induction in the mutant strains. Further microscopic analysis, e.g. by expression of a redox-sensitive GFP variant (roGFP; Heller and Tudzynski 2011) will elucidate the ROS status in the interaction between *F. graminearum* and its hosts. The presented results regarding the *in-vitro* DON-production disagrees with a previous analysis of DON production in OS-2-deficient strains of *F. graminearum* (Ochiai et al., 2007). The authors described a lack of DON production in aerial hyphae of mutants after being cultivated on a medium containing glucose and yeast extract. The DON quantification was performed using thin layer chromatography (TLC) and HPLC. It is likely that the different experimental setup contributed to this disagreement. DON analysis in this study was performed using the highly sensitive DON ELISA technique instead of TLC. For the measurement of DON in rice medium, which seems to be equivalent to the wheat kernel assay in this study, Ochiai and co-workers (2007a) used an HPLC method. The results obtained in this experiment fit nicely to the results reported here of reduced DON contents in wheat kernels inoculated with OS-2-deficient strains. A reduced DON content in sterilized wheat kernels was also shown in mutants deficient in the upstream response regulator FgRrg1 (Jiang et al., 2011).

ZEA production is also regulated by FgOS-2 and Fgatf1 in a growth condition dependent manner. Interestingly, however, only during wheat infection FgOS-2 and Fgatf1 seem to be necessary for proper regulation of ZEA production. *In-vitro* ZEA levels are nearly wild-type like. In *F. graminearum*, production of ZEA and other secondary metabolites depends on culture conditions. Generally, ZEA production was much higher on solid substrates such as rice and wheat compared to liquid media. The expression of the genes required for ZEA production is influenced by different culture conditions such as nutrient starvations or pH in

the medium (Keller and Hohn, 1997; Calvos et al., 2002; Linnemannstons et al., 2002; Kim et al., 2005b).

Jahn and co-workers (1997; 2000) showed that the loss of melanin production in different *Aspergillus* species led to an increased sensitivity to oxidative stress. The deletion of *OS-2* and *Atf1* in *F. graminearum* led to an increase in aurofusarin production compared to the wild type. The expression of genes involved in aurofusarin biosynthesis (*gip1*, encoding a putative laccase; *gip2*, transcription factor; *pks12*, polyketide synthase) were up-regulated in $\Delta FgOS-2$ and $\Delta Fgatf1$ mutants compared to the wild type under *in-vitro* conditions. A gene encoding a putative laccase involved in the biosynthesis of aurofusarin (*gip1*; Frandsen et al. 2006) drastically up regulated in the mutants both *in vitro* and *in planta* ($\Delta Fgatf1$ mutants only *in vitro*). This laccase may exhibits anti oxidantial potential (Giardina et al. 2010; Thurston 1994). This might lead to a higher resistance to ROS and thereby facilitate better growth. Maybe acting antagonistically, aurofusarin was shown to inhibit the growth of fungal hyphae (Malz et al., 2005). Surprisingly, the expression of genes involved in aurofusarin production in $\Delta FgOS-2$ mutants was also up-regulated during *in planta* growth of the mutant when compared to the wild type (Fig. 40B); hence, the reduced growth rate of mutant strains on agar plates ($\Delta FgOS-2$ and $\Delta Fgatf1$ mutants) and *in planta* ($\Delta FgOS-2$ mutants) might also be due to this increased aurofusarin production. Deletion of *PKS12*, a gene coding or the precursor for aurofusarin in *F. graminearum*, leads to an enhanced growth rate compared to the wild type. *PKS12* deletion does not harm virulence towards wheat and barley (Malz et al., 2005).

In summary, FgOS-2 and its putative downstream target Fgatf1 control secondary metabolite production in *F. graminearum*. They positively influence DON and ZEA production *in planta* and repress DON biosynthesis *in vitro*. FgOS-2 and Fgatf1 negatively regulate aurofusarin biosynthesis (Fig. 81).

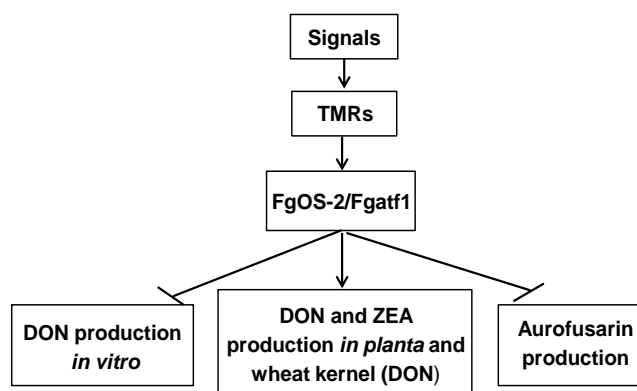


Figure 81. Proposed regulation model for secondary metabolite production by the FgOS-2/Fgatf1 signaling pathway in *F. graminearum*. FgOS-2 and Fgatf1 repress DON production *in vitro*, whereas they activate DON and ZEA production *in planta* and on wheat kernel. FgOS-2 and Fgatf1 negatively regulate aurofusarin biosynthesis.

4.8. FgOS-2 and Fgatf1 influence the expression of genes involved light reception and circadian rhythmicity

Light reception and circadian rhythmicity have a profound impact on nearly all physiological processes within fungal hyphae including DNA, RNA and protein metabolism, cell cycle, carbon metabolism, and stress response (Correa et al., 2003; Dong et al., 2008); (Rodriguez-Romero et al., 2010). A current model of circadian rhythmicity (Dunlap and Loros, 2004) describes the central role of the light receptor proteins White Collar 1 and 2 (WC-1 and WC-2) which build up a regulatory complex (White Collar Complex, WCC) and the regulatory protein Frq. The WCC promotes expression of Frq which in turn is acting as a repressor of the WCC and is subject to a tightly regulated degradation. This equilibrium between synthesis and degradation of Frq builds up the circadian clock. White collar-dependent blue light receptor VIVID (Vvd) is a small protein. It functions downstream of the WCC and acts as a repressor of the light responses (Cheng et al., 2003; Schwerdtfeger and Linden, 2003). In the constant light, the Vvd protein interacts with WCC in the nucleus to regulate photoadaptation by attenuating WCC activity (Chen et al., 2010). Vvd has been also shown to take part in regulating various circadian clock properties through its effects on the WCC (Heintzen et al., 2001). The results presented in this thesis suggest that the stress-activated FgOS-2/Fgatf1 is involved in the light reception and circadian rhythmicity in *F. graminearum*. Briefly, the wild type, $\Delta FgOS-2$ mutants and the *Fgatf1* mutants responded differently to light conditions (Fig. 72 and 73). Under permanent darkness condition, the formation of rings was weaker in the wild type and $\Delta FgOS-2$ mutant strains and absent in $\Delta Fgatf1$ as well as *Fgatf1*^{oe} mutants. Under permanent light condition, none of the strains produced coloured rings. However, all strains revealed a significant increase in red pigment formation compared to permanent darkness condition. Therefore, gene expression patterns of the *F. graminearum* homologues of *frq1*, *vvd1* and *opsins* genes under different light conditions were analyzed by RT-PCR. In the wild type, *frq1* and *vvd1* expression was induced in the darkness and repressed in the light. This regulation pattern was inverted in $\Delta Fgatf1$, *Fgatf1*^{oe} and $\Delta FgOS-2$ mutants. These results suggest that FgOS-2 and Fgatf1 repress *frq1* and *vvd1* in the light but activate in the darkness. Nonetheless, *frq1* and *vvd1* expression in the light and darkness were nearly the same between the $\Delta Fgatf1$ and *Fgatf1*^{oe} mutants. Interestingly, in *Fgatf1*^{oe}:: $\Delta FgOS-2$ mutants, *frq1* and *vvd1* transcript level were elevated both in the darkness and in the light. There have to be other factors which influence the expression of *frq1* and *vvd1*. Protein kinase C (PKC) and several kinases have been implicated in the light response processes. PKC affects light responses in *N. crassa* by negatively regulating the light receptor WC-1 (Arpaia et al., 1999; Yang et al., 2002; Franchi et al., 2005; Tang et al., 2009). These results might also explain why the wild type, but

not the mutants, developed pericentric rings of yellowish and reddish regions in the darkness. In contrast, all mutants were more reddish than the wild type in the light. In the darkness, the expression of genes involved in aurofusarin biosynthesis was up-regulated in the $\Delta FgOS-2$ and $\Delta Fgatf1$ mutants. Thus, $\Delta FgOS-2$ and $\Delta Fgatf1$ mutants were more reddish compared to the wild type and *Fgatf1* overexpression strains. Whether this regulation is also connected to the expression of *frq* and *vvd* genes, remains vague. In both *Fgatf1* over-expressing mutants the expression of *ops3* was absent and the expression of *ops2* was strongly down-regulated in the light and in the darkness. These results may explain why in both *Fgatf1* over-expressing mutants the red color was evenly distributed in the centre of the colonies. Upon *Fgatf1* deletion, the induction of *ops2* expression in the light was absent. In $\Delta FgOS-2$ mutants in the light, *ops2* and *ops3* expression were strongly induced compared to the wild type. This might explain why the pericentric rings of yellowish and reddish regions in $\Delta FgOS-2$ mutants appeared more pronounced compared to the wild type and $\Delta Fgatf1$ mutants. Furthermore, this might also explain why pericentric rings of yellowish and reddish regions in $\Delta Fgatf1$ mutants were weaker compared to the wild type and $\Delta FgOS-2$ mutants in the light-darkness rhythm.

The *N. crassa* OS-2 and Atf1 orthologue directly control some genes involved in circadian rhythm (Watanabe et al., 2007; Yamashita et al., 2008). In *B. cinerea*, the light sensor opsin1 (homologous to *ops1* and *ops3* in *F. graminearum*) is activated by BcAtf1 under stress conditions (Temme et al., 2012). In this study the induction of *ops2* expression in the light was absent in $\Delta Fgatf1$ mutants and was down-regulated in the *Fgatf1* overexpression strains compared to the wild type and $\Delta FgOS-2$ mutants. On the contrary, the expression of *ops2* was up-regulated in $\Delta Fgatf1$ mutants in the darkness conditions compared to the *Fgatf1* overexpression strains. These results suggest that *Fgatf1* activates *ops2* in the light conditions but represses *ops2* in the darkness. In $\Delta FgOS-2$ mutants in the light, the expression *ops2* and *ops3* were strongly induced compared to the wild type. These results suggest that FgOS-2 represses *ops2* and *ops3* in the light conditions. However, the expression of *ops2* was equal in the $\Delta FgOS-2$ mutants in the light and in the darkness and similar to the *ops2* expression in the $\Delta Fgatf1$ mutants in the darkness. The expression of *ops3* was down-regulated in $\Delta FgOS-2$ mutants in the darkness. Therefore, FgOS-2 positively regulates the expression of *ops3* in the darkness. This once again confirms that *Fgatf1* represses the expression of *ops2* in the darkness.

In summary, FgOS-2 and *Fgatf1* have a dominant influence on the expression of the *ops2*, *ops3*, *frq1* and *vvd1*. FgOS-2 and *Fgatf1* are positive regulators or repressors of these circadian genes depending on the light conditions. There might be a cross talk between the FgOS-2/*Fgatf1* signaling pathway and other signaling pathways in the regulation of light reception and circadian rhythmicity.

Altogether, this study highlights that the diverse physiological functions are controlled by a complex signaling machinery. I identified the stress-activated MAP-kinase FgOS-2 as a central regulator in the life cycle of *F. graminearum*. FgOS-2 influences vegetative growth, perithecia formation, the production of secondary metabolites and virulence. Many of these functions are executed through the regulation of ROS. In *F. graminearum*, Atf1 acts as a downstream target of FgOS-2 and is mainly involved in regulation of ROS metabolism. Atf1 shares some functions with the stress-activated MAP kinase FgOS-2 but has important-independent features (Fig. 82).

This study also provides evidences that TMRs are involved in numerous physiological functions and different signaling cascades in *F. graminearum*. TMRs perceive external signals and communicate them to intracellular heterotrimeric G-protein-signaling cascades. The results presented here further indicate a signaling crosstalk between the TMRs and MAP kinases and cAMP/PKA signaling pathways. Deletion of some TMRs compromised pathogenicity or influences several physiological processes, such as vegetative growth, sexual development, (secondary) metabolite products (DON, lipase secretion) and stress response (Fig. 82). Several TMRs turned out to be dispensable for normal vegetative growth, sexual reproduction, secondary metabolite production and virulence of *F. graminearum* (FGSG_07716, FGSG_05239 and FGSG_09693). It is feasible that—after deletion of the respective gene from the genome— the function of this receptor is taken over by another TMR. Multiple parallel gene deletions will most likely answer this question. Furthermore, it is possible that some TMRs lost their function in evolution. The large number of TMRs in the genome of *F. graminearum* might also hint to gene duplications that gave rise to new proteins with very specialized functions.

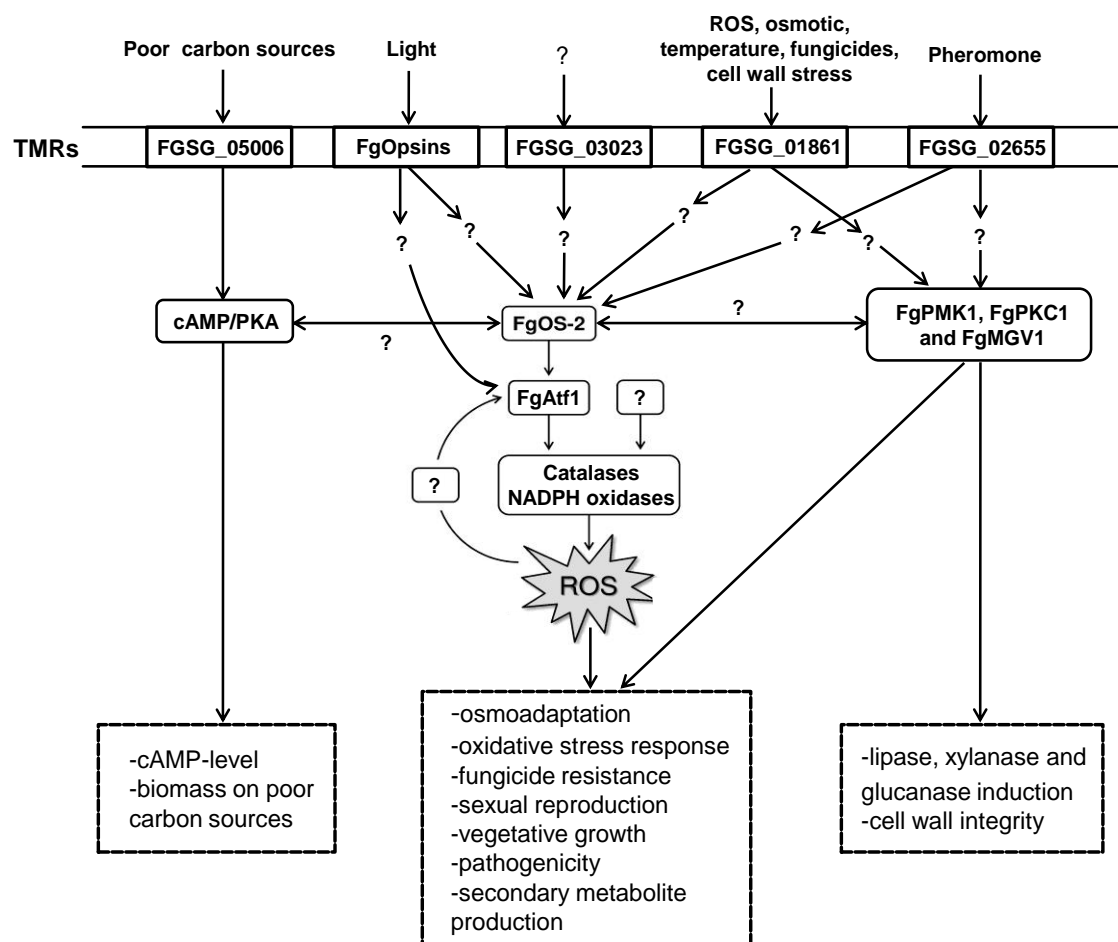


Figure 82. Proposed model: FgOS-2 orchestrates numerous physiological functions like sexual reproduction, secondary metabolism, virulence and stress response in *F. graminearum*. FgOS-2 controls ROS production and degradation, presumably by regulating ROS metabolic enzymes such as catalases and NADPH oxidases. Transmembrane receptors are involved in several physiological functions and different signaling cascades in *F. graminearum*.

Future investigations will focus on discovery of downstream targets of TMRs in different signaling pathways by quantitative RT-PCR and antibody against phosphorylated and unphosphorylated kinases PMK1, MGV1 and HOG1. The identification of cross talks between different signaling cascades is necessary in order to fully understand the complex signaling network in *F. graminearum*. By use of microarray analysis, metabolomics and western blot (using different TMR, MAP kinase and PKA mutants under different *in-vitro* culture conditions and *in planta*), the complete cross talks between TMRs, FgOS-2 signaling cascade and other signaling cascades will be elucidated. This approach will most likely also answer the questions how the central regulator FgOS-2 and its putative downstream target Fgatf1 are able to differentially regulate developmental processes depending on the environment in the connection with ROS metabolism. How do they positively influence DON production *in planta* and repress this synthesis *in vitro*. What exactly causes the reduced virulence towards wheat and maize.

5. Summary

The filamentous ascomycete *Fusarium graminearum* is a highly organ specific pathogen that resides on small grain cereals like rice, wheat, and maize. Once the host plants are infected, crops yielded from them are unsuited for food and feed production. This is mainly due to massive mycotoxin accumulation but also due to reductions in grain development. The most devastating mycotoxins produced by *F. graminearum* are deoxynivalenol (DON) and zearalenone (ZEA). The signaling cascades that are necessary for pathogenicity and mycotoxin production as well as the external stimuli that trigger those cascades are yet not fully understood. Aim of this thesis was to analyse a complete signaling cascade starting at membrane-bound receptors down to a transcriptional response. Transmembrane receptors (TMRs) are specialized integral membrane proteins that perceive external signals and communicate them to intracellular heterotrimeric G-protein-signaling cascades. Thus, TMRs play a pivotal role in the adaptation of entities to environmental stresses. In this study I present a comprehensive functional characterization of seven TMRs of *Fusarium graminearum*. They are involved in numerous physiological functions and different signaling cascades in *F. graminearum*. It was found that TMR FGSG_01861 is involved in stress tolerance towards oxidative, osmotic, fungicide, temperature and cell wall stress. Two TMRs (FGSG_03023 and FGSG_02655) play roles in pathogenicity, DON production, lipase secretion and sexual reproduction (the latter only FGSG_02655). Another TMR (FGSG_05006) was necessary for utilization of poor carbon sources and the intracellular level of the second messenger cAMP. Three other TMRs (FGSG_07716, FGSG_05239 and FGSG_09693) did not provoke any obvious phenotype. Acting downstream in the signaling cascade there are several transcription factors and mitogen-activated protein kinases (MAPK). MAPK signaling is a ubiquitous and well preserved regulation system for nearly all developmental processes throughout all eukaryotic organisms in response to several external stimuli like biotic or abiotic stresses or hormones. As shown in this study, the stress-activated MAP-kinase FgOS-2 (*S. cerevisiae* HOG1p) as a central regulator in the life cycle of *F. graminearum*. It is involved in nearly all developmental processes, such as perithecia formation, oxidative and osmotic stress tolerance, fungicide resistance, virulence, metabolism of reactive oxygen species (ROS) and secondary metabolite production, including mycotoxins. The results also highlight the possibility that the diverse physiological functions controlled by FgOS-2 are executed through the regulation of ROS. Functional characterization of the putative downstream target of FgOS-2, the ATF/CREB activating transcription factor Fgatf1, revealed that it plays a pivotal role in stress adaptation, secondary metabolism, sexual reproduction and virulence towards wheat and maize. Moreover, under stress conditions, Fgatf1 and FgOS-2 physically interact in the

nucleus. Furthermore, results obtained from overexpression experiments indicate that Fgatf1 is the main downstream target of FgOS-2.

Taken together, the results obtained in the course of this thesis, help to develop a signaling network starting from the signal perception and ending in the physiological response of the fungus to the environmental cues executed by the action of MAP-kinases and transcriptional regulators. Elaboration of such signaling cascades will most likely help to understand the molecular basis of pathogenicity and mycotoxin production and facilitates the invention of counter measures against this devastating plant pathogen.

6. Zusammenfassung

Der filamentöse Ascomycet *Fusarium graminearum* ist ein organspezifischer Schädling auf kleinkörnigen Getreidesorten wie z.B. Reis, Weizen und Mais. Infizierte Wirtspflanzen sind für die Nahrungs- und Futtermittelproduktion ungeeignet. Dies liegt zum einen in der massiven Akkumulation von Mykotoxinen aber auch an einer Verkürzung der Kornentwicklung begründet. Die prominentesten Mykotoxine, die von *F. graminearum* produziert werden, sind Deoxynivalenol (DON) und Zearalenon (ZEA). Die Regulation von Signalkaskaden, die für die Pathogenität und die Mykotoxin-Produktion sowie für die Perzeption äußerer Reize verantwortlich sind, ist noch nicht vollständig verstanden. Ziel dieser Arbeit war es, eine komplette Signalkaskade beginnend bei membrangebundenen Rezeptoren bis hin zu einer transkriptionellen Antwort zu analysieren. Transmembran-Rezeptoren (TMRs) sind spezialisierte, integrale Membranproteine, die externe Signale wahrnehmen und sie an intrazelluläre heterotrimere G-Protein-Signalkaskaden weiterleiten. TMRs spielen eine entscheidende Rolle bei der Anpassung von Organismen an wechselnde Umweltbedingungen. Die vorliegende Arbeit beschreibt die umfassende funktionelle Charakterisierung von insgesamt sieben TMRs von *F. graminearum*. Die Untersuchungen ergaben, dass diese Proteine an zahlreichen physiologischen Funktionen und verschiedenen Signalkaskaden in *F. graminearum* beteiligt sind. Es wurde festgestellt, dass TMR FGSG_01861 involviert ist in die Stresstoleranz gegenüber oxidativem, osmotischem, Fungizid-, Temperatur- und Zellwandstress. Zwei TMRs (FGSG_03023 und FGSG_02655) spielen eine Rolle in der Pathogenität, DON Produktion, Lipase-Sekretion und sexueller Fortpflanzung (letztere nur FGSG_02655). Ein weiterer TMR (FGSG_05006) war notwendig für die Nutzung bestimmter Kohlenstoffquellen und die Regulation intrazellulärer Level des sekundären Botenstoffs cAMP. Die Deletion dreier weiterer TMRs (FGSG_07716, FGSG_05239 und FGSG_09693) ergab keinen offensichtlichen Phänotyp. In der Signalkaskade abwärts befinden sich mehrere Transkriptionsfaktoren und Mitogen-aktivierte Proteinkinasen (MAPK). MAPKs sind ubiquitäre und konservierte Regelsysteme für nahezu alle Entwicklungsprozesse in allen eukaryotischen Organismen. Ihre Aktivität wird in Reaktion auf externe Stimuli wie biotischen oder abiotischen Stress oder Hormone moduliert. In der vorliegenden Arbeit wird die stress-aktivierte MAP-Kinase FgOS-2 (*S. cerevisiae* HOG1p) als zentralen Regulator im Lebenszyklus von *F. graminearum* beschrieben. Sie ist an der Regulation fast aller Entwicklungsprozesse wie Perithezienbildung, Stresstoleranz, Fungizidresistenz, Virulenz, Metabolismus reaktiver Sauerstoffspezies und Sekundärstoffproduktion, einschließlich der Mykotoxine, beteiligt. Die Ergebnisse deuten darauf hin, dass die vielfältigen, durch FgOS-2 gesteuerten Prozesse, durch die Regulierung intrazellulärer ROS-

Level gesteuert werden. Die funktionelle Charakterisierung eines putativen targets von FgOS-2, des ATF/CREB Transkriptionsfaktors Fgatf1, ergab, dass dieser eine zentrale Rolle bei der Stressanpassung, dem sekundären Stoffwechsel, der sexuellen Reproduktion und der Virulenz spielt. Unter Stressbedingungen interagieren Fgatf1 und FgOS-2 physisch miteinander. Darüber hinaus belegen Überexpressionsexperimente, dass Fgatf1 ein target stromabwärts von FgOS-2 ist. Zusammengenommen zeichnen die Ergebnisse dieser Arbeit erhalten wird ein komplexes Bild eines Signaltransduktionsnetzwerks ausgehend von der signalwahrnehmung bis hin zur physiologischen Reaktion des Pilzes auf wechselnde Umweltreize. Die Mitwirkung von MAP-Kinasen und transkriptionellen Regulatoren wird dargelegt. Die Aufklärung solcher Signalnetzwerke wird helfen, die molekularen Grundlagen der Pathogenität und Mykotoxin-Produktion zu verstehen. Die Kenntnis hiervon wird die Suche nach geeigneten Gegenmaßnahmen gegen dieses verheerende Pflanzenpathogen begünstigen.

7. References

- Ádám, A.L., Kohut, G., and Hornok, L. 2008. Fphog1, a HOG-type MAP kinase gene, is involved in multistress response in *Fusarium proliferatum*. *Journal of Basic Microbiology* 48:151-159.
- Alberts, B., Johnson, A., Lewis, J., Raff, M., Roberts, K., and Walter, P. 2002. *Molecular Biology of the Cell*. 4th edition. New York: Garland Science.
- Alonso-Monge, R., Real, E., Wojda, I., Bebelman, J.P., Mager, W.H., and Siderius, M. 2001. Hyperosmotic stress response and regulation of cell wall integrity in *Saccharomyces cerevisiae* share common functional aspects. *Mol Microbiol* 41:717-730.
- Alsbaugh, J.A., Perfect, J.R., and Heitman, J. 1997. *Cryptococcus neoformans* mating and virulence are regulated by the G-protein alpha subunit GPA1 and cAMP. *Genes Dev* 11:3206-3217.
- Arpaia, G., Cerri, F., Baima, S., and Macino, G. 1999. Involvement of protein kinase C in the response of *Neurospora crassa* to blue light. *Mol Gen Genet* 262:314-322.
- Ausubel, F.M., Brent, R., Kingston, R.E., Moore, D.D., Seidman, J.G., Smith, J.A., and Struhl, K. 2002. *Short protocols in molecular biology: a compendium of methods from current protocols in molecular biology*. Wiley, New York.
- Bahn, Y.S., Kojima, K., Cox, G.M., and Heitman, J. 2006. A unique fungal two-component system regulates stress responses, drug sensitivity, sexual development, and virulence of *Cryptococcus neoformans*. *Mol Biol Cell* 17:3122-3135.
- Becher, R., Hettwer, U., Karlovsky, P., Deising, H.B., and Wirsel, S.G. 2010. Adaptation of *Fusarium graminearum* to tebuconazole yielded descendants diverging for levels of fitness, fungicide resistance, virulence, and mycotoxin production. *Phytopathology* 100:444-453.
- Bennett, R.J., and Johnson, A.D. 2006. The role of nutrient regulation and the Gpa2 protein in the mating pheromone response of *C. albicans*. *Mol Microbiol* 62:100-119.
- Beyer, M., Röding, S., Ludewig, A., and J-A, V. 2004. Germination and survival of *Fusarium graminearum* macroconidia as affected by environmental factors. *Journal of Phytopathology* 152:92-97.
- Bluhm, B.H., Zhao, X., Flaherty, J.E., Xu, J.R., and Dunkle, L.D. 2007. RAS2 regulates growth and pathogenesis in *Fusarium graminearum*. *Mol. Plant-Microbe Interact* 20:627-636.

- Brewster, J.L., de Valoir, T., Dwyer, N.D., Winter, E., and Gustin, M.C. 1993. An osmosensing signal transduction pathway in yeast. *Science* 259:1760-1763.
- Buchenauer, H. 1987. Mechanism of action of triazolyl fungicides and related compounds. Pages 205-232 in: *Modern Selective Fungicides*. H. Lyr, ed. Gustav-Fischer-Verlag, Jena, Germany.
- Calvos, A.M., Wilson, R.A., Bok, J.W., and Keller, N.P. 2002. Relationship between secondary metabolism and fungal development. *Microbiol Mol Biol Rev* 66:447-459.
- Cano-Dominguez, N., Alvarez-Delfin, K., Hansberg, W., and Aguirre, J. 2008. NADPH oxidases NOX-1 and NOX-2 require the regulatory subunit NOR-1 to control cell differentiation and growth in *Neurospora crassa*. *Eukaryot. Cell* 7:1352-1361.
- Carla, J.E., Isabelle, J., Simon J. F., Jeremy S. H., and Barry, S. 2008. Functional analysis of a fungal endophyte stress-activated MAP kinase. *Current genetics* 53:163-174.
- Chang, Y.C., Miller, G.F., and Kwon-Chung, K.J. 2003. Importance of a developmentally regulated pheromone receptor of *Cryptococcus neoformans* for virulence. *Infect Immun* 71:4953-4960.
- Chen, C.H., DeMay, B.S., Gladfelter, A.S., Dunlap, J.C., and Loros, J.J. 2010. Physical interaction between vivid and white collar complex regulates photoadaptation in *Neurospora*. *Proceedings of the National Academy of Sciences of the United States of America* 107:16715-16720.
- Cheng, P., He, Q., Yang, Y., Wang, L., and Liu, Y. 2003. Functional conservation of light, oxygen, or voltage domains in light sensing. *Proc Natl Acad Sci U S A* 100:5938-5943.
- Chi, M.H., Park S.Y., Kim, S., and Lee, Y.H. 2009. A Novel pathogenicity gene is required in the rice blast fungus to suppress the basal defenses of the host. *PLoS Pathogens* 5:e1000401.
- Chung, S., Karos, M., Chang, Y.C., Lukszo, J., Wickes, B.L., and Kwon-Chung, K.J. 2002. Molecular analysis of CPR α , a MAT α -specific pheromone receptor gene of *Cryptococcus neoformans*. *Eukaryot Cell* 1:432-439.
- Clare, D.A., Minh Ngoc, D., Darr, D., Archibald, F., and Fridovich, I. 1984. Effects of molecular oxygen on detection of superoxide radical with nitroblue tetrazolium and on activity stains for catalase. *Anal. Biochem.* 140:532-537.
- Clark, J.M. 1988. Novel non-templated nucleotide addition reactions catalyzed by procaryotic and eucaryotic DNA polymerases. *Nucleic Acids Res* 16:9677-9686.

- Clergeot, P.H., Gourgues, M., Cots, J., Laurans, F., Latorse, M.P., Pepin, R., Tharreau, D., Notteghem, J.L., and Lebrun, M.H. 2001. PLS1, a gene encoding a tetraspanin-like protein, is required for penetration of rice leaf by the fungal pathogen *Magnaporthe grisea*. Proc Natl Acad Sci USA 98:6963–6968.
- Correa, A., Lewis, Z.A., Greene, A.V., March, I.J., Gomer, R.H., and Bell-Pedersen, D. 2003. Multiple oscillators regulate circadian gene expression in *Neurospora*. Proc Natl Acad Sci U S A 100:13597-13602.
- Cuatrecasas, P. 1974. Membrane Receptors. Annual Review of Biochemistry 43:169–214.
- Davidson, M.K., Shandilya, H.K., Hirota, K., Ohta, K., and Wahls, W.P. 2004. Atf1-Pcr1-M26 complex links stress-activated MAPK and cAMP-dependent protein kinase pathways via chromatin remodeling of *cgs2+*. J Biol Chem 279:50857-50863.
- De Backer, M., Ilyina, T., Ma, X., Vandoninck, S., Luyten, W.H.M., and Bossche, H., V. 2001. Genomic profiling of the response of *Candida albicans* to itraconazole treatment using a DNA microarray. Antimicrob Agents Chemother 45:1660–1670.
- Dean, R.A., Talbot, N.J., Ebbole, D.J., Farman, M.I., Mitchell, T.K., Orbach, M.J., Thon, M., Kulkarni, R., Xu, J.R., Pan, H., Read, N.D., Lee, Y.H., Carbone, I., Brown, D., Oh, Y.Y., Donofrio, N., Jeong, J.S., Soanes, D.M., Djonovic, S., Kolomiets, E., Rehmeyer, C., Li, W., Harding, M., Kim, S., Lebrun, M.H., Bohnert, H., Coughlan, S., Butler, J., Calvo, S., ma, L.J., Nicol, R., Purcell, S., Nusbaum, C., Galagan, J.E., and Birren, B.W. 2005. The genome sequence of the rice blast fungus *magnaporthe grisea*. Nature 434:980-986.
- Desmond, O.J., Manners, J.M., Stephens, A.E., Maclean, D.J., Schenk, P.M., Gardiner, D.M., Munn, A.L., and Kazan, K. 2008. The Fusarium mycotoxin deoxynivalenol elicits hydrogen peroxide production, programmed cell death and defence responses in wheat. Mol. Plant Pathol 9:435-445.
- DeZwaan, T.M., Carroll, A.M., Valent, B., and Sweigard, J.A. 1999. *Magnaporthe grisea* pth11p is a novel plasma membrane protein that mediates appressorium differentiation in response to inductive substrate cues. Plant Cell 11:2013-2030.
- Dixon, K.P., Xu, J.R., Smirnov, N., and Talbot, N.J. 1999. Independent signaling pathways regulate cellular turgor during hyperosmotic stress and appressorium-mediated plant infection by *Magnaporthe grisea*. Plant Cell 11:2045-2058.

- Dong, W., Tang, X., Yu, Y., Nilsen, R., Kim, R., Griffith, J., Arnold, J., and Schuttler, H.B. 2008. Systems biology of the clock in *Neurospora crassa*. PLoS One 3:e3105.
- Dunlap, J.C., and Loros, J.J. 2004. The neurospora circadian system. J Biol Rhythms 19:414-424.
- Eaton, C., Jourdain, I., Foster, S., Hyams, J., and Scott, B. 2008. Functional analysis of a fungal endophyte stress-activated MAP kinase. Current Genet. 53:163-174.
- Egan, M.J., Wang, Z.Y., Jones, M.A., Smirnov, N., and Talbot, N.J. 2007. Generation of reactive oxygen species by fungal NADPH oxidases is required for rice blast disease. Proc Natl Acad Sci U S A 104:11772-11777.
- Escoté, X., Miranda, M., Rodríguez-Porrata, B., Mas, A., Cordero, R., Posas, F., and Vendrell, J. 2011. The stress-activated protein kinase Hog1 develops a critical role after resting state. Mol. Microbiol. 80:423-435.
- Félix, G.S., and Edivaldo, X.F.F. 2010. Plant cell call as a substrate for the production of enzymes with industrial applications. Mini-Reviews in Organic Chemistry 7:54-60.
- Franchi, L., Fulci, V., and Macino, G. 2005. Protein kinase C modulates light responses in *Neurospora* by regulating the blue light photoreceptor WC-1. Mol Microbiol 56:334-345.
- Gacto, M., Soto, T., Vicente-Soler, J., Villa, T.G., and Cansado, J. 2003. Learning from yeasts: intracellular sensing of stress conditions. Int Microbiol 6:211-219.
- Gaffoor, I., Brown, D.W., Plattner, R., Proctor, R.H., Qi, W., and Trail, F. 2005. Functional analysis of the polyketide synthase genes in the filamentous fungus *Gibberella zeae* (anamorph *Fusarium graminearum*). Eukaryot. Cell 4:1926-1933.
- Giesbert, S., SchÜRg, T., Scheele, S., and Tudzynski, P. 2008. The NADPH oxidase Cpnox1 is required for full pathogenicity of the ergot fungus *Claviceps purpurea*. Mol. Plant Pathol. 9:317-327.
- Gilbert, H.J. 2010. The biochemistry and structural biology of plant cell wall deconstruction. Plant Physiol 153:444-455.
- Godet, F., and Limpert, E. 1998. Recent evolution of multiple resistance of *Godet, F.*, and *Limpert, E* to selected DMI and morpholine fungicides in France. Pestic. Sci 54:244-252.
- Goswami, R.S., and Kistler, H.C. 2004. Heading for disaster: *Fusarium graminearum* on cereal crops. Mol. Plant Pathol. 5:515-525.

- Gourgues, M., Brunet-Simon, A., Lebrun, M.H., and C., L. 2004. The tetraspanin BcPls1 is required for appressorium-mediated penetration of *Botrytis cinerea* into host plant leaves. *Mol Microbiol* 51:619–629.
- Green, C.E., and Phillips, R.L. 1975. Plant regeneration from tissue cultures of maize. *Crop Sci.* 15:417-421.
- Guenther, J.C., and Trail, F. 2005. The development and differentiation of *Gibberella zeae* (anamorph: *Fusarium graminearum*) during colonization of wheat. *Mycologia* 97:229-237.
- Guo, M., Guo, W., Chen, Y., Dong, S., Zhang, X., Zhang, H., Song, W., Wang, W., Wang, Q., Ruili Lv, R., Zhang, Z., Wang, Y., and Zheng, X. 2010. The basic leucine zipper transcription factor Moatf1 mediates oxidative stress responses and is necessary for full virulence of the rice blast fungus *Magnaporthe oryzae*. *Mol. Plant-Microbe Interact* 23:1053–1068.
- Gustin, M.C., Albertyn, J., Alexander, M., and Davenport, K. 1998. MAP kinase pathways in the yeast *Saccharomyces cerevisiae*. *Microbiol. Mol. Biol. Rev.* 62:1264-1300.
- Hagiwara, D., Asano, A., Yamashini, T., and Mizuno, T. 2008. Characterization of bZip-type transcription factor AtfA with reference to stress responses of conidia of *Aspergillus nidulans*. *Biosci Biotechnol Biochem* 72:2756-2760.
- Hagiwara, D., Asano, Y., Marui, J., Yoshimi, A., Mizuno, T., and Abe, K. 2009. Transcriptional profiling for *Aspergillus nidulans* HogA MAPK signaling pathway in response to fludioxonil and osmotic stress. *Fungal Genet. Biol.* 46:868-878.
- Han, K.H., and Prade, R.A. 2002. Osmotic stress-coupled maintenance of polar growth in *Aspergillus nidulans*. *Mol. Microbiol.* 43:1065–1078.
- Hanks, S.K., Quinn, A.M., and 1991. Protein kinase catalytic domain sequence database: Identification of conserved features of primary structure and classification of family members. *Methods Enzymol.* 200:38-62
- Harris, L.J., Alexander, N.J., Saparno, A., Blackwell, B., McCormick, S.P., Desjardins, A.E., Robert, L.S., Tinker, N., Hattori, J., and Piche, C. 2007. A novel gene cluster in *Fusarium graminearum* contains a gene that contributes to butenolide synthesis. *Fungal Genet. Biol.* 44:293-306.
- Heintzen, C., Loros, J.J., and Dunlap, J.C. 2001. The PAS protein VIVID defines a clock-associated feedback loop that represses light input, modulates gating, and regulates clock resetting. *Cell* 104:453–464.

- Heller, J., Ruhnke, N., Espino, J.j., Massaroli, M., Collado, I.G., and Tudzynski, P. 2012. The mitogen-activated protein kinase BcSak1 of *Botrytis cinerea* is required for pathogenic development and has broad regulatory functions beyond stress response. *Mol. Plant-Microbe Interact* 25 802-816.
- Hoff, B., and Kück, U. 2005. Use of bimolecular fluorescence complementation to demonstrate transcription factor interaction in nuclei of living cells from the filamentous fungus *Acremonium chrysogenum*. *Curr Genet* 47:132–138.
- Hohmann, S. 2002. Osmotic stress signaling and osmoadaptation in yeasts. *Microbiol Mol Biol Rev* 66:300-372.
- Hou, Z., Xue, C., Peng, Y., Katan, T., Kistler, H.C., and Xu, J.R. 2002. A mitogenactivated protein kinase (MGV1) in *Fusarium graminearum* is required for female fertility, heterokaryon formation, and plant infection.. *Mol. Plant-Microbe Interact* 15:1119-1127.
- Igbaria, A., Lev, S., Rose, M., Lee, B., Hadar, R., Degani, O., and Horwitz, B. 2008. Distinct and combined roles of the MAP kinases of *Cochliobolus heterostrophus* in virulence and stress responses. *Mol. Plant-Microbe Interact* 21:769-780.
- Ilgen, P., Hadelers, B., Maier, F.J., and Schafer, W. 2009. Developing kernel and rachis node induce the trichothecene pathway of *Fusarium graminearum* during wheat head infection. *Mol Plant-Microbe Interact* 22:899-908.
- Ivey, F.D., Hodge, P.N., Turner, G.E., and A., B.K. 1996. The G_{zi} homologue gna-1 controls multiple differentiation pathways in *Neurospora crassa*. *Mol. Biol. Cell* . 7:1283–1297.
- Jahn, B., Boukhallouk, F., Lotz, J., Langfelder, K., Wanner, G., and Brakhage, A.A. 2000. Interaction of human phagocytes with pigmentless *Aspergillus* conidia. *Infect. Immun* 68:3736.
- Jahn, B., Koch, A., Schmidt, A., Wanner, G., Gehringer, H., Bhakdi, S., and Brakhage, A.A. 1997. Isolation and characterization of a pigmentless-conidium mutant of *Aspergillus fumigatus* with altered conidial surface and reduced virulence. *Infect. Immun.* 65:5110.
- Jansen, C., von Wettstein, D., Schäfer, W., Kogel, K.H., Felk, A., and Maier, F.J. 2005. Infection patterns in barley and wheat spikes inoculated with wild-type and trichodiene synthase gene disrupted *Fusarium graminearum*. *Proc. Natl. Acad. Sci. U.S.A.* 102:16892-16897.

- Jenczmionka, N.J., and Schäfer, W. 2005. The Gpmk1 MAP kinase of *Fusarium graminearum* regulates the induction of specific secreted enzymes. *Current Genet.* 47:29-36.
- Jenczmionka, N.J., Maier, F.J., Lösch, A.P., and Schäfer, W. 2003. Mating, conidiation and pathogenicity of *Fusarium graminearum*, the main causal agent of the head-blight disease of wheat, are regulated by the MAP kinase gpmk1. *Current Genet.* 43:87-95.
- Jensen-Pergakes, K.L., Kennedy, M.A., Lees, N.D., Barbuch, R., Koegel, C., and Bard, M. 1998. Sequencing, disruption, and characterization of the *Candida albicans* sterol methyltransferase (ERG6) gene: drug susceptibility studies in *erg6* mutants. *Antimicrob Agents Chemother* 42:1160-1167.
- Jiang, J., Yun, Y., Fu, J., Shim, W.-B., and Ma, Z. 2011. Involvement of a putative response regulator FgRrg-1 in osmotic stress response, fungicide resistance and virulence in *Fusarium graminearum*. *Mol. Plant Pathol.* 12:425-436.
- Jonkers, W., Dong, Y., Broz, K., and Kistler, H.C. 2012. The Wor1-like protein Fgp1 regulates pathogenicity, toxin synthesis and reproduction in the phytopathogenic fungus *Fusarium graminearum*. *PLoS Pathog* 8:e1002724.
- Joseph-Horne, T., Manning, N.J., Hollomon, D., and Kelly, S.L. 1995. Defective sterol $\Delta 5(6)$ desaturase as a cause of azole resistance in *Ustilago maydis*. *FEMS Microbiol. Lett* 127:29-34.
- Joseph-Horne, T., Hollomon, D., Manning, N., and Kelly, S.L. 1996. Investigation of the Sterol Composition and Azole Resistance in Field Isolates of *Septoria tritici*. *Appl Environ Microbiol* 62:184-190.
- Kawasaki, L., Sánchez, O., Shiozaki, K., and Aguirre, J. 2002. Saka MAP kinase is involved in stress signal transduction, sexual development and spore viability in *Aspergillus nidulans*. *Mol. Microbiol.* 45:1153-1163.
- Keller, N.P., and Hohn, T.M. 1997. Metabolic pathway gene clusters in filamentous fungi. *Fungal Genet Biol* 21:17-29.
- Kim, H.K., Lee, T., and Yun, S.H. 2008. A putative pheromone signaling pathway is dispensable for self-fertility in the homothallic ascomycete *Gibberella zeae*. *Fungal Genet Biol* 45:1188–1196.
- Kim, J.E., Jin, J., Kim, H., Kim, J.C., Yun, S.H., and Lee, Y.W. 2006. GIP2, a putative transcription factor that regulates the aurofusarin biosynthetic gene cluster in *Gibberella zeae*. *Appl. Environ. Microb.* 72:1645.

- Kim, J.E., Han, K.H., Jin, J., Kim, H., Kim, J.C., Yun, S.H., and Lee, Y.W. 2005a. Putative polyketide synthase and laccase genes for biosynthesis of aurofusarin in *Gibberella zeae*. *Appl. Environ. Microb.* 71:1701-1708.
- Kim, K.-H., Willger, S.D., Park, S.-W., Puttikamonkul, S., Grahl, N., Cho, Y., Mukhopadhyay, B., Cramer, R.A., Jr., and Lawrence, C.B. 2009. TmpL, a transmembrane protein required for intracellular redox homeostasis and virulence in a plant and an animal fungal pathogen. *PLoS Pathog.* 5:e1000653.
- Kim, Y.T., Lee, Y.R., Jin, J., Han, K.H., Kim, H., Kim, J.C., Lee, T., Yun, S.H., and Lee, Y.W. 2005b. Two different polyketide synthase genes are required for synthesis of zearalenone in *Gibberella zeae*. *Mol Microbiol* 58:1102-1113.
- Klittich C, J.R., and Leslie, J.F. 1988. Nitrate reduction mutants of *Fusarium moniliforme* (*Gibberella fujikuroi*). *Genetics* 118:417 – 423.
- Klix, M.B., Verreet, J.A., and Beyer, M. 2007. Comparison of the declining triazole sensitivity of *Gibberella zeae* and increased sensitivity achieved by advances in triazole fungicide development. *Crop Prot* 26:683-690.
- Kobayashi, T., Abe, K., Asai, K., Gomi, K., Juvvadi, P.R., Kato, M., Kitamoto, K., Takeuchi, M., and Machida, M. 2007. Genomics of *Aspergillus oryzae*. *Biosci Biotechnol Biochem* 71:646-670.
- Kojima, K., Bahn, Y.S., and Heitman, J. 2006. Calcineurin, Mpk1 and Hog1 MAPK pathways independently control fludioxonil antifungal sensitivity in *Cryptococcus neoformans*. *Microbiology* 152:591-604.
- Kojima, K., Takano, Y., Yoshimi, A., Tanaka, C., Kikuchi, T., and Okuno, T. 2004. Fungicide activity through activation of a fungal signalling pathway. *Mol. Microbiol.* 53:1785-1796.
- Krems, B., Charizanis, C., and Entian, K.D. 1996. The response regulator-like protein Pos9/Skn7 of *Saccharomyces cerevisiae* is involved in oxidative stress resistance. *Curr. Genet* 29:327-334.
- Krystofova, S., and Borkovich, K.A. 2006. The Predicted G-Protein-Coupled Receptor GPR-1 Is Required for Female Sexual Development in the Multicellular Fungus *Neurospora crassa*. *Eukaryot Cell* 5:1503–1516.
- Kültz, D. 1998. Phylogenetic and functional classification of mitogen- and stress-activated protein kinases. *J Mol Evol* 46 46:571-588.

- Lara-Ortiz, T., Riveros-Rosas, H., and Aguirre, J. 2003. Reactive oxygen species generated by microbial NADPH oxidase NoxA regulate sexual development in *Aspergillus nidulans*. *Mol. Microbiol.* 50:1241-1255.
- Lara-Ortiz, T., Riveros-Rosas, H., and J., A. 2003. Reactive oxygen species generated by microbial NADPH oxidase NoxA regulate sexual development in *Aspergillus nidulans*. *Mol Microbiol.* 50:1241-1255.
- Lara-Rojas, F., Sánchez, O., Kawasaki, L., and Aguirre, J. 2011. *Aspergillus nidulans* transcription factor AtfA interacts with the MAPK SakA to regulate general stress responses, development and spore functions. *Mol. Microbiol.* 80:436-454.
- Lawrence, C.L., Botting, C.H., Antrobus, R., and Coote, P.J. 2004. Evidence of a new role for the high-osmolarity glycerol mitogen-activated protein kinase pathway in yeast: regulating adaptation to citric acid stress. *Mol Cell Biol* 24:3307-3323.
- Leach, J., Lang, B.R., and Yoder, O.C. 1982. Methods for selection of mutants and *in vitro* culture of *cochliobolus heterostrophus*. *J. Gen. Microbial* 128:1719-1729.
- Leberer, E., Thomas, D.Y., and Whiteway, M. 1997. Pheromone signalling and polarized morphogenesis in yeast. *Curr Opin Genet Dev* 7:59-66.
- Lee, J.K., Leslie, J.F., and Bowden, R.L. 2008. Expression and Function of Sex Pheromones and Receptors in the Homothallic Ascomycete *Gibberella zeae*. *Eukaryot Cell* 7:1211–1221.
- Lemaire, K., Van de Velde, S., Van Dijck, P., and Thevelein, J.M. 2004. Glucose and sucrose act as agonist and mannose as antagonist ligands of the G protein-coupled receptor Gpr1 in the yeast *Saccharomyces cerevisiae*. *Mol Cell* 16:293-299.
- Lenardon, M.D., Munro, C.A., and Gow, N.A. 2010. Chitin synthesis and fungal pathogenesis. *Curr Opin Microbiol* 13:416-423.
- Leroux, P., Albertini, C., Gautier, A., Gredt, M., and Walker, A.S. 2007. Mutations in the CYP51 gene correlated with changes in sensitivity to sterol 14 alpha-demethylation inhibitors in field isolates of *Mycosphaerella graminicola*. *Pest Manag Sci* 63:688-698.
- Leslie, J.F., and Summerell, B.A. 2006. *The Fusarium laboratory manual*. Wiley Online Library.
- Li, L., and Borkovich, K.A. 2006. GPR-4 is a predicted G-protein-coupled receptor required for carbon source-dependent asexual growth and development in *Neurospora crassa*. *Eukaryot Cell* 5:1287-1300.

- Li, L., Sara J. W., Krystofova, S., Park, G., and Katherine, A.B. 2007. Heterotrimeric G Protein Signaling in Filamentous Fungi. *Annual Review of Microbiology* 61:423-452.
- Li, S., Ault, A., Malone, C.L., Raitt, D., Dean, S., Johnston, L.H., Deschenes, R.J., and Fassler, J.S. 1998. The yeast histidine protein kinase, Sln1p, mediates phosphotransfer to two response regulators, Ssk1p and Skn7p. *EMBO J.* 17:6952-6962.
- Liang, S., Wang, Z.Y., Liu, P.J., and Li, D.B. 2006. A G γ subunit promoter T-DNA insertion mutant: A1-412 of *Magnaporthe grisea* is defective in appressorium formation, penetration and pathogenicity *Chin. Sci. Bull* 51:2214–2218.
- Linnemannstons, P., Schulte, J., del Mar Prado, M., Proctor, R.H., Avalos, J., and Tudzynski, B. 2002. The polyketide synthase gene *pk4* from *Gibberella fujikuroi* encodes a key enzyme in the biosynthesis of the red pigment bikaverin. *Fungal Genet Biol* 37:134-148.
- Liu, S., and Dean, R.A. 1997. G protein alpha subunit genes control growth, development, and pathogenicity of *Magnaporthe grisea*. *Mol. Plant-Microbe Interact* 10:1075-1086.
- Liu, W., Leroux, P., and Fillinger, S. 2008. The HOG1-like MAP kinase Sak1 of *Botrytis cinerea* is negatively regulated by the upstream histidine kinase Bos1 and is not involved in dicarboximide- and phenylpyrrole-resistance. *Fungal Genet. Biol.* 45:1062-1074.
- Liu, X., Jiang, J., Shao, J., Yin, Y., and Ma, Z. 2010. Gene transcription profiling of *Fusarium graminearum* treated with an azole fungicide tebuconazole. *Appl Microbiol Biotechnol* 85:1105-1114.
- Lodish, H., Berk, A., Matsudaira, P., Kaiser, C.A., and Krieger, M. 2003. *Molecular Cell Biology*. 5th Edition W.H. Freeman.
- Lorenz, M.C., Pan, X., Harashima, T., Cardenas, M.E., Xue, Y., Hirsch, J.P., and Heitman, J. 2000. The G protein-coupled receptor Gpr1 is a nutrient sensor that regulates pseudohyphal differentiation in *Saccharomyces cerevisiae*. *Genetics* 154:609–622.
- Maidan, M.M., De Rop, L., Serneels, J., Exler, S., Rupp, S., Tournu, H., Thevelein, J.M., and Van Dijck, P. 2005 The G protein-coupled receptor Gpr1 and the G α protein Gpa2 act through the cAMP-protein kinase A pathway to induce morphogenesis in *Candida albicans*. *Mol Biol Cell* 16:1971-1986.
- Maier, F.J., Miedaner, T., Hadel, B., Felk, A., Salomon, S., Lemmens, M., Kassner, H., and Schafer, W. 2006. Involvement of trichothecenes in fusarioses of wheat, barley and

- maize evaluated by gene disruption of the trichodiene synthase (Tri5) gene in three field isolates of different chemotype and virulence. *Mol. Plant Pathol.* 7:449-461.
- Malagnac, F., Lalucque, H., Lepere, G., and Silar, P. 2004. Two NADPH oxidase isoforms are required for sexual reproduction and ascospore germination in the filamentous fungus *Podospora anserina*. *Fungal Genet. Biol.* 41:982-997.
- Malz, S., Grell, M.N., Thrane, C., Maier, F.J., Rosager, P., Felk, A., Albertsen, K.S., Salomon, S., Bohn, L., Schäfer, W., and Giese, H. 2005. Identification of a gene cluster responsible for the biosynthesis of aurofusarin in the *Fusarium graminearum* species complex. *Fungal Genet. Biol.* 42:420-433.
- McMullen, M., Jones, R., and Gallenberg, D. 1997. Scab of wheat and barley: a re-emerging disease of devastating impact. *Plant Dis.* 81:1340-1348.
- Michael, C.G., Jacobus, A., Matthew, A., and Kenneth, D. 1998. MAP kinase pathways in the Yeast *Saccharomyces cerevisiae*. *Microbiology and Molecular Biology Reviews* 62:1264-1300.
- Millar, J.B., Buck, V., and Wilkinson, M.G. 1995 Pyp1 and Pyp2 PTPases dephosphorylate an osmosensing MAP kinase controlling cell size at division in *fission yeast*. *Genes Dev* 9:2117-2130.
- Min Guo, Wang Guo., Yue Chen., Suomeng Dong., Xing Zhang., Haifeng Zhang., Wenwen Song., Wei Wang., Qi Wang., Ruili Lv., Zhengguang Zhang., Yuanchao Wang., and Zheng., X. 2010. The Basic Leucine Zipper Transcription Factor Moatf1 Mediates Oxidative Stress Responses and Is Necessary for Full Virulence of the Rice Blast Fungus *Magnaporthe oryzae*. *MPMI* 23:1053-1068.
- Moriwaki, A., Kubo, E., Arase, S., and Kihara, J. 2006 Disruption of SRM1, a mitogen-activated protein kinase gene, affects sensitivity to osmotic and ultraviolet stressors in the phytopathogenic fungus *Bipolaris oryzae*. *FEMS Microbiol Lett* 257:253-261.
- Mösch, H.U., Roberts, R.L., and Fink, G.R. 1996. Ras2 signals via the Cdc42/Ste20/mitogen-activated protein kinase module to induce filamentous growth in *Saccharomyces cerevisiae*. *Proc Natl Acad Sci U S A* 93:5352-5356.
- Nakaune, R., Adachi, K., Nawata, O., Tomiyama, M., Akutsu, K., and Hibi, T. 1998. A novel ATP-binding cassette transporter involved in multidrug resistance in the phytopathogenic fungus *Penicillium digitatum*. *Appl Environ Microbiol* 64:3983-3988.

- Nathues, E., Joshi, S., Tenberge, K.B., von den Driesch, M., Oeser, B., Baumer, N., Mihlan, M., and Tudzynski, P. 2004. CPTF1, a CREB-like transcription factor, is involved in the oxidative stress response in the phytopathogen *Claviceps purpurea* and modulates ROS level in its host *Secale cereale*. *Mol. Plant-Microbe Interact.* 17:383-393.
- Nguyen, L.N., Bormann, J., Le, G.T., Starkel, C., Olsson, S., Nosanchuk, J.D., Giese, H., and Schafer, W. 2010. Autophagy-related lipase FgATG15 of *Fusarium graminearum* is important for lipid turnover and plant infection. *Fungal Genet. Biol.* 48:217-224.
- Nguyen, T.V., Schäfer, W., and Bormann, J. 2012. The Stress-Activated Protein Kinase FgOS-2 Is a Key Regulator in the Life Cycle of the Cereal Pathogen *Fusarium graminearum*. *Mol. Plant-Microbe Interact* 25:1142-1156.
- Nirenberg, H. 1981. A simplified method for identifying *Fusarium* spp. occurring on wheat. *Can. J. Bot* 59:1599-1609.
- Nishimura M., Park, G., and Xu, J.R. 2003. The G- β subunit MGB1 is involved in regulating multiple steps of infection-related morphogenesis in *Magnaporthe grisea*. *Mol. Microbiol.* 50:231–243.
- Noguchi, R., S. Banno, R. Ichikawa, F. Fukumori, A. Ichiishi, M. Kimura, I. Yamaguchi, and Fujimura., M. 2007. Identification of OS-2 MAP kinasedependent genes induced in response to osmotic stress, antifungal agent fludioxonil, and heat shock in *Neurospora crassa*. *Fungal Genet. Biol.* 44:208–218.
- O'Rourke, S.M., Herskowitz, I., and O'Shea, E.K. 2002. Yeast go the whole HOG for the hyperosmotic response. *Trends Genet.* 18:405-412.
- O'Rourke, S.M., and Herskowitz, I. 1998. The Hog1 MAPK prevents cross talk between the HOG and pheromone response MAPK pathways in *Saccharomyces cerevisiae*. *Genes Dev* 12:2874–2886.
- Ochiai, N., Tokai, T., Takahashi-Ando, N., Fujimura, M., and Kimura, M. 2007. Genetically engineered *Fusarium* as a tool to evaluate the effects of environmental factors on initiation of trichothecene biosynthesis. *FEMS Microbiol. Lett.* 275:53-61.
- Ochiai, N., Tokai, T., Nishiuchi, T., Takahashi-Ando, N., Fujimura, M., and Kimura, M. 2007a. Involvement of the osmosensor histidine kinase and osmotic stress-activated protein kinases in the regulation of secondary metabolism in *Fusarium graminearum*. *Biochem. Bioph. Res. Co.* 363:639-644.

- Paper, J.M., Scott-Craig, J.S., Adhikari, N.D., Cuomo, C.A., and Walton, J.D. 2007. Comparative proteomics of extracellular proteins in vitro and in planta from the pathogenic fungus *Fusarium graminearum*. *Proteomics* 7:3171-3183.
- Park, S.M., Choi, E.S., Kim, M.J., Cha, B.J., Yang, M.S., and Kim, D.H. 2004. Characterization of HOG1 homologue, Cpmk1, from *Cryphonectria parasitica* and evidence for hypovirus-mediated perturbation of its phosphorylation in response to hypertonic stress. *Mol Microbiol* 51:1267-1277.
- Pascual-Ahuir, A., Serrano, R., and Proft, M. 2001. The Sko1p repressor and Gcn4p activator antagonistically modulate stress-regulated transcription in *Saccharomyces cerevisiae*. *Mol Cell Biol* 21:16-25.
- Peraldi, A., Beccari, G., Steed, A., and Nicholson, P. 2011. *Brachypodium distachyon*: a new pathosystem to study *Fusarium* head blight and other *Fusarium* diseases of wheat. *BMC Plant Biol* 11:100.
- Phalip, V., Delalande, F., Carapito, C., Goubet, F., Hatsch, D., Leize-Wagner, E., Dupree, P., Dorselaer, A.V., and Jeltsch, J.M. 2005. Diversity of the exoproteome of *Fusarium graminearum* grown on plant cell wall. *Curr Genet* 48:366-379.
- Pillonel, C., and Meyer, T. 1997. Effect of phenylpyrroles on glycerol accumulation and protein kinase activity of *Neurospora crassa*. *Pestic. Sci.* 49:229-236.
- Ponts, N., Pinson Gadais, L., Verdal Bonnin, M.N., Barreau, C., and Richard Forget, F. 2006. Accumulation of deoxynivalenol and its 15 acetylated form is significantly modulated by oxidative stress in liquid cultures of *Fusarium graminearum*. *FEMS Microbiol. Lett.* 258:102-107.
- Posas, F., Wurgler-Murphy, S.M., Maeda, T., Witten, E.A., Thai, T.C., and Saito, H. 1996. Yeast HOG1 MAP kinase cascade is regulated by a multistep phosphorelay mechanism in the SLN1-YPD1-SSK1 "two-component" osmosensor. *Cell* 86:865-875.
- Proctor, R.H., Hohn, T.M., and McCormick, S.P. 1995. Reduced virulence of *Gibberella zeae* caused by disruption of a trichothecene toxin biosynthetic gene. *Mol. Plant-Microbe Interact.* 8:593-601.
- Reid, L.M. 1996. Screening maize for resistance to *Gibberella* ear rot. Agriculture and Agri-Food Canada, Research Branch.

- Reid, L.M., Hamilton, R.I., and Mather, D.E. 1995. Effect of macroconidial suspension volume and concentration on expression of resistance to *Fusarium graminearum* in maize. *Plant Dis.* 79:461-466.
- Reimann, S., and Deising, H.B. 2005. Inhibition of efflux transporter-mediated fungicide resistance in *Pyrenophora tritici-repentis* by a derivative of 4'-hydroxyflavone and enhancement of fungicide activity. *Appl. Environ. Microbiol* 71:3269-3275.
- Robertson, E.F., Dannelly, H.K., Malloy, P.J., and Reeves, H.C. 1987. Rapid isoelectric focusing in a vertical polyacrylamide minigel system. *Anal. Biochem* 167:290-294.
- Rodriguez-Romero, J., Hedtke, M., Kastner, C., Muller, S., and Fischer, R. 2010. Fungi, hidden in soil or up in the air: light makes a difference. *Annu Rev Microbiol* 64:585-610.
- Román, E., David M.Arena., Ce'sar, N., Rebeca, A.M., and Pla, J.s. 2007. MAP kinase pathways as regulators of fungal virulence. *TRENDS in Microbiology* 15:181-190.
- Rosen, S., Yu, J.H., and Adams, T.H. 1999. The *Aspergillus nidulans* *sfaD* gene encodes a Gprotein β subunit that is required for normal growth and repression of sporulation. *EMBO J* 18:5592-5600.
- Sakamoto, K., Iwashita, K., Yamada, O., Kobayashi, K., Mizuno, A., Akita, O., Mikami, S., Shimoi, H., and Gomi, K. 2009. *Aspergillus oryzae* *atfA* controls conidial germination and stress tolerance. *Fungal Genet. Biol.* 46:887-897.
- Sambrook, J., Fritsch, E.F., and Maniatis, T. 1989. *Molecular cloning: a laboratory manual*. Cold Spring Harbor Laboratory, Cold Spring Harbor, N.Y.
- Schnabel, G., and Jones, A.L. 2001. The 14 alpha-demethylase (CYP51A1) gene is overexpressed in *Venturia inaequalis* strains resistant to myclobutanil. *Phytopathology* 91:102-110.
- Schwerdtfeger, C., and Linden, H. 2003. VIVID is a flavoprotein and serves as a fungal blue light photoreceptor for photoadaptation. *EMBO J* 22:4846-4855.
- Segmüller, N., Ellendorf, U., Tudzynski, B., and Tudzynski, P. 2007. BcSAK1, a stress-activated mitogen-activated protein kinase, is involved in vegetative differentiation and pathogenicity in *Botrytis cinerea*. *Eukaryot. Cell* 6:211-221.
- Segmüller, N., Kokkelink, L., Giesbert, S., Odinius, D., van Kan, J., and Tudzynski, P. 2008. NADPH oxidases are involved in differentiation and pathogenicity in *Botrytis cinerea*. *Mol Plant-Microbe Interact* 21:808-819.

- Selmecki, A., Gerami-Nejad, M., Paulson, C., Forche, A., and Berman, J. 2008. An isochromosome confers drug resistance in vivo by amplification of two genes, ERG11 and TAC1. *Mol Microbiol* 68:624-641.
- Seo, J.A., and Yu, J.H. 2006. The phosphatidylinositol 3-kinase-like protein PhnA is required for G $\beta\gamma$ -mediated signaling for vegetative growth, developmental control, and toxin biosynthesis in *Aspergillus nidulans*. *Eukaryot. Cell* 5:400–410.
- Seo, J.A., Han, K.H., and Yu, J.H. 2004. The gprA and gprB genes encode putative G protein-coupled receptors required for self-fertilization in *Aspergillus nidulans*. *Mol Microbiol* 53:1611-1623.
- Seo, J.A., Han, K.H., and Yu, J.H. 2005. Multiple roles of a heterotrimeric G-protein gamma-subunit in governing growth and development of *Aspergillus nidulans*. *Genetics* 171:81-89.
- Seong, K.Y., Zhao, X., Xu, J.R., Guldener, U., and Kistler, H.C. 2008. Conidial germination in the filamentous fungus *Fusarium graminearum*. *Fungal Genet. Biol* 45:389-399.
- Shiozaki, K., and Russell, P. 1995. Cell-cycle control linked to extracellular environment by MAP kinase pathway in *fission yeast*. *Nature* 378:739-743.
- Singh, P., Chauhan, N., Ghosh, A., Dixon, F., and Calderone, R. 2004. SKN7 of *Candida albicans*: mutant construction and phenotype analysis. *Infect Immun* 72:2390-2394.
- Sutton, J.C. 1982. Epidemiology of wheat head blight and maize ear rot caused by *Fusarium graminearum*. *Can. J. Plant Pathol* 4:195-209.
- Takada, H., Nishimura, M., Asayama, Y., Mannse, Y., Ishiwata, S., Kita, A., Doi, A., Nishida, A., Kai, N., Moriuchi, S., Tohda, H., Giga-Hama, Y., Kuno, T., and Sugiura, R. 2007. Atf1 Is a Target of the Mitogen-activated Protein Kinase Pmk1 and Regulates Cell Integrity in *Fission Yeast*. *Mol Biol Cell* 18:4794–4802.
- Tanaka, A., Christensen, M.J., Takemoto, D., Park, P., and Scott, B. 2006. Reactive oxygen species play a role in regulating a fungus-perennial ryegrass mutualistic interaction. *Plant Cell* 18:1052-1066.
- Tang, C.T., Li, S., Long, C., Cha, J., Huang, G., Li, L., Chen, S., and Liu, Y. 2009. Setting the pace of the *Neurospora* circadian clock by multiple independent FRQ phosphorylation events. *Proc Natl Acad Sci U S A* 106:10722-10727.

- Temme, N., Oeser, B., Massaroli, M., Heller, J., Simon, A., González Collado, G., and Tudzynski, P. 2012. BcAtf1, a global regulator, controls various differentiation processes and phytotoxin production in *Botrytis cinerea*. *Mol. Plant Pathol* 13:704-718.
- Trail, F. 2009. For blighted waves of grain: *Fusarium graminearum* in the postgenomics era. *Plant Physiol* 149:103-110.
- Veneault-Fourrey, C., Parisot, D., Gourgues, M., Lauge, R., Lebrun, M.H., and Langin, T. 2005. The tetraspanin gene CIPLS1 is essential for appressorium-mediated penetration of the fungal pathogen *Colletotrichum lindemuthianum*. *Fungal Genet Biol.* 42:306–318.
- Verna, J., Lodder, A., Lee, K., Vagts, A., and Ballester, R. 1997. A family of genes required for maintenance of cell wall integrity and for the stress response in *Saccharomyces cerevisiae*. *Proc Natl Acad Sci U S A* 94:13804-13809.
- Voigt, C., von Scheidt, B., Gácsér, A., Kassner, H., Lieberei, R., Schäfer, W., and Salomon, S. 2007. Enhanced mycotoxin production of a lipase-deficient *Fusarium graminearum* mutant correlates to toxin-related gene expression. *Eur. J. Plant Pathol.* 117:1-12.
- Voigt, C.A., Schäfer, W., and Salomon, S. 2005. A secreted lipase of *Fusarium graminearum* is a virulence factor required for infection of cereals. *Plant J* 42:364-375.
- Wang, P., Perfect, J.R., and Heitman, J. 2000. The G-protein β subunit GPB1 is required for mating and haploid fruiting in *Cryptococcus neoformans*. *Mol. Cell Biol* 20:352–362.
- Wanjiru, W.M., Kang, Z., and Buchenauer, H. 2002. Importance of cell wall degrading enzymes produced by *Fusarium graminearum* during infection of wheat heads. *European Journal of Plant Pathology* 108:803-810.
- Waskiewicz, A.J., and Cooper, J.A. 1995. Mitogen and stress response pathway; MAPK kinase cascade and phosphatase regulation in mammals and yeast. *Curr opin cell biol* 7:798-805.
- Watanabe, S., Yamashita, K., Ochiai, N., Fukumori, F., Ichiishi, A., Kimura, M., and Fujimura, M. 2007. OS-2 Mitogen Activated Protein Kinase Regulates the Clock-Controlled Gene *cgc-1* in *Neurospora crassa*. *Biosci. Biotechnol. Biochem* 71:2856–2859.
- Winkler, A., Arkind, C., Mattison, C.P., Burkholder, A., Knoche, K., and Ota, I. 2002. Heat stress activates the yeast high-osmolarity glycerol mitogen-activated protein kinase pathway, and protein tyrosine phosphatases are essential under heat stress. *Eukaryot Cell* 1:163-173.

- Winkler, U.K., and Stuckmann, M.J. 1979. Glycogen, hyaluronate, and some other polysaccharides greatly enhance the formation of exolipase by *Serratia marcescens*. J. Bacteriol 138: 663–670.
- Wood, P.J., and Fulcher, R.G. 1983. Dye interactions. A basis for specific detection and histochemistry of polysaccharides. J Histochem Cytochem 31:823-826.
- Wyand, R.A., and Brown, J.K. 2005. Sequence variation in the CYP51 gene of *Blumeria graminis* associated with resistance to sterol demethylase inhibiting fungicides. Fungal Genet Biol 42:726-735.
- Xue, C., Bahn, Y.S., Cox, G.M., and Heitman, J. 2006. G Protein-coupled Receptor Gpr4 Senses Amino Acids and Activates the cAMP-PKA Pathway in *Cryptococcus neoformans*. Mol Biol Cell 17:667–679.
- Xue, Y., Battle, M., and Hirsch, J.P. 1998. GPR1 encodes a putative G protein-coupled receptor that associates with the Gpa2p Galpha subunit and functions in a Ras-independent pathway. EMBO J 17:1996–2007.
- Yamashita, K., Shiozawa, A., Watanabe, S., Fukumori, F., Kimura, M., and Fujimura, M. 2008. ATF-1 transcription factor regulates the expression of *cgc-1* and *cat-1* genes in response to fludioxonil under OS-2 MAP kinase in *Neurospora crassa*. Fungal Genet Biol 45:1562-1569.
- Yang, Q., and Borkovich, K.A. 1999. Mutational activation of a *Gai* causes uncontrolled proliferation of aerial hyphae and increased sensitivity to heat and oxidative stress in *Neurospora crassa*. Genetics 151:107–117.
- Yang, Y., Cheng, P., and Liu, Y. 2002. Regulation of the *Neurospora* circadian clock by casein kinase II. Genes Dev 16:994-1006.
- Yu, H.Y., Seo, J.A., Kim, J.E., Han, K.H., Shim, W.B., Yun, S.H., and Lee, Y.W. 2008. Functional analyses of heterotrimeric G protein Galpha and Gbeta subunits in *Gibberella zeae*. Microbiology 154:392–401.
- Yu, L., Zhang, W., Wang, L., Yang, J., Liu, T., Peng, J., Leng, W., Chen, L., Li, R., and Jin, Q. 2007. Transcriptional profiles of the response to ketoconazole and amphotericin B in *Trichophyton rubrum*. Antimicrob Agents Chemother 51:144-153.
- Yun, C.W., Tamaki, H., Nakayama, R., Yamamoto, K., and Kumagai, H. 1997. G-protein coupled receptor from yeast *Saccharomyces cerevisiae*. Biochem Biophys Res Commun 240:287-292.

- Yun, C.W., Tamaki, H., Nakayama, R., Yamamoto, K., and Kumagai, H. 1998. Gpr1p, a putative G-protein coupled receptor, regulates glucose-dependent cellular cAMP level in yeast *Saccharomyces cerevisiae*. *Biochem Biophys Res Commun* 252:29-33.
- Zhang, Y., Lamm, R., Pillonel, C., Lam, S., and Xu, J.R. 2002. Osmoregulation and fungicide resistance: the *Neurospora crassa* os-2 gene encodes a HOG1 mitogen-activated protein kinase homologue. *Appl. Environ. Microbiol.* 68:532-538.

Acknowledgments

First, I am deeply grateful to my supervisor **Prof. Dr. Wilhelm Schäfer** for the opportunity of participate in this study at his laboratory, and for his excellent supervisor. Thank for his guidance and patience through the good times and bad times. His faith in me kept me going during the times when it felt like nothing was working and I questioned whether I could ever finish.

I am thankful to **Prof. Dr. Christian Axel Voigt** for being the second reviewer of this study.

I would like to thank **Prof. Dr. Myron Peck** for his linguistic assessment of this writing.

I am very thankful to **Dr. Jörg Bormann**. Without his kind guidance and valuable discussions many results presented in this study could not have been achieved. I have valued his help, advice and most importantly his friendship. I would also like to thank him for proofreading my dissertation. Without his support all this would not have been possible.

I am grateful to **Dr. Ana Lilia Martinez-Rocha** for many useful discussions and advices. It is also the time to express my thanks to her for support and encouragement during my PhD time.

I will forever be grateful to **Associate Prof. Dr. Quyen Dinh Thi** for giving me a chance and valuable advices to enhance my academic study before doing PhD.

Thanks to all present and former colleagues of **Molecular Phytopathology and Genetics**: Cathrin Kröger, Birgit Hadel, Dr. Anke Lösch, Brigitte Doormann, Dr. Le Thi Thu Giang, Dr. Cornelia Stärkel, Jakob Bönnighausen and Marike Boenisch. They all helped me in so many ways. Special thanks to Cathrin Kröger and Birgit Hadel for technical assistance. I would also like to thank all colleagues and friends from **Molecular Phytopathology and Genetics** as well as from the **Biocenter Klein Flottbek**.

I would like to thank the Hong Duc University, Thanh Hoa, Vietnam for the PhD fellowship.

Lastly, my deepest thanks must go to my wife and my children for their love and moral support. Without their support and love none of this would have been possible.

CURRICULUM VITAE

Personal

Name: Mr. Thuat Van Nguyen

Date of Birth: March 23th, 1973

Nationality: Vietnamese

Education

3/2009 – 2/2013: Ph.D student

Biology Department, University of Hamburg, Germany

Study Project: Signal transduction pathways in the fungal wheat pathogen *Fusarium graminearum*

Certificate: Doctorate

Speciality: Molecular Biology/Genetics/Phytopathology

1/2007 - 3/2008: DE Course

DE Course (Diploma Equivalence) by the corporation between Vietnam and Greifswald University (Germany).

Certificate: Diploma Equivalence Degree

Speciality: Experimental Biotechnology

1/2006 - 12/2006: Intensive English Course

Intensive English Course by IIG Vietnam-ETS country Representative

Certificate: TOEFL iBT

10/1998 - 10/2000: Master Course

Biology Department- Hanoi University of Education, Vietnam

Certificate: Master Degree

Speciality: Biology Teaching

8/1991 - 8/1995: Full time student

Biology Department- Hanoi University of Education, Vietnam

Certificate: Bachelor of Science

Language Proficiency

Vietnamese (native), English (good)